Cellular models for liver toxicity:
keeping track of time

Annelieke Suzanne de Wit

Cellular models for liver toxicity: keeping track of time

Cellulaire modellen voor levertoxiciteit: blijf bij de tijd

Proefschrift

ter verkrijging van de graad van doctor
aan de Erasmus Universiteit Rotterdam
op gezag van de rector magnificus

Prof. dr. H.A.P. Pols

en volgens besluit van het College van Promoties.
De openbare verdediging zal plaatsvinden op

25 juni 2014 om 11:30

door

Annelieke Suzanne de Wit

geboren te Amsterdam

ERASMUS UNIVERSITEIT ROTTERDAM

Promotiecommissie

Promotor   prof. dr. Gijsbertus T.J. van der Horst

Copromotor   dr. Inês Chaves

Overige leden   dr. ing. Ron W.F. de Bruin
prof. dr. Harry van Steeg
prof. dr. Leon H.F. Mullenders

Table of contents

Chapter 1: Introduction

Hepatotoxicity and the clock: a timely matter

Annelieke S. de Wit, Romana M. Nijman, Eugin Destici, Inês Chaves, and Gijsbertus T.J. van der Horst

1

Circadian rhythms

As a direct result of the composition of our solar system, life on earth is continuously exposed to temporal changes to the environment. Apart from annual, seasonal and lunar cycles, we experience 24-hour light/dark and temperature cycles, caused by the rotation of the earth around its own axis. To cope with these cyclic changes organisms have acquired an internal timing mechanism with a periodicity of approximately 24 hour (Edery, 2000). This circadian clock (Lat. circa = near, dies = day) is an anticipatory mechanism that allows an organism to adjust behavior, physiology and metabolism (e.g. body temperature, sleep-wake cycle, blood pressure and locomotor activity) to the specific needs at defined stages over the day (Lowrey & Takahashi, 2004; Reppert & Weaver, 2002). The importance of circadian clocks is well illustrated by the fact that they evolved multiple times during evolution and are present in almost all life forms on earth, ranging from single cellular organisms (e.g. bacteria) to multicellular organisms (e.g. plants and animals) (Bell-Pedersen et al., 2005; Dunlap, 1999). Circadian clock research has largely focused on a series of model organisms, notably the filamentous fungus Neurospora crassa, the plant *Arabidopsis thaliana*, the fruit fly *Drosophila melanogaster*, zebrafish, rodents, and humans (Dunlap, 1999; Kantermann et al., 2007).

Circadian rhythms are defined as being endogenous, self-sustained, persisting in the absence of any environmental cues (such as the light/dark cycle) and their close approximation to the period of the earth's rotation (Pittendrigh, 1960). For instance, mice kept in constant darkness exhibit sleep/wake and locomotor activity cycles with a periodicity around 23.5 hour. Such rhythms are called free running rhythms, its periodicity defined by the Greek symbol *tau* (τ). Likewise, humans have been demonstrated to maintain a free-running sleep/wake cycle with a periodicity slightly longer than 24 hours (Czeisler et al., 1999; Sack et al., 2000). Circadian rhythms are temperature compensated and will therefore sustain the same period under different temperatures (Izumo et al., 2003). As circadian rhythms have a period of approximately, but not exactly, 24-hours, it is necessary that they are synchronized to the environment. This process is called entrainment and requires external factors, known as *Zeitgebers*, of which light is the most reliable cue (Bell-Pedersen et al., 2005). In its simplest form, a circadian clock can be said to be composed of three components: a central clock (an internal oscillator, generating body time), an input (keeping the clock in phase with environmental cues, notably the light-dark cycle), and an output (coupling the oscillations to biological processes). This basic scheme applies to all known circadian clocks, regardless of the species involved.

The mammalian circadian clock

In mammals, the central clock is located in the suprachiasmatic nucleus (SCN), a small bilateral paired structure of approximately 10.000-20.000 neurons located in the ventral hypothalamus in the brain (Moore & Eichler, 1972; Moore, 1983; Van den Pol, 1980). These neurons are able to generate circadian rhythms in electrical, neuronal, and hormonal activities, which regulate several biological functions and output processes, including circadian patterns in behavioral activity (Lowrey & Takahashi, 2004; Takahashi et al., 2008).

To keep pace with the day/night cycle, the SCN is entrained by light. This process is called photoentrainment and is best illustrated in free-running mammals. Brief light pulses have been shown to phase shift behavioral rhythms and the direction and magnitude of the phase shift depend on the moment of the light pulse within the circadian cycle. For instance, a phase delay occurs when a light pulse is given during the early subjective night, while a phase advance is seen when a light pulse is given during the late subjective night. There is no phase shift when a light pulse is given during the subjective day (Pittendrigh, 1988).

The light information required for photo-entrainment of the mammalian circadian clock, is perceived by the eye and transmitted to the SCN through the retinohypothalamic tract. To this end, the inner nuclear layer of the retina is equipped with a redundant set of photoreceptor cells and pigments, notably the opsin-containing rods and cones and subset of ganglion cells that con-

tain the photopigment melanopsin and project specifically to the SCN (Berson et al., 2002; Gooley et al., 2001; Hattar et al., 2002; Provencio et al., 2002; Ukai et al., 2007).

The molecular clock

At the cellular level, circadian rhythms are generated by a cell-autonomous molecular oscillator, composed of a series of clock genes and proteins (see Figure 1). The organization of the mammalian circadian oscillator is based on a complex auto-regulatory transcriptional-translation feedback loop (TTFL) mechanism (Brown et al., 2012; Canaple et al., 2006; Hastings et al., 2008; Haydon et al., 2013; Reppert & Weaver, 2002; Rey & Reddy, 2013). The TTFL drives the transcription and translation of the clock genes, which in turn are able to rhythmically repress their own expression with a periodicity of approximately 24-hours (Lowrey & Takahashi, 2004).

The CLOCK and BMAL1 proteins, the positive regulators in the mammalian TTFL, are members of the basic helix loop helix and Period-ARNT-Single-minded (bHLH/PAS) family of transcription factors. Through interactions via their PAS domains, CLOCK and BMAL1 are able to form a heterodimeric complex in the cytoplasm and, upon translocation to the nucleus, drive the transcription of genes that contain E-box enhancer elements in their promoter region (Lowrey & Takahashi, 2004). Among the genes activated by the CLOCK/BMAL1 complex are the negative components of the TTFL, the *Period* (*Per1* and *Per2*) and *Cryptochrome* genes (*Cry1* and *Cry2*). When PER and CRY proteins are synthesized, they are able to form PER/CRY protein complexes in the cytoplasm that shuttle between the cytoplasm and the nucleus (Chaves et al., 2006; Yagita et al., 2002). When the nuclear concentration of PER/CRY complexes is sufficiently high, they inhibit the CLOCK/BMAL1 complex, thereby shutting down transcription of E-box genes, including their own transcription (Griffin et al., 1999; Sato et al., 2006; Shearman et al., 2000). Posttranslational modifications such as ubiquitination and phosphorylation, affect the stability of clock proteins and thereby contribute to period length modulation (Gallego & Virshup, 2007; Harms et al., 2004; Lamia et al., 2009).

The CLOCK/BMAL1 complex also drives the transcription of the two orphan nuclear receptor genes *retinoic acid receptor related orphan receptor α* (*Rorα*) and *nuclear receptor subfamily 1, group D, member 1* (*Nr1d1* or *Rev-erbα*). Both RORα and REV-ERBα are involved in stabilizing the circadian oscillator by driving cyclic expression of *Bmal1*, through binding via the ROR-E elements in its promoter (Lowrey & Takahashi, 2004). RORα is responsible for the transcriptional activation of *Bmal1*, while REV-ERBα represses the transcription of *Bmal1*.

Circadian clocks in peripheral tissues and cells

Initially, the SCN was considered to be the only structure to generate circadian rhythms. Today, however, virtually all tissues and organs throughout the body have been shown to contain a circadian clock (Reppert & Weaver, 2002; Yamazaki et al., 2000). Clocks in non-SCN cells are generally referred to as peripheral clocks and make use of the same set of clock genes and transcriptional-translation feedback loop mechanism (Yagita et al., 2001). The master clock keeps the clocks of individual cells in peripheral tissues synchronized by neural and humoral signals (Takahashi et al., 2008). The phase of the molecular clock in peripheral tissues, however, is 3-9 hours delayed compared to the master clock in the SCN (Field et al., 2000; Lee et al., 2001).

In vivo, the clocks of the peripheral tissues are kept synchronized by hormonal stimuli from the SCN in normal conditions. In experiments in which mice were provided with food only during the light period, during which they normally do not eat (time restricted feeding), the phase of the peripheral clocks was dissociated from the central clock. In the liver, restricted feeding can thus result in complete phase reversal of hepatic expression of many genes, including core clock and clock controlled genes such as *Bmal1, Rev-erbα, Per2* and *Dbp* (Damiola et al., 2000, Hara et al., 2001, Stokkan et al., 2001).

When cells are taken out of the body and are kept in culture, they retain their ability to exhibit circadian oscillations. Immortalized rat fibroblast cultures showed rhythmic expression of
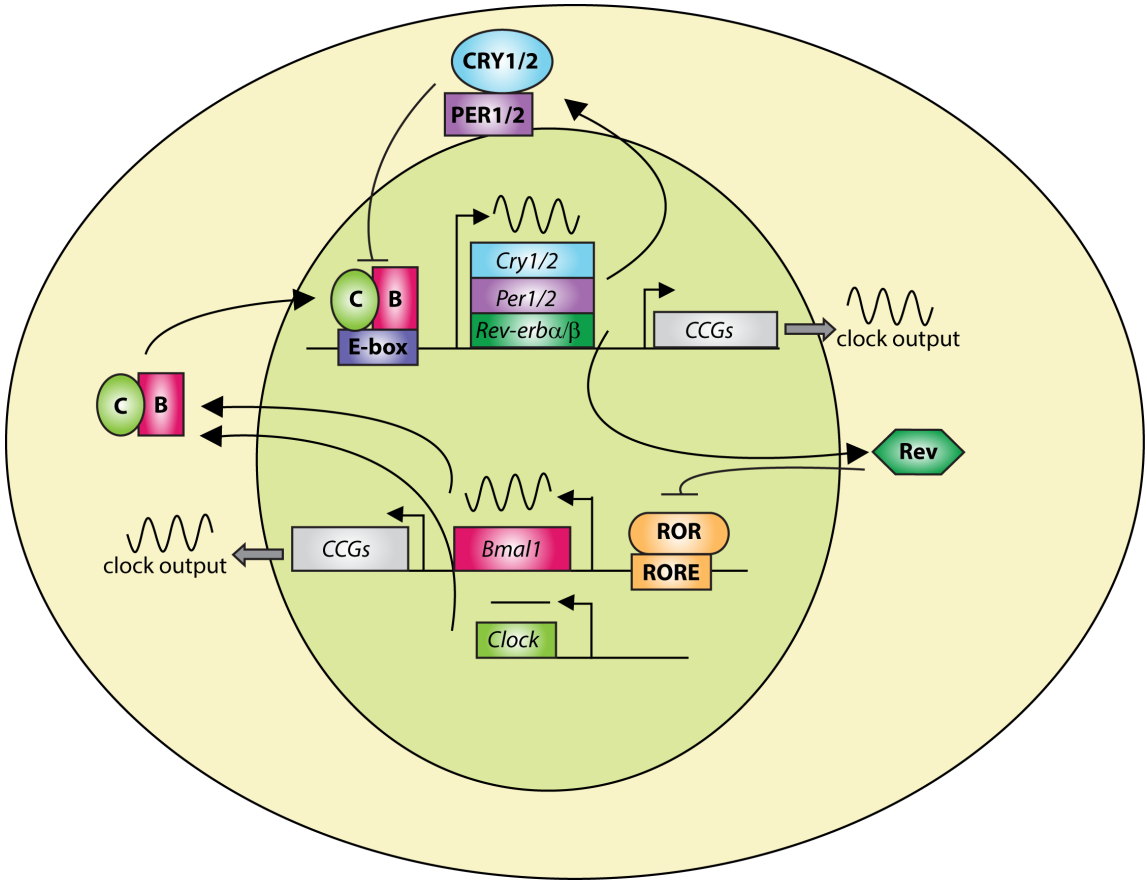
Figure 1: The mammalian circadian oscillator. Simplified scheme showing the mammalian circadian oscillator, composed of a negative feedback loop and one auxiliary feedback loop. Key elements in this model include CLOCK/BMAL1 drive expression of the *Cry* and *Per* genes through E-box elements in their promoters and subsequent inhibition of CLOCK/BMAL1 driven expression by CRY/PER complexes. This system is stabilized by REV-ERBα/β driven cyclic expression of the *Bmal1* gene. This molecular oscillator is coupled to output processes through a series of E-box or RORE promoter element containing clock-controlled genes (CCGs). [Reprinted with permission from Elsevier, Destici et al., 2009]

the core clock genes not only after serum stimulation resembling hormonal cues from the SCN, but also after forskolin and corticosteroid treatment (Balsalobre et al., 2000; Yagita et al., 2000; Yamazaki et al., 2000). After these treatments, several signal transduction pathways, such as the mitogen-activated protein kinase (MAPK) cascade pathway and cAMP are activated. These transduction pathways are able to reset the circadian oscillation and thus synchronize expression of the core clock genes in a similar manner as in the SCN neurons upon treatment of animals with a clock-resetting light pulse (Akashi & Nishida, 2000; Balsalobre et al., 2000).

Clock-controlled genes

The main function of the circadian system is to drive daily rhythms in behavior, physiology and metabolism, which requires that the molecular oscillator is coupled to clock output processes. Indeed, in addition to the core clock genes, expression patterns of several other genes and proteins show a 24-hour rhythm.. The circadian core oscillator regulates the transcription of these clock controlled genes (CCGs) via clock regulatory elements, i.e. E-box, D-Box and REV-ERB responsive (RORE) elements (Reppert & Weaver, 2002; Ueda et al., 2005). Amongst these CCGs are transcription factor encoding genes, which further add to the complexity and dynamics of circadian gene expression by rhythmically driving output genes with a phase different from that obtained with aforementioned promoter elements alone (Kumaki et al., 2008; Ueda et al., 2002). In rodents, approximately 8-10% of the SCN and peripheral tissue transcriptome is under circadian control (Hughes et al., 2009; Miller et al., 2007; Panda et al., 2002; Storch et al., 2002; Ueda et al., 2002). The genes that oscillate vary from tissue to tissue, possibly reflecting the specific requirements for each tissue (Lamia et al., 2008; Storch et al., 2007). An important example of CCG's is the group of the Basic Leucin Zipper (PARbZip) family of transcription factors, which is highly conserved in all organisms (Gachon et al., 2006). Members of this family, the albumin D-element binding protein (DBP), hepatic leukemia factor (HLF) and thyrotroph embryonic factor (TEF), are rhythmically expressed in the liver, kidney lungs and brain and are known to drive rhythmic expression of various enzymes in the liver (Reppert & Weaver, 2002; Ripperger et al., 2000), among which several P450 enzymes (Lavery et al., 1999).

Liver metabolism and the circadian clock

The liver is a major organ involved in metabolism. A large number of the oscillating clock controlled genes in the liver are involved in physiological and metabolic processes (Asher et al., 2011), many of which are nuclear receptors that work as transcriptional regulators capable of binding hormones and sensing concentrations of metabolites including lipids, oxysterols, heme and bile acids, linking the clock machinery to metabolic pathways (Yang et al., 2006) (reviewed in detail by Mazzoccoli et al., 2012). In turn, ligand binding to nuclear receptors regulates the recruitment of co-activators and -repressors, which modulates their transcriptional activity and thus plays an important role in the control of glucose, lipid and mitochondrial oxidative metabolism (Finck et al., 2006).

Various enzymes in the endoplasmic reticulum membrane are involved in metabolism and xenobiotic detoxification and some of these enzymes have been shown to play a role in many human metabolic diseases such as obesity, insulin resistance, diabetes type 2 and atherosclerosis (Hummasti et al., 2010). A critical role in the pathogenesis of chronic metabolic diseases is played by the crosstalk between the core clock machinery, nutrient sensors such as PPARs (peroxisome proliferator-activated receptors, involved in glucose and lipid metabolism), FXR (farnesoid X receptor, involved in bile acid binding), and LXR (liver X receptor, involved in cholesterol homeostasis and lipoprotein secretion) (Yang et al., 2006), and pathogen-sensing systems (Yamamura et al., 2010).

The clock machinery orchestrates the expression of enzymes involved in cyclic production of ligands for nuclear receptors; in turn these receptors regulate the clock machinery through cis-regulatory elements on specific clock genes and thus play a part in the synchronization of

peripheral clocks. For instance, the intracellular NAD+/NADH ratio displays circadian oscillation (Nakahata et al., 2009; Ramsey et al., 2010) ultimately dependent on the presence of BMAL1/CLOCK. The levels of NAD^+ determine the activity of the energy sensor SIRT1 (NAD^+-dependent deacetylase sirtuin-1), which deacetylates PER2 and BMAL1 (Asher et al., 2008; Nakahata et al., 2008) and also LXR (Li et al., 2007) and FXR (Kemper et al., 2009), raising the possibility that the latter two are regulated through a post-translational mechanism (Yang et al., 2010).

PPARs are key players in fatty acid metabolism and function as transcriptional regulators that sense and respond to circulating fatty acids and their metabolites. PPARα and PPARγ are under circadian control, but have also been shown to modulate transcription of core clock genes. PPARα controls the expression of genes involved in peroxisomal and mitochondrial fatty acid beta-oxidation and regulates transcription of genes involved in lipid, cholesterol and glucose uptake and metabolism upon binding to fatty acids (Gachon et al., 2011). Transcription of *Pparα* is induced by CLOCK and BMAL1 (Canaple et al., 2006) and repressed by PER2 and CRY1 (Hayashida et al., 2010). *PPARγ* is a regulator of adipogenesis and fat storage. It modulates genes involved in lipogenesis and storage of triglycerides, and regulates insulin sensitivity (Takahashi et al., 2010). Transcription and recruitment to target promoters are inhibited by PER2 (Grimaldi et al., 2010) and E4BP4 (Takahashi et al., 2010), and a reciprocal positive regulation has been shown for *Pparγ* and *Bmal1* (Canaple et al., 2006). Both *Pparα* and *Pparγ* are positively regulated by clock controlled members of the PARbZIP family of transcription factors, including DBP, HFL and TEF (Takahashi et al., 2010).

Another group of core clock genes which have been demonstrated in several studies to have direct influence on both lipid and bile acid metabolism are *Rev-erbα* and *β*. *Rev-erbα* expression is induced by the CLOCK-BMAL1 heterodimer and its gene product modulates normal physiology by controlling rhythmic regulation of bile acid production via SHP and E4BP4. Likewise, REV-ERBα influences lipid metabolism by driving circadian rhythmicity in epigenetic changes, chromatin remodeling and histone modifications of transcription factors (Sun et al., 2011). The latter is exemplified by circadian recruitment of constitutively expressed HDAC3 to promoter regions in the mouse liver, which is in phase with *Rev-erbα* expression. Histone acetylation at genes regulating lipid homeostasis is inversely related to HDAC3 colocalization with REV-ERBα. Deletion of either protein or misalignment of the recruitment rhythm with fasting/feeding cycles causes perturbations in normal metabolic function and leads to hepatic steatosis (Feng et al., 2011). The core clock genes *Bmal1* and *Clock* are direct target genes of both REV-ERBs (Crumbley & Burris, 2011; Preitner et al., 2002). REV-ERBα is also involved in the regulation of bile acid synthesis, including expression of P450 cytochrome CYP7a1 and sterol response element binding protein (SREBF1) (Duez et al., 2008; Le Martelot et al., 2009). The latter two are suppressed when mice are treated with synthetic REV-ERB agonists (Solt et al., 2012) and dual depletion of *Rev-erbα* and β genes disrupts both circadian expression of core clock and lipid homeostatic gene networks (Cho et al., 2012). In accordance with this, enzymes involved in the glycolytic pathway and beta-oxidation of fatty acids were elevated upon treatment with REB-ERB agonists and enzymes involved in lipogenesis and cholesterologenesis were decreased, making REV-ERBs interesting targets for studying and treating various metabolic disorders (Solt et al., 2012).

Cholesterol and bile acid metabolism and homeostasis are biological mechanisms in which various nuclear receptors, transcription factors and transporters are involved, many of which are under circadian control (Ma et al., 2009). Bile acid metabolism is a major mechanism for elimination of cholesterol *in vivo*. Cholesterol has been identified as a ligand in the binding pocket of RORα. Changes in intracellular levels of cholesterol and its derivatives may modulate its transcriptional activity, suggesting a role for RORα in the regulation of cholesterol homeostasis (Wang et al., 2010). The nuclear receptors FXR and SHR, mainly involved in controlling bile acid homeostasis, are under circadian control and thus form a hinge between key mechanisms of metabolism and circadian rhythmicity (Bookout et al., 2006, Yang et al., 2006). FXR responds to elevated bile acid levels by inducing expression of SHP, which is a potent co-repressor of the rate limiting enzyme in bile biosynthesis CYP7a1 (Lu et al., 2000, Goodwin et al., 2000, Moore et al., 2002). The *Cyp7a1* gene shows a distinct circadian oscillation under the control of DBP (Wuarin

et al., 1992; Lavery & Schibler, 1993) and *Rev-erbα* (Duez et al., 2008). Consistently, bile flow and biliary secretion of bile acids, cholesterol and phospholipids exhibit daily rhythms that are in accordance with the *Cyp7a1* rhythms (Nakano et al., 1990). Disruption of this coordinately regulated pathway can result in the accumulation of bile acids in the liver, a condition known as hepatic cholestasis (Alvarez et al., 2004, De Vree et al., 1998), eventually leading to liver cell necrosis (Woolbright & Jaeschke, 2012).

The FXR-SHP pathway controls several other genes involved in bile acid synthesis (e.g. *Cyp8b1* and *Cyp27*), basolateral bile acid uptake by NTCP, which has also been shown to be under direct control of DBP (Ma et al., 2009), and apical bile acid export by BSEP (Kalaany et al., 2005). These and many other bile acid transporters which may or may not be under circadian control, have been linked to drug induced cholestasis (Wagner et al., 2009), of which posttranslational mechanisms such as localization of the transporters may be affected by immediate cholestatic effects, where the long-term maintenance of cholestasis is likely due to disruption of transcriptional mechanisms (Trauner et al., 1999).

Xenobiotic metabolism and the circadian clock

Touching upon these many genes, regulators and pathways involved in liver homeostasis that are also intertwined with the core clock machinery and clock regulated genes, it is not very surprising that various aspects of xenobiotic metabolism, a major hepatic function, are dependent on the phase of the clock as well. In mammals, the xenobiotic defense system can be divided into three functionally separate groups, referred to as phase I, II and III enzymes.

Phase I enzymes are mainly microsomal CYPs with oxidative, reductive and hydrolytic function adding a functional group (e.g. OH, SH or NH_2) to the substrate, but also alcohol and aldehyde dehydrogenases and paraoxonases (Zhang et al., 2009). All CYPs require heme as a prosthetic group. Heme is also an endogenous ligand for REV-ERBα (Raghuram et al., 2007; Yin et al., 2007) and is reciprocally regulated by the circadian clock via the CLOCK paralogue NPAS2 and PER2, and the rate-limiting heme biosynthesis enzyme aminolevulinate synthase 1 (ALAS1) (Kaasik & Lee, 2004). CYP activity is also regulated by P450 oxidoreductase (POR) expression, which is a membrane-bound enzyme required for electron transfer to CYPs (Gutierrez et al., 2003). Both ALAS1 and POR are regulated by the constitutive androstane receptor (CAR), a direct target of the clock-controlled PARbZIP factors DBP, HLF and TEF (Gachon et al., 2006). Moreover, some CYPs are additionally regulated by core circadian clock genes directly (Matsunaga et al., 2008). In general, phase I enzymes show the highest levels of expression and/or activity at times when animals are feeding and likely to encounter xenobiotics, i.e. during the night in mice (Zhang et al., 2009).

Phase II consists of conjugating enzymes, comprising sulfotransferases (SULT), UDP-glucuronotransferases (UGT), NAD(P)H:quinine oxidoreductases (NQO), epoxide hydrolases (EPH), glutathione-S-transferases (GSH), and N-acetyltransferases (NAT) (Xu et al., 2005). These enzymes contribute to the conversion of lipophilic compounds to hydrophilic forms, to render them soluble enough for secretion from the liver in bile by transporters in the phase III group (Claudel et al., 2007; Xu et al., 2005). Most phase II enzymes show diurnal variation, but their pattern is not the same for the entire group; in mice, glutathione conjugation is mainly active during the early light phase, followed by glucuronidation in the late light phase and sulfation in the early dark phase (Zhang et al., 2009; Zmrzljak & Rozman, 2012).

Phase III is represented by transport proteins, like multidrug-associated proteins (MRPs) or P-glycoproteins (P-gp), which serve as barriers to limit the penetration of xenobiotics. They are involved in both import and export of compounds. On the basolateral or sinusoidal membrane, key transporters are the Na^+-taurocholate cotransporter polypeptide (NTCP or SLC10A1, major bile salt uptake transporter), organic anion transporting polypeptides (OATPs, involved in uptake of unconjugated bile salts, estrogen-conjugates and xenobiotics) and the organic cation transporter 1 (OCT1 or SLC22A1), but also conjugate export pumps (MRP1 and 3). The canalicular membrane houses many export pumps, such as multidrug resistance protein 2 (MRP2), multidrug

export pump (MDR1), breast cancer resistance protein (BCRP), multidrug and toxin extrusion 1 (MATE1) and the bile salt export pump (BSEP or ABCB11) (Koepsell, 2004; Meier et al., 1997; reviewed in Zmrzljak & Rozman, 2012). Many of the transporters on the sinusoidal and canalicular membranes of the mouse liver show circadian oscillations (Akhtar et al., 2002; Miller et al., 2007; Panda et al., 2002; Storch et al., 2002; reviewed by Zhang et al., 2009).

Aryl hydrocarbon receptor dependent metabolism

A well-studied xenobiotic receptor system is the aryl hydrocarbon receptor (AHR), which forms a complex with the AHR nuclear translocator (ARNT). These proteins are critical components of the xenobiotic detoxification system, in which the nuclear receptor pregnane X receptor (PXR), CAR and PPARα, various P450-enzymes and heme-synthesizing enzymes also play a major role (Anderson et al., 2013; Claudel et al., 2007; Mazzoccoli et al., 2012; Shimba & Watabe, 2009). Under normal conditions, AHR resides in the cytoplasm bound to heat shock proteins, but binding to hydrophobic ligands that enter the cell through the membrane induces conformational changes causing translocation to the nucleus and its association with ARNT. In the nucleus, AHR-ARNT heterodimers induce transcriptional activation of xenobiotic metabolism pathways by binding to promoter regions of xenobiotic response elements (XREs), also called dioxin response elements (DREs) (Mimura & Fuji-Kuriyama, 2003). As a negative feedback, AHR is transported back to the cytoplasm and degraded by the proteasome-ubiquitin system (Stejskalova et al., 2011), and induces its own repressor (Zudaire et al., 2008).

Because AHR is conserved in vertebrates and invertebrates, it is suggested that it has played an essential function through evolution (Shimba & Watabe, 2009). AHR-ARNT complexes have been demonstrated to modulate reproductive, cardiovascular, metabolic, developmental, central nervous system and immunological functions (Zmrzljak & Rozman, 2012). Organisms encounter both endogenous and exogenous ligands capable of binding AHR on a daily basis. Endogenous ligands are represented by endogenously synthesized chemicals such as indigoids, equilenin, arachidonic acid metabolites, heme metabolites and tryptophan metabolites. Exogenous natural compounds capable of AHR are mainly encountered as dietary chemicals such as polyphenols, flavonoids, carotenoids and berberine (Zmrzljak & Rozman, 2012). AHR can also be translocated to the nucleus independent of ligand binding by cAMP, a core component of the circadian pacemaker, driving signaling which is significantly different from that induced by exogenous ligands (Oesch-Bartlomowicz & Oesch, 2009). It is suggested that cAMP-mediated transcription is the evolutionary derived primary endogenous regulator of AHR. Disrupting cAMP-mediated AHR signaling is thus considered to play a major role in the mechanisms of toxicity represented by environmental pollutants and toxic compounds (Oesch-Bartlomowicz et al., 2005). Another endogenous ligand, the tryptophan photoproduct 6-formylindolo[3,2-b]carbazole (FICZ) is capable of influencing the circadian expression of clock genes by blocking the glutamate pathway and regulates the light-dependent circadian rhythm through AHR signaling activation (Mukai & Tischkau, 2007; Rannug & Fritsche, 2006). Exogenous ligands capable of binding and translocating AHR are represented by various polycyclic aromatic hydrocarbons (PAHs), of which benzo[a]pyrene (B[a]P) has been studied the most, halogenated dioxins, polychlorinated biphenyls and other compounds such as 2,3,7,8-tetrachlorodibenzo-p-dioxin (TCDD).

Many promutagens are inactive as mutagens prior to biotransformation by phase I enzymes, but oxidative metabolites can form DNA adducts, leading to toxicity and/or ultimately triggering mutagenesis and carcinogenesis. Additionally, B[a]P and TCDD induce cAMP, leading to increased levels of Ca^{2+} and activity of the Ca^{2+}/calmodulin dependent kinase pathway that are normally modulated by melatonin, one of the principal humoral outputs for the circadian timing system. Together, this leads to increased and prolonged effects of their toxic properties (Dai et al., 2002; Mayati et al., 2012; Monteiro et al., 2008). Mice treated with TCDD and dioxin show altered behavioral circadian rhythmicity and gene expression, and reduced responsiveness of the circadian clock to changes in light/dark regimes, thus showing that xenobiotics are able to interfere with proper working of the clock machinery via activation of the AHR pathway (Garrett & Gasiewicz,

2006; Hogenesch et al., 1997; Mukai et al., 2008; Xu et al., 2010), disrupting CLOCK-BMAL1 transcriptional activity and thereby repressing and deregulating *Per1* gene expression (Xu et al., 2010; Qu et al., 2009). Although dimerization studies have demonstrated that AHR does not interact with many core clock protein complexes directly, shared co-mediators provide multiple interaction platforms allowing for altered influence on transcriptional machinery (reviewed in Anderson et al., 2013). PER1 and PER2 have opposite impact on the regulation of xenobiotic responses in the liver; PER1 is functioning as an inhibitory factor, whereas PER2 acts as a positive regulator in the AHR-mediated and ligand binding-dependent activation of AHR-signaling (Qu et al., 2009). Studies performed with liver explants and cells from *Per2::luciferase* mice have demonstrated that activation of AHR does not cause direct changes in core clock gene expression, but the phase of the circadian clock does influence the transcriptional activity of P450 enzymes (Pendergast & Yamazaki, 2012; chapter 2, chapter 3, chapter 5).

AHR signaling and circadian pathways are closely engaged in the pathophysiological basis of metabolic, immune-related and neoplastic diseases (Zmrzljak & Rozman, 2012). For instance, there is evidence underlying the crosstalk between AHR activation, PPARα signaling and altered clock machinery in the development of type 2 diabetes related to toxic exposure by altering glucose metabolism (Wang et al., 2011). Also, epidemiological studies have found links between shift work and many forms of cancer, particularly those that have a strong link to AHR-mediated toxicity including prostate, colorectal and lung cancer, and non-Hodgkin lymphoma. Activation or deregulation of AHR has been associated with development of lymphomas and leukemia in mice and man (reviewed by Anderson et al., 2013). There is countless evidence for a link between cancer development and exposure to B[a]P and other PAHs (Krawczak & Cooper, 1998).

DNA damage and the circadian clock

Our DNA is continuously exposed to physical and chemical genotoxic compounds of exogenous and endogenous origin (e.g. ultraviolet light, ionizing radiation, chemical pollutants, reactive byproducts of metabolism) which can damage our genome. When not repaired in time, lesions can block transcription and (depending on the DNA damage level) cause the cell to undergo apoptosis. On the other hand, replication of damaged DNA can give rise to mutations, ultimately leading to induction of cancer (Hoeijmakers, 2001). To counteract the deleterious effects of exposure to genotoxic agents, cells have evolved an intricate network of DNA damage repair pathways wilt (partially) overlapping substrate specificity. One such repair pathway is Nucleotide Excision Repair, a multi-step cut and patch mechanism involving some 30 proteins (Hoeijmakers, 2001). Interestingly, one of the key NER factors, XPA (involved in damage recognition/verification), has been reported to be under circadian control, as evident from its rhythmic expression pattern in liver and brain (Kang et al., 2009). The XPA gene exhibits two E-box elements in its promoter region, allowing transcription activation by CLOCK/BMAL, and as such is considered a CCG (Kang et al., 2009; Sancar et al., 2010). In line with the circadian expression pattern of XPA, repair of cisplatin induced DNA lesions in the liver has been shown to fluctuate over the day (Kang et al., 2010).

The connection between the core clock and DNA damage appears bidirectional. It has been shown that DNA damage can reset the mammalian circadian clock in a time dependent manner (Oklejewicz et al., 2008). In this study, clock synchronized rat fibroblasts were treated with a single dose of γ-radiation at a defined moment of the day, after which circadian phase and dose dependent phase advance of circadian rhythms was observed. This phase advance was reduced after treatment of cells with ATM inhibitors, suggesting that resetting of the circadian clock by γ-radiation might depend on ATM (Oklejewicz et al., 2008). Likewise, DNA damage induced by UV, oxidative stress and methyl methane sulfonate (MMS) was shown to induce a phase advance the circadian clock (Gamsby et al., 2009; Oklejewicz et al., 2008).

Chronotoxicity

Considering the tight link between the circadian clock and cellular metabolism, including

xenobiotic metabolism and DNA damage repair, it may not come as a surprise that the (geno) toxic effect of chemical agents may depend on the time-of-day of exposure. This phenomenon is referred to as chronotoxicity and is well illustrated by animal exposure studies with the genotoxic agent cyclophosphamide, a chemotherapeutic and immunosuppressive agent that is widely used for treatment of several types of cancer, blood and bone marrow transplantations and autoimmune disorders. Cyclophosphamide is a prodrug that requires metabolic activation by several cytochrome P450 enzymes (Gurtoo et al., 1981). Interestingly, as illustrated by animal exposure studies, cyclophosphamide sensitivity is greatly dependent on the time of drug administration. (Gorbacheva et al., 2005). Mice treated with cyclophosphamide for 3 consecutive days at the beginning of the night were shown to be more tolerant to cyclophosphamide than animals treated at the beginning of the day. Likewise, other rodent studies revealed for more than 30 anti-cancer drugs (e.g. doxorubicin, 5-fluorourcil, celecoxib) that the animals tolerance to the drug depends on the time of administration (Blumenthal et al., 2001; Gorbacheva et al., 2005; Granda et al 2001; Ohdo, 2007).

The chronotoxic properties of compounds can be very useful when treating cancer with chemotherapeutic or other anti-cancer agents (Innominato et al., 2010; Lévi & Okyar, 2011; Levi & Schibler, 2007). Such drugs usually damage both malignant and (proliferating) healthy cells, the latter resulting in severe side effects such as nausea, vomiting, anemia and hair loss (Carey & Burish, 1988; Kondratov et al., 2007). Chronomodulated therapy or chronotherapy involves protocols in which chemotherapeutic agents are given at a specific moment of the day in order to minimize the side effects and cause damage predominantly to the malignant cells. As such, chronotherapy can either be used to maximize efficacy, to minimize unwanted side effects or improve drug tolerance (Griffett & Burris, 2013; Kondratov et al., 2007; Lévi & Okyar, 2011).

The circadian clock and *in vitro* alternatives for hepatotoxic risk assessment

By law, our society demands chemical compounds to be assessed for their potential to elicit (hepato)toxic and carcinogenic effects. To this end, a battery of routinely performed *in vitro* tests (e.g. measurement of mutations, DNA damage, chromosomal changes) are available to determine the toxicity of the agent (Kirkland et al., 2007; Thybaud et al., 2007). Yet, as such assays are not always conclusive and many compounds are identified as false positive or negative in at least one of these tests, *in vivo* rodent studies are necessary in order to identify and correctly classify compounds (Kirkland et al., 2007). Apart from the high costs of animal experiments, society wants us to obey the 3R's principle, refinement, replacement and reduction of laboratory animals (Liebsch et al., 2011).

To decrease and ultimately replace the number of laboratory animals used, many *ex vivo* and *in vitro* alternatives have been and are being investigated; the liver is a major organ involved in compound metabolism and therefore often at the center of these alternative assays (reviewed in Guillouzo, 1998 and Soldatow et al., 2013). Several *in vitro* models (e.g. stable cell lines, 3D tissue models) are available and frequently used to determine the (geno)toxic properties of compounds (Kirkland et al., 2007; Liebsch et al., 2011). Nowadays, a popular approach to predict the (geno)toxic and (non)carcinogenic properties of compounds *in vitro* include proteomic and transcriptomic profiling methods to establish predictive risk marker profiles (Liebsch et al., 2011). However, in such risk assessment assays, including toxicogenomics studies, the circadian clock is usually not taken into account. Yet, the circadian clock can be predicted to prominently influence the outcome of *in vivo* and *in vitro* transcriptomics studies (and as such the comparison of *in vivo* and *in vitro* data) in multiple ways.

First, as xenobiotic metabolism, DNA repair and various other toxicity related processes are subject to circadian variation, the toxic response of the liver upon *in vivo* exposure to chemical compounds may depend on the time of day of exposure. Accordingly, it can be predicted that the response of the transcriptome may also depend on circadian phase of the liver at the moment of treatment. Indeed, in a first study addressing this issue, we uncovered pronounced day-night differences in the number and category of differentially expressed genes after exposure of mice

to cyclophosphamide during the day or night (Nijman et al. unpublished data). Accordingly, when interpreting (published) *in vivo* exposure studies, it is important to take into account at which time of the day animals have been exposed. With respect to the latter, it is also important to note that many rodent toxicity studies have been performed during the day, which corresponds to the inactive phase (sleep) of the animal.

Second, comparison of *in vivo* and *in vitro* exposure studies are hampered by the fact that (as discussed above) intracellular circadian clocks of cultured cells tend to desynchronize in the absence of clock resetting signals from the master clock in the SCN because of small variations in period length, for instance due to interactions between the core clock machinery and machinery involved in metabolism. Therefore, at the population level the average expression level of oscillating clock controlled genes in cultured cells may be flat, even though there are large intercellular variations between gene or protein expression level. As a consequence, *in vivo/ in vitro* differences in gene expression levels will occur. Moreover, in a series of experiments in which we compared clock-synchronized and non-synchronized cultures, we demonstrated that in the absence of a synchronizing stimulus such as glucocorticoids (e.g. dexamethasone), cell cultures can still be partially synchronous (De Wit and Chaves, unpublished data). Indeed, culture conditions such as (but not limited to) replacing the medium (containing serum-derived clock resetting factors), changes in temperature, glucose availability during long-term culturing, can temporarily reset the circadian clock. This implicates that, in the classic experimental setup, cultures are often synchronized to some extent but the phase is unknown, making inter-experimental comparison unreliable, especially when experiments are conducted by different researchers and/or within different laboratories.

Last but not least, DNA damaging agents are able to reset the circadian clock (Gamsby et al., 2009; Oklejewicz et al., 2008). Since many *in vitro* systems are based on established cell lines and intracellular clocks are usually desynchronized (or partially synchronized with unknown phase) in cell cultures, exposure to DNA damaging agents might synchronize or reset the cellular clocks, and accordingly affect the expression level of core circadian clock genes and thousands of CCGs. Such genes may accidentally be considered as (geno)toxic stress responsive genes. For example, when studying the mRNA expression level of a certain gene after exposure to a genotoxic compound, one may find the expression level of that particular gene to be increased 12-hour after exposure, and return to a lower level 24-hour after exposure (Figure 2A), which might suggest that this gene is a DNA damage responsive gene. However, when a DNA damaging compound is able to reset the circadian clock, it might very well be that the gene of interest is not a DNA damage responsive gene, but rather a CCG and as such should be considered as a false positive gene (Figure 2B).

In vitro chronotoxicity assays

Given the impact of the circadian clock on liver performance (including xenobiotic metabolism and DNA repair), it is crucial that this endogenous time keeper is taken into account when designing and performing toxicity studies. We have previously proposed a new approach for *in vitro* toxicological and toxicogenomics studies, based on the use of clock synchronized cell cultures (Destici et al., 2009). In this approach (outlined in Figure 2C), intracellular clocks are synchronized prior to starting an exposure experiment. To control for clock synchronization, and to facilitate the calculation of the time of exposure, one can make use of primary cells and tissues obtained from mice with a luciferase-based circadian clock reporter gene, or alternatively introduce lentiviral- or plasmid-based clock reporter constructs in established cell lines of choice. Such *in vitro* liver model systems allow real time recording of circadian clock phase. Subsequently, exposure with a chemical compound of interest (e.g. a pollutant, an industrial chemical, a pharmaceutical drug) can be initiated at defined (pre-calculated) phases of the circadian clock. In case the tested chemical compound harbors chronotoxic properties (e.g. through clock controlled metabolism) major differences in gene expression profiles and biological endpoints (e.g. apoptosis, steatosis, cholestasis) can be expected depending on the phase of the clock at the moment of exposure

1

(see Figure 2C).

The advantage of this approach over classical liver derived systems is that it enables us to quantify the genotoxic sensitivity of the cells in relation to circadian clock phase, thereby not only classifying an compound as being chronotoxic, but also providing novel insights on the kinetics and amplitude of (geno)hepatotoxic responses. Moreover, when the magnitude of the toxic response is dependent on circadian clock phase, the output (e.g. gene expression, proteomics, cell death) is likely to be observed at lower compound concentrations and/or shorter treatment periods than in classical toxicological experiment, thereby increasing the sensitivity of the assay. Moreover, the use of synchronized cells also eliminates the risk of non-toxic response related transcriptional changes originating from potential clock-resetting properties of chemical compounds, which will increase the specificity of the assay.

Concluding remarks

It has become evidently clear that the kinetics and dynamics of toxicological responses and side effects of drugs, poisons or toxic substances can be influenced by the circadian clock. Over ten percent of the liver transcriptome displays robust mRNA cycling, which not only well illustrates the impact of the circadian clock on various cellular key processes, but also explains why the sensitivity of tissues to environmental toxicant and drug induced toxicity may depend on the time of exposure cq administration (i.e. circadian clock phase). Accordingly, it is strongly recommended that the circadian clock is implemented in mechanistic research aiming at understanding (hepato)toxic responses elicited by chemical compounds, as well as in efforts to replace animal-based risk assessment assays by validated *in vitro* assays.

Insight in the chronotoxic properties of chemicals will have an important societal impact. In case of toxic industrial chemicals, knowledge on the chronotoxic properties of such compounds will contribute to the improvement of labor hygiene as employees (in addition to wearing protective cloths) can be advised to handle such chemicals only at the time of day when accidental exposure has the least impact on the body. Likewise, information on potential chronotoxic properties of anti-cancer drugs may help to improve therapeutic efficacy and reduce undesired side-effects and as such will improve quality of life of the cancer patient. Rather than conventional drug administration courses in which the blood levels of drugs in patients are kept more or less constant (thereby increasing the total drug burden and contributing to toxic side effects), pharmaceutical companies should focus on intelligent drug delivery systems in which slow-release technology is combined with the patient individual circadian rhythms (Farrow et al., 2012; Lévi & Okyar, 2011).
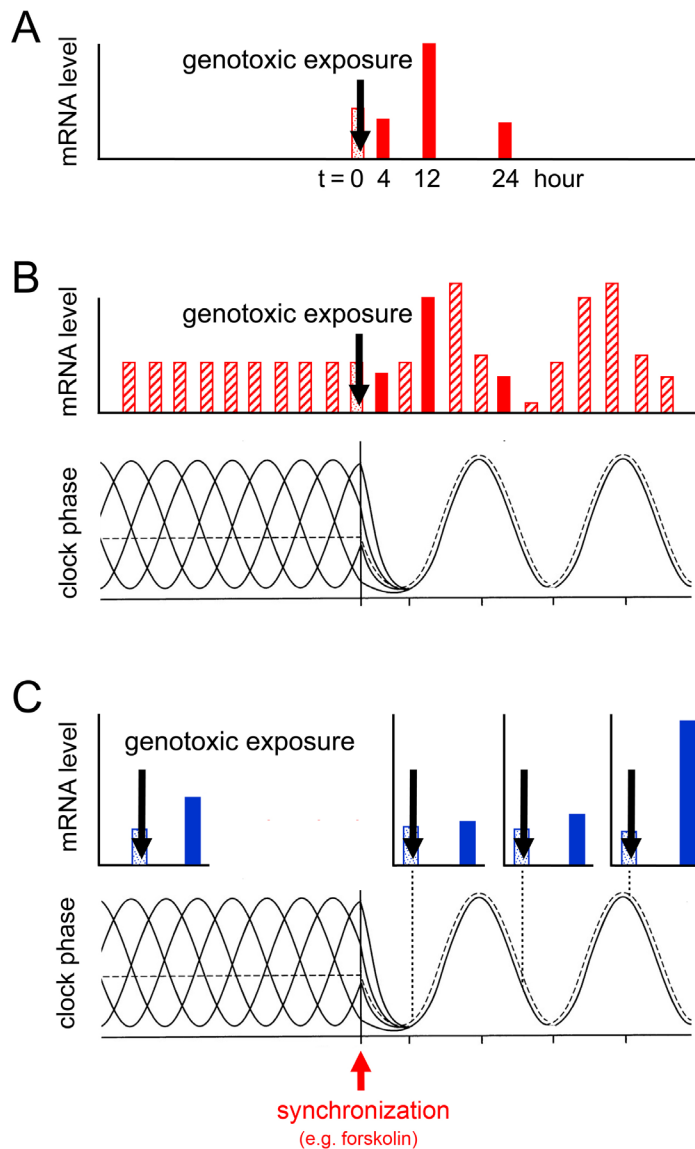
Figure 2: Implications of DNA damage resetting of the circadian clock for *in vitro* genotoxic risk assessment assays. (A) Imaginary *in vitro* experiment for identification of genotoxic stress markers. Cultured cells are exposed to a DNA damaging agent. mRNA profiles are determined at various times after exposure (solid bars) and compared to those obtained from mock-treated cells (not shown) or cells harvested prior to treatment (dashed bars). The data obtained for gene X suggest that this gene is a DNA damage responsive gene. (B) Same experiment as described under A, except that mRNA levels were analyzed at 4 hour intervals (additional data represented by hatched bars). Note that exposure to the DNA damaging agent is synchronizing the individual cellular circadian clocks, and accordingly transcription of clock (output) genes. On the basis of this experiment, gene X is likely a clock controlled output gene. (C) Modified version of the *in vitro* experiment for identification of genotoxic stress markers, in which the circadian clock of the individual cells is synchronized by treatment with forskolin (or another known synchronizing compound) and cells are exposed to the DNA damaging agent at defined phases of the circadian day. Expression profiles are determined 12 hours after treatment (solid bars) and compared to those obtained cells harvested prior to treatment (dashed bars). Note the time-of-day differences in the response of gene Y, indicative for chronotoxic effects of the DNA damaging agent. Also note the stronger response of gene Y in synchronized cells, as compared to non-synchronized cells. [Reprinted with permission from Elsevier, Destici et al., 2009]

1

Scope of this thesis

In vitro assays have been and are being developed in order to test compounds for chemical safety while reducing the number of laboratory animals needed at the same time. These newly developed assays have to be validated against *in vivo* data, obtained in both laboratory animals and humans. As part of the Netherlands Toxicogenomics Centre, several studies including the one described in this thesis, have focused on the development and validation of *ex vivo* and *in vitro* systems derived from mice. Because the liver is the major organ involved in xenobiotics metabolism, many toxicogenomics projects have focused on this organ. We have focused on setting up alternative *in vitro* systems to study liver toxicity. We compared obtained results to experiments performed with liver slices, primary hepatocytes and commercially available liver cell lines, as well as to data from *in vivo* exposure studies performed in mice. All these *in vitro* systems have their own strengths and drawbacks. Liver slices and primary hepatocytes are the most similar to the *in vivo* situation but have limited lifespan and thus require new animals for each experiment. Moreover, both options are relatively expensive, require great skill to obtain material, are prone to large inter-researcher variations and are consequently not suitable for high throughput chemical testing. Slices retain their original architecture but contain other cell types next to hepatocytes and depending on the thickness of the slice, nutrients and oxygen might not be accessible for all interior cells. Primary hepatocytes can be isolated and grown in a monolayer collagen sandwich but undergo extensive temporal changes in gene expression and other hepatocyte specific functions. Immortalized liver cell lines are available unlimitedly but are either derived from hepatocarcinomas or developed by introducing oncogenes. These lines can be grown in various desired structures, many of which improve liver function, but their hepatocyte specific functions are limited and the metabolic competence is often not representative of the *in vivo* situation. Therefore, there is a large demand for a system combining high hepatocyte specific function with unlimited growth and under standard culturing conditions, making it suitable for fast, easy and reproducible chemical testing.

An additional layer of complexity in developing *in vitro* alternatives for chemical testing is the circadian clock. *In vivo*, the moment of exposure has been shown to have large influence on chemical toxicity in rodents and on therapeutical drug efficacy and tolerability in humans. However, *in vitro*, the influence of circadian rhythmicity is not acknowledged while there is ample proof for the intimate relationship between the clock and (xenobiotics) metabolism. Next to 24 hour variations in general and xenobiotic metabolism *in vivo*, in *in vitro* experiments it is important to know if the system retains a functional circadian clock and to what extent individual clocks are synchronized in cell populations. Furthermore, unintended clock synchronizing events can play a major role in *in vitro* assays, leading to larger interexperimental variations and decreasing the predictive value of such systems for *in vivo* toxicity.

In order to overcome *in vivo*-*in vitro* differences in toxicological assays as a result of the circadian clock, we aimed to develop novel *in vitro* assays in which chemical exposure can be performed at defined phases of the circadian clock. In this thesis, we optimized mouse liver slices and mouse primary hepatocytes for long term culturing and used these systems to assess chronotoxicity, i.e. the extent of toxicity depending on the time of exposure, for the environmental carcinogenic pollutant benzo[a]pyrene and the immunosuppressant drug cyclosporine A that causes cholestasis *in vivo* (chapters 2 and 3). In chapter 4 we describe the development of a novel immortalized mouse hepatocyte cell line (SIMH4/SIMH[CLOCK] cells) that combines high hepatocyte specific function with ease of handling, validate that these cells are more similar to primary hepatocytes than other liver cell lines and demonstrate that the system can be used to induce biologically relevant end points for liver injury. We investigate the clock and clock dependent properties of SIMH4/SIMH[CLOCK] cells by performing similar exposure regimes as for primary hepatocytes (chapter 5) and prove that the immortalized hepatocytes retain proper and robust rhythmicity with similar results after chronotoxic exposure as in primary hepatocytes. In chapter 6 we provide experimental proof that a chronotoxic exposure approach increases the specificity and sensitivity of chemical exposure assays, as compared to standard protocols.

References

Akashi, M., & Nishida, E. (2000). Involvement of the MAP kinase cascade in resetting of the mammalian circadian clock. Genes Dev, 14(6), 645–649.

Akhtar, R. A., Reddy, A. B., Maywood, E. S., Clayton, J. D., King, V. M., Smith, A. G., Gant, T. W., et al. (2002). Circadian cycling of the mouse liver transcriptome, as revealed by cDNA microarray, is driven by the suprachiasmatic nucleus. Current biology, 12(7), 540–50.

Alvarez, L., Jara, P., Sánchez-Sabaté, E., Hierro, L., Larrauri, J., Díaz, M. C., Camarena, C., et al. (2004). Reduced hepatic expression of farnesoid X receptor in hereditary cholestasis associated to mutation in ATP8B1. Human molecular genetics, 13(20), 2451–60.

Anderson, G., Beischlag, T. V, Vinciguerra, M., & Mazzoccoli, G. (2013). The circadian clock circuitry and the AHR signaling pathway in physiology and pathology. Biochemical pharmacology.

Asher, G., Gatfield, D., Stratmann, M., Reinke, H., Dibner, C., Kreppel, F., Mostoslavsky, R., et al. (2008). SIRT1 regulates circadian clock gene expression through PER2 deacetylation. Cell, 134(2), 317–28.

Asher, G., & Schibler, U. (2011). Crosstalk between components of circadian and metabolic cycles in mammals. Cell metabolism, 13(2), 125–37.

Balsalobre, A., Marcacci, L., & Schibler, U. (2000). Multiple signaling pathways elicit circadian gene expression in cultured Rat-1 fibroblasts. Current biology, 10(20), 1291–4.

Bell-Pedersen, D., Cassone, V., Earnest, D., Golden, S., Hardin, P., Thomas, T., & Zoran, M. (2005). Circadian rhythms from multile oscillators: lessons from diverse organisms. Nature Reviews Genetics, 6(7), 544–556.

Berson, D. M., Dunn, F. a, & Takao, M. (2002). Phototransduction by retinal ganglion cells that set the circadian clock. Science, 295(5557), 1070–3.

Blumenthal, R. D., Waskewich, C., Goldenberg, D. M., Lew, W., Flefleh, C., & Burton, J. (2001). Chronotherapy and Chronotoxicity of the Cyclooxygenase-2 Inhibitor , Celecoxib , in Athymic Mice Bearing Human Breast Cancer Xenografts Chronotherapy and Chronotoxicity of the Cyclooxygenase-2 Inhibitor , Celecoxib , in Athymic Mice Bearing Human Breast C. Clinical Cancer Research, 7, 3178–3185.

Bookout, A., Jeong, Y., Downes, M., Yu, R. T., Evans, R. M., & Mangelsdorf, D. J. (2006). Anatomical profiling of nuclear receptor expression reveals a hierarchical transcriptional network. Cell, 126(4), 789–99.

Brown, S. a, Kowalska, E., & Dallmann, R. (2012). (Re)inventing the circadian feedback loop. Developmental cell, 22(3), 477–87.

Canaple, L., Rambaud, J., Dkhissi-Benyahya, O., Rayet, B., Tan, N. S., Michalik, L., Delaunay, F., et al. (2006). Reciprocal regulation of brain and muscle Arnt-like protein 1 and peroxisome proliferator-activated receptor alpha defines a novel positive feedback loop in the rodent liver circadian clock. Molecular endocrinology, 20(8), 1715–27.

Carey, M. P., & Burish, T. G. (1988). Etiology and treatment of the phychological side effects associated with cander chemotherapy: A critical review and discussion. Phychological Bulletin, 104(3), 307–325.

Chaves, I., Yagita, K., Barnhoorn, S., Horst, G. T. J. Van Der, & Tamanini, F. (2006). Functional Evolution of the Photolyase / Cryptochrome Protein Family: Importance of the C Terminus of Mammalian CRY1 for Circadian Core Oscillator Performance. Molecular and Cellular Biology, 26(5), 1743–1753.

1

Cho, H., Zhao, X., Hatori, M., Yu, R. T., Barish, G. D., Lam, M. T., Chong, L.-W., et al. (2012). Regulation of circadian behaviour and metabolism by REV-ERB-α and REV-ERB-β. Nature, 485(7396), 123–7.

Claudel, T., Cretenet, G., Saumet, A., & Gachon, F. (2007). Crosstalk between xenobiotics metabolism and circadian clock. FEBS letters, 581(19), 3626–33.

Crumbley, C., & Burris, T. P. (2011). Direct regulation of CLOCK expression by REV-ERB. PloS one, 6(3), e17290.

Czeisler, C. A., Duffy, J. F., Shanahan, T. L., Brown, E. N., Mitchell, J. F., Rimmer, D. W., Ronda, J. M., et al. (1999). Stability, Precision, and Near-24-Hour Period of the Human Circadian Pacemaker. Science, 284(5423), 2177–2181.

Dai, J., Inscho, E., Yuan, L., & Hill, S. (2002). Modulation of intracellular calcium and calmodulin by melatonin in MCF-7 human breast cancer cells. J Pineal Res, 32(2), 112–119.

Damiola, F., Le Minh, N., Preitner, N., Kornmann, B., Fleury-Olela, F., & Schibler, U. (2000). Restricted feeding uncouples circadian oscillators in peripheral tissues from the central pacemaker in the suprachiasmatic nucleus. Genes & Development, 14(23), 2950–2961.

De Vree, J. M., Jacquemin, E., Sturm, E., Cresteil, D., Bosma, P. J., Aten, J., Deleuze, J. F., et al. (1998). Mutations in the MDR3 gene cause progressive familial intrahepatic cholestasis. Proceedings of the National Academy of Sciences of the United States of America, 95(1), 282–7.

Destici, E., Oklejewicz, M., Nijman, R., Tamanini, F., & Van der Horst, G. T. J. (2009). Impact of the circadian clock on in vitro genotoxic risk assessment assays. Mutation research, 680(1-2), 87–94.

Duez, H., Van der Veen, J. N., Duhem, C., Pourcet, B., Touvier, T., Fontaine, C., Derudas, B., et al. (2008). Regulation of bile acid synthesis by the nuclear receptor Rev-erbalpha. Gastroenterology, 135(2), 689–98.

Dunlap, J. C. (1999). Molecular Bases for Circadian Clocks. Cell, 96, 271–290.

Edery, I. (2000). Circadian rhythms in a nutshell. Physiological genomics, 3(2), 59–74.

Farrow, S. N., Solari, R., & Willson, T. M. (2012). The importance of chronobiology to drug discovery. Expert opinion on drug discovery, 7(7), 535–41.

Feng, D., Liu, T., Sun, Z., Bugge, A., Mullican, S. E., Alenghat, T., Liu, X. S., et al. (2011). A circadian rhythm orchestrated by histone deacetylase 3 controls hepatic lipid metabolism. Science, 331(6022), 1315–9.

Field, M. D., Maywood, E. S., O'Brien, J. A., Weaver, D. R., Reppert, S. M., & Hastings, M. H. (2000). Analysis of clock proteins in mouse SCN demonstrates phylogenetic divergence of the circadian clockwork and resetting mechanisms. Neuron, 25(2), 437–447.

Finck, B. N., & Kelly, D. P. (2006). Review series PGC-1 coactivators : inducible regulators of energy metabolism in health and disease. The Journal of Clinical Investigation, 116(3), 615–622.

Gachon, F., Leuenberger, N., Claudel, T., Gos, P., Jouffe, C., Fleury Olela, F., De Mollerat du Jeu, X., et al. (2011). Proline- and acidic amino acid-rich basic leucine zipper proteins modulate peroxisome proliferator-activated receptor alpha (PPARalpha) activity. Proceedings of the National Academy of Sciences of the United States of America, 108(12), 4794–9.

Gachon, F., Olela, F. F., Schaad, O., Descombes, P., & Schibler, U. (2006). The circadian PAR-domain basic leucine zipper transcription factors DBP, TEF, and HLF modulate basal and inducible xenobiotic detoxification. Cell metabolism, 4(1), 25–36.

Gallego, M., & Virshup, D. (2007). Post-translational modifications regulate the ticking of the circadian clock. Nature Reviews Molecular Cell Biology, 8, 139–148.

Gamsby, J. J., Loros, J. J., & Dunlap, J. C. (2009). A phylogenetically conserved DNA damage response resets the circadian clock. Journal of biological rhythms, 24(3), 193–202.

Garrett, R., & Gasiewicz, T. (2006). The aryl hydrocarbon receptor agonist 2,3,7,8-tetrachlorodibenzo-p-dioxin alters the circadian rhythms, quiescence, and expression of clock genes in murine hematopoietic stem and progenitor cells. Mol Pharmacol, 69(6), 2076–83.

Goodwin, B., Jones, S., Price, R., Watson, M., McKee, D., Moore, L., Galardi, C., et al. (2000). A regulatory cascade of the nuclear receptors FXR, SHP-1, and LRH-1 represses bile acid biosynthesis. Molecular cell, 6(3), 517–26.

Gooley, J. J., Lu, J., Chou, T. C., Scammell, T. E., & Saper, C. B. (2001). Melanopsin in cells of origin of the retinohypothalamic tract. Nature neuroscience, 4(12), 1165.

Gorbacheva, V. Y., Kondratov, R. V, Zhang, R., Cherukuri, S., Gudkov, A. V, Takahashi, J. S., & Antoch, M. P. (2005). Circadian sensitivity to the chemotherapeutic agent cyclophosphamide depends on the functional status of the CLOCK/BMAL1 transactivation complex. Proceedings of the National Academy of Sciences of the United States of America, 102(9), 3407–12.

Granda, T. G., Filipski, E., & Attino, R. M. D. (2001). Experimental Chronotherapy of Mouse Mammary Adenocarcinoma MA13 / C with Docetaxel and Doxorubicin as Single Agents and in Combination Experimental Chronotherapy of Mouse Mammary Adenocarcinoma MA13 / C with Docetaxel and Doxorubicin as Single Agents and. Cancer Research, 61, 1996–2001.

Griffett, K., & Burris, T. P. (2013). The mammalian clock and chronopharmacology. Bioorganic & medicinal chemistry letters, 23(7), 1929–34.

Griffin, E. J., Staknis, D., & Weitz, C. (1999). Light-independent role of CRY1 and CRY2 in the mammalian circadian clock. Science, 286(5440), 768–771.

Grimaldi, B., Bellet, M. M., Katada, S., Astarita, G., Hirayama, J., Amin, R. H., Granneman, J. G., et al. (2010). PER2 controls lipid metabolism by direct regulation of PPARγ. Cell metabolism, 12(5), 509–20.

Guillouzo, A. (1998). Liver cell models in in vitro toxicology. Environmental health perspectives, 106 Suppl, 511–32.

Gurtoo, H., Marinello, A., Struck, R., Paul, B., & Dahms, R. (1981). Sudies on the mechanism of denaturation of cytochrome P-450 by cyclophosphamide and its metabolites. J Biol Chem, 256, 11691–11701.

Gutierrez, A., Grunau, A., Paine, M., Munro, A. W., Wolf, C. R., Roberts, G. C. K., & Scrutton, N. S. (2003). Electron transfer in human cytochrome P450 reductase. Biochemical Society Transactions, 31, 497–501.

Hara, R., Wan, K., Wakamatsu, H., Aida, R., Moriya, T., Akiyama, M., & Shibata, S. (2001). Restricted feeding entrains liver clock without participation of the suprachiasmatic nucleus. Genes to cells : devoted to molecular & cellular mechanisms, 6(3), 269–78.

Harms, E., Kivimäe, S., Young, M., & Saez, L. (2004). Posttranscriptional and Posttranslational Regulation of Clock Genes. J Biol Rhythms, 19(5), 361–373.

Hastings, M. H., Maywood, E. S., & O'Neill, J. S. (2008). Cellular circadian pacemaking and the role of cytosolic rhythms. Current biology, 18(17), R805–R815.

1

Hattar, S., Liao, H. W., Takao, M., Berson, D. M., & Yau, K. W. (2002). Melanopsin-containing retinal ganglion cells: architecture, projections, and intrinsic photosensitivity. Science, 295(5557), 1065–70.

Hayashida, S., Kuramoto, Y., Koyanagi, S., Oishi, K., Fujiki, J., Matsunaga, N., Ikeda, E., et al. (2010). Proxisome proliferator-activated receptor-α mediates high-fat, diet-enhanced daily oscillation of plasminogen activator inhibitor-1 activity in mice. Chronobiology international, 27(9-10), 1735–53.

Haydon, M. J., Hearn, T. J., Bell, L. J., Hannah, M. a., & Webb, A. a. R. (2013). Metabolic regulation of circadian clocks. Seminars in Cell & Developmental Biology, 24(5), 414–421.

Hoeijmakers, J. H. J. (2001). Genome maintenance mechanisms for preventing cancer. Nature, 411, 366–374.

Hogenesch, J. B., Chan, W. K., Jackiw, V. H., Brown, R. C., Gu, Y. Z., Pray-Grant, M., Perdew, G. H., et al. (1997). Characterization of a subset of the basic-helix-loop-helix-PAS superfamily that interacts with components of the dioxin signaling pathway. The Journal of biological chemistry, 272(13), 8581–93.

Hughes, M. E., DiTacchio, L., Hayes, K. R., Vollmers, C., Pulivarthy, S., Baggs, J. E., Panda, S., et al. (2009). Harmonics of circadian gene transcription in mammals. PLoS genetics, 5(4), e1000442.

Hummasti, S., & Hotamisligil, G. S. (2010). Endoplasmic reticulum stress and inflammation in obesity and diabetes. Circulation research, 107(5), 579–91.

Innominato, P. F., Lévi, F. a, & Bjarnason, G. a. (2010). Chronotherapy and the molecular clock: Clinical implications in oncology. Advanced drug delivery reviews, 62(9-10), 979–1001.

Izumo, M., Johnson, C. H., & Yamazaki, S. (2003). Circadian gene expression in mammalian fibroblasts revealed by real-time luminescence reporting: temperature compensation and damping. Proceedings of the National Academy of Sciences of the United States of America, 100(26), 16089–94.

Kaasik, K., & Lee, C. C. (2004). Reciprocal regulation of haem biosynthesis and the circadian clock in mammals. Letters to Nature, 430(July), 467–471.

Kalaany, N. Y., Gauthier, K. C., Zavacki, A. M., Mammen, P. P. a, Kitazume, T., Peterson, J. a, Horton, J. D., et al. (2005). LXRs regulate the balance between fat storage and oxidation. Cell metabolism, 1(4), 231–44.

Kang, T.-H., Lindsey-Boltz, L. a, Reardon, J. T., & Sancar, A. (2010). Circadian control of XPA and excision repair of cisplatin-DNA damage by cryptochrome and HERC2 ubiquitin ligase. PNAS, 106(11), 4890–5.

Kang, T.-H., Reardon, J. T., Kemp, M., & Sancar, A. (2009). Circadian oscillation of nucleotide excision repair in mammalian brain. PNAS, 106(8), 2864–7.

Kantermann, T., Juda, M., Merrow, M., & Roenneberg, T. (2007). The human circadian clock's seasonal adjustment is disrupted by daylight saving time. Current biology, 17(22), 1996–2000.

Kemper, J. K., Xiao, Z., Ponugoti, B., Miao, J., Kanamaluru, D., Tsang, S., Wu, S., et al. (2009). FXR acetylation is normally dynamically regulated by p300 and SIRT1 but constitutively elevated in metabolic disease states. Cell. Metab., 10(5), 392–404.

Kirkland, D., Pfuhler, S., Tweats, D., Aardema, M., Corvi, R., Darroudi, F., Elhajouji, A., et al. (2007). How to reduce false positive results when undertaking in vitro genotoxicity testing and thus avoid unnecessary follow-up animal tests: Report of an ECVAM Workshop. Mutation research, 628(1), 31–55.

Koepsell, H. (2004). Polyspecific organic cation transporters: their functions and interactions with drugs. Trends Pharma-

col Science, 25(7), 375–381.

Kondratov, R. V, Gorbacheva, V. Y., & Antoch, M. P. (2007). The role of mammalian circadian proteins in normal physiology and genotoxic stress responses. Current topics in developmental biology, 78(06), 173–216.

Krawczak, M., & Cooper, D. (1998). p53 mutations, benzo(a)pyrene and lung cancer. Mutagenesis, 13, 319–320.

Kumaki, Y., Ukai-tadenuma, M., Uno, K. D., Nishio, J., Masumoto, K., & Nagano, M. (2008). Analysis and synthesis of high-amplitude Cis-elements. PNAS, 105(39), 14946–51.

Lamia, K. a, Storch, K.-F., & Weitz, C. J. (2008). Physiological significance of a peripheral tissue circadian clock. Proceedings of the National Academy of Sciences of the United States of America, 105(39), 15172–7.

Lamia, K., Sachdeva, U., DiTacchio, L., Williams, E., Alvarez, J., Egan, J., Vasquez, J., et al. (2009). AMPK Regulates the Circadian Clock by Cryptochrome Phosphorylation and Degradation. Science, 326(5951), 437–440.

Lavery, D. J., & Schibler, U. (1993). Circadian transcription of the cholesterol 7 alpha hydroxylase gene may involve the liver-enriched bZIP protein DBP. Genes & Development, 7(10), 1871–1884.

Lavery, D., Lopez-Molina, L., Margueron, R., Fleury-Olela, F., Conquet, F., Schibler, U., & Bonfils, C. (1999). Circadian expression of the steroid 15 alpha-hydroxylase (Cyp2a4) and coumarin 7-hydroxylase (Cyp2a5) genes in mouse liver is regulated by the PAR leucine zipper transcription factor DBP. Mol Cell Biol., 19(10), 6488–99.

Le Martelot, G., Claudel, T., Gatfield, D., Schaad, O., Kornmann, B., Lo Sasso, G., Moschetta, A., et al. (2009). REV-ERBalpha participates in circadian SREBP signaling and bile acid homeostasis. PLoS biology, 7(9), e1000181.

Lee, C., Etchegaray, J.-P., Cagampang, F. R. A., Loudon, A. S. I., & Reppert, S. M. (2001). Posttranslational mechanisms regulate the mammalian circadian clock. Cell, 107(7), 855–867.

Lévi, F., & Okyar, A. (2011). Circadian clocks and drug delivery systems: impact and opportunities in chronotherapeutics. Expert opinion on drug delivery, 8(12), 1535–41.

Levi, F., & Schibler, U. (2007). Circadian rhythms: mechanisms and therapeutic implications. Annual review of pharmacology and toxicology, 47, 593–628.

Li, X., Zhang, S., Blander, G., Tse, J. G., Krieger, M., & Guarente, L. (2007). SIRT1 deacetylates and positively regulates the nuclear receptor LXR. Molecular cell, 28(1), 91–106.

Liebsch, M., Grune, B., Seiler, A., Butzke, D., Oelgeschläger, M., Pirow, R., Adler, S., et al. (2011). Alternatives to animal testing: current status and future perspectives. Archives of toxicology, 85(8), 841–58.

Lowrey, P. L., & Takahashi, J. S. (2004). Mammalian circadian biology: elucidating genome-wide levels of temporal organization. Annual review of genomics and human genetics, 5, 407–41.

Lu, T. T., Makishima, M., Repa, J. J., Schoonjans, K., Kerr, T. A., Auwerx, J., Mangelsdorf, D. J., et al. (2000). Molecular Basis for Feedback Regulation of Bile Acid Synthesis by Nuclear Receptors at Dallas. Molecular cell, 6, 507–515.

Ma, K., Xiao, R., Tseng, H.-T., Shan, L., Fu, L., & Moore, D. D. (2009). Circadian dysregulation disrupts bile acid homeostasis. PloS one, 4(8), e6843.

Matsunaga, N., Ikeda, M., Takiguchi, T., Koyanagi, S., & Ohdo, S. (2008). The molecular mechanism regulating 24-hour rhythm of CYP2E1 expression in the mouse liver. Hepatology, 48(1), 240–51.

1

Mayati, A., Levoin, N., Paris, H., N'Diaye, M., Courtois, A., Uriac, P., Lagadic-Gossmann, D., et al. (2012). Induction of intracellular calcium concentration by environmental benzo(a)pyrene involves a beta2-adrenergic receptor/adenylyl cyclase/Epac-1/inositol 1,4,5-trisphosphate pathway in endothelial cells. J Biol Chem, 287(6), 4041–52.

Mazzoccoli, G., Pazienza, V., & Vinciguerra, M. (2012). Clock genes and clock-controlled genes in the regulation of metabolic rhythms. Chronobiology international, 29(3), 227–51.

Meier, P. J., Eckhardt, U., Schroeder, A., Hagenbuch, B., & Stieger, B. (1997). Special Article Substrate Specificity of Sinusoidal Bile Acid and Organic Anion Uptake Systems in Rat and Human Liver. Hepatolgy, 26(6), 1667–1676.

Miller, B. H., McDearmon, E. L., Panda, S., Hayes, K. R., Zhang, J., Andrews, J. L., Antoch, M. P., et al. (2007). Circadian and CLOCK-controlled regulation of the mouse transcriptome and cell proliferation. Proceedings of the National Academy of Sciences of the United States of America, 104(9), 3342–7.

Mimura, J., & Fuji-Kuriyama, Y. (2003). Functional role of AhR in the expression of toxic effects by TCDD. Biochim Biophys Acta, 1619(3), 263–268.

Monteiro, P., Gilot, D., Le Ferrec, E., Rauch, C., Lagadic-Gossmann, D., & Fardel, O. (2008). Dioxin-mediated up-regulation of aryl hydrocarbon receptor target genes is dependent on the calcium/calmodulin/CaMKIalpha pathway. Mol Pharmacol, 73(3), 769–777.

Moore, J., Goodwin, B., Willson, T., & Klieuwer, S. (2002). Nuclear receptor regulation of genes involved in bile acid metabolism. Crit Rev Eukaryot Gene Expr, 12(2), 119–35.

Moore, R. (1983). Organization and Function of a Central Nervous System Circadian Oscillator: the Suprachiasmatic Hypothalamic Nucleus. Federation Proceedings, 42(11), 2783–2789.

Moore, R., & Eichler, V. (1972). Loss of a Circadian Adrenal Corticosterone Rhythm Following Suprachiasmatic Lesions in the Rat. Brain Research, 42(1), 201–206.

Mukai, M., Lin, T., Peterson, R., Cooke, P., & Tischkau, S. (2008). BehavioralBehavioral rhythmicity of mice lacking AhR and attenuation of light-induced phase shift by 2,3,7,8-tetrachlorodibenzo-p-dioxin. J Biol Rhythms, 23(3), 200–210.

Mukai, M., & Tischkau, S. (2007). Effects of tryptophan photoproducts in the circadian timing system: searching for a physiological role for aryl hydrocarbon receptor. Toxicol Sci, 95(1), 172–181.

Nakahata, Y., Kaluzova, M., Grimaldi, B., Sahar, S., Chen, D., Guarente, L. P., & Sassone-corsi, P. (2008). The NAD+-Dependent Deacetylase SIRT1 Modulates CLOCK- Mediated Chromatin Remodeling and Circadian Control. Cell, 134(2), 329–340.

Nakahata, Y., Sahar, S., Astarita, G., Kaluzova, M., & Sassone-Corsi, P. (2009). Circadian control of the NAD+ salvage pathway by CLOCK-SIRT1. Science, 324(5927), 654–7.

Nakano, A., Tietz, P., & LaRusso, N. (1990). Circadian rhythms of biliary protein and lipid excretion in rats. Am J Physiol Gastrointest Liver Physiol, 258(5), G653–G659.

Oesch-Bartlomowicz, B., Huelster, A., Wiss, O., Antoniou-Lipfert, P., Dietrich, C., Arand, M., Weiss, C., et al. (2005). Aryl hydrocarbon receptor activation by cAMP vs dioxin: divergent signaling pathways. PNAS, 102(26), 9218–9223.

Oesch-Bartlomowicz, B., & Oesch, F. (2009). Role of cAMP in mediating AHR-signaling. Biochemical Pharmacology, 77(4), 627–641.

Ohdo, S. (2007). Review Chronopharmacology Focused on Biological Clock. Drug Metab Pharmacokinet, 22(1), 3–14.

Oklejewicz, M., Destici, E., Tamanini, F., Hut, R. a, Janssens, R., & Van der Horst, G. T. J. (2008). Phase resetting of the mammalian circadian clock by DNA damage. Current biology, 18(4), 286–91.

Panda, S., Antoch, M. P., Miller, B. H., Su, A. I., Schook, A. B., Straume, M., Schultz, P. G., et al. (2002). Coordinated transcription of key pathways in the mouse by the circadian clock. Cell, 109(3), 307–20.

Pendergast, J., & Yamazaki, S. (2012). The mammalian circadian system is resistant to dioxin. J Biol Rhythms, 27(2), 156–163.

Pittendrigh, C. (1960). Circadian Rhythms and the Circadian Organization of Living Systems. Cold Spring Harb Symp Quant Biol, 25, 159–184.

Pittendrigh, C. (1988). The Photoperiodic Phenomena: Seasonal Modulation of the "Day Within". J Biol Rhythms, 3, 173–188.

Preitner, N., Damiola, F., Zakany, J., Duboule, D., Albrecht, U., & Schibler, U. (2002). The Orphan Nuclear Receptor REV-ERBalpha Controls Circadian Transcription within the Positive Limb of the Mammalian Circadian Oscillator. Cell, 110, 251–260.

Provencio, I., Rollag, M. D., & Bakun, A. (2002). Photoreceptive net in the mammalian retina. Nature Brief Communications, 415, 493.

Qu, X., Metz, R. P., Porter, W. W., Cassone, V. M., & Earnest, D. J. (2009). Disruption of period gene expression alters the inductive effects of dioxin on the AhR signaling pathway in the mouse liver. Toxicology and applied pharmacology, 234(3), 370–7.

Raghuram, S., Stayrook, K. R., Huang, P., Rogers, P. M., Amanda, K., Mcclure, D. B., Burris, L. L., et al. (2007). Identification of heme as the ligand for the orphan nuclear receptors REV-ERBα and REV-ERBβ. Nat. Struct. Mol. Biol, 14(12), 1207–1213.

Ramsey, K. M., Yoshino, J., Brace, C. S., Abrassart, D., Kobayashi, Y., Marcheva, B., Hong, H., et al. (2009). Circadian Clock Feedback Cycle Through NAMPT-Mediated NAD+ Biosynthesis. Science, 324(5927), 651–654.

Rannug, A., & Fritsche, E. (2006). The aryl hydrocarbon receptor and light. Biological chemistry, 387(9), 1149–57.

Reppert, S. M., & Weaver, D. R. (2002). Coordination of circadian timing in mammals. Nature, 418(6901), 935–41.

Rey, G., & Reddy, A. B. (2013). Connecting cellular metabolism to circadian clocks. Trends in cell biology, 23(5), 234–241.

Ripperger, J., Shearman, L., Reppert, S., & Schibler, U. (2000). CLOCK, an essential pacemaker component, controls expression of the circadian transcription factor DBP. Genes Dev, 14(6), 679–689.

Sack, R., Brandes, R., Kendal, A., & Lewy, A. (2000). Entrainment of Free-Running Circadian Rhythms by Melatonin in Blind People. The New England Journal of Medicine, 343, 1070–1077.

Sancar, A., Lindsey-Boltz, L. a, Kang, T.-H., Reardon, J. T., Lee, J. H., & Ozturk, N. (2010). Circadian clock control of the cellular response to DNA damage. FEBS letters, 584(12), 2618–25.

Sato, T., Yamada, R., Ukai, H., Baggs, J., Miraglia, L., Kobayashi, T., Welsh, T., et al. (2006). Feedback repression is required for mammalian circadian clock function. Nature Genetics, 38, 312–319.

Shearman, L. P., Sriram, S., Weaver, D. R., Maywood, E. S., Chaves, I., Zheng, B., Kume, K., et al. (2000). Interacting molecular loops in the mammalian circadian clock. Science, 288(5468), 1013–9.

1

Shimba, S., & Watabe, Y. (2009). Crosstalk between the AHR signaling pathway and circadian rhythm. Biochemical pharmacology, 77(4), 560–5.

Soldatow, V. Y., Lecluyse, E. L., Griffith, G., & Rusyn, I. (2013). In vitro models for liver toxicity testing. Toxicology Research, 2(23), 23–39.

Solt, L. A., Wang, Y., Banerjee, S., Hughes, T., Kojetin, D. J., Lundasen, T., Shin, Y., et al. (2012). Regulation of circadian behaviour and metabolism by synthetic REV-ERB agonists. Nature, 485(7396), 62–8.

Stejskalova, L., Dvorak, Z., & Pavek, P. (2011). Endogenous and exogenous ligands of aryl hydrocarbon receptor: current state of art. Curr Drug Metab, 12, 198–212.

Stokkan, K., Yamazaki, S., Tei, H., Sakaki, Y., & Menaker, M. (2001). Entrainment of the circadian clock in the liver by feeding. Science, 291(5503), 490–3.

Storch, K.-F., Lipan, O., Leykin, I., Viswanathan, N., Davis, F. C., Wong, W. H., & Weitz, C. J. (2002). Extensive and divergent circadian gene expression in liver and heart. Nature, 417(6884), 78–83.

Storch, K.-F., Paz, C., Signorovitch, J., Raviola, E., Pawlyk, B., Li, T., & Weitz, C. J. (2007). Intrinsic circadian clock of the mammalian retina: importance for retinal processing of visual information. Cell, 130(4), 730–41.

Sun, Z., Feng, D., Everett, L., Bugge, A., & Lazar, M. (2011). Circadian Epigenomic Remodeling and Hepatic Lipogenesis: Lessons from HDAC3. Cold Spring Harb. Symp. Quant. Biol., 76, 49–55.

Takahashi, J., Hong, H., Ko, C., & McDearmon, E. (2008). The Genetics of Mammalian Circadian Order and Disorder: Implications for Physiology and Disease. Nature Reviews Genetics, 9(10), 764–775.

Takahashi, S., Inoue, I., Nakajima, Y., Seo, M., Nakano, T., & Yang, F. (2010). A Promoter in the Novel Exon of hPPAR Directs the Circadian Expression of PPAR. Journal of Atherosclerosis and Thrombosis, 17(1), 73–83.

Thybaud, V., Aardema, M., Clements, J., Dearfield, K., Galloway, S., Hayashi, M., Jacobson-Kram, D., et al. (2007). Strategy for genotoxicity testing: hazard identification and risk assessment in relation to in vitro testing. Mutation research, 627(1), 41–58.

Trauner, M., Meier, P. J., & Boyer, J. L. (1999). Molecular regulation of hepatocellular transport systems in cholestasis. Journal of hepatology, 31(1), 165–78.

Ueda, H., Hayashi, S., Chen, W., Sano, M., Machida, M., Shigeyoshi, Y., Iino, M., et al. (2005). System-level identification of transcriptional circuits underlying mammalian circadian clocks. Nature Genetics, 37(2), 187–192.

Ueda, H. R., Chen, W., Adachi, A., Wakamatsu, H., Hayashi, S., Takasugi, T., Nagano, M., et al. (2002). A transcription factor response element for gene expression during circadian night. Letters to Nature, 418(August), 534–539.

Ukai, H., Kobayashi, T. J., Nagano, M., Masumoto, K., Sujino, M., Kondo, T., Yagita, K., et al. (2007). Melanopsin-dependent photo-perturbation reveals desynchronization underlying the singularity of mammalian circadian clocks. Nature cell biology, 9(11), 1327–34.

Van den Pol, A. (1980). The hypothalamic suprachiasmatic nucleus of rat: intrinsic anatomy. The Journal of comparative neurology, 191(4), 661–702.

Wagner, M., Zollner, G., & Trauner, M. (2009). New molecular insights into the mechanisms of cholestasis. Journal of hepatology, 51(3), 565–80.

Wang, C., Xu, C., Krager, S., Bottum, K., Liao, D., & Tischkau, S. (2011). Aryl hydrocarbon receptor deficiency enhances insulin sensitivity and reduces PPAR-α pathway activity in mice. Environ Health Perspect, 119(12), 1739–1744.

Wang, Y., Kumar, N., Solt, L. A., Richardson, T. I., Helvering, L. M., Crumbley, C., Garcia-Ordonez, R. D., et al. (2010). Modulaton of Retinoid Acid Receptor-regulated Orphan Receptor alpha and gamma Activity by 7-Oxygenated Sterol Ligands. J Biol Chem, 285(7), 5013–25.

Woolbright, B. L., & Jaeschke, H. (2012). Novel insight into mechanisms of cholestatic liver injury. World journal of gastroenterology : WJG, 18(36), 4985–93.

Wuarin, J., Falvey, E., Lavery, D., Talbot, D., Schmidt, E., Ossipow, V., Fonjallaz, P., et al. (1992). The role of the transcriptional activator protein DBP in circadian liver gene expression. J Cell Sci Suppl, 16, 123–7.

Xu, C., Li, C., & Kong, A. (2005). Induction of phase I, II and III drug metabolism/transport by xenobiotics. Arch Pharm Res, 3, 249–68.

Xu, C.-X., Krager, S. L., Liao, D.-F., & Tischkau, S. a. (2010). Disruption of CLOCK-BMAL1 transcriptional activity is responsible for aryl hydrocarbon receptor-mediated regulation of Period1 gene. Toxicological sciences : an official journal of the Society of Toxicology, 115(1), 98–108.

Yagita, K, Tamanini, F., & Yasuda, M. (2002). Nucleocytoplasmic shuttling and mCRY-dependent inhibition of ubiquitylation of the mPER2 clock protein. The EMBO Journal, 21(6), 1301–1314.

Yagita, Kazuhiro, & Okamura, H. (2000). Forskolin induces circadian gene expression of rPer1, rPer2 and dbp in mammalian rat-1 fibroblasts. FEBS Letters, 465(1), 79–82.

Yagita, Kazuhiro, Tamanini, F., Horst, G. T. J. Van Der, & Okamura, H. (2001). Molecular Mechanisms of the Biological Clock in Cultured Fibroblasts. Science, 292(April), 278–281.

Yamamura, Y., Yano, I., Kudo, T., & Shibata, S. (2010). Time-dependent inhibitory effect of lipopolysaccharide injection on Per1 and Per2 gene expression in the mouse heart and liver. Chronobiology international, 27(2), 213–32.

Yamazaki, S., Numano, R., Abe, M., Hida, A., Takahashi, R., Ueda, M., Block, G. D., et al. (2000). Resetting central and peripheral circadian oscillators in transgenic rats. Science, 288(5466), 682–685.

Yang, X. (2010). A wheel of time: the circadian clock, nuclear receptors, and physiology. Genes & Development, 24, 741–747.

Yang, X., Downes, M., Yu, R. T., Bookout, A. L., He, W., Straume, M., Mangelsdorf, D. J., et al. (2006). Nuclear receptor expression links the circadian clock to metabolism. Cell, 126(4), 801–10.

Yin, L., Wu, N., Curtin, J. C., Qatanani, M., Szwergold, N. R., Reid, R. a, Waitt, G. M., et al. (2007). Rev-erbalpha, a heme sensor that coordinates metabolic and circadian pathways. Science, 318(5857), 1786–9.

Zhang, Y. J., Yeager, R. L., & Klaassen, C. D. (2009). Circadian Expression Profiles of Drug-Processing Genes and Transcription Factors in Mouse Liver ABSTRACT : Drug Metabolism and Disposition, 37(1), 106–115.

Zmrzljak, U. P., & Rozman, D. (2012). Circadian regulation of the hepatic endobiotic and xenobitoic detoxification pathways: the time matters. Chemical research in toxicology, 25(4), 811–24.

Zudaire, E., Cuesta, N., Murty, V., Woodson, K., Adams, L., Gonzalez, N., Martínez, A., et al. (2008). The aryl hydrocarbon receptor repressor is a putative tumor suppressor gene in multiple human cancers. J Clin Invest, 118(2), 640–650.

Chapter 2

Chronotoxic effects of benzo[a]pyrene, assessed in cultured liver slices

Romana M. Nijman, César E. Payan Gomez, Paul Wackers, Annelieke S. de Wit, António Carvalho da Silva, Inês Chaves and Gijsbertus T.J. van der Horst

2

Abstract

The circadian clock is an internal timekeeping system that not only imposes 24 hour rhythmicity on behavior and physiology, but also on metabolism, including liver xenobiotic metabolism. Accordingly, the severity of the response of the liver to (geno)toxic chemicals can depend on the time of day of exposure, a phenomenon referred to as chronotoxicity. Yet, in most *in vivo* and *in vitro* toxicological and toxicogenomics experiments, time is not taken into consideration. Here, we describe the establishment of an *ex vivo* chronotoxicity assay that allows treatment of liver slices at defined circadian phase. We have used this system to investigate the chronotoxic properties of benzo[a]pyrene (B[a]P), an environmental pollutant that requires metabolism to exert its carcinogenic DNA damaging effect. We have treated liver slices with B[a]P at two different time points, corresponding to late afternoon and late night, and determined changes in the liver transcriptome by microarray analysis. We observed that B[a]P triggers common responses, as well as responses that are unique for the late day and late night, suggesting that B[a]P has chronotoxic properties. Moreover, these results show that the moment of treatment should be taken into account when studying the toxic effect of compounds.

Introduction

Environmental xenobiotic compounds are man-made substances which can be harmful to organisms as well as to the entire ecosystem. Xenobiotic compounds are found in air, soil and water (pollutants), as well as in food (e.g. pesticides). Likewise, chemicals and drugs produced by industry can be hazardous for living organisms (Wogan, 1989). As such, risk assessment of xenobiotic compounds for their hazardous effects on humans, animals, and on the environment is of prime importance for regulatory decision making with respect to the approval and registration of chemicals and setting the maximum tolerable exposure level (Dearfield et al., 2002; Dearfield and Moore, 2005; Thybaud et al., 2007).

In genetic toxicology research, xenobiotic compounds are characterized with respect to their potential to induce DNA damage, and as a consequence mutations and/or chromosomal damage that ultimately cause adverse health effects, including cancer (Kirkland et al., 2007; Liebsch, et al., 2011). Evaluation of the (geno)toxic properties of compounds usually relies on a minimum of two *in vitro* tests (e.g. the Ames bacterial mutation assay, *in vitro* mammalian mutation and/or cytogenetic assays) and one *in vivo* test (e.g. rodent assays for DNA damage and/or chromosomal aberrations) (Dearfield and Moore, 2005; Thybaud et al., 2007). However, apart from the fact that *in vivo* studies are very costly and time consuming, and as such do not allow large scale screening (Liebsch, et al., 2011), society wants to reduce the use of rodents for these types of studies. Nowadays, several *in vitro* systems such as hepatic cell lines and liver slices are frequently used to study toxicity of compounds (Liebsch et al., 2011; Boess et al., 2003; Holme and Dybing, 2002). These *in vitro* studies (i) require fewer or no animals, (ii) are cheaper, and (iii) when combined with modern omics-based technologies, can be used as (semi)high through-put systems to test large numbers of toxic compounds (Afshari et al., 1999; Burczynski et al., 2000; van Delft et al., 2004; Farkas et al., 2005; Staal., et al., 2008). Liver slices have been successfully used as a model system for toxicogenomic studies addressing hepatotoxic properties of chemical compounds (Staal et al., 2008; Elferink et al., 2008). Importantly, while primary hepatocytes and established hepatoma cell lines (e.g. HepG2) dedifferentiate and may lose liver specific functions (Ogino et al., 2002; Wilkening et al., 2003; de Graaf et al., 2010), liver slices offer the advantage of preserving tissue structure, cell-cell and cell matrix interactions, as well as expression of xenobiotic enzymes (de Graaf et al., 2010; Boess et al., 2003; Moronvalle-Halley et al., 2005).

Apart from structure, another, yet poorly recognized, factor that can influence the outcome of a toxicological or toxicogenomics experiment is time, notably the temporal (i.e. daily) variations in gene expression, as well as protein and metabolite levels. The circadian clock is an internal timekeeping system that imposes 24 hour rhythmicity on behavior, physiology and metabolism in most if not all organisms (Lowrey and Takahashi, 2011). At the cellular level, rhythms are generat-

ed by a molecular oscillator, organized in positive and negative transcription translation feedback loops (TTFL) (Lowrey and Takahashi, 2011). In short, the Basic-Helix-Loop-Helix/Per-ARNT-Sim (BHLH/PAS) domain containing transcription factors CLOCK and BMAL1 form a heterodimeric complex that drives transcription of the *Period* (*Per1* and *Per2*) and *Cryptochrome* (*Cry1* and *Cry2*) genes through binding to E-box promoter elements. Once generated, the PER and CRY proteins dimerize and accumulate in the nucleus, where they shut down their own expression by repressing CLOCK/BMAL1 driven transcription (Lowrey and Takahashi, 2004; Lowrey and Takahashi, 2011). This molecular clock contains an additional stabilizing feedback loop involving CLOCK/BMAL1-mediated rhythmic expression of *Rev-Erbα*, which gene product drives cyclic expression of *Bmal1* by competing with retinoic-acid-receptor-related orphan receptor (ROR) proteins for binding to ROR elements in the *Bmal1* promoter (Preitner et al., 2002). Importantly, the circadian clock is coupled to output processes through a series of clock-controlled genes (for an in depth review of the circadian oscillator, see Ko and Takahashi 2006).

Transcriptomic analysis revealed that approximately 10% of the liver transcriptome is under circadian control, including many genes involved in the metabolism and detoxification of xenobiotics, such as cytochrome P450 (CYP450) enzymes (Akhtar et al., 2002; Levi and Schibler, 2007; Panda et al., 2002; Storch et al., 2002). This suggests that the toxic effect of compounds that require metabolic activation may depend on the time of day of exposure (e.g. morning vs. evening), a process which nowadays is referred to as chronotoxicity. Among the pathways that may contribute to liver chronotoxicity is the aryl hydrocarbon receptor (AhR) signaling pathway. The AhR protein contains a bHLH/PAS domain and is known to interact with the core clock component BMAL1 (Hogenesch et al., 1997), resulting in rhythmic AhR protein levels in liver, lung, thymus and brain (i.e. suprachiasmatic nucleus) (Richardson et al., 1998). Several Cyp450 genes, such as *Cyp1a1*, are induced by AhR, and therefore may also be rhythmically expressed. Indeed, *Cyp1a1* (as well as AhR) expression was shown to oscillate, with mRNA levels peaking at light-dark transition. Moreover, rhythmic expression of *Cyp1a1* was abolished when the circadian clock was disrupted (Tanimura et al., 2011; Qu et al., 2010; Tischkau et al., 2011).

Among the environmental pollutants that require metabolic activation by CYP1A1 is the polycyclic aromatic hydrocarbons (PAHs), benzo[a]pyrene (B[a]P), a well-studied environmental pollutant, mainly found in cigarette smoke, exhaust, and industrial waste (Samanta et al., 2002; Wogan, 1989). B[a]P has been demonstrated to be carcinogenic in rodents (Hattemer-Frey and Travid, 1991; Wolterbeek et al., 1995; Harrigan et al., 2006) and is also classified as a human carcinogen (Hussain et al., 2001; Mukhopadhyay et al., 2004). B[a]P is a pro-drug and in order to cause damage it needs to be converted into its ultimate carcinogenic metabolite B[a]P-7,8-diol 9,10-epoxide (BPDE) through the subsequent action of CYP1A1, epoxide hydrolase and CYP1B1 (Miller and Ramos, 2001; Xiao et al., 2007). BPDE is a highly reactive metabolite that damages the genome by intercalating with DNA and formation of cytotoxic and mutagenic BPDE-DNA adducts (Dipple, 1995; Phillips, 1983; Rubin, 2001). B[a]P is able to enhance its own metabolism through binding to AhR, which results in the induction of phase I and phase II metabolizing enzymes (Shimada et al., 1996; Hankinson, 2005).

In the present study, we describe the establishment of an *ex vivo* chronotoxicity assay on the basis of mouse liver slices and address the effect of time of exposure on B[a]P-induced genotoxic response by transcriptome analysis. We show that the magnitude of *Cyp1a1* induction by B[a]P varies with circadian phase. Moreover, marked differences in gene expression patterns and related biological functions and pathways were observed depending on the time of day of exposure. This study highlights the involvement of the circadian clock in the severity of toxic responses and proves liver slices to be a valuable tool to study chronotoxic effects of chemical compounds.

Materials & methods

Animals

Per2::Luc circadian clock reporter mice, expressing the firefly luciferase gene from the *Per2* pro-

2

moter and backcrossed to a C57BL/6J background (Chaves et al., 2011) were kept at the Animal Resource Center (Erasmus University Medical Center), which operates in compliance with the European guidelines (European Community 1986) and The Netherlands legislation for the protection of animals used for research. Animals were kept in a 12 hr. light/12 hr. dark cycle (LD12:12) with ad libitum access to food and water. For the isolation of liver slices, adult male *Per2::Luc* mice (10-15 weeks) were sacrificed by cervical dislocation between ZT2 and ZT5 (ZT means *Zeitgeber* time, in which ZT0 represents time of lights on). Livers were rapidly removed and placed in ice cold Hank's balanced salt solution (GIBCO), supplemented with 50 mM glucose, 4 mM sodium bicarbonate, 10 mM HEPES, 100 U/ml penicillin and 100 μg/ml streptomycin (Yoo, et al., 2004). Animal studies at Erasmus University Medical Center were approved by DEC Consult, an independent Animal Ethical Committee (Dutch equivalent of the IACUC) under permit numbers 139-09-11 (EUR1760), 139-10-04 (EUR2026) and 139-11-07 (EMC2383).

Liver slice cultures

Within 45 min after isolation of the liver, slices (200-250 μm thickness) were prepared using a Krumdieck tissue slicer (Alabama, R&D, TSE). Individual liver slices were placed on a Biopore CM hydrophilized (PTFE) Insert (Millipore, PICM ORG50) in a 35-mm dish in imaging medium, composed of DMEM (GIBCO), supplemented with 0.1 mM luciferin (Sigma), 2% B27 supplement, 4 mM sodium bicarbonate, 10 mM HEPES, 25 U/ml penicillin and 25 μg/ml streptomycin). *Ex vivo* cultures were continuously monitored for circadian clock phase through real-time bioluminescence imaging of *Per2::Luc* clock reporter gene activity. To this end culture dishes were placed in a LumiCycle 32-channel automated luminometer (Actimetrics) in a dry, temperature-controlled incubator at 37°C. Data was analyzed using the Actimetrics software. For *in vivo* vs. *ex vivo* comparison of clock gene and clock controlled gene expression by qRT-PCR, liver slices were collected 2-3 days after slice preparation at relative circadian time (CTr) 0, 8, 12 or 20 (in which the trough of *Per2::Luc* expression is set at CTr0).

B[a]P exposure of liver slices

After stabilization of bioluminescence rhythms, liver slices were exposed to B[a]P or DMSO (vehicle control) at CTr0, 4, 8, 12, 16 or 20. Individual slices were incubated with 1.2 ml recording medium containing B[a]P (Sigma; dissolved in DMSO, dose as indicated in the text), or DMSO. After 4 hours, slices were collected and immediately frozen in liquid nitrogen and stored at -80°C for later analysis.

Cytotoxicity assay

Viability of the liver slices was measured using the Cytotoxicity Detection Kit LDH (Roche) following the manufacturer's instructions. This enzymatic assay is based on the release of thermo-stable lactate dehydrogenase by apoptotic and necrotic cells. Medium was collected at various time points during slice culturing, or before and after B[A]P treatment. As a positive control (maximum LDH release), we used liver slices treated with 1% triton X-100 for 2 hr. at 37°C. The LDH leakage was measured from 4 liver slices per time point/condition.

RNA isolation

Total RNA was isolated from liver slices using TRIzol Reagent (Invitrogen) following manufacturer's instructions. RNA samples for transcriptomics analysis were further purified using the RNeasy MinElute Cleanup Kit (Qiagen). RNA concentrations were determined using the NanoDrop ND-1000 (NanoDrop Technologies) and the RNA quality was assessed with the Agilent 2100 Bioanalyzer (Agilent Technologies) in combination with the RNA 6000 Pico Chip. Only RNA samples with a RIN value above 7 were used for transcriptomic analysis and quantitative RT-PCR.

Quantitative RT-PCR

cDNA was generated using 1 μl of total RNA, oligo(dT) primers and SuperScript III reverse transcriptase (Invitrogen), following manufacturer's instructions. Quantitative PCR amplification

was performed with the iCycler iQ™ Real-Time PCR Detection System (BioRad), using SYBR-green and primers generating intron-spanning products of 150-300 bp. The following forward and reverse primers were used: *Hprt*: 5'-CGA AGT GTT GGA TAC AGG CC-3' and 5'-GGC AAC ATC AAC AGG ACT CC-3'; *Cyp1a1*: 5'-ACG AGA ATG CCA ATG TCC AG-3' and 5'-CCA ATC ACT GTG TCT AGT TCC T-3'; *Cyp1a2*: 5'-ACA TCA CAA GTG CCC TGT TCA AGC-3' and 5'-ATC TTC CTC TGC ACG TTA GGC CAT-3'; *Cyp2a5*: 5'- ATG AGG ACC GAA TGA AGA TGC CCT-3' and 5'-ACA GAG CCC AGC ATA GGA AAC ACT-3'; *Cyp2b10*: TTC TGC GCA TGG AGA AGG AGA AGT-3' and 5'-TGC CAG CAA AGA AGA GAG AGA GCA-3'; *Nr1d1*: 5'-ACC TTA CTG CTC AGT GCC TGG AAT-3' and 5'-TGG ACC TTG ACA CAA ACT GGA GGT-3'; *Wee1*: 5'-AGG ATG TGG GTC ACT GTT GGA TGT-3' and 5'-TTC GCA GTA AAG CCC TTG AGT CCT-3'; *Bmal1*: 5'-AAG CTT CTG CAC AAT CCA CAG CAC-3' and 5'-TGT CTG GCT CAT TGT CTT CGT CCA-3'; *Per2*: 5'-TTC CTA CAG CAT GGA GCA GGT TGA-3' and 5'-ATG AGG AGC CAG GAA CTC CAC AAA-3'; *Bhmt*: 5'-TGC CGG AGA AGT TGT GAT TGG AGA-3' and 5'-AAC TCC CGA TGA AGC TGA CGA ACT-3'; *Gls2*: 5'-GGT TCA GCA ATG CCA CAT CCC AGT-3' and 5'-AGA GAT CAA GGG CAG CAG CCA TCA TGT-3'; *Agxt*: 5'-TCA TCT CCT TCA ACG ACA AGG CCA-3' and 5'-AAG CTG GTG ACA GGT GTG GTA TGA-3'; *Apoa1*: 5'-TTC AAC CGT TAG TCA GCT GCA GGA-3' and 5'-TAG GGC TGC ACC TTC TGT TTC ACT-3'; *Car3*: 5'-ACA ACC AGT CAC CCA TTG AAC TGC-3' and 5'-ACA CAA CTC TGC AGG TCT TCC CAT-3'; *Tiparp*: 5'-GGC ACT TGC ATT TAT GGC AGG GAT-3' and 5'- ACT CTG CCA CTT CTG AGT GGT TGT-3'; and *Ccl24*: 5'-TTG ACG CTT TAC CAG CTG CTT TG-3' and 5'- TTC ACT CAG CAC AGG AGA CAC CA-3'. Expression levels were normalized to hypoxanthine-guanine phosphoribosyl transferase (*Hprt*) mRNA levels. The generation of specific products was confirmed by melting curve analysis, and primer pairs were tested with a logarithmic dilution of a cDNA mix to generate a linear standard curve, which was used to calculate primer pair efficiencies. The significance of circadian oscillations in relative mRNA expression levels was analyzed by CircWave Batch v3.3 for cosinor analysis with a 24 hour wave, using forward linear harmonic regression and an F-test. User defined alpha was 0.05.

RNA labeling and hybridization
Biotin-labled cRNA was synthesized using the 3' IVT Express Kit (Affymetrix). The fragmented cRNA was utilized for hybridization to a GeneChip® HT MG-430 PM Array Plate (Affymetrix), processed using GeneTitan™ Hybridization, Wash, and Stain Kit for 3' IVT Arrays and the GeneTitan™ instrument (Affymetrix). The software program Affymetrix GeneChip Command Console (v3.2) was used to operate the GeneTitan™ instrument (Affymetrix) fully automated. After scanning, the array images as well as the correct alignment of the grid were inspected using Affmetrix GeneChip Command Console Viewer software.

Data analysis
The Data Quality Control, comprising sample independent (hybridization controls) and sample dependent controls (RNA degradation controls, Background CG12, Perfect Match Mean, Relative Signal, and Statistical correlation) was performed using Affymetrix Expression Console v1.1 software. Next, arrays were annotated according to De Leeuw et al (2008) and expression levels were calculated using the robust multi-array average (RMA) algorithm (Affy package, version 1.22.0; Irizarry et al., 2003) from the Bioconductor project (http://www.bioconductor.org) for the R statistical language. Using a mixed linear model with coefficients the normalized data were statistically analyzed for differential gene expression. False discovery rate (FDR) correction was performed across all contrasts, and only annotated genes were used for further analysis. The top 1000 differentially expressed genes (DEGs) were used for further analysis. Pathway and Gene ontology analysis were performed using Database for Annotation, Visualization and Integration Discovery (DAVID) and Ingenuity Pathway Analysis (IPA).

Statistical analysis
Data are presented as the mean SEM and the Student's t-test was used to compare between the

2

groups. P-values < 0.05 were considered statistically significant.

Results

Optimization of liver slice cultures for chronotoxicity measurements

Previous studies have established liver slices as a valid *ex vivo* system to investigate the response to toxic compounds. Although it is possible to culture liver slices up to 7 days (Amin et al., 2006; Vickers and Fischer, 2004), most toxicology studies are performed within 24 to 96 hours after isolation in order to maintain a good viability of the slices. Moreover, it is known that the expression level of CYP450 enzymes tends to decline during culturing (De Graaf, et al., 2010). However, in order to establish an *ex vivo* chronotoxicity assay in liver slices, it will be necessary to first determine the phase of circadian oscillation of the slices in order to predict the time of treatment. To this end, we have made use of a transgenic mouse model, ubiquitously expressing an *mPer2::Luc* clock reporter gene for real-time imaging of circadian phase (Chaves et al., 2011). As shown in Figure 1A, we were able to follow bioluminescence rhythms in *Per2::luc* mouse liver slices for more than 7 days. After a recovery period of approximately 36 to 48 hours, robust circadian rhythms were detected with a periodicity of 24.19 ± 0.79 hours. Moreover, the amplitude of oscillations remained stable for at least seven days, suggesting that the slices remained viable. Nonetheless, we determined the viability of the slices by measuring the LDH leakage in the medium (originating from apoptotic/necrotic cells). LDH levels remained relatively constant up to day 5, but started to increase upon prolonged culturing (Fig. 1B). Therefore, taking into consideration the recovery period of the slices (1.5-2 days) and the time required to assess clock phase and period (2 days), exposure studies are best performed at day 4.

In order to get an impression of the circadian gene expression in liver slices and to further validate the system, we measured the relative expression levels of several core clock and clock-controlled genes (CCGs) in liver slices at day 4. Slices were collected at 4 hour intervals over a 24 hour period, starting from the trough of the *Per2::Luc* signal (set as relative circadian time 0, or CTr0). Similar to the liver *in vivo* (Panda et al., 2002; Hughes et al., 2009), the relative
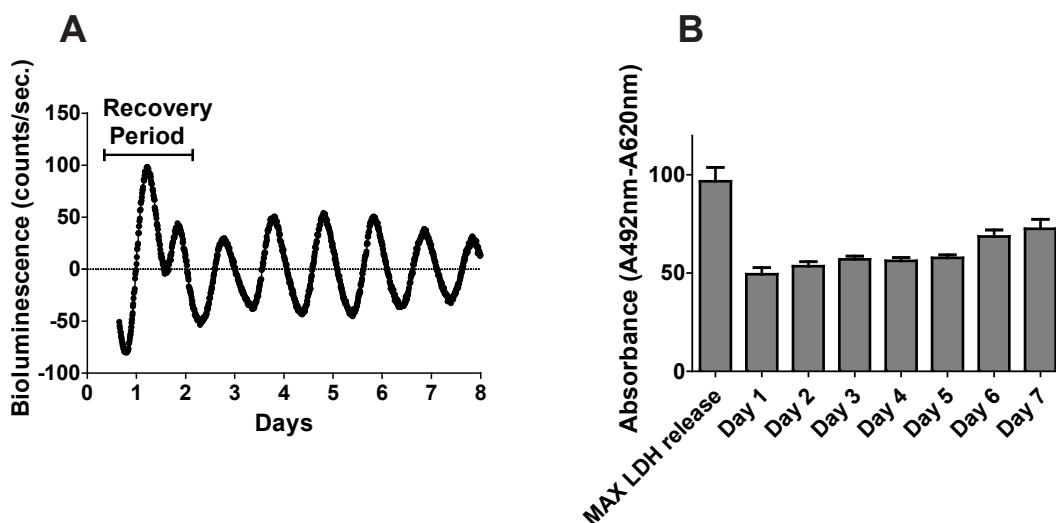

Figure 1: Characterization of circadian clock and viability in liver slices. A. Representative example of a bioluminescence recording of *Per2::Luc* a mouse liver slice. The Y-axis represents the baseline subtracted bioluminescence value, the X-axis the time after slicing. Note that liver slices need approximately 2 day to recover and adjust to the culturing conditions (recovery period, indicated by a bar). B. Representative example of the viability of a liver slice, cultured for 7 days. Medium from liver slices (n= 4) was collected at the indicated days and assayed for LDH leakage .

expression levels of the core circadian clock genes, *Bmal1, Rev-Erbα* and *Per2* in the liver slices showed a clear circadian oscillation with the peak of *Bmal1* anti-phase to that of *Per2*, and *Rev-Erbα* peaking 4 to 6 hours before *Per2*. Likewise, the clock controlled *Cyp2a5, Cyp2b10* and *Wee1* genes also show the expected circadian expression pattern (Suppl. Fig. 1A). The relative expression levels were analyzed by CircWave to statically confirm the circadian oscillation (Suppl. Fig. 1B).

Taken together, these findings lead us to conclude that under the conditions used, the viability and clock performance of the liver slices meets the reproducibility and robustness required for use in chronotoxicity assay.

Expression of Cyp1a1 mRNA in liver slices after B[a]P exposure

As the level of induction of *Cyp1a1* gene expression in the lungs of B[a]P treated mice has previously been shown to be under control of the circadian clock (Tanimura et al., 2011), we have chosen this genotoxic agent as a test compound to investigate whether liver slices can serve as an *ex vivo* chronotoxicity assay.

To this end, we first exposed liver slices to various concentrations of B[a]P at day 2 to identify the optimal B[a]P dose for *Cyp1a1* induction (Fig. 2A). On the basis of this dose response curve, and in line with several other studies (Harrigan et al., 2006; Staal et al., 2007; Plazar et al., 2007), we have chosen for a 4 hour treatment with 10 µM B[a]P. Next, liver slices were treated with B[a]P or mock treated with the solvent DMSO on day 4 at 6 individual time points over a 24 hour period, i.e. CTr0, 4, 8, 12, 16, and 20. Liver slices were collected 4 hour after the start of B[a]P or DMSO (vehicle control) treatment (annotated in sample names as T4 and C4, respectively, in which T and C refer to treatment and control). As shown in Figure 2B, the relative induction level of *Cyp1a1* in the liver slices after B[a]P exposure is dependent on the time of treatment, with the highest and lowest *Cyp1a1* mRNA levels observed in the CTr8-T4 and CTr20-T4 samples, respectively. In line with circadian control over *Cyp1a1* induction, peak and through levels are separated by 12 hour. Moreover, the rhythm in B[a]P-mediated *Cyp1a1* induction appears in phase with *Per2::Luc* reporter gene expression.
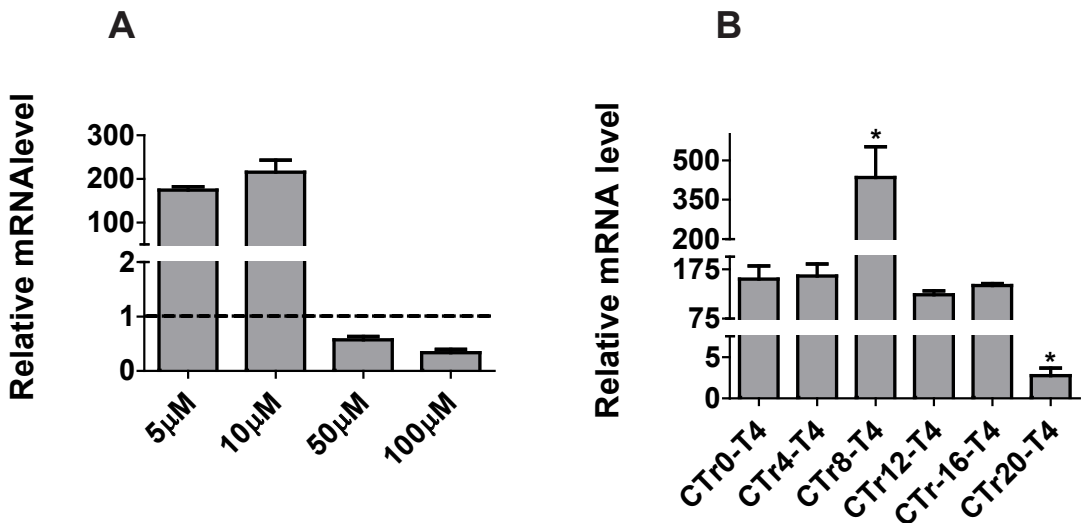

Figure 2: B[a]P treatment of liver slices. A. Dose response curve of B[a]P treatment. Liver slices (n= 4) were treated at day 2 for 4 hrs. with B[a]P. Induction of *Cyp1a1* gene expression, measured by qRT-PCR, was used as a readout. B. Representative examples of qRT-PCR of *Cyp1a1 in* liver slices (n= 4) exposed to B[a]P for 4 hrs. The liver slices were harvested every 4 hrs.

Transcriptome analysis of B[a]P exposed liver slices

The difference in *Cyp1a1* induction observed at CTr8-T4 and CTr20-T4 are highly indicative for the occurrence of chronotoxic effect upon B[a]P exposure. To determine the effect of time of exposure on the genotoxic response elicited by B[a]P, we performed transcriptome analysis on the CTr8-T4 and CTr20-T4 (B[a]P treated) samples, using CTr8-C4 and CTr20-C4 (DMSO vehicle treated) samples as time-matched controls. To obtain a first visual impression of the transcriptional response after B[a]P exposure, we performed a Principle Component Analysis (PCA), and we plotted the two principal components with the higher amount of variance explained (Fig. 3). The PCA plot revealed a separation of data in four distinguishable clusters, corresponding to the four conditions analyzed, notably B[a]P vs. DMSO treatment and exposure at ZT8 vs. exposure at ZT20.
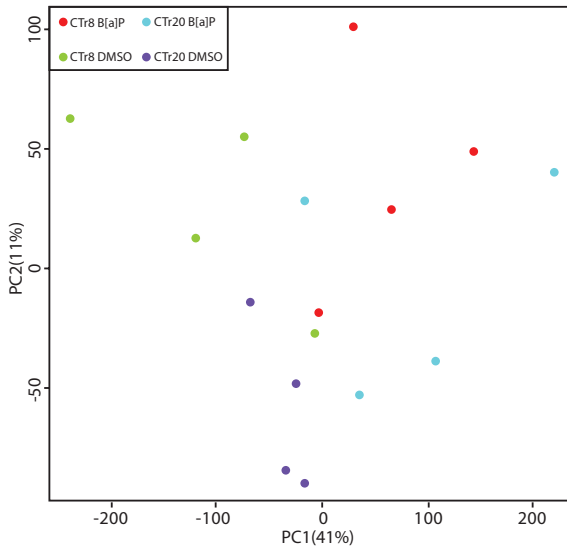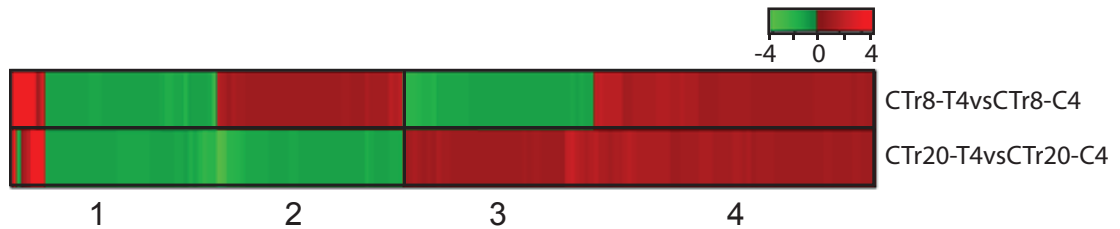

Figure 3: Differentially expressed genes after B[a]P exposure. Principle Component analysis of all genes after 4 hr. B[a]P (T4) or DMSO exposure (C4) of liver slices at CTr8 and CTr20. Red dots: CTr8-T4, green dots: CTr8-C4, blue dots: CTr20-T4 and purple dots: CTr20-C4.

1.   Carbohydrate metabolism
     Drug metabolism
     Small molecule biochemistry

2.   Drug metabolism
     Protein synthesis
     Cell morphology

3.   Nervous System development and function
     Neurological disease
     Lipid metabolism

4.   Connective tissue development and function
     Tissue morphology
     Cellular development

Figure 4: Heat map of common DEGs. Normalized log 2 values (experimental/reference) of the 181 overlapping genes between CTr8-T4 vs CTr8-C4 and CTr20-T4 vs CTr20-C4 were used to create a hierarchical clustering across genes using the package gplots from Bioconductor.

Differences in gene expression levels between the (DMSO vehicle treated) CTr8-C4/ CTr20-C4 samples are likely originating from circadian regulation. We surveyed previously published transcriptomics-based *in vivo* mouse liver data sets (Miller et al. 2007; Akhtar et al. 2002; Panda et al. 2002; Ueda et al. 2002; Hughes et al. 2009) for clock (controlled) genes and identified 108 genes that are rhythmically expressed in at least 3 out of 5 studies (Suppl. Table 1). Using this panel as a test set for truly oscillating genes, we next analyzed how many of those genes were present among the top 500 differentially expressed genes (DEGs) in the CTr8-C4/CTr20-C4 comparison. On the basis of fold change, we could find back 8 out of those 108 genes, a number that significantly exceeds the 1-2 genes that are expected to occur by chance in a panel of 500 genes. Moreover, the direction in gene expression change matches the phase of the oscillation for these genes (data not shown). Taking into consideration that we only compare two time points (CTr0 and CTr12, the time of isolation of the CTr8-C4 and CTr20-C4 samples, respectively, and corresponding with trough and peak of *Per2::Luc* reporter derived bioluminescence), this number is an underestimation as in this approach genes for which expression peaks considerably out of phase with *Per2* expression escape detection. Therefore, the overrepresentation of true oscillating genes in the CTr8-C4/CTr20-C4 comparison further highlights the presence of robust synchronous circadian oscillations in our liver slice cultures.

Next, we determined for each exposure time the DEGs by comparing the CTr8T4 vs. CTr8C4 and CTr20T4 vs. CTr20C4 samples. By using time-matched DMSO exposed control samples, we exclude non-B[a]P responsive clock controlled genes as well as genes that respond

Table 1. The top 10 upregulated and downregulated genes found at CTr8-T4/CTr8-C4 and CTr20-T4 / CTr20-C4-. A grey background highlight the genes that are unique at one time point. We used a lineal fold change cut-off of ≤ -1.2 or ≥ 1.2.

Upregulated							
CTr8-T4/CTr8-C4				**CTr20-T4/CTr20-C4**			
Genes	**FC**	**P value**	**FDR**	**Genes**	**FC**	**P value**	**FDR**
CYP1A1	19.76	1,40E-08	0,001	CYP1A1	12.11	0	0
CYP1B1	8.94	1,90E-07	0,003	CYP1B1	7.36	1,18E-06	0,003
DCLK3	6.03	1,50E-06	0,011	SERPINE1	5.76	2,28E-07	0,003
SERPINE1	5.27	2,60E-07	0,003	TIPARP	5.64	0	0
TIPARP	5.07	8,60E-08	0,002	DCLK3	2.75	0,00063	0,202
CYP1A2	2.78	1,50E+00	0,006	NRG1	2.6	1,55E-05	0,046
ARHGAP28	2.52	1,50E-04	0,071	NQO1	2.45	6,13E-07	0,006
HPGD	2.19	1,80E-03	0,207	ARHGAP28	2.29	0,00045	0,176
AHRR	2.18	6,80E-06	0,033	P2RY13	2.12	0,00029	0,154
LMO7	2.17	1,40E-05	0,045	CSF2BR*	2.02	5,71E-05	0,088
Downregulated							
CTr8-T4/CTr8-C4				**CTr20-T4/CTr20-C4**			
Genes	**FC**	**P value**	**FDR**	**Genes**	**FC**	**P value**	**FDR**
CCL5	-2.5	7,40E-04	0,215	BHMT	-4.2	3,04E-05	0,064
HAL	-2.24	2,00E-02	0,425	HAL	-3.48	0,00106	0,234
SSTR2	-2.21	6,30E-03	0,345	SSTR2	-2.51	0,00221	0,278
GLS2	-2.19	5,00E-03	0,328	CYP2F1	-2.3	0,00105	0,234
BHMT	-2.08	9,30E-03	0,375	CCL5	-2.26	0,00193	0,267
CYP2F1	-1.88	7,80E-03	0,363	Cyp2a12/Cyp2a22	-2.17	0,00124	0,237
Cyp2a12/Cyp2a22	-1.87	6,00E-03	0,342	GLS2	-2.12	0,00654	0,348
IRX3	-1.69	1,50E-03	0,251	FOXA3	-2.02	0,00105	0,234
FOXA3	-1.6	1,60E-02	0,412	PPM1K	-1.87	5,65E-05	0,088
TAF15	-1.57	0,00059	0,195	TAF15	-1.62	0,00033	0,159

to exposure to the solvent. Given the low number of significant DEGs (i.e. 38 and 36 DEGs at CTr8-T4/CTr8-C4 and 36 DEGs at CTr20-T4/CTr20-C4, respectively; FDR<0.05), precluding analysis of the biological processes and pathways associated with B[a]P exposure at the different time points, we selected the top 1000 DEGs (on the basis of P value) for further analysis, and identified 819 unique and 181 overlapping DEGs in the CTr8-T4/CTr8-C4 and CTr20-T4/CTr20-C4 data sets. Next, we analyzed the fold change differences for the 181 overlapping DEGs and found 101 genes regulated in the same direction (65 upregulated and 36 downregulated) and 80 genes regulated in the opposite direction (40 upregulated and 40 downregulated) for both time points (Suppl. Table 2 and Fig. 4). Table 1 indicates the top 10 upregulated and downregulated genes in CTr8-T4/CTr8-C4 and CTr20-T4/CTr20-C4. The expression levels of nine genes (*Cyp1a1, Cyp1a2, Tiparp, Agxt, Bhmt, Apoa1, Gls2, Car3, Ccl24*) were validated by quantitative RT-PCR (qRT-PCR) (Suppl. Fig. 1C). As expected, most genes display comparable gene expression patterns in both qRT-PCR and transcriptome analysis.

Chronotoxic effects of B[a]P: gene ontology and pathway analysis

The biological processes that respond to B[a]P exposure at CTr8 and CTr20 were identified using Gene Ontology with the DAVID tool, applied to the top 1000 DEGs in the CTr8-T4/CTr8-C4 and CTr20-T4/CTr20-C4 comparisons, respectively. Not completely unexpected, the 181 common DEGs in both CTr8-T4/CTr8-C4 and CTr20-T4/CTr20-C4 data sets (listed in Suppl. Table 2) are associated with biological processes involved in xenobiotic metabolism (Table 2). The biological processes that are unique for the response of liver slices at CTr8 (the time point at which induction of *Cyp1a1* is at its highest) included cell proliferation regulation, as well as cellular macromolecular complex subunit organization. Oppositely, biological processes affected by B[a]P treatment at CTr20 were amine catabolism and organic acid biosynthesis (Table 2).

Subsequently, the B[a]P responsive genes after exposure at CTr8 and CTr20, as identified in the CTr8-T4/CTr8-C4 and CTr20-T4/CTr20-C4 data sets respectively, were submitted to IPA, allowing the identification of biological functions and pathways common and unique for treatment at CTr8 and CTr20. The top 10 canonical pathways identified in the overlapping DEGs after B[a]P exposure at CTr8 and CTr20 included pathways involved in xenobiotic and lipid metabolism (Table 3). However, due to the difference in gene expression and P value of the common overlapping genes, we found "Glucocorticoid receptor signaling" and the "Role of IL7-a in arthritis" after B[a]P exposure at CTr8 and CTr20, respectively, in the list of top 10 canonical pathways (Suppl. Fig. 3).

Furthermore, IPA pathway analysis of the unique DEGs revealed that most pathways show time of day specific responses to B[a]P exposure at CTr8 or CTr20, including "AMPK Signaling", "Glycerolipid Metabolism" and "NF-κB Signaling" at CTr8, and "Glycine, Serine, Threonine Metabolism", "Atherosclerosis Signaling", "Phospholipase C Signaling" and "Leukocyte Extravasation Signaling" at CTr20 (Table 3). However, "Liver X Receptor (LXR)/Retinoid X Receptor (RXR) activation" is identified at both time points, suggesting differential expression of a different set of genes belonging to the same pathway at CTr8 and CTr20. The LXRs are transcription factors involved in the transport and metabolism of steroids and fatty acids, and RXRs are transcriptional activators of several CYP450 enzymes after xenobiotic activation (Xu et al., 2005). Since this comparison is done with the unique DEGs found after B[a]P exposure at CTr8 and CTr20, LXR/RXR activation might be differently affected at these time points.

Next, we analyzed the significant biological functions linked to the biological processes occurring after exposure of liver slices to B[a]P at CTr8 vs. CTr20. The overlapping DEGs after comparison of the CTr8-T4/CTr8-C4 and CTr20-T4/CTr20-C4) data sets identified an increase in biological functions cellular growth and proliferation, lipid and nucleic acid metabolism (Suppl.

Table 2: Gene ontology identified by DAVID. The top 5 biological functions of the common and unique DEGs based on P-value were selected.

2

Upregulated		
CTr8-T4/CTr-C4 vs. CTr20-T4-CTr20-C4 (common DEGs)	**Genes**	**p-values**
xenobiotic metabolic process	AHRR, CYP1B1, CYP2F2, CYP1A1, CYP1A2	2.80E-06
response to xenobiotic stimulus	AHRR, CYP1B1, CYP2F2, CYP1A1, CYP1A2	7.10E-06
benzene and derivative metabolic process	CYP1B1, CYP2F2, CYP1A1, CYP1A2	1.00E-05
dibenzo-p-dioxin metabolic	CYP1B1, CYP1A1, CYP1A2	2.00E-04
toxin metabolic process	CYP1B1, CYP1A1, CYP1A2	6.50E-04

CTr8-T4/CTr8-C4 (unique DEGs)		
regulation of cell proliferation	SAT1, FGFR1, FGFR4, PPARD, NBN, HMX2, APOBEC1, PDGFA, FGFRL1, PPARG, BCL2L1, SOX9, TGFB2, KISS1R, TGFA, INPP5D, TRAF5, LTA, MLL1, IHH, CLEC2I, EFNB1, SF1, IGF1, MBD2, AGER, LEFTY1, PTHLH, ATF5, TNS3, ADRB2, NOTCH1, CDKN1A, SERPINF1, GLMN, IL2	3.80E-05
growth	GDF3, NBN, PPARD, LOC100044968, ZFX, TBCE, IGF1, BCL2L1, MREG, SOX9, TGFB2, LEFTY1, PTHLH, NOTCH1, RASGRP4, IHH	1.20E-03
positive regulation of cell	FGFR1, HMX2, PPARD, FGFR4, PDGFA, EFNB1, IGF1, BCL2L1, AGER, TGFB2, PTHLH, TNS3, ADRB2, CDKN1A, NOTCH1, TGFA, TRAF5, LTA, IHH, IL2	1.60E-03
cellular macromolecular complex subunit organization	HIST1H1C, HP1BP3, CEBPG, NASP, TBCE, MBD2, TARBP2, TUBA8, PSMG1, TSPYL2, TPPP, ICT1, TUBA4A, TUBA1A, ASF1A, H1FOO, HIST1H4H, CLEC2I	1.90E-03
neuron development	FGFR1, IRX5, MYO6, ATL1, AFNB1, KIF5C, TBCE, NTN4, RPE65, RGNEF, TBR1, THY1, TGFB2, ATP7A, NOTCH1, SRPX, CXCR4, ROBO1, PBX3, IHH	2.20E-03

CTr20-T4/CTr20-C4 (unique DEGs)		
amine catabolic process	BCKDHA, AMDHD1, TDO2, MAOA, GLS, DMGDH, PRODH2, AASS, CDO1, TAT, AFMID	1.10E-04
cellular amino acid catabolic process	BCKDHA, AMDHD1, TDO2, GLS, DMGDH, PRODH2, AASS, CDO1, TAT, AFMID	1.30E-04
sulfur metabolic process	BHMT2, STAT5A, GSTT1, CDO1, CSGALNACT1, GSR, GGT6, CTH, GSTK1, MTR, PHGDH, LIAS, HS3ST3B1	1.50E-04
cellular amino acid biosynthetic process	CTH, BHMT2, 4933437F05RIK, MTR, SRR, PHGDH, PRODH2, ALDH4A1, AGXT	1.60E-04
carboxylic acid biosynthetic process	BHMT2, PTGS2, OLAH, 4933437F05RIK, FADS6, AGXT, ACSM1, CTH, MTR, PHGDH, SRR, PRODH2, ALDH4A1, LIAS, ELOVL6, 2010111I01RIK	1.80E-04

2

Table 3). The biological functions identified when liver slices were exposed to B[a]P at CTr8 demonstrated that invasion of mammary tumor cells is increased. However, development of lymphatic system component and development of cancer and metabolism of terpenoid were decreased (Suppl. Table 3). When exposed at CTr20, IPA predicted that the biological functions, tumor genesis, vascularization and growth of tumor to be increased. Moreover, cell viability and transport of molecules was predicted to be decreased.

Taken together, these results demonstrate that a 4 hour B[a]P exposure at different time points during the circadian day (CTr8 and CTr20) elicits common and differential responses in liver slices, which may explain why B[a]P can exert chronotoxic effects.

Table 3: The top 10 Pathways identified by IPA. A grey background highlights the pathways that are unique for each time point. We used a lineal fold change cut-off of ≤ -1.2 or ≥ 1.2.

Overlapping DEGs			
CTr8-T4/CTr8-C4	p-value	CTr20-T4/CTr20-C4	p-value
Arachidonic acid metabolism	3.60E-05	Arachidonic acid metabolism	3.63E-05
Linoleid acid metabolism	0.00012	Linoleid acid metabolism	0.00012
MSP-RON signaling pathway	0.00013	MSP-RON signaling pathway	0.000126
Aryl hydrocarbon receptor signaling	0.00013	Aryl hydrocarbon receptor signaling	0.000129
Xenobiotic metabolism signaling	0.00013	Xenobiotic metabolism signaling	0.000166
Fatty acid metabolism	0.0003	Fatty acid metabolism	0.000302
Metabolism of xenobiotics by CYP450	0.00043	Metabolism of xenobiotics by CYP450	0.000427
HMGB1 signaling	0.00178	HMGB1 signaling	0.001778
Tryptophan metabolism	0.00282	Tryptophan metabolism	0.002818
Glucocorticoid receptor signaling	0.00347	Role of IL-17A in arthritis	0.003548

Unique DEGs			
CTr8-T4/CTr8-C4	p-value	CTr20-T4/CTr20-C4	p-value
LXR/RXR activation	1.10E-03	Tryptophan metabolism	3.16E-04
VDR/RXR activation	0.00182	RhoDGI signaling	0.000389
Clathrin-mediated endocytosis signaling	0.00372	Glycine, Serine, Threonine metabolism	0.000457
IL-17A signaling in gastritic cells	0.00759	Atherosclerosis signaling	0.000562
Hepatic fibrosis/ hepatic stallate cell activation	0.00813	Phospholipase C signaling	0.000646
AMPK signaling	0.01047	Leukocyte extravasation signaling	0.000871
Role of CHK proteins in cell cycle	0.01148	LXR/RXR activation	0.000871
Glycerolipid metabolism	0.01514	Coagylation system	0.001349
NF-κB signaling	0.01995	Lysine degradation	0.003388
Human embryonic stem cell pluripotency	0.02188	Signaling by Rho family GTPases	0.00389

Discussion

The aim of this study was to set up an *ex vivo* chronotoxicity assay to determine whether the toxic response of hepatotoxic compounds depends on the time of day of exposure. To this end, we have chosen to use cultured liver slices as a model system. Although the use of liver slices in toxicological studies is well accepted, there are certain requirements to which an *in vitro*/ *ex vivo* hepatochronotoxicity assay should fit. Firstly, it is important to use a system that is able to metabolize compounds, and secondly, the system must exhibit rhythmic oscillation of core clock and clock controlled genes. After having optimized liver slicing and culture conditions, we have shown that liver slices from *Per2::Luc* clock reporter mice (allowing real time monitoring of circadian phase) can be successfully used as a chronotoxicity assay system. After an adaptation period of approximately two days, liver slices were shown to exhibit stable circadian bioluminescence rhythms and remain viable for up to 7 days. In addition, we confirmed proper performance of the circadian oscillator in the liver slices by qRT-PCR analysis of clock (controlled) genes.

Whereas in most toxicology studies with liver slices treatment with toxic compounds is performed immediately or within 48 hours after slicing (Staal et al., 2008; Harrigan et al., 2004; Harrigan et al., 2006; Plazar et al., 2007), we have chosen to treat the slices around day four, thus (i) circumventing potential negative effects of adjustment to culture environment, and (ii) allowing to determine clock phase and calculate time of treatment. As a model agent, we used B[a]P.

Several studies demonstrated that *Cyp1a1* induction by PAH is regulated in a circadian manner (Tanimura et al., 2011; Qu et al., 2010; Mukai et al., 2008). This induction is mediated by the AHR, which was shown to be under circadian control, indicating that the toxic effects of AHR agonists such as B[a]P and dioxin TCDD might vary depending on the moment of exposure (Shimba and Warabe, 2009). When liver slices were treated with B[a]P, the highest induction of *Cyp1a1* gene expression was seen at CTr8-T4 and the lowest induction at CTr20-T4, which is in phase with the reported circadian rhythm in *Cyp1a1* induction by TCDD (Qu et al., 2009, 2010).

Cyp1a1 is the main CYP450 enzyme responsible for the metabolization of PAHs into reactive species (Roberts-Thomson et al., 1993; Shimada et al., 1996). Elevated levels of *Cyp1a1* are related to an increased risk of cancer progression and have been associated with higher levels of DNA adducts (Geneste et al., 1991; Puga et al., 1997; Raunio et al., 1995). Additionally, several studies have shown that polymorphisms in regions of *Cyp1a1* are also related to increased *Cyp1a1* activity and link it to cancer (Hu et al., 2008; Rojas et al., 2000). *Cyp1a1* is also involved in the detoxification of PAHs (Shi et al., 2010; Uno et al., 2004, 2006). It is therefore possible that depending on the moment of exposure, *Cyp1a1* can either increase carcinogenesis or inactivate PAHs, leading to time dependent effects of exposure to toxic compounds.

The transcriptome data revealed a clear difference in biological functions and pathways when liver slices were exposed to B[a]P at CTr8 or CTr20. Exposure at CTr8 induced an increase in cellular movement and tumor morphology related functions. However, at this time point, the incidence of tumor and cancer was predicted to be decreased. The biological functions of liver slices exposed at CTr20, suggested an increase in cancer while the cell viability was predicted to be decreased. This suggests that B[a]P exposure at CTr20 might influence the expression of genes involved in DNA damage repair and apoptosis, explaining the decrease in cell viability. The *Xpa* gene, involved in nucleotide excision repair (NER), was shown to be under direct control of the CLOCK/BMAL1 complex. Likewise, the XPA protein demonstrated a robust circadian oscillation with a peak and trough at ZT12 and ZT22, respectively (Kang et al., 2009; Sancar et al., 2010). In our liver slice assay, ZT12 corresponds with the time at which B[a]P slices, (mock) treated at CTr8 were collected (CTr8-T4). Since the NER activity peaks around CTr8-T4, the DNA damage caused by B[a]P might be repaired more efficiently at this time point, which may explain the possible chronotoxic effects of B[a]P. At CTr20, the induction of Cyp1a1 is reduced compared to exposure at CTr8. Nevertheless, this might still lead to enough reactive metabolites that may cause DNA adducts damage when not repaired. Interestingly, a combined *in vivo/ in vitro* study by Kesteren et al. (2013) suggests that the common pathways affected by B[a]P treatment of mice or primary hepatocytes are related to xenobiotic metabolism, which is in line with our data. However, cancer-related pathways appeared differentially regulated in the mouse liver, as compared to isolated primary hepatocytes. Our analysis revealed differences in cancer related functions when liver slices were treated at different times. Therefore, in the light of the results presented here, we propose that the differences identified by Kesteren et al (2013) are not intrinsic to the model systems, but may have arisen from differences in the time of day of treatment. It is therefore recommended that toxicology studies are interpreted in relation to the moment of treatment. Unfortunately, this information is usually not provided.

In conclusion, our results provide evidence that B[a]P has chronotoxic properties and when liver slices are treated at defined moments during the day there are differences in gene expression and different pathways and networks are triggered. Our data show the importance of the circadian clock when performing toxicological studies, as treatment at different moments of the day has completely different outcomes.

2

Acknowledgements

References

Amin, K., Ip, C., Sato, B., Le, T., Green, C.E., Tyson, C.A., and Behrsing, H.P. (2006). Characterization of ANIT-induced toxicity using precision-cut rat and dog liver slices cultured in a dynamic organ roller system. Toxicol Pathol 34: 776-84.

Afshari, C.A., Nuwaysir, E.F., and Barrett, J.C. (1999) Application of complementary DNA microarray technology to carcinogen identification, toxicology, and drug safety evaluation. Cancer Res 59: 4759-4760.

Akhtar, R.A., Reddy., A.B., Maywood., E.S., Clayton, J.D., King. V,M., Smith, A.G., Hastings, M.G., and Kyriacou, C.P. (2002) Circadian cycling of the mouse liver transcriptome, as revealed by cDNA microarray, is driven by the suprachiasmatic nucleus. Curr. Biol 12: 540-550.

Boess, F., Kamber, M. Romer, S., Gasser, R., Muller, D., Albertini, S., and Suter, L. (2003). Gene expression in two hepatic cell lines, cultured primary hepatocytes, and liver slices compared to the in vivo liver gene expression in rats: possible implications for toxicogenomics use of in vitro systems. Toxicol Sci 73: 386-402.

Burczynski, M.E., McMillian, M., Ciervo, J.. Li, L., Parker, J,B., Dunn, R.T. 2nd, Hicken, S., Farr, S., and Johnson, M.D. (2000) Toxicogenomics-based discrimination of toxic mechanism in HepG2 human hepatoma cells. Toxicol Sci 58: 399-415.

Chaves, I., Nijman, R.M., Biernat, M.A., Bajek, M.I., Brand, K., da Silva, A.C., Saito, S., Yagita, K., Eker, A.P., and van der Horst, G.T. (2011) The Potorous CPD photolyase rescues a cryptochrome-deficient mammalian circadian clock. PLos One 6:e23447.

de Graaf, I.A., Olinga, P., de Jager, M.H, Merema, M.T, de Kanter, R., van de Kerkhof, E.G., and Groothuis, G.M. (2010) Preparation and incubation of precision-cut liver and intestinal slices for application in drug metabolism and toxicity studies. Nat Protoc 5: 1540-1551.

Dearfield, K.L., Cimino, M.C., McCarroll, N.E., Mauer, I., and Valcovic, L.R. (2002) US Environmental Protection Agency. Genotoxicity risk assessment: a proposed classification strategy. Mutat Res 521: 121-135.

Dearfield, K.L., and Moore, M.M. (2005) Use of genetic toxicology information for risk assessment. Environ Mol Mutagen 46: 236-245.

de Leeuw, W.C., Rauwerda, H., Jonker, M.J., and Breit, T.M. (2008) Salvaging Affymetrix probes after probe-level re-annotation. BMC Res Notes 1:66.

Dipple, A. (1995) DNA adducts of chemical carcinogens. Carcinogenesis 16: 437-441.

Elferink, M.G., Olinga, P., Draaisma, A.L., Merema, M.T., Bauerschmidt, S., Polman, J., Schoonen, W.G., and Groothuis, G.M. (2008) Microarray analysis in rat liver slices correctly predicts in vivo hepatotoxicity. Toxicol Appl Pharmacol 229: 300-309.

Farkas, D., Bhat, V.B., Mandapati, S., Wishnok, J.S. and Tannenbaum, S.R. (2005). Characterization of the secreted proteome of rat hepatocytes cultured in collagen sandwiches. Chem Res Toxical 18: 1132-1139.

Geneste, O., Camus, A.M., Petruzzelli, S., Macchiarini, P., Angeletti, C.A., Giuntini, C., and Bartsch, H. (1991) Comparison of pulmonary DNA adduct levels, measured by 32P-postlabelling and aryl hydrocarbon hydroxylase activity in lung paren-chyma of smokers and ex-smokers. Carcinogenesis 12: 1301-1305.

Hankison, O. (2005) Role of coactivators in transcriptional activation by the aryl hydrocarbon receptor. Arch Biochem Biophys 433: 379-386.

Harrigan, J.A., Vezina, C.M., McGarrigle, B.P., Ersing, N., Box, H.C., Maccubbin, A.E., and Olson, J.R. (2004) DNA adduct formation in precision-cut rat liver and lung slices exposed to benzo[a]pyrene. Toxicol. Sci 77: 307-314.

Harrigan, J.A., McGarrigle, B.P., Sutter, T.R., and Olson, J.R. (2006) Tissue specific induction of cytochrome P450 (CYP) 1A1 and 1B1 in rat liver and lung following in vitro (tissue slice) and in vivo exposure to benzo(a)pyrene. Toxicol In Vitro 20: 426-438.

Hattermer-Frey, H.A., and Travis, C.C. (1991) Benzo-a-pyrene: environmental partitioning and human exposure. Toxicol Ind Health 7: 141-157.

Hogenesch, J.B., Chan, W.K., Jackiw, V.H., Brown, R.C., Gu, Y.Z., Pray-Grant, M., Perdew, G.H., and Brandfield, C.A. (1997) Characterization of a subset of the basic-helix-loop-helix-PAS superfamily that interacts with components of the dioxin signaling pathway. (Translated from eng) J Biol Chem 272: 8581-8593.

Holme, J.A., and Dybing, E. (2002) The use of in vitro methods for hazard characterisation of chemicals. Toxicol Lett 127: 135-141.

Hu, Y., Li, P., Xue, X., Zhou, Z., Li, X., Fu, J., Cohen, B., Roy, N., Li, D., Sun, J., Nan, P., Tang, M.S., and Qu, Q. (2008) PAH-DNA adducts in a Chinese population: relationship to PAH exposure, smoking and polymorphisms of metabolic and DNA repair genes. Biomarkers 13: 27-40.

Hughes, M.E., Ditacchio, L., Hayes, K.R., Vollmers, C., Pulivarthy, S., Baggs, J.E., Panda, S., and Hogenesch, J.B. (2009) Harmonics of circadian gene transcription in mammals. PLos Genet 5:e1000442.

Hussain, S.P., Amstad, P., Raja, K., Sawyer, M., Hofseth, L., Shields, P,G., Hewer, A., Phillips, D.H., Ryberg, D., Haugen, A., and Harris, C.C. (2001) Mutability of p53 hotspot codons to benzo(a)pyrene diol epoxide (BPDE) and the frequency of p53 mutations in nontumorous human lung. Cancer Res 61: 6350-6355.

Irizarry, R.A., Bolstad, B.M., Collin, F., Cope, L.M., Hobbs, B., and Speed, T.P. (2003). Summaries of Affymetrix GeneChip probe level data. Nucleic Acids Res 31:e15.

Kang, T.H., and Sancar A. (2009) Circadian regulation of DNA excision repair: implications for chrono-chemotherapy. Cell Cycle 8: 1665-1667.

Kirkland, D., Pfuhler, S., Tweats, D., Aardema, M., Corvi, R., Darroudi, F., Elhajouji, A., Glatt, H., Hastwell, P., Hayashi, M., Kasper, P., Kirchner, S., Lynch, A., Marzin, D., Maurici, D., Meunier, J.R., Müller, L., Nohynek, G., Parry, J., Parry, E., Thybaud, V., Tice, R., van Benthem, J., Vanparys, P., and White, P. (2007) How to reduce false positive results when un-dertaking in vitro genotoxicity testing and thus avoid unnecessary follow-up animal tests: Report of an ECVAM Workshop. Mutat Res. 628: 31-55.

Ko, C.H. and Takahashi, J.S. (2006) Molecular components of the mammalian circadian clock. Hum Mol Genet 15: 271-277.

Levi, F., and Schibler, U. (2007) Circadian rhythms: mechanisms and therapeutic implications. Annu Rev Pharmacol Toxicol 47: 593-628.

Liebsch, M., Grune, B., Seiler, A., Butzke, D., Oelgeschläger, M., Pirow, R., Adler, S., Riebeling, C., and Luch, A. (2011) Alternatives to animal testing: current status and future perspectives. Arch Toxicol 85: 841-858.

Lowrey, P.L., and Takahashi, J.S. (2004) Mammalian circadian biology: elucidating genome-wide levels of temporal organization. Annu Rev Genomics Hum Genet 5: 407-41.

Lowrey, P.L., and Takahashi, J.S. (2011) Genetics of circadian rhythms in Mammalian model organisms. Adv Genet 74: 175-230.

Miller, B.H., McDearmon, E.L., Panda, S., Hayesm K.R., Zhang, J., Andrews, J.L., Antoch, M.P., Walker, J.R., Esser, K.A., Hogenesch, J.B., and Takahashi, J.S. (2007) Circadian and CLOCK-controlled regulation of the mouse transcriptome and cell proliferation. Proc Natl Acad Sci U S A 104: 3342-3347.

Miller, K.P., and Ramos, K.S. (2001) Impact of cellular metabolism on the biological effects of benzo[a]pyrene and related hydrocarbons. Drug Metab Rev 33: 1-35.

Moronvalle-Halley, V., Sacré-Salem, B., Labbe, G., and Gautier, J.C. (2005) Evaluation of cultured, precision-cut rat liver slices as a model to study drug-induced liver apoptosis. Toxicology 07: 203-214.

Mukai, M., Lin, T.M., Peterson, R.E., Cooke, P.S., and Tischkau, S.A. (2008) Behavioral rhythmicity of mice lacking AhR and attenuation of light-induced phase shift by 2,3,7,8-tetrachlorodibenzo-p-dioxin. J Biol Rhythms 23: 200-210.

Mukhopadhyay, S., Clark, D.R., Watson, N.B., Zacharias, W., and McGragor, W.G. (2004). REV1 accumulates in DNA damage-induced nuclear foci in human cells and is implicated in mutagenesis by benzo[a]pyrenediolepoxide. Nucleic Acids Res 32: 5820-5826.

Ogino, M., Nagata, K., and Yamazoe, Y. (2002) Selective suppressions of human CYP3A forms, CYP3A5 and CYP3A7, by troglitazone in HepG2 cells. Drug Metab Pharmacokinet 17: 42-46

Panda, S., Hogenesch, J.B., and Kay, S.A. (2002) Circadian rhythms from flies to human. Nature 417: 329-335.

Phillips, D.H. (1983) Fifty years of benzo(a)pyrene. Nature 303: 468-472.

Plazar, J., Hreljac, I., Pirih, P., Filipic, M., and Groothuis, G.M. (2007) Detection of xenobiotic-induced DNA damage by the comet assay applied to human and rat precision-cut liver slices. Toxicol In Vitro 21: 1134-1142.

Preitner, N., Damiola, F., Lopez-Molina, L., Zakany, J., Duboule, D., Albrecht, U., and Schibler, U. (2002) The orphan nuclear receptor REV-ERBalpha controls circadian transcription within the positive limb of the mammalian circadian oscillator. Cell 110: 251-260.

Puga, A., Nebert, D.W., McKinnon, R.A. and Menon, A.G. (1997) Genetic polymorphisms in human drug-metabolizing enzymes: potential uses of reverse genetics to identify genes of toxicological relevance. Crit Rev Toxicol 27: 199-222.

Qu, X., Metz, R.P., Porter, W.W., Cassone, V.M., Earnest, D.J. (2009) Disruption of period gene expression alters the inductive effects of dioxin on the AhR signaling pathway in the mouse liver. Toxicol Appl Pharmacol 234: 370-377.

Qu, X., Metz, R.P., Porter, W.W., Neuendorff, N., Earnest, B.J., and Earnest D.J. (2010) The clock genes period 1 and period 2 mediate diurnal rhythms in dioxin-induced Cyp1A1 expression in the mouse mammary gland and liver. Toxicol Lett 196: 28-32.

Raunio, H., Husgafvel-Pursiainen, K., Anttila, S., Hiertanen, E., Hirvonen, A., and Pelkonen, O. (1995) Diagnosis of polymorphisms in carcinogen-activating and inactivating enzymes and cancer susceptibility--a review. Gene 159: 113-121.

2

Richardson, V.M., Santostefano, M.J, and Birnbaum, L.S. (1998) Daily cycle of bHLH-PAS proteins, Ah receptor and Arnt, in multiple tissues of female Sprague-Dawley rats. Biochem Biophys Res Commun 252: 225-231.

Roberts-Thomson, S.J., McManus, M.E., Tukey, R.H., Gonzalez, F.F., and Holder, G.M. (1993) The catalytic activity of four expressed human cytochrome P450s towards benzo[a]pyrene and the isomers of its proximate carcinogen. Biochem Biophys Res Commun 192: 1373-1379.

Rojas, M., Cascorbi, I., Alexandrov, K., Kriek, E., Auburtin, G., Mayerm L., Kopp-Schneider, A., Roots, I., and Bartsch, H. (2000) Modulation of benzo[a]pyrene diolepoxide-DNA adduct levels in human white blood cells by CYP1A1, GSTM1 and GSTT1 polymorphism. Carcinogenesis 21: 35-41.

Rubin, H. (2001) Synergistic mechanisms in carcinogenesis by polycyclic aromatic hydrocarbons and by tobacco smoke: a bio-historical perspective with updates. Carcinogenesis 22: 1903-1930.

Samanta, S.K., Singh, O.V., and Jain, R.K. (2002) Polycyclic aromatic hydrocarbons: environmental pollution and bioremediation. Trends Biotechnol 20: 243-248.

Sancar, A., Lindsey-Bolts, L.A., Kang, T.H., Reardon, J.T., Lee, J.H., and Ozturk, N. (2010). Circadian clock control of the cellular response to DNA damage. FEBS Lett 584: 2618-2625.

Shi, Z., Dragin, N., Gálvez-Peralta, M., Jorge-Nebert, L.F., Miller, M.L., Wang, B., and Nebert, D.W. (2010) Organ-specific roles of CYP1A1 during detoxication of dietary benzo[a]pyrene. Mol Pharmacol 78: 46-57.

Shimada, T., Hayes, C.L., Yamazaki, H., Amin, A., Hecht, S.S. Guengerich, F.P., and Sutter, T.R. (1996) Activation of chemically diverse procarcinogens by human cytochrome P-450 1B1. Cancer Res 56: 2979-2984.

Shimba, S., and Watabe, Y. (2009) Crosstalk between the AHR signaling pathway and circadian rhythm. Biochem Pharmacol 77: 560-565.

Staal, Y.C., van Herwijnen, M.H., Pushparajah, D.S., Umachandran, M., Ioannides, C., van Schooten, F.J., and van Delft, J.H. (2007) Modulation of gene expression and DNA-adduct formation in precision-cut liver slices exposed to polycyclic aromatic hydrocarbons of different carcinogenic potency. Mutagenesis 22: 55-62.

Staal, Y.C., Pushparajah, D.S., van Herwijnen, M.H., Gottschalk, R.W., Maas, L.M., Ioannides, C., van Schooten, F,J, and van Delft, J.H. (2008) Interactions between polycyclic aromatic hydrocarbons in binary mixtures: effects on gene expression and DNA adduct formation in precision-cut rat liver slices. Mutagenesis 23: 491-499.

Storch, K.F., Lipan, O,m Leykin, I., Viswanathan, N., Davis, F.C., Wong, W.H., and Weitz, C.J. (2002) Extensive and divergent circadian gene expression in liver and heart. Nature 417: 78-83.

Tanimura, N., Kusunose, N., Matsunaga, N., Koyanagi, S., and Ohdo, S. (2011) Aryl hydrocarbon receptor-mediated Cyp1a1 expression is modulated in a CLOCK-dependent circadian manner. Toxicology 290: 203-207

Thybaud, V., Aardema, M., Clements, J., Dearfield, K., Galloway, S., Hayashi, M., Jacobson-Kram, D., Kirkland, D., MacGregor, J.T., Marzin, D., Ohyama, W., Schuler, M., Suzuki, H., and Zeiger, E. (2007) Expert Working Group on Hazard Identification and Risk Assessment in Relation to In Vitro Testing. Mutat Res 627: 41-58.

Tischkau, S.A., Jaeger, C.D., and Krager, S.L. (2011) Circadian clock disruption in the mouse ovary in response to 2,3,7,8-tetrachlorodibenzo-p-dioxin. Toxicol Lett 201:116-122.

Ueda, H.R., Chen, W., Adachi, A., Wakamatsu, H., Hayashi, S., Tajasugi, T., Nagano, M., Nakahama, K., Suzuki, Y., Sugano, S., Lino, M., Shigeyoshi, Y., and Hashimoto, S. (2002) A transcription factor response element for gene expression during circadian night. Nature 418: 534-539.

2

Uno, S., Dalton, T.P., Derkenne, S., Curran, C.P., Miller, M.L., Shertzer, H.G. and Nebert, D.W. (2004) Oral exposure to benzo[a]pyrene in the mouse: detoxication by inducible cytochrome P450 is more important than metabolic activation. Mol Pharmacol 65: 1225-1237.

Uno, S., Dalton, T.P., Dragin, N., Curran, C.P., Derkenne, S., Miller, M.L., Shertzer, H.G. Gonzales, F.J. and Nebert, D.W. (2006) Oral benzo[a]pyrene in Cyp1 knockout mouse lines: CYP1A1 important in detoxication, CYP1B1 metabolism required for immune damage independent of total-body burden and clearance rate. Mol Pharmacol 69: 1103-1114.

Van Delft, J.H., van Agen, E., van Breda, S.G, Herwijnen, M.H., Staal, Y.C., and Kleinjans, J.C. (2004) Discrimination of genotoxic from non-genotoxic carcinogens by gene expression profiling. Carcinogenesis 25: 1265-1276.

Van Kesteren, P.C., Zwart, P.E., Schaap, M.M., Pronk, T.E., van Herwijnen, M.H., Kleinjans, J.C., Bokkers, B.G., Godschalk, R.W., Zeilmaker, M.J., van Steeg, H., and Luijten, M. (2013) Benzo[a]pyrene-induced transcriptomic responses in primary hepatocytes and in vivo liver: Toxicokinetics is essential for in vivo-in vitro comparisons. Arch. Toxicol 87: 505-515

Vickers, A.E., and Fisher, R.L. (2004) Organ slices for the evaluation of human drug toxicity. Chem Biol Interact 150: 87-96.

Wilkening, S., Stahl, F., and Bader, A. (2003) Comparison of primary human hepatocytes and hepatoma cell line HepG2 with regard to their biotransformation properties. Drug Metab. Dispos 31: 1035–1042.

Wogan, G.N. (1989) Markers of exposure to carcinogens. Environ Health Perspect 81: 9-17.

Wolterbeek, A.P., Schoevers, E.J., Bruyntjes J.P., Rutten, A.A., and Feron, V.J. (1995) Benzo[a]pyrene-induced respiratory tract cancer in hamsters fed a diet rich in beta-carotene. A histomorphological study. J Environ Pathol Toxicol Oncol 14: 35-43.

Xiao, H., Rawal, M., Hahm, E.R., and Singh, S.V. (2007) Benzo[a]pyrene-7,8-diol-9,10-epoxide causes caspase-mediated apoptosis in H460 human lung cancer cell line. Cell Cycle 6: 2826-34

Xu, C., Li, C.Y., and Kong A.N. (2005) Induction of phase I, II and III drug metabolism/transport by xenobiotics. Arch Pharm Res 28: 249-268.

Yoo, S.H., Yamazaki, S., Lowrey, P.L., Shimomura, K., Ko, C.H., Buhr, E.D., Siepka, S.M., Hong,H.K., Oh, W.J., Yoo, O.J., Menaker, M., and Takahashi, J.S. (2004) PERIOD2::LUCIFERASE real-time reporting of circadian dynamics reveals persistent circadian oscillations in mice peripheral tissues. Proc Natl Acad Sci U S A 101: 5339-5346.

A
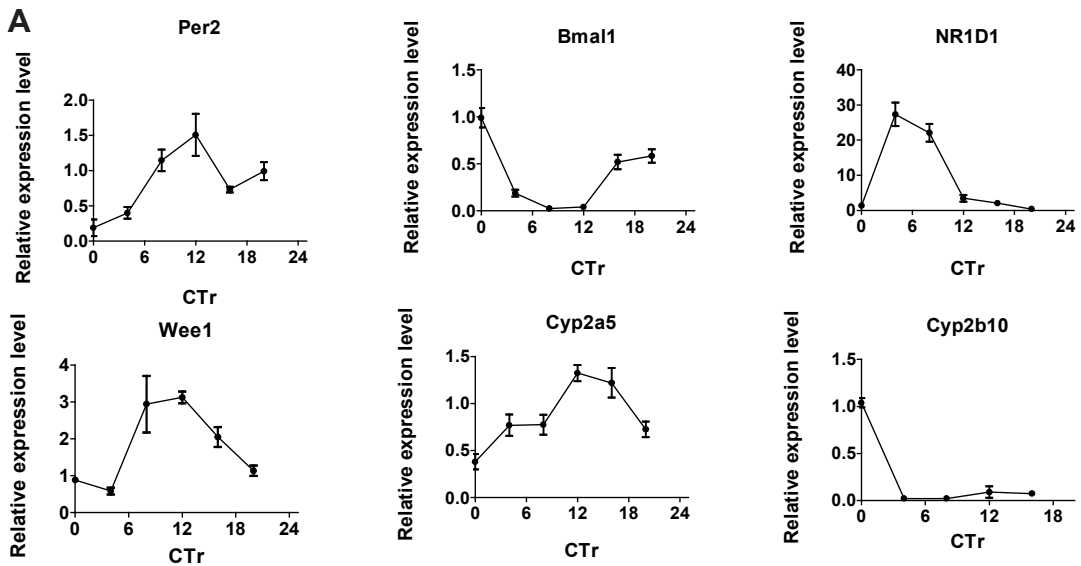
B

Genes	Tau	pAnova	p1
Per2	24	0.0008	0.0025
Cyp2a5	24	0.0005	0.0002
Bmal1	24	0	0
Nr1d1	24	0	0.0001
Wee1	24	0.0007	0.0002
Cyp2b10	24	0	0

C

Validation gene expression by RT-PCR				
	CTr8-T4		**CTr20-T4**	
Genes	**RT-PCR**	**Microarray**	**RT-PCR**	**Microarray**
Cyp1a1	64.61	19.76	16.96	12.11
Cyp1a2	5.34	2.78	3.06	1.89
Tiparp	10.27	5.07	7.14	5.64
Agxt	0.96	1.45	0.43	0.46
Bhmt	0.45	0.48	0.15	0.2
Apoa1	0.91	1.08	0.31	0.68
Gls2	0.81	0.46	0.52	0.47
Car3	1.44	0.88	0.16	0.44
Ccl24	0.91	1.06	1.97	1.46

Supplementary Figure 1: identification of circadian rhythms of core clock genes and clock control genes in liver slices. A. Core clock gene (*Per2, Bmal1,* and *Rev-Erbα)* and clock controlled gene (*Wee1, Cyp2a5* and *Cyp2b10*) expression profiles in liver slices harvest every 4 hrs. (n = 4). B. Statistical analysis of expression profiles. The relative mRNA levels were analyzed by CircWave in order to statistically test if there is a circadian oscillation. We used the P-ANOVA test and a Harmonic regression to calculate the shape of the oscillation. C. qRT-PCR validation of micro array data. Validate microarray analysis by analyzing a few genes by qRT-PCR. Table indicates the lineal fold change found by microarray and qRT-PCR.

2

Number of genes present in existing databases
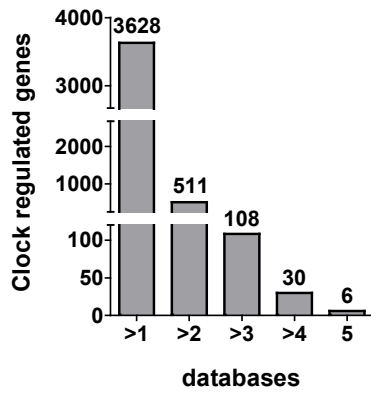
Supplementary Figure 2: Identification of true circadian regulated genes in existing dataset. Number of circadian regulated genes identified by Miller et al., 2002, Akhtar et al., 2002, Panda et al., 2002, Ueda et al., 2002 and Hughes et al., 2009.

Supplementary Table 1 True circadian regulated genes identified in more than 3 existing dataset. List demonstrated the circadian regulated genes identified by Miller et al., 2002, Akhtar et al., 2002, Panda et al., 2002, Ueda et al., 2002 and Hughes et al., 2009 that are present in more than 3 datasets. The 8 DEGs in the CTr8-C4/ CTr20-C4 comparison that were identified as true oscillating genes are present in grey.

2

Clock controlled genes	Akhtor	Miller	Huges	Panda	Ueda	Total
1110007M04Rik	0	0	1	1	1	3
1300001I01Rik	0	1	1	1	0	3
1300002A08Rik	0	0	1	1	1	3
1810063B05Rik	0	0	1	1	1	3
2810425J22Rik	0	1	0	1	1	3
3732413I11Rik	0	0	1	1	1	3
Adfp	0	1	1	1	0	3
Agxt	0	1	1	1	0	3
Ahcy	0	0	1	1	1	3
AI842396	0	1	1	0	1	3
Ak2	0	1	1	0	1	3
Ak4* (Ak4)	0	1	0	1	1	3
Aqp8	0	1	1	0	1	3
Arl6ip2	0	0	1	1	1	3
Atp1a1	0	1	1	1	0	3
Avpr1a (avpr1)	0	1	1	1	0	3
BC004728	0	1	1	0	1	3
Bhmt	0	1	1	1	0	3
Bri3	0	0	1	1	1	3
Btg1	0	1	1	0	1	3
Car14	**0**	**1**	**1**	**0**	**1**	**3**
Casp6	1	1	1	0	0	3
Cdh1	1	1	1	0	0	3
Cebpb	0	0	1	1	1	3
Cldn1	0	1	1	0	1	3
Clock	0	1	1	0	1	3
Crot	1	1	1	0	0	3
Cyp2a4	1	0	1	0	1	3
Cyp7a1	0	0	1	1	1	3
Cyp8b1	**0**	**1**	**1**	**0**	**1**	**3**
D3Ucla1	0	0	1	1	1	3
Ddc	**1**	**1**	**1**	**0**	**0**	**3**
Dscr1	0	1	1	0	1	3
Egr1	1	0	1	1	0	3
Elovl3	0	1	1	1	0	3
Enpep	1	0	1	1	0	3

2

Clock controlled genes	Akhtor	Miller	Huges	Panda	Ueda	Total
Esrra	1	0	1	0	1	3
Fgb	0	1	1	1	0	3
Fgf1	0	0	1	1	1	3
Fh1	0	0	1	1	1	3
Gabarapl1	0	1	1	0	1	3
Gdap10	0	0	1	1	1	3
Gstt2	1	1	1	0	0	3
Herpud1	0	0	1	1	1	3
Hes6	0	1	1	0	1	3
Hsp105	1	1	0	0	1	3
Hspa8	0	0	1	1	1	3
Igfbp2	1	1	1	0	0	3
Igfbp4	1	0	0	1	1	3
Krt1 -18	0	0	1	1	1	3
Krt2 -8	0	0	1	1	1	3
Mapk14	1	0	0	1	1	3
Mbl2	1	1	0	1	0	3
Mgea5	0	1	1	0	1	3
Nfix	1	0	1	1	0	3
Npc1	0	0	1	1	1	3
Pah	1	1	1	0	0	3
Pbx1	1	0	0	1	1	3
Pdk4	0	1	1	0	1	3
Peci	0	1	1	1	0	3
Ppp1r3c	0	1	1	0	1	3
Psen2	0	1	1	0	1	3
Rbpms	0	0	1	1	1	3
Rdh7	0	1	1	1	0	3
Rev -ErbAalpha (NR1D1)	0	1	1	0	1	3
Rgs16	0	1	1	0	1	3
RORgamma (rorc)	**0**	**0**	**1**	**1**	**1**	**3**
S100a10 (calgizzarin)	0	1	1	0	1	3
Sc5d	0	1	1	1	0	3
Sfrs5	0	0	1	1	1	3
Slc10a1	0	1	1	1	0	3
Slc2a2	**0**	**1**	**1**	**0**	**1**	**3**

Clock controlled genes	Akhtor	Miller	Huges	Panda	Ueda	Total
Sqstm1 (osi)	0	0	1	1	1	3
Stra13 (Bhlhb2)	0	1	1	0	1	3
Tfdp1	1	0	1	1	0	3
Ulk1	1	0	1	0	1	3
Uox	**0**	**1**	**1**	**1**	**0**	**3**
Wee1	1	1	1	0	0	3
1810015C04Rik	0	1	1	1	1	4
Adh4* (Adh4)	0	1	1	1	1	4
Alas1	0	1	1	1	1	4
Atf5	0	1	1	1	1	4
Bmal1 (Arntl)	1	1	1	0	1	4
Bnip3	0	1	1	1	1	4
Cd9	0	1	1	1	1	4
Cdo1	0	1	1	1	1	4
Cpt1a	1	0	1	1	1	4
E4BP4 (Nfil3)	**0**	**1**	**1**	**1**	**1**	**4**
Fkbp4* //Fkbp4	0	1	1	1	1	4
Hmgcr	0	1	1	1	1	4
Hsd17b2	0	1	1	1	1	4
Mknk2	0	1	1	1	1	4
Ndrg1// Ndrl	0	1	1	1	1	4
Pnp	1	0	1	1	1	4
Por	1	0	1	1	1	4
Ppara	1	0	1	1	1	4
Ptp4a1	0	1	1	1	1	4
Serpinf2	0	1	1	1	1	4
Slc9a3r1	0	1	1	1	1	4
Tfpi2	0	1	1	1	1	4
Tubb5	1	0	1	1	1	4
Wrnip1 (Wrnip)	1	1	1	1	0	4
Col4a1	1	1	1	1	1	5
Fdx1	1	1	1	1	1	5
Hal	1	1	1	1	1	5
Map2k3	1	1	1	1	1	5
Per2	**1**	**1**	**1**	**1**	**1**	**5**
Usp2	1	1	1	1	1	5

Supplementary Table 2: common DEGS identified at CTr8-T4/CTr8-C4 and CTr20-T4/CTr20-C4. The 181 common DEGs identified after comparison of the CTr8-T4/CTr8-C4 and CTr20-T4/CTr20-C4 data sets. Fold changes are indicated. The grey background marks for which gene expression changes in the same direction in gene expression at both time points.

Overlapping genes	CTr8-T4/ CTr8-C4	CTr20-T4/ CTr20-C4	Overlapping genes	CTr8-T4/ CTr8-C4	CTr20-T4/ CTr20-C4
1700054O10Rik	1.16	-1.16	Lepr	1.26	-1.12
1700056N10Rik	1.27	-2.12	Lin54	1.18	-1.16
1810013L24Rik	1.16	-1.37	Lrrc42	-1.15	2.28
2010001J20Rik	-1.11	1.42	Lcrc46	-1.26	1.20
2010011I20Rik	-1.39	1.55	Malt1	1.24	-1.32
4930434J08Rik	2.08	-1.54	Meox2	-1.12	1.29
9430051O21Rik	-1.25	1.26	Nefl	1.31	-1.39
Acox2	-1.26	1.34	Npat	1.16	1.41
Adamts6	-1.49	1.20	Nrg1	2.16	-1.46
Ahdc1	-1.18	1.16	Nuak2	-1.35	2.75
AI413194	1.15	-1.19	P2ry5	1.47	-1.73
AW987390	1.35	-1.18	Pard3b	-1.43	1.38
BC004728	-1.20	1.89	Pde8a	-1.11	1.28
BC032203	1.12	-1.13	Pik3r5	-1.29	1.26
Btnl9	-1.29	1.20	Ppm1k	-1.49	1.26
C79557	1.12	-1.14	Ptgs1	1.47	-1.12
Cbr3	1.49	-1.14	Rbm7	1.11	-1.11
Cbr4	-1.17	1.20	Rbpms	-1.14	1.13
Cd274	1.39	-1.13	Rbpms2	-1.21	1.44
Cpeb4	1.36	-1.87	Rcbtb2	1.17	-1.18
Creb3l1	1.57	-1.21	Samd7	-1.19	1.11
Csf1	-1.37	1.25	Sbk1	2.11	-4.20
Csf2rb	1.68	-3.48	Sdccag10	-1.69	1.39
Cyp2a12	-1.87	1.57	Setd3	1.19	-1.45
Cyp2f2	-1.88	1.27	Slc7a11	1.61	-1.62
Dci	-1.15	1.26	Snx20	-1.22	1.18
Dclk3	6.03	-1.55	Sorbs3	1.21	-1.22
Dmrt3	-1.44	1.87	Sstr2	-2.21	1.78
Dsg2	-1.28	1.19	Tbp	-1.21	2.60
ENSMUSG0000007398	-1.69	1.18	Tenc1	-1.23	1.80
Galc	-1.54	1.64	Tifab	1.29	-1.35
Gatad2b	-1.24	1.14	Tk1	1.59	-2.17
Gls2	-2.19	1.43	Tpst1	-1.13	1.29
Glyat	-1.39	1.14	Trex2	-1.14	1.29
Gtf3c3	1.13	-1.11	Txnl4a	1.17	-1.24
Hal	-2.24	1.31	Uba3	1.18	-1.14
Hpgd	2.19	-1.34	Usp42	1.10	-1.46
Iffo2	1.53	-1.40	Wsb1	1.25	-1.11
Josd1	1.20	-1.32	Zfp213	-1.20	1.29
Klhl9	1.14	-1.38	Zfp87	1.28	-1.12

Overlapping genes	CTr8-T4/ CTr8-C4	CTr20-T4/ CTr20-C4	Overlapping genes	CTr8-T4/ CTr8-C4	CTr20-T4/ CTr20-C4
100042616	-1.23	-1.53	Dfna5h	1.97	1.34
1110031I02Rik	-1.11	-1.15	Dock4	1.50	1.90
2700038C09Rik	-1.17	-1.39	Edc3	1.90	1.77
3110035C09Rik	1.44	1.42	EG624866	1.79	2.02
4921509J17Rik	1.52	1.34	Eme2	-1.15	-1.11
9130221J17Rik	1.32	1.33	Entpd2	1.42	1.54
9430076G02Rik	-1.18	-1.64	Erbb2ip	1.15	1.28
9530006C21Rik	-1.27	-1.20	Exoc3	1.32	1.28
9630050E16Rik	-1.38	-1.46	Fbxl5	1.19	1.41
AA386476	-1.23	-1.41	Foxa3	-1.60	-1.14
Abcd6	-1.16	-1.18	Frat2	-1.23	-1.25
Acot4	1.56	1.34	Gas2l3	1.37	1.33
Add2	-1.11	-1.16	Glis3	1.63	1.20
Aftph	1.20	1.35	Gnat2	-1.39	-1.23
Ahrr	2.18	1.60	Hspa4l	1.34	1.27
AI415730	1.31	1.42	Hyal1	-1.40	-1.19
AL023051	-1.16	-2.02	Il1r1	1.69	1.12
Amot	1.33	1.56	Irx3	-1.69	-1.22
Amz1	1.48	1.21	Klf7	-1.26	-2.51
Ankrd10	1.51	1.29	Krit1	1.25	1.14
Ankrd27	-1.12	-1.34	Lincr	1.90	1.63
Arhgap28	2.52	1.73	Lmo7	2.17	1.63
Arl6ip5	1.72	1.62	LOC74457	1.77	1.50
Avl9	1.09	1.20	Lrp4	2.12	1.83
Bcl2l11	1.72	1.35	Mad2l2	-1.23	-1.37
Bhmt	-2.07	-1.12	Mefv	1.44	1.14
C130050O18Rik	1.81	1.64	Naga	-1.14	-1.19
C430049A07Rik	1.10	1.21	Nfe2l2	1.54	5.76
C78878	-1.20	-1.12	Nfkbil1	-1.26	-1.31
Ccl5	-2.50	-2.30	Nqo1	2.15	2.15
Cenpc1	1.19	1.40	Nrp1	-1.33	-2.26
Cib2	1.30	1.29	Onecut1	-1.54	-1.48
Cldnd1	1.27	1.13	P2ry13	1.97	1.77
Clpx	-1.30	-1.23	Pdcl	1.23	1.62
Comt1	1.43	1.20	Pik3r3	2.15	1.56
Csf2rb2	1.54	1.63	Pkm2	1.52	1.26
Cyp1a1	19.76	12.11	Plk2	1.28	1.19
Cyp1a2	2.78	7.36	Plscr2	1.69	1.60
Cyp1b1	8.94	2.45	Ppp1cb	1.14	1.63
D430019H16Rik	1.27	1.17	Prox1	-1.23	-1.08

2

Overlapping genes	CTr8-T4/ CTr8-C4	CTr20-T4/ CTr20-C4
Prpf40b	-1.19	1.33
Rnf181	-1.15	-1.16
Rtn4rl2	1.72	1.71
S1pr3	1.84	1.35
Sall2	1.20	1.71
Sema3e	-1.20	-1.13
Serpine1	5.27	1.43
Slc12a6	1.37	1.71
Slc28a3	-1.31	-1.12
Spag17	-1.39	-1.30
Taf15	-1.57	-1.24
Taf1b	-1.17	-1.35
Thap4	-1.17	-1.37
Tiparp	5.07	5.64
Tnfaip2	1.58	2.12
Usp14	1.16	1.45
Usp6nl	1.14	1.15
Xdh	1.47	1.47
Ythdc1	1.17	1.16
Zfp28	1.47	1.59
Zfp326	1.35	1.22

Supplementary Table 3: Biological functions identified at CTr8-T4/CTr8-C4 and CTr20-T4/CTr20-C4 by IPA. The predicted increased and decreased biological functions by IPA for CTr8-T4 and CTr20-T4 for both the overlapping and the unique DEGs. Biofunctions with a Activation z-score of >2 or <-2 are shown.

Biological functions CTr8-T4/ CTr8-C4 common			
Category	**Functions Annotation**	**Activation z-score**	**#**
Increased			
Cellular Development	proliferation of tumor cell lines	2.897	18
Cellular Growth and Proliferation	proliferation of tumor cell lines	2.897	18
Cellular Growth and Proliferation	proliferation of cells	2.566	36
Small Molecule Biochemistry	conversion of lipid	2.197	5
Lipid Metabolism	conversion of lipid	2.197	5
Small Molecule Biochemistry	oxidation of lipid	2.194	6
Lipid Metabolism	oxidation of lipid	2.194	6
Energy Production	oxidation of lipid	2.194	6
Nucleic Acid Metabolism	metabolism of nucleic acid component or derivative	2.161	12
Biological functions CTr20-T4/CTr20-C4 common			
Category	**Functions Annotation**	**Activation z-score**	**#**
Increased			
Cellular Growth and Proliferation	proliferation of tumor cell lines	2.897	18
Cellular Growth and Proliferation	proliferation of cells	2.737	34
Small Molecule Biochemistry	conversion of lipid	2.197	5
Lipid Metabolism	conversion of lipid	2.197	5
Small Molecule Biochemistry	oxidation of lipid	2.194	6
Lipid Metabolism	oxidation of lipid	2.194	6
Energy Production	oxidation of lipid	2.194	6
Nucleic Acid Metabolism	metabolism of nucleic acid component or derivative	2.161	12
Hematological System Development and Function	Hematocrit	2	4

Biological functions CTr8-T4/CTr8-C4 unique			
Category	**Functions Annotation**	**Activation z-score**	**#**
increased			
Cellular Movement	invasion of mammary tumor cells	2.236	5
Tumor Morphology	invasion of mammary tumor cells	2.236	5
decreased			
Lymphoid Tissue Structure and Development	development of lymphatic system component	-2.2	14
Cancer	incidence of tumor	-2.155	11
Tissue Development	development of connective tissue	-2.102	14
Cellular Development	differentiation of blood cells	-2.073	28
Hematological System Development and Function	differentiation of blood cells	-2.073	28
Lipid Metabolism	metabolism of terpenoid	-2.039	14
Small Molecule Biochemistry	metabolism of terpenoid	-2.039	14
Vitamin and Mineral Metabolism	metabolism of terpenoid	-2.039	14
Cellular Development	differentiation of leukocytes	-2.023	26
Hematological System Development and Function	differentiation of leukocytes	-2.023	26
Hematopoiesis	differentiation of leukocytes	-2.023	26
Tissue Morphology	quantity of connective tissue cells	-2.005	10
Connective Tissue Development and Function	quantity of connective tissue cells	-2.005	10
Biological functions CTr20-T4/CTr20-C4 unique			
Category	**Functions Annotation**	**Activation z-score**	**#**
increased			
Cancer	Tumorigenesis	3.236	145
Cardiovascular System-Development and Function	Vascularization	2.758	15
Cancer	growth of tumor	2.65	16
Tissue Development	mammary gland development	2.335	10
Organismal Development	mammary gland development	2.335	10
Reproductive System-Development and Function	mammary gland development	2.335	10
Immunological Disease	immediate hypersensitivity	2.236	16
Cell Morphology	shape change of fibroblast cell lines	2.213	6
Connective Tissue Development and Function	shape change of fibroblast cell lines	2.213	6
Cellular Movement	migration of prostate cancer celllines	2.166	5
Cell Cycle	Mitogenesis	2.019	10
decreased			
Cell Death	cell viability of muscle cells	-2.219	5
Skeletal and Muscular System-Development and Function	cell viability of muscle cells	-2.219	5
Molecular Transport	transport of molecule	-3.546	49

Chapter 3

Chronotoxic and chronomutagenic properties of benzo[a]pyrene, assessed in cultured mouse primary hepatocytes

Annelieke S. de Wit, Inês Chaves, Edwin Zwart, António Carvalho da Silva, Harry van Steeg, Mirjam Luijten, Gijsbertus T.J. van der Horst

3

Abstract

Worldwide, many efforts are undertaken to establish *in vitro* alternatives for the use of animals in chemical risk assessment assays. Given the prominent role of the liver in xenobiotic metabolism, comprising both bioactivation and detoxification of chemicals, considerable attention is given to primary hepatocytes as a model system for hepatotoxicity. Over the last decade, it has become strikingly clear that the metabolic activation and detoxification of chemical compounds is controlled by the circadian clock. Accordingly, though largely ignored in the toxicology field thus far, the toxic outcome of chemical exposure not only depends on exposure time, but also on time of day of exposure, which is known as chronotoxicity. Here, we show that mouse primary hepatocytes from *Per2::Luc* circadian clock reporter mice can be maintained in a collagen sandwich culture for at least 14 days, while retaining hepatocyte-specific gene expression and functions. Importantly, circadian clock performance in synchronized mouse primary hepatocytes could be visualized by time lapse bioluminescence imaging, allowing exposure studies at defined phases of the circadian clock. Exposure of synchronized cell cultures to the environmental carcinogen benzo[a]pyrene (B[a]P) at 4 hour intervals revealed a distinct time-of-day dependent difference in the induction of *Cyp1a1* gene expression, the peak of which coincided with that of *Per2* clock gene expression. Moreover, using primary hepatocytes from the pUR288 LacZ mutation reporter, we show that at this time point B[a]P has the highest mutagenic potential. In conclusion, these data not only provide the first demonstration that chemical mutagenesis can be under circadian control, but also show the applicability of this novel mouse primary hepatocyte-based *in vitro* chronotoxicity assay for chronotoxic risk analysis.

Introduction

Toxicity can be defined as the ability of a substance to cause damage to the cells and tissues of a living organism. Although dose is considered the most important determinant of toxicity, followed by duration (exposure time) and frequency (number of exposures), it has become evidently clear that also time of exposure (i.e. the moment of the day) can modulate toxic responses. This is well illustrated by the observation that mice injected with cyclophosphamide at the end of the day show a higher survival than litter mates injected at the end of the night (Gorbacheva et al., 2005). Likewise, time of day dependent tolerability has been shown for over 30 anticancer drugs (reviewed by Ohdo, 2007). This phenomenon is known as chronotoxicity and finds its origin in the fact that mammalian behavior, physiology and metabolism are regulated by an internal time keeping mechanism, referred to as the circadian clock.

The mammalian circadian system is composed of a self-sustained master clock in the neurons of the Suprachiasmatic Nuclei (SCN) in the brain. As these cellular clocks have a near (circa) 24 hour (dies) periodicity, they are daily reset by light to keep pace with the light-dark cycle. Likewise, virtually all organs and cells contain their own (light-insensitive) clock, referred to as peripheral clocks, which remain synchronized by humoral stimuli originating from the SCN master clock (Takahashi et al., 2008). At the molecular level, circadian rhythms in SCN neurons and peripheral cells are generated by transcription/translation feedback loops (TTFL) composed of a set of clock genes and proteins (reviewed by Dibner et al., 2010). In short, the main loop consists of the CLOCK/BMAL1 heterodimeric transcription activator complex that induces transcription of the *Cryptochrome* (*Cry1, Cry2*) and *Period* (*Per1, Per2*) genes through E-box elements in their promoters. PER/CRY complexes in turn dislocate BMAL1/CLOCK complexes from these regions, thus inhibiting transcription of their own genes. Similarly, the CLOCK/BMAL1 complex drives rhythmic transcription of a set of E-box promoter containing clock controlled genes that couple the molecular oscillator to circadian output processes. Among these clock-controlled genes are transcription factor genes that further relay rhythmicity to other output genes with a phase different from that of E-box genes (Kumaki et al., 2008; Lowrey and Takahashi, 2011). Following these mechanisms, over 10% of a tissues transcriptome is under circadian control. Among the clock controlled processes are cell metabolism (including xenometabolism and antioxidant defense)

and the DNA damage response (including DNA repair, cell cycle progression, thus explaining an organism's sensitivity to toxic agents in relation to the moment of exposure (Akhtar et al., 2002; Hughes et al., 2009; Panda et al., 2002).

Our society demands environmental, industrial and pharmaceutical chemicals to be tested for adverse health effects. Despite the availability of established *in vitro* assays, human health risk assessment still requires the use of laboratory animals for hazard identification and risk estimation. In order to comply with the European regulations regarding the use of laboratory animals, new alternative *in vitro* systems are being developed to reduce, and ultimately replace animal experiments. Often, difficulties are encountered when comparing similar data from different labs or when extrapolating *in vitro* results to *in vivo* risk analysis studies, especially in the field of pharmacology, toxicology, and toxicogenomics (Eisenbranda et al., 2002; Kienhuis et al., 2011; Oberemm et al., 2005). These dissimilarities may find their origin in that most of the animal and cell/ tissue-based studies ignore the impact of the circadian clock. For instance, we have recently shown a 10-fold difference in the number of responsive genes and pathways in the liver transcriptome of mice exposed to cyclophosphamide during the day or during the night, highlighting the importance of providing information on time of day of exposure for *in vivo* toxicogenomics studies (Van Dycke et al., 2014). When explanted from the body, tissues and cells retain their individual endogenous clocks, but upon subsequent culturing in the absence of synchronizing stimuli from the master clock in the brain, these clocks rapidly desynchronize (Yoo et al., 2004) Moreover, as serum has been shown to resynchronize the circadian clocks of individual cultured cells (Balsalobre et al., 2000), timing of cell passaging and/or medium replacement impinges on the phase of the circadian clock and thus cellular (Mazzoccoli et al., 2012) and xenobiotic metabolism (Claudel et al., 2007). Adding to the complexity is our observation that DNA damage, introduced by treatment of cells with genotoxic agents, can resynchronize or phase shift the circadian clock (Oklejewicz et al., 2008). Thus, (uncontrolled) timing of medium refreshment and (geno)toxic exposure itself may affect the outcome of an *in vitro* toxicity experiment.

To circumvent aforementioned sources for intraexperimental variation, we have previously proposed a setup for *in vitro* toxicity assays in which (i) individual cellular clocks of the cultured cells are synchronized prior to toxic exposure, and (ii) exposure is started at defined phases of the circadian clock (Destici et al., 2009). Acknowledging this additional layer of complexity not only leads to higher predictive value of *in vitro* systems, but also provides insight in potential chronotoxic properties of chemical compounds. Benzo[a]pyrene (B[a]P), for example, is a pro-carcinogen that requires the subsequent action of CYP1A1, epoxide hydrolase and CYP1B1 to be converted into the highly genotoxic metabolite B[a]P-7,8-diol 9,10-epoxide (BPDE) (Miller and Ramos, 2001; Xiao and Singh, 2007), which forms cytotoxic and mutagenic BPDE-DNA adducts (Dipple, 1995; Rubin, 2001). B[a]P activates the aryl hydrocarbon receptor (AhR) signaling pathway by binding to the AhR, which in turn leads to the induction of several *Cyp450* genes, including *Cyp1a1* (reviewed by De Wit et al., 2014). Using an *ex vivo* mouse liver slice system, we have recently shown that B[a]P-mediated *Cyp1a1* induction follows a circadian pattern, suggesting that B[a]P has chronotoxic properties.

Because the liver is the major organ involved in xenobiotic metabolism, many *in vitro* chemical toxicity assays involve liver-derived systems such as primary hepatocytes (reviewed by Hewitt et al., 2007; Ramboer et al., 2013). In the present study, we optimized culturing conditions for mouse primary hepatocytes for analysis of chronotoxic properties of chemical compounds. Using mouse primary hepatocytes from *Per2::Luc* clock reporter mice, grown in a collagen sandwich, we show that cells can be maintained for at least 14 days, while retaining stable hepatocyte specific gene expression, metabolic functioning and circadian clock performance. To determine the potency of this *in vitro* liver model system for use in chronotoxic risk analysis assays, we treated the cells with B[a]P at defined phases of the circadian clock and demonstrate that this environmental genotoxin not only acts as a chronotoxicant, but also as a chronomutagen.

3

Materials & methods

Animals

Per2::Luc circadian clock reporter mice expressing the firefly luciferase gene from the *Period2* promoter (Chaves et al., 2011), and pUR288 LacZ mutation reporter mice (Boerrigter et al., 1995; Dollé et al., 1996), all backcrossed to a C57BL/6J genetic background, were housed at the Animal Resource Facility of the Erasmus University Medical Center, which operates in compliance with the European guidelines (European Community 1986) and the Dutch legislation for the protection of research animals. Mice were kept in a climate controlled room in a 12 light/12h dark cycle, with ad libitum access to food and water. All studies were approved by the Dutch Animal Ethical Committee under permit numbers EMC2027 and EMC2382.

Primary hepatocyte isolation, plating and maintenance

Primary hepatocytes were isolated from 10-16 week old male *Per2::Luc* and pUR288 LacZ mice by a two-step collagenase perfusion method (Seglen, 1976) with modifications. In short, animals were anesthetized with an intraperitoneal injection with pentobarbital (300 μg/g body weight) and the liver was perfused in situ via cannulation of the abdominal vena cava using wash buffer, composed of Hank's balanced salt solution (HBSS; Invitrogen) without phenol red, Mg^{2+} and Ca^{2+} and supplemented with 10 mM Hepes (Lonza) and 16 mM $NaHCO_3$ at a temperature of 37^0C and a flow rate of 7 ml/min. After 10 minutes, the wash buffer was substituted by perfusion buffer (wash buffer supplemented with 150 U/ml collagenase type IV (Sigma) and 5 mM $CaCl_2$) and perfusion was continued for 12-16 minutes, depending on the size of the liver. After perfusion, the liver was excised and cells were filtered using a sterile 70 μm filter in primary hepatocyte culture medium (DMEM containing 10% FCS (Gibco), 100 U/ml pen/strep, 0.5 U/ml insulin (Sigma), 20 ng/ml EGF (Sigma), 7 ng/ml glucagon (Sigma) and 7.5 μg/ml hydrocortisone (Sigma)). Cells were centrifuged 3 times (4^0C, 50 g) and during the last centrifugation step Percoll (GE Healthcare) in 1x HBSS was added to separate viable cells from death cells and debris. Yield and viability (ca. 90% for all mice) were determined using Trypan Blue exclusion. Unless stated otherwise, viable cells were seeded at 1.3×10^6 cells/well in 6-wells plates or 35 mm dishes in a collagen type I (BD Bioscience) gel sandwich with a strength of 1.5 mg/ml and pH 7.0-7.5 and cultured in primary hepatocyte culture medium in a humidified incubator at 37^0C with 5% CO_2.

Analysis of secreted products in the medium

Secreted albumin was determined in serum using a Mouse Albumin ELISA Kit (GenWay) according to the manufacturer's protocol and absorbance was measured at 450 nm using a GloMax-96 Microplate reader (Promega). Urea was determined with the Urea Assay Kit (BioChain) according to the manufacturer's protocol and absorbance was measured at 430 nm using a Varioskan Microplate reader (ThermoFisher Scientific). Cell viability measurements in primary hepatocyte cultures were performed using the Cytotoxicity Detection KitPLUS (LDH) (Roche Diagnostics) according to the manufacturer's protocol. Maximum LDH release (indicative for 100% cell death) was determined by lysing separate cultures with a comparable number of cells using 1% Triton X-100 in medium for 1 hour at 370C. Absorbance at 490 nm was measured using a Varioskan microplate reader (ThermoFisher Scientific). All measurements were background corrected for medium-derived LDH activity.

Isolation of RNA and RT-qPCR analysis

Total RNA was isolated using TriPure reagent (Roche Diagnostics) according to the manufacturer's protocol. Following analysis of RNA quality and concentration using the NanoDrop ND-1000 (NanoDrop Technologies), 1 μg of RNA was used for cDNA preparation using iScript (Biorad) according to the manufacturer's protocol. Semi-quantitative RT-qPCR was performed using Platinum Taq DNA polymerase (Invitrogen) according to the manufacturer's protocol and a C1000 Touch Thermal Cycler (Bio-Rad) using a standard 2-step amplification program with annealing/extension at 60^0C. Reactions for samples with housekeeping gene transcripts (*B2M, Hprt, Gap-*

dh and *β-Actin*) were always included on the same plate as reactions for transcripts of interest. All samples were analyzed in triplicate and expression levels were normalized separately to 3 housekeeping genes. Afterwards, the average of these 3 analyses was used for calculations for each sample separately. The following primers were used: *B2M* Fwd 5'-CCG GCC TGT ATC CAG AAA-3' Rev 5'-ATT TCA ATG TGA GGC GGG TGG AAC-3'; *Hprt* Fwd 5'-CGA AGT GTT GGA TAC AGG CC-3' Rev 5'-GGC AAC ATC AAC AGG ACC TCC-3'; *Gapdh* Fwd 5'-CAG AAC ATC ATC CCT GCA TCC-3' Rev 5'-GTC ATC ATA CTT GGC AGG TTT CTC-3'; *β-Actin* Fwd 5'-GGC TGT ATT CCC CTC CAT CG-3' Rev 5'-CCA GTT GGT AAC AAT GCC ATG T-3'; *Alb* Fwd 5'-TAA GAA ACA AAC GGC TCT TGC T -3' Rev 5'-GAA GCA GGT GTC CTT GTC AG-3'; *CK18* Fwd 5'-TTG CCG CCG ATG ACT TTA GA -3' Rev 5'GGA TGT CGC TCT CCA CAG AC-3'; *cMet* Fwd 5'-TCT GGG AGC TCA TGA CGA GA-3' Rev 5'-ATC CTG GAG ACC AGT TCG GA-3'; *Pck1* Fwd 5'-TGC GGA TCA TGA CTC GGA TG-3' Rev 5'-AGG CCC AGT GTT GA CCA AA-3'; *Mrp2* Fwd 5'-TCA TGG ACA GTG ACA AGA TAA TGG-3' Rev 5'-GGC CAT CAA GTA GAA GGG AC-3'; *Mrp3* Fwd 5'-CTC TCA GCT CAC CAT CAT CC-3' Rev 5'-TGG CCA ACA CTG AGA TTA TCC-3'; *Cyp1a1* Fwd 5'-GCA CTA CAG GAC ATT TGA GAA GG-3' Rev 5'-AAT CAC TGT GTC TAG TTC CTC C-3'; *Bmal1* Fwd 5'-GCA CTG CCA CTG ACT ACC AAG A-3' Rev 5'- TCC TGG ACA TTG CAT TGC AT-3'; *DBP* Fwd 5'-ACC GTG GAG GTG CTA ATG AC-3' Rev 5'-CCT CTT GGC TGC TTC ATT GTT-3'; *Per1* Fwd 5'-CAG GCT AAC CAG GAA TAT TAC CAG C-3' Rev 5'-CAC AGC CAC AGA GAA GGT GTC CTG G-3'; *Per2* Fwd 5'-GGC TTC ACC ATG CCT GTT GT-3' Rev 5'-GGA GTT ATT TCG GAG GCA AGT GT-3'; *Cry1* Fwd 5'-CAG ACT CTC GTC AGC AAG ATG-3' Rev 5'-CAA ACG TGT AAG TGC CTC AGT-3'; *Cry2* Fwd 5'-GGG ACT CTG TCT ATT GGC ATC TG-3' Rev 5'-GTC ACT CTA GCC CGC TTG GT-3'; *DnaJb9* Fwd 5'-TCA GAG CGA CAA ATC AAA AAG GC-3' Rev 5'-CTA TTG GCA TCC GAG AGT GTT T-3'. Relative gene expression was calculated using the comparative C(t) method described by Schmittgen et al and normalized to relative expression after exposure to the vehicle (relative expression = 1) (Schmittgen and Livak, 2008).

Time-lapse recording of circadian performance
For experiments involving recording of circadian oscillations, *Per2::Luc* primary hepatocytes were seeded at 1.3×10^6 cells/well in 35 mm dishes in a collagen type I (BD Bioscience) gel sandwich with a strength of 1.5 mg/ml and pH 7.0-7.5. Time-lapse bioluminescence measurements (60 sec measurements at 10 min intervals) were performed using a LumiCycle 32-channel automated luminometer (Actimetrics), placed in a temperature-controlled dry incubator at 37^0C. Prior to placing 35 mm dishes in the lumicycle, 0.1 mM luciferin (Sigma) was added and the lid was replaced by a glass coverslip and sealed with parafilm. Data was analyzed using Actimetrics software.

In vitro exposure studies
Sandwich cultured *Per2::Luc* primary hepatocytes were maintained under continuous monitoring of circadian performance. At defined circadian phase (i.e. relative Circadian Time CTr0, 4, 8, 12, 16 and 20, in which CTr0 represents the trough of *Per2::Luc* expression), cells were treated with benzo[a]pyrene (Sigma), cyclosporine A (Sigma) or 0.1% DMSO (solvent), dissolved in conditioned medium (i.e. medium taken from, and transferred back to each well) to prevent unexpected synchronization by medium composition. After 4 hours, RNA was isolated for further analysis.

LacZ mutant frequency determination
Primary hepatocytes from pUR288 LacZ mice were seeded on collagen coated 10 cm dishes (50 ug/ml). After attachment, pUR288 LacZ cells were maintained in proliferating hepatocyte medium (William's E containing 100 U/ml pen/strep, 2 mM ultraglutamine (Lonza), 1 mM sodium pyruvate (Invitrogen), 0.35 mM L-proline (Sigma), 3.5 μM glucagon and 1 ng/ml EGF) in a humidified incubator at 37^0C with 5% CO_2, as described (Zwart et al., 2012). At least 24 hours prior to starting the exposures, 0.1 μM dexamethasone was added to the medium to synchronize the clock of the individual cells. After genotoxic exposure to B[a]P at defined circadian phase for 4 hour, cells were washed twice with prewarmed PBS and cultured for another 44 hour in conditioned medium. Cells

were lysed and plasmid DNA was recovered for mutation frequency analysis as described (Dollé et al., 1996).

Bromodeoxyuridine assay

To determine the percentage of proliferating hepatocytes in the mutagenesis experiments, BrdU was added to the medium to a final concentration of 10 µM. Prior to fixation with 4% paraformaldehyde for 15 minutes, cells were permeabilized using 1% Triton X-100 for 15 minutes, followed by breaking the structure of the DNA for 10 minutes at 4^0C in 1 M HCl, 10 minutes and 20 minutes at 37^0C in 2 M HCl. Cells were blocked in PBS with 1% Triton X-100, 5% goat serum and 1 M glycine for 1 hour, followed by 1 hour binding to primary antibody (anti-BrdU, Sigma) in block buffer. Secondary antibody (goat anti-mouse-FITC, Jackson Immuno Research) was added for 45 minutes in permeabilization buffer before mounting with Vectashield with DAPI (Vector Laboratories). Unless stated otherwise, steps were performed at room temperature and separated by a 3 x 5 minutes washing step with permeabilization buffer. Pictures were taken using a Leica DM4000B microscope.

Statistical analysis

Harmonic regression analysis of circadian oscillation was performed using CircWave Batch v5.0 (courtesy of Dr. Roelof Hut, http://www.euclock.org/) for cosinor analysis with a 24 hour wave unless stated otherwise, with forward linear harmonic regression using an F-test. User defined alpha was 0.05.

Results

Temporal changes in mouse primary hepatocytes in a collagen sandwich

Primary hepatocytes are usually grown on extracellular matrices, with exposure studies being performed within 48 hours (Baker et al., 2001; Harris et al., 2004; Luttringer et al., 2002), although re-establishment of cell-cell interactions is incomplete (reviewed by (Swift et al., 2010). Chronotoxicity assays include establishing circadian phase prior to exposure, which requires culturing of primary hepatocytes for longer than two days.

We first evaluated the functional state of mouse primary hepatocytes, isolated from male *Per2::Luc* mice and grown in a collagen sandwich for two weeks. RNA was isolated every 24h and expression levels of liver specific genes were compared to that observed in freshly prepared primary hepatocytes. As shown in Figure 1, and in accordance with observations for cultured human and rat primary hepatocytes (Baker et al., 2001; Harris et al., 2004; Luttringer et al., 2002), extensive temporal changes were observed during the first 48 hours. Albumin (*Alb*), Multidrug resistance protein 2 (*Mrp2*) and Multispecific organic anion transporter 3 (*Mrp3*) expression stabilized at 50-70% of the level measured in fresh primary hepatocytes, while Tyrosine aminotransferase (*Tat*) expression gradually decreased from 40% at day 3 to 10% at day 14. Expression of Solute carrier organic anion transporter 1a1 (*Sclo1a1* or *Oatp1*) and 1b2 (*Sclo1b2* or *Lst-1*), as well as Phosphoenolpyruvate carboxykinase 1 (*Pck1*) were reduced to less than 10% of the levels in fresh primary hepatocytes. Expression levels of Met proto-oncogene (*cMet*) increased to 180% and remained stable for a week, while Keratin 18 (*CK18*) expression increased in between 300 and 500% of levels in fresh primary hepatocytes. *cMet* is involved in DNA synthesis and liver regeneration and *CK18* is associated with the phenotypic changes occurring when primary hepatocytes are placed in culture. Both genes have been reported to be upregulated in cultured primary hepatocytes (Baffet et al., 1991; Michalopoulos and DeFrances, 1997).

In order to evaluate hepatocyte specific function, we measured secreted albumin and urea in the medium of cultured primary hepatocytes. Initially, cells secreted albumin and urea at rather constant rate (18.76 and 4.37 mg/24h/106 cells; Figure 2a and b). After 4 days cells continued to secrete albumin, though at lower level (5.75 mg/24h/10^6 cells), while urea excretion dropped to a low level (0.44 mg/24h/10^6 cells).

To determine the viability of the hepatocyte cultures, we measured the spontaneous leak-

3
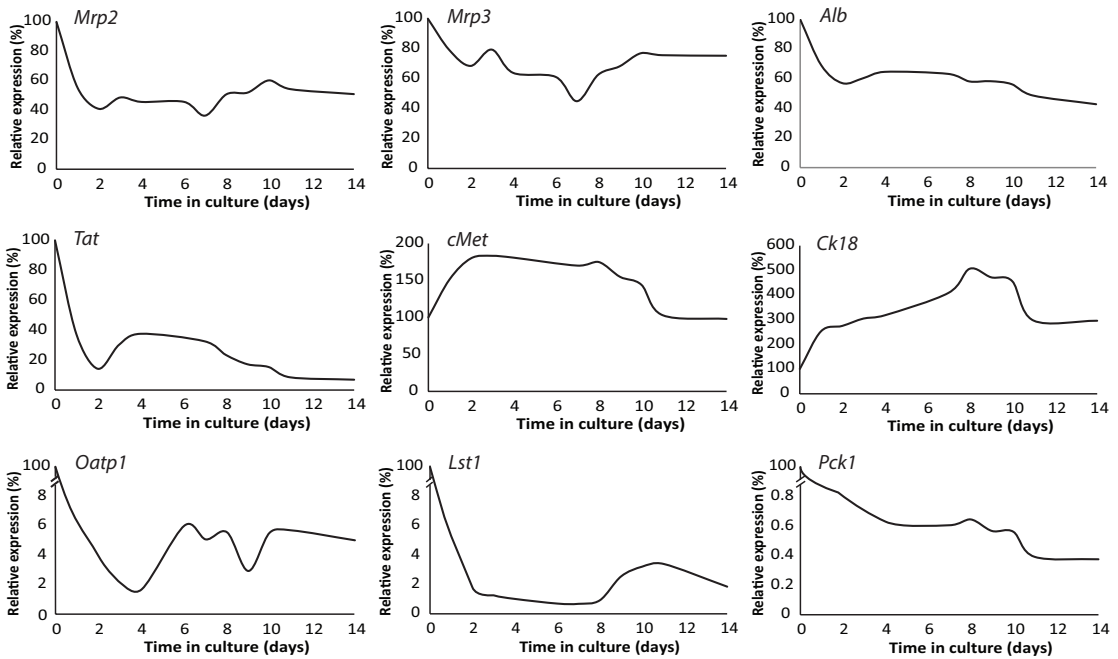
Figure 1. Temporal changes in liver-specific gene expression in sandwich cultured mouse primary hepatocytes.
RNA was isolated every 24 hours and gene expression was determined by RT-qPCR. Expression levels are plotted using a 3-day moving average (n=3 independent experiments with biological triplicates per experiment). The 100% value represents the expression levels directly after perfusion.
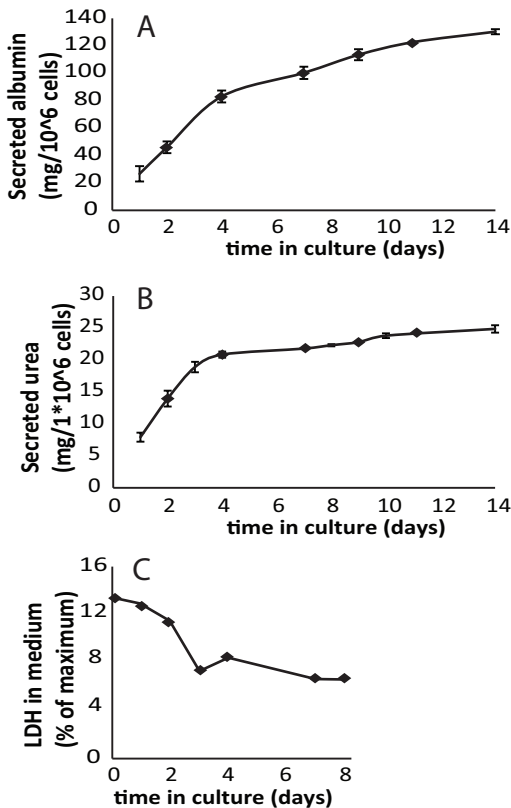
Figure 2. Temporal changes in biological activity and viability of sandwich cultured mouse primary hepatocytes. Cells were seeded at a density of 1.3×10^6 cells per 35 mm dish and medium was collected every 24 hours (n=3 independent experiments with biological triplicates per experiment). (A) Cumulative albumin secretion, (B) cumulative urea secretion, (C) LDH leakage, expressed as the percentage of the total LDH activity (the extracellular LDH activity plus the intracellular LDH activity). Diamonds indicate days of medium change. Error bars represent SD.
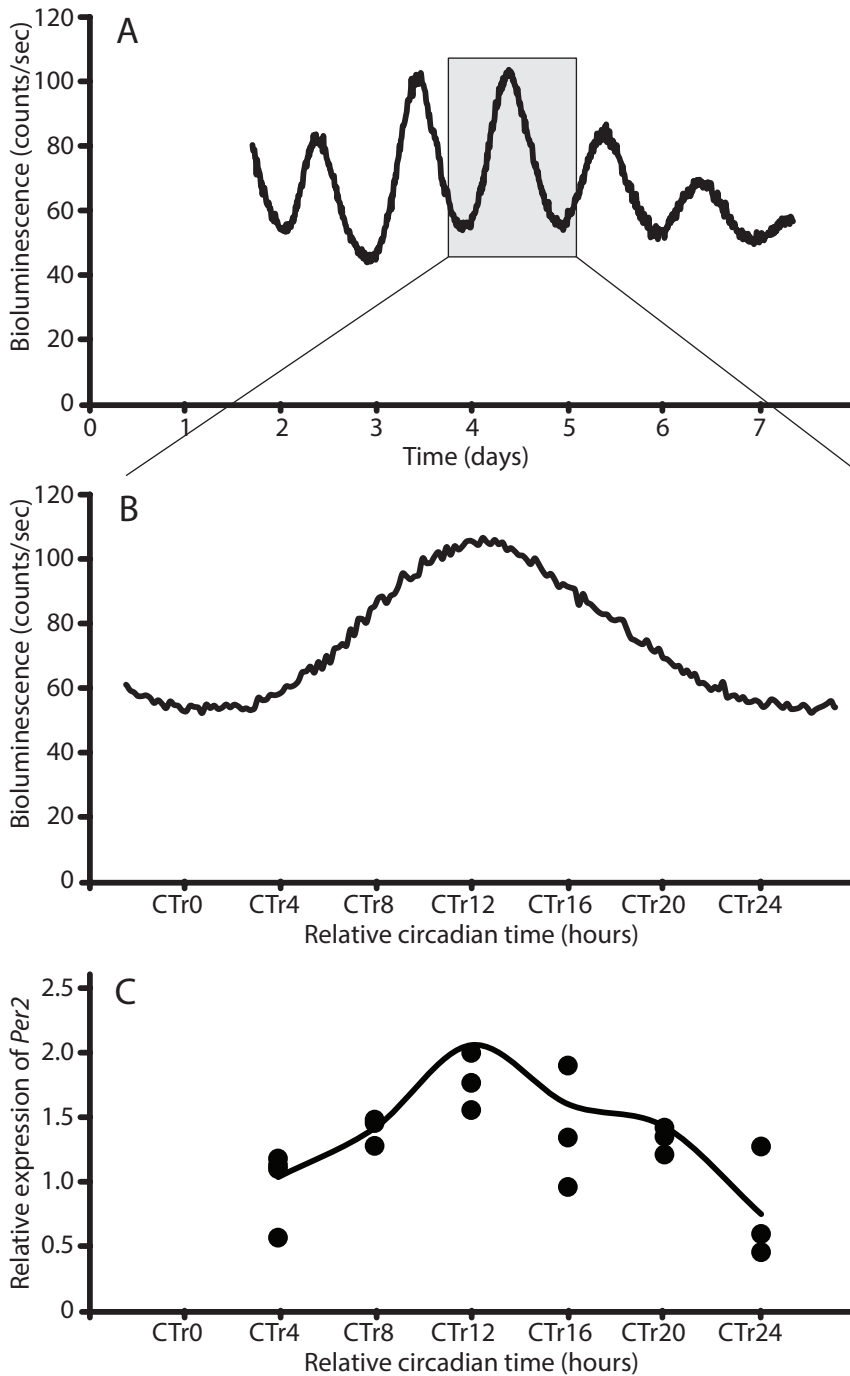
Figure 3. Circadian performance of sandwich cultured mouse primary hepatocytes. (A) Representative example of bioluminescence rhythms in sandwich cultured mouse primary hepatocytes, τ = 24.10 ± 0.59 hours (n=8 independent experiments). Data from the first 36 hours are removed for clarity. (B) Enlarged view of one cycle of *Per2::Luc* oscillations. Relative circadian time (CTr) is represented on the x-axis. (C) RT-qPCR data from primary hepatocytes at relative time points CTr4, 8, 12, 16, 20 and 24 hours. Dots represent one sample and the line represents the average value of samples collected in one experiment.
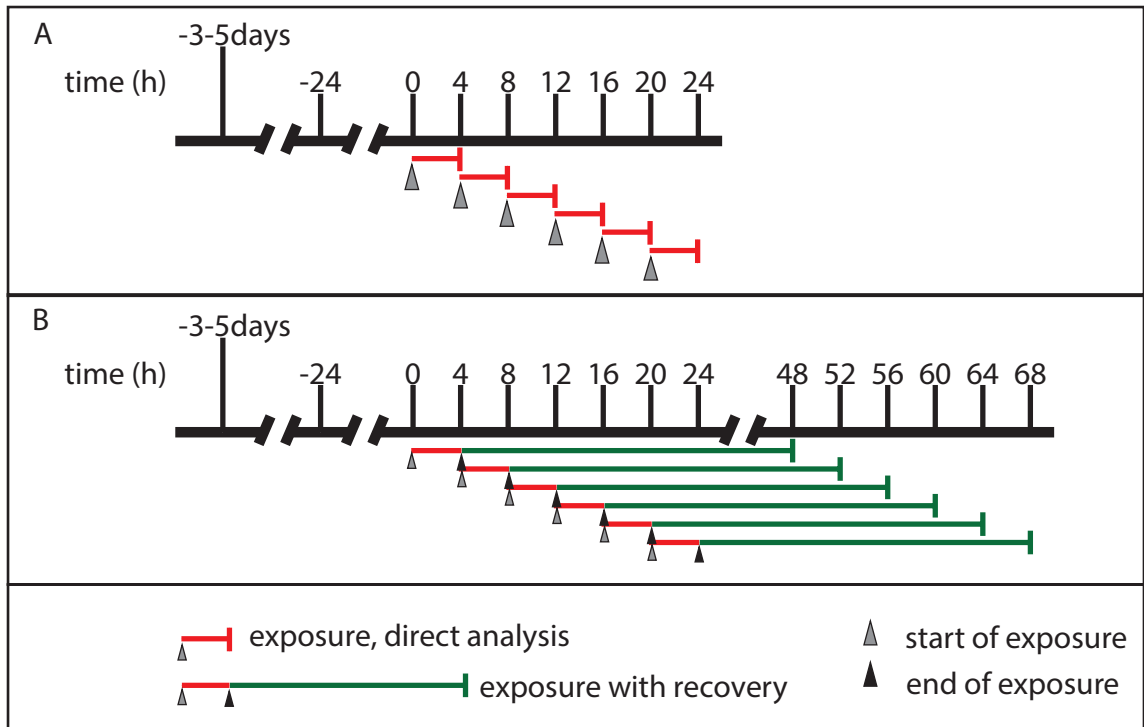
Figure 4. Schematic representation of chronotoxicity studies. Primary hepatocytes are seeded in a collagen sandwich and allowed to grow for 3 to 5 days. After reaching confluency, cells are placed in the LumiCycle for time-lapse bioluminescence measurements and establishing circadian phase. Cells are exposed to a compound for 4 hours, starting at a predefined phase of the clock. In experimental setup (A), RNA is collected directly after the exposure to measure gene expression. In experimental setup (B), cells are washed after exposure and further maintained for 44 hours in conditioned medium. Cells lysates were collected for further analysis 48 hours after the start of the exposure.

age of lactate dehydrogenase (LDH) in the medium, originating from the loss of membrane integrity by apoptotic/necrotic cells). Medium LDH levels decreased from 13 to 6% of the maximum value in the first 3 days, to remain stable throughout the experiment (Figure 2c), indicating limited cell death in the sandwich cultured hepatocytes.

Taken together, these data show that mouse primary hepatocytes in a collagen sandwich can be stably maintained in culture for at least 14 days. The cultures are subject to profound changes in gene expression within the first 48 hours after isolation, while hepatic secretion of albumin and urea are higher during the first 4 days in culture. Both findings are consistent with the re-establishment of polarized cultures of hepatocytes during the first 4 days in culture (Swift et al., 2010; Zhang et al., 2005). After this period, the cells were stable in gene expression and secretion of hepatic products for another 10 days.

Circadian clock performance of cultured mouse primary hepatocytes

We next determined circadian core oscillator performance of sandwich cultured primary hepatocytes obtained from a *Per2::Luc* clock reporter mice. Cells were clock-synchronized by replacing the medium (containing glucagon as a synchronizing factor (Saini et al., 2011)) and bioluminescence was monitored for the next seven days. As shown in Figure 3a, robust oscillations of the bioluminescent *Per2* reporter gene were observed with a period of 24.10 ± 0.59 hours (n= 8), indicating that the primary hepatocyte culture responds well to clock synchronizing stimuli. As an additional control, we isolated RNA from parallel grown cells at 4 hour intervals over a period of 24 hours, spanning the 4th cycle (Figure 3b) and determined *Per2* mRNA levels by quantitative RT-qPCR. In this analysis, we defined the trough of *Per2::Luc* expression as relative circadian

time CTr0. As expected, we observed a significant oscillation of endogenous *Per2* gene expression (Figure 3c) which is in phase with bioluminescence rhythms originating from the *Per2::Luc* reporter gene (Figure 3b). In conclusion, sandwich cultured primary hepatocytes possess a robust, synchronisable circadian clock.

Assays aimed at determining chronotoxic properties of chemicals require (short periods of exposure during different phases of the circadian clock. Taking into consideration the recovery period of primary hepatocytes (2 days) and the time required to assess clock phase and period (2 days), exposure studies are best performed at day 4.

Synchronized primary hepatocytes reveal chronotoxic properties of B[a]P

In order to determine whether primary hepatocytes serve as a good *in vitro* system for chronotoxicity assays, we have used benzo[a]pyrene (B[a]P) as a model compound. We have previously shown that B[a]P exerts chronotoxic responses in a mouse liver slice system and that induction levels of *Cyp1a1* (encoding a key component in the metabolism of B[a]P) depend on circadian phase at the time of exposure (chapter 2). We first performed a dose-range experiment for non-clock synchronized *Per2::Luc* primary hepatocytes and measured *Cyp1a1* mRNA levels 4 hour after exposure. *Cyp1a1* induction increases with concentration (as compared to 0.1% DMSO solvent treatment), saturating around 2.5 µM (Supplementary Figure S1a) without triggering cytotoxic effects (Supplementary Figure S1b). To avoid saturation of the xenobiotic metabolism pathway, we have chosen to perform the chronotoxicity assay at a dose that elicits half-maximal *Cyp1a1* induction.

As outlined in Figure 4a, we exposed synchronized *Per2::Luc* primary hepatocytes to 0.5 µM B[a]P or 0.1% DMSO vehicle for 4 hours starting at 6 different phases of the clock (i.e. CTr 4, 8, 12, 16, 20, and 24, in which CTr0 refers to the trough of *Per2::Luc* expression) and isolated RNA directly after exposure (Figure 4a). We show that there is a clear rhythm in the induction of *Cyp1a1* expression, peaking at exposure from CTr8-12 (Figure 5). Harmonic regression of B[a]P-induced levels of *Cyp1a1* mRNA revealed a highly significant oscillation (p=0.0002). As an additional control, we measured the expression levels of several core clock genes by RT-qPCR (Supplementary Figure S2). In line with the *Per2::Luc* bioluminescence recordings, endogenous *Per2* mRNA levels peak at CTr12. As expected on the basis of the core circadian oscillator mechanism, other E-box clock (*Per1, Cry1* and *Cry2*) and clock-controlled (*Dbp*) genes also peak at CTr12, while *Bmal1* expression proceeds in antiphase (Supplementary Figure S2).

Taken together, our data demonstrate that clock-synchronized primary hepatocytes can be used for *in vitro* chronotoxicity assays and that B[a]P is to determine chronotoxic properties of chemical compounds and that B[a]P has chronotoxic properties.

Synchronized primary hepatocytes reveal chronomutagenic properties of B[a]P

Benzo[a]pyrene-7,8-diol-9,10-epoxide (BPDE), the active metabolite of B[a]P after xenobiotic bioactivation, damages the DNA and is highly mutagenic. Recently, primary mouse hepatocytes from pUR288 LacZ mutation reporter mice have been used to demonstrate the mutagenic properties of B[a]P *in vitro* (Zwart et al., 2012). Given the significant circadian phase-dependent differences in *Cyp1a1* induction, and assuming that higher levels of CYP1A1 translate in a more efficient metabolism of B[a]P, we hypothesize that time-of-day of exposure may translate into circadian variation in mutagenic outcome.

To test this hypothesis, we exposed dexamethasone synchronized, proliferating primary hepatocytes from a pUR288 LacZ mouse at RTr0-4, 4-8, 8-12, 12-16, 16-20 or 20-24 to 10 µM B[a]P or 0.1% DMSO (solvent) for 4 hours, where RTr0 was defined as 24 hours after dexamethasone synchronization. After exposure, culturing was continued in conditioned medium for 44 hours to allow fixation of mutations (Figure 4b). In this period, BrdU incorporation was used to indicate DNA replication in parallel dishes (>50% of nuclei, Supplementary Figure S4). To determine the phase of the circadian clock at the time of exposure, clock gene expression was measured by RT-qPCR in RNA isolated from parallel dishes (Supplementary Figure S3). For purposes of comparing the results with our gene induction data in previous experiments, we normalized the relative exposure

time (RTr) of the cells to relative circadian time (CTr) in the mutagenesis experiment on the basis of expression levels of core clock genes. A slight shift is likely to be induced by the difference of adding dexamethasone in this experimental setup. Interestingly, we observed a marked peak in the B[a]P induced mutation frequency for cells treated from CTr8-12, coinciding with the peak in *Cyp1a1* induction, suggesting that B[a]P acts as a chronomutagen. To this point, these analyses are based on the results of one experiment (n=1) and should be repeated in order to know whether they are reproducible.

3
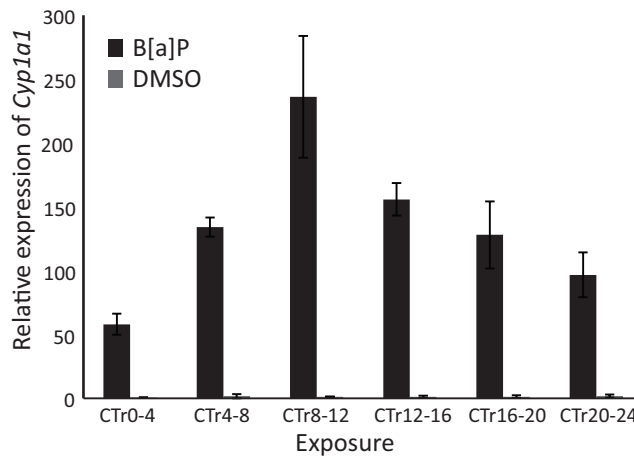
Figure 5. Time of day dependent induction of *Cyp1a1* after exposure to B[a]P. Sandwich cultured mouse primary hepatocytes were treated with 0.5 µM B[a]P or its solvent DMSO (0.1%) at different phases of the circadian clock as indicated (CTr12 represents the peak of *Per2::Luc* expression, see Figure 3). Relative *Cyp1a1* expression was measured by RT-qPCR. n=3 independent experiments with biological triplicates per experiment. Error bars represent SD..
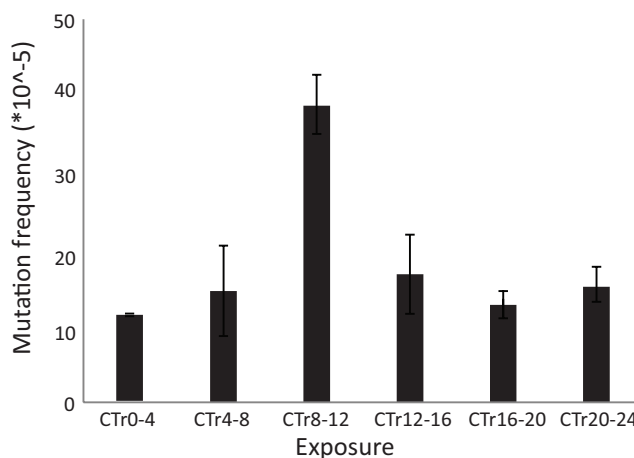
Figure 6. Time of day dependent mutagenesis after exposure to B[a]P. Proliferating, dexamethasone synchronized mouse primary hepatocytes from pUR288 LacZ mutation reporter mice were exposed to B[a]P or its solvent DMSO (0.1%) for 4 hours at defined phases of the circadian clock and allowed to grow for another 2 days in order to allow mutation fixation. LacZ mutation frequency was determined as described in the Materials section and plotted as mutants per 10^5 colonies (n=1 experiment). Error bars represent SD.

3

Discussion

The circadian clock plays an important role in many processes and is retained when cells are explanted from the body (Reppert and Weaver, 2002). In chemical risk analysis assays many *in vitro* liver derived systems are being used, however most of them do not consider the influence of the circadian clock on normal cellular metabolism and on the efficiency of processes involved in xenobiotics metabolism. *In vitro* assays often suffer from poor reproducibility between labs or studies and the predictive value for *in vivo* exposure experiments is variable. We suggest that both problems can be ameliorated by acknowledging the influence of circadian rhythms.

In order to perform exposure studies at defined phases of the circadian clock, we optimized conditions for sandwich cultured mouse primary hepatocytes to obtain stable expression of hepatocyte specific gene expression. Extensive temporal changes were observed for all genes measured, but after 48 in culture, expression stabilized at intermediate (40-70%; *Alb, Mrp2, Mrp3* and *Tat*), low (1-10%; *Oatp1, Lst-1* and *Pck1*) or high (180-500%; *cMet* and *CK18*) levels, as compared to freshly isolated mouse primary hepatocytes. The latter two genes have been previously reported to be upregulated in cultured primary hepatocytes (Baffet et al., 1991; Michalopoulos and DeFrances, 1997). Secreted levels of albumin and urea were higher in the first 4 days in culture than from day 4-14, but stable through the whole experiment. Serum levels of lactate dehydrogenase (LDH) can be used as a measure for cytotoxicity. After 4 days in culture, spontaneous LDH release was less than 10% and stable, indicating that cell populations were viable. Combined, these data show that cultures of mouse primary hepatocytes can be maintained for at least 14 days, with stable hepatocyte specific functioning. The altered expression of some genes and lower rates of albumin and urea secretion from day 4 are consistent phenotypic alterations in sandwich cultured hepatocytes, such as the re-establishment of cell-cell interactions and polarized cell architecture (reviewed by Swift et al., 2010). Previously, expression of P450 genes was demonstrated in cultured primary hepatocytes, indicating that cultured hepatocytes are suitable for xenobiotics metabolism studies (Boess et al., 2003; Jacobsen et al., 2011; Page et al., 2007). We were able to follow the phase of the clock in hepatocytes from *Period2::luciferase (Per2::Luc)* mice by time lapse bioluminescence recording and confirmed circadian oscillation by RT-qPCR analysis of clock and clock output gene expression. Our findings fit well with a recent study on the circadian clock in mouse primary hepatocytes in terms of period length, variation, amplitude and dampening (Guenthner et al., 2014).

Circadian expression of many genes involved in xenobiotics metabolism in the liver was demonstrated previously (Akhtar et al., 2002; Hughes et al., 2009; Miller et al., 2007; Panda et al., 2002; Zhang et al., 2009). We exposed synchronized cultures of mouse primary hepatocytes to the polycyclic aromatic hydrocarbon benzo[a]pyrene (B[a]P), an environmental pollutant and a ligand for the aryl hydrocarbon receptor (AHR). We have shown that exposure to B[a]P at defined phases of the clock causes time of day dependent differences in the induction of *Cyp1a1*, with the highest induction around the peak of *Per2* (exposure at CTr8-12), which is in line with diurnal variations in AHR rhythmicity (reviewed by De Wit et al., 2014) and our previous observations of *Cyp1a1* induction in mouse liver slices (chapter 2). The implications of these findings are that the cellular metabolic response to B[a]P is highly variable depending on exposure time, and that B[a]P is likely to act as a chronotoxic compound.

Last, we exposed proliferating hepatocytes from pUR288 LacZ mice to B[a]P at different phases of the clock and determined the mutation frequency. We observed that the mutagenic potential of B[a]P was higher when cells were treated at CTr8-12 than at other time points. Interestingly the peak in B[a]P induced mutagenesis coincides with the peak of B[a]P-induced *Cyp1a1* expression. Therefore, it is tempting to speculate that at CTr8-12, B[a]P is metabolized by CYP1A1 at higher rates causing higher intracellular levels of the genotoxic metabolite BPDE, and as a consequence higher DNA damage levels, leading to increased mutagenesis. Although these experiments should be repeated to confirm reproducibility, this is a first indication for the occurrence of time of day of exposure dependent variations in mutagenic events (chronomutagenesis).

Taken together, these data provide further insight in the interplay between the circadian

clock and the molecular mechanisms of B[a]P toxicity and has major implications for toxicogenomics and the future use of *in vitro* assays. Acknowledging the influence of the circadian clock will (i) improve interexperimental reproducibility because of more similar testing conditions, (ii) improve risk analysis by being able to assess responses in a more *in vivo*-like manner, likely accelerating go/no go decisions, (iiI) provide additional information on high and low risk exposure times in terms of labor hygiene and cancer susceptibility and (iv) have a large impact on personalized medicine, especially in terms of chronotherapy.

In conclusion, sandwich cultured mouse primary hepatocytes are suitable for stable long term maintenance, enabling chronotoxic exposure studies. Validation of time of day dependent gene induction was performed using B[a]P, resulting in circadian differences with high statistical significance. Analysis of the mutagenic potential of B[a]P showed increased mutagenesis overlapping with the moment of highest gene induction in both mouse primary hepatocytes and liver slices. Acknowledging the circadian clock in *in vitro* toxicogenomics assays thus increases the reproducibility, sensitivity and specificity of these assays and has major implications for labor hygiene and chronotherapy.

Acknowledgements

References

Akhtar, R.A., Reddy, A.B., Maywood, E.S., Clayton, J.D., King, V.M., Smith, A.G., Gant, T.W., Hastings, M.H., Kyriacou, C.P., 2002. Circadian cycling of the mouse liver transcriptome, as revealed by cDNA microarray, is driven by the suprachiasmatic nucleus. Curr. Biol. 12, 540–50.

Baffet, G., Loyer, P., Glaise, D., Corlu, A., Etienne, P.L., Guguen-Guillouzo, C., 1991. Distinct effects of cell-cell communication and corticosteroids on the synthesis and distribution of cytokeratins in cultured rat hepatocytes. J. Cell Sci. 99 (Pt 3), 609–15.

Baker, T.K., Carfagna, M.A., Gao, H., Dow, E.R., Li, Q., Searfoss, G.H., Ryan, T.P., 2001. Temporal gene expression analysis of monolayer cultured rat hepatocytes. Chem. Res. Toxicol. 14, 1218–1231.

Balsalobre, A., Marcacci, L., Schibler, U., 2000. Multiple signaling pathways elicit circadian gene expression in cultured Rat-1 fibroblasts. Curr. Biol. 10, 1291–4.

Boerrigter, M., Dollé, M., Martus, H., Gossen, J., Vijg, J., 1995. Plasmid-based transgenic mouse model for studying in vivo mutations. Nature 377, 657–659.

Boess, F., Kamber, M., Romer, S., Gasser, R., Muller, D., Albertini, S., Suter, L., 2003. Gene expression in two hepatic cell lines, cultured primary hepatocytes, and liver slices compared to the in vivo liver gene expression in rats: possible implications for toxicogenomics use of in vitro systems. Toxicol. Sci. 73, 386–402.

Chaves, I., Nijman, R., Biernat, M., Bajek, M., Brand, K., Carvalho da Silva, A., Saito, S., Yagita, K., Eker, A., van der Horst, G., 2011. The Potorous CPD photolyase rescues a cryptochrome-deficient mammalian circadian clock. PLoS One 6, e23447.

Claudel, T., Cretenet, G., Saumet, A., Gachon, F., 2007. Crosstalk between xenobiotics metabolism and circadian clock. FEBS Lett. 581, 3626–33.

De Wit, A.S., Nijman, R., Destici, E., Chaves, I., van der Horst, G.T.J., 2014. Hepatotoxicity and the circadian clock, a timely matter, in: Toxicogenomics-Based Cellular Models: Alternatives to Animal Testing for Safety Assessment. Academic Press, pp. 251–270.

Destici, E., Oklejewicz, M., Nijman, R., Tamanini, F., van der Horst, G.T.J., 2009. Impact of the circadian clock on in vitro genotoxic risk assessment assays. Mutat. Res. 680, 87–94.

Dibner, C., Schibler, U., Albrecht, U., 2010. The mammalian circadian timing system: organization and coordination of central and peripheral clocks., Annual review of physiology.

Dipple, A., 1995. DNA adducts of chemical carcinogens. Carcinogenesis 16, 437–441.

Dollé, M., Martus, H., Gossen, J., Boerrigter, M., Vijg, J., 1996. Evaluation of a plasmid-based transgenic mouse model for detecting in vivo mutations. Mutagenesis 11, 111–118.

Eisenbranda, G., Pool-Zobelb, B., Bakerc, V., Ballsd, M., Blaauboere, B.., Boobisf, A., Carereg, A., Kevekordesh, S., Lhuguenoti, J.-C., Pieterse, R., Kleiner, J., 2002. Methods of in vitro toxicology. Food Chem. Toxicol. 40, 193–236.

Gorbacheva, V.Y., Kondratov, R. V, Zhang, R., Cherukuri, S., Gudkov, A. V, Takahashi, J.S., Antoch, M.P., 2005. Circadian sensitivity to the chemotherapeutic agent cyclophosphamide depends on the functional status of the CLOCK/BMAL1 transactivation complex. Proc. Natl. Acad. Sci. U. S. A. 102, 3407–12.

Guenthner, C.J., Luitje, M.E., Pyle, L. a, Molyneux, P.C., Yu, J.K., Li, A.S., Leise, T.L., Harrington, M.E., 2014. Circadian Rhythms of PER2::LUC in Individual Primary Mouse Hepatocytes and Cultures. PLoS One 9, e87573.

Harris, A.J., Dial, S.L., Casciano, D. a, 2004. Comparison of basal gene expression profiles and effects of hepatocarcinogens on gene expression in cultured primary human hepatocytes and HepG2 cells. Mutat. Res. 549, 79–99.

Hewitt, N.J., Lechón, M.J.G., Houston, J.B., Hallifax, D., Brown, H.S., Maurel, P., Kenna, J.G., Gustavsson, L., Lohmann, C., Skonberg, C., Guillouzo, A., Tuschl, G., Li, A.P., LeCluyse, E., Groothuis, G.M.M., Hengstler, J.G., 2007. Primary hepatocytes: current understanding of the regulation of metabolic enzymes and transporter proteins, and pharmaceutical practice for the use of hepatocytes in metabolism, enzyme induction, transporter, clearance, and hepatotoxicity studies. Drug Metab. Rev. 39, 159–234.

Hughes, M.E., DiTacchio, L., Hayes, K.R., Vollmers, C., Pulivarthy, S., Baggs, J.E., Panda, S., Hogenesch, J.B., 2009. Harmonics of circadian gene transcription in mammals. PLoS Genet. 5, e1000442.

Jacobsen, J.K., Jensen, B., Skonberg, C., Hansen, S.H., Badolo, L., 2011. Time-course activities of Oct1, Mrp3, and cytochrome P450s in cultures of cryopreserved rat hepatocytes. Eur. J. Pharm. Sci. 44, 427–436.

Kienhuis, A.S., Bessems, J.G.M., Pennings, J.L.A., Driessen, M., Luijten, M., Delft, J.H.M. van, Peijnenburg, A.A.C.M., Ven, L.T.M. van der, 2011. Application of toxicogenomics in hepatic systems toxicology for risk assessment: Acetaminophen as a case study. Toxicol. Appl. Pharmacol. 250, 96–107.

Kumaki, Y., Ukai-tadenuma, M., Uno, K.D., Nishio, J., Masumoto, K., Nagano, M., 2008. Analysis and synthesis of high-amplitude Cis-elements. PNAS 105, 14946–51.

Lowrey, P., Takahashi, J., 2011. Genetics of circadian rhythms in Mammalian model organisms, in: Adv Genet. pp. 74:175–230.

Luttringer, O., Theil, F.P., Lavé, T., Wernli-Kuratli, K., Guentert, T.W., de Saizieu, A., 2002. Influence of isolation procedure, extracellular matrix and dexamethasone on the regulation of membrane transporters gene expression in rat hepatocytes. Biochem. Pharmacol. 64, 1637–50.

Mazzoccoli, G., Pazienza, V., Vinciguerra, M., 2012. Clock genes and clock-controlled genes in the regulation of metabolic rhythms. Chronobiol. Int. 29, 227–51.

Michalopoulos, G., DeFrances, M., 1997. Liver regeneration. Science (80-.). 276, 60–66.

Miller, B.H., McDearmon, E.L., Panda, S., Hayes, K.R., Zhang, J., Andrews, J.L., Antoch, M.P., Walker, J.R., Esser, K., Hogenesch, J.B., Takahashi, J.S., 2007. Circadian and CLOCK-controlled regulation of the mouse transcriptome and cell proliferation. Proc. Natl. Acad. Sci. U. S. A. 104, 3342–7.

Miller, K.P., Ramos, K.S., 2001. Impact of cellular metabolism on the biological effects of benzo[a]pyrene and related hydrocarbons. Drug Metab. Rev. 33, 1–35.

Oberemm, A., Onyon, L., Gundert-Remy, U., 2005. How can toxicogenomics inform risk assessment? Toxicol. Appl. Pharmacol. 207, 592–598.

Ohdo, S., 2007. Review Chronopharmacology Focused on Biological Clock. Drug Metab Pharmacokinet 22, 3–14.

Page, J.L., Johnson, M.C., Olsavsky, K.M., Strom, S.C., Zarbl, H., Omiecinski, C.J., 2007. Gene expression profiling of extracellular matrix as an effector of human hepatocyte phenotype in primary cell culture. Toxicol. Sci. 97, 384–97.

Panda, S., Antoch, M.P., Miller, B.H., Su, A.I., Schook, A.B., Straume, M., Schultz, P.G., Kay, S.A., Takahashi, J.S., Hogenesch, J.B., 2002. Coordinated transcription of key pathways in the mouse by the circadian clock. Cell 109, 307–20.

Ramboer, E., Vanhaecke, T., Rogiers, V., Vinken, M., 2013. Primary hepatocyte cultures as prominent in vitro tools to study hepatic drug transporters. Drug Metab. Rev. 45, 196–217.

Reppert, S.M., Weaver, D.R., 2002. Coordination of circadian timing in mammals. Nature 418, 935–41.

Rubin, H., 2001. Synergistic mechanisms in carcinogenesis by polycyclic aromatic hydrocarbons and by tobacco smoke: a bio-historical perspective with updates. Carcinogenesis 22, 1903–1930.

Saini, C., Suter, D.M., Liani, A., Gos, P., Schibler, U., 2011. The Mammalian Circadian Timing System: Synchronization of Peripheral Clocks. Cold Spring Harb Symp Quant Biol 76, 39–47.

Schmittgen, T.D., Livak, K.J., 2008. Analyzing real-time PCR data by the comparative CT method. Nat. Protoc. 3, 1101 – 1108.

Seglen, P., 1976. Preparation of isolated rat liver cells. Methods Cell Biol 13, 29–83.

Swift, B., Pfeifer, N.D., Brouwer, K.L.R., 2010. Sandwich-cultured hepatocytes: an in vitro model to evaluate hepatobiliary transporter-based drug interactions and hepatotoxicity. Drug Metab. Rev. 42, 446–71.

Takahashi, J., Hong, H., Ko, C., McDearmon, E., 2008. The Genetics of Mammalian Circadian Order and Disorder: Implications for Physiology and Disease. Nat. Rev. Genet. 9, 764–775.

Van Dycke, K.C.G., Nijman, R.M., Wackers, P.F., Jonker, M.J., Rodenburg, W., van Oostrom, C.T.M., Salvatori, D.C.F., Breit, T.M., van Steeg, H., Luijten, M., van der Horst, G.T.J. (2014), 2014. A day and night difference in the response of the hepatic transcriptome to cyclophosphamide treatment. Arch. Toxicol. In press.

Xiao, H., Singh, S., 2007. p53 regulates cellular responses to environmental carcinogen benzo[a]pyrene-7,8-diol-9,10-epoxide in human lung cancer cells. Cell cycle 6, 1753–1761.

Yoo, S.-H., Yamazaki, S., Lowrey, P.L., Shimomura, K., Ko, C.H., Buhr, E.D., SiepkaH, S.M., Hong, E.-K., Oh, W.J., Yoo,

3

O.J., Menaker, M., Takahashi, J.S., 2004. PERIOD2:: LUCIFERASE real-time reporting of circadian dynamics reveals persistent circadian oscillations in mouse peripheral tissues. Proc. Natl. Acad. Sci. U. S. A. 101, 5339–5346.

Zhang, P., Tian, X., Chandra, P., Brouwer, K.L.R., 2005. Role of Glycosylation in Trafficking of Mrp2 in Sandwich-Cultured Rat Hepatocytes. Mol. Pharmacol. 67, 1334–1341.

Zhang, Y.J., Yeager, R.L., Klaassen, C.D., 2009. Circadian Expression Profiles of Drug-Processing Genes and Transcription Factors in Mouse Liver. Drug Metab. Dispos. 37, 106–115.

Zwart, E.P., Schaap, M.M., Dungen, M.W. Van Den, Braakhuis, H.M., White, P.A., Steeg, H. Van, Benthem, J. Van, Luijten, M., 2012. Proliferating Primary Hepatocytes From the pUR288 LacZ Plasmid Mouse Are Valuable Tools for Genotoxicity Assessment In Vitro. Environ. Mol. Mutagen. 53, 376–383.

Supplementary figures
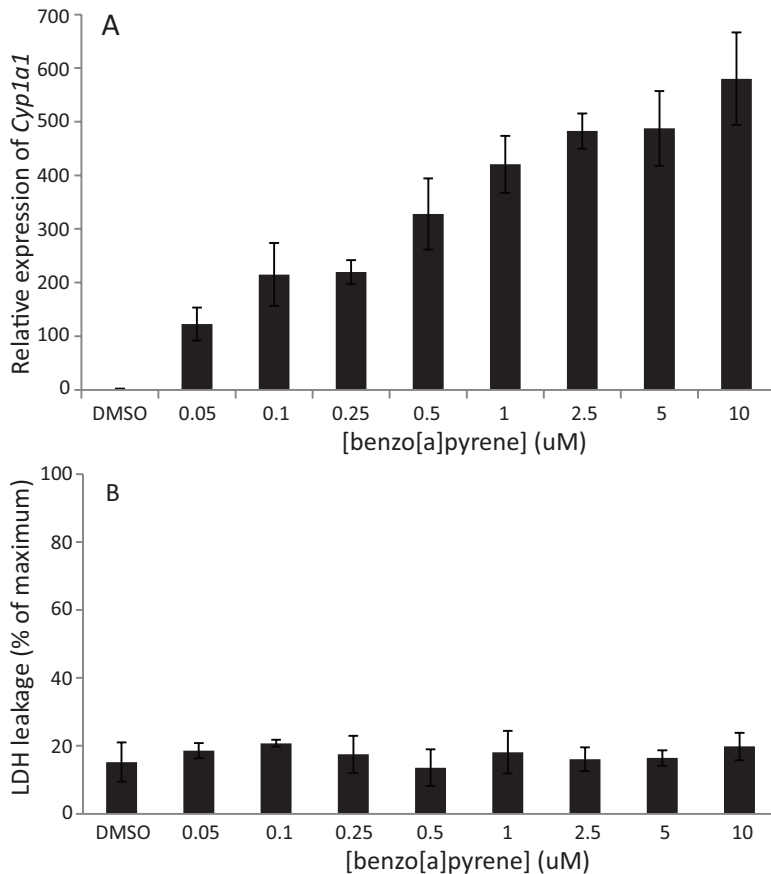
Figure S1. B[a]P dose response curve for *Cyp1a1* induction in mouse primary hepatocytes. Sandwich cultured mouse primary hepatocytes were exposed to increasing doses of B[a]P or its solvent DMSO (0.1%). (A) Dose dependent induction of *Cyp1a1* after 4 hour exposure, as measured by RT-qPCR (n=2 independent experiments with biological triplicates). (B) LDH secretion after 4 hour exposure (n=2 independent experiments with biological triplicates). Error bars represent SD.
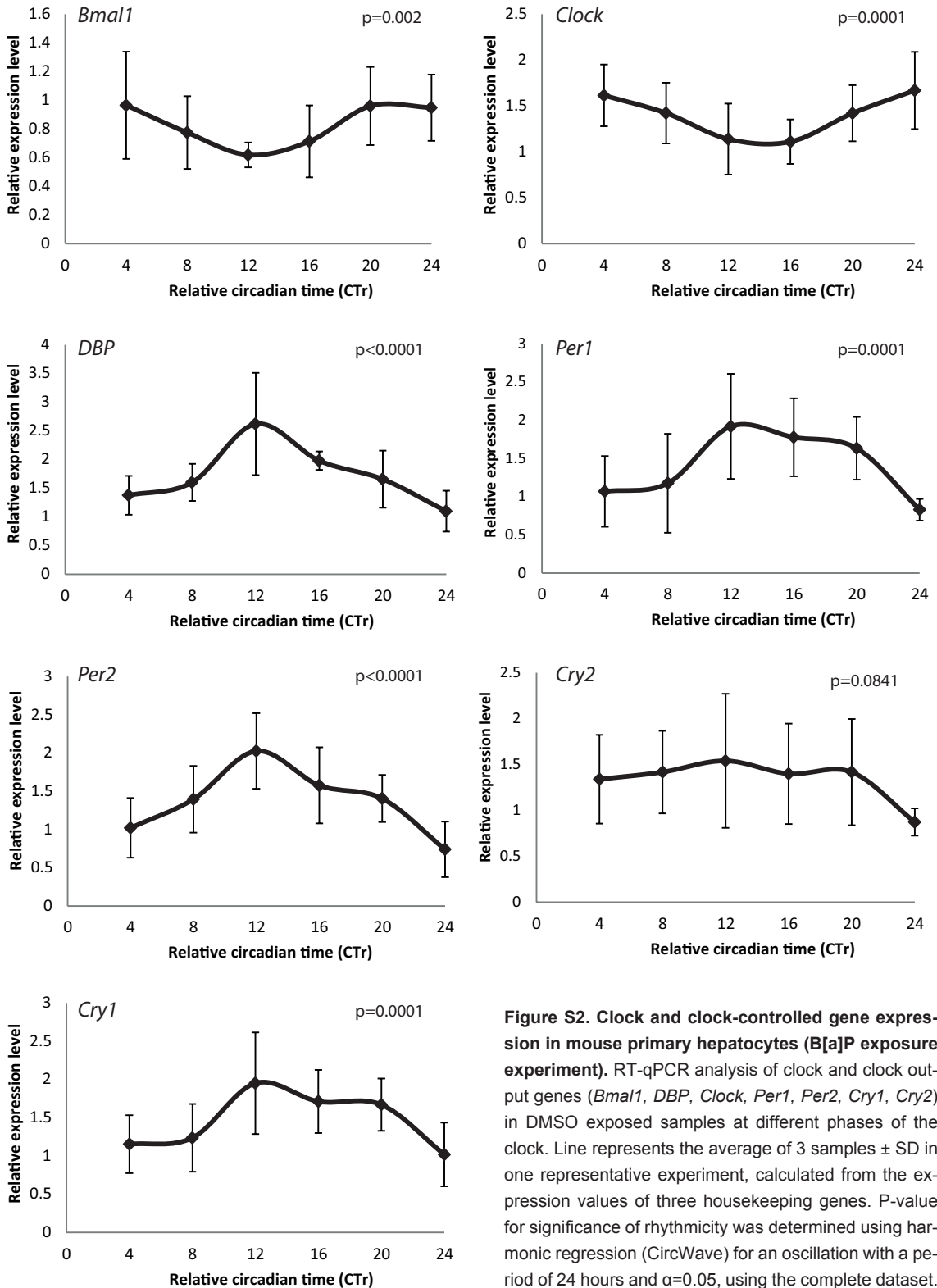
Figure S2. Clock and clock-controlled gene expression in mouse primary hepatocytes (B[a]P exposure experiment). RT-qPCR analysis of clock and clock output genes (*Bmal1, DBP, Clock, Per1, Per2, Cry1, Cry2*) in DMSO exposed samples at different phases of the clock. Line represents the average of 3 samples ± SD in one representative experiment, calculated from the expression values of three housekeeping genes. P-value for significance of rhythmicity was determined using harmonic regression (CircWave) for an oscillation with a period of 24 hours and α=0.05, using the complete dataset.

3
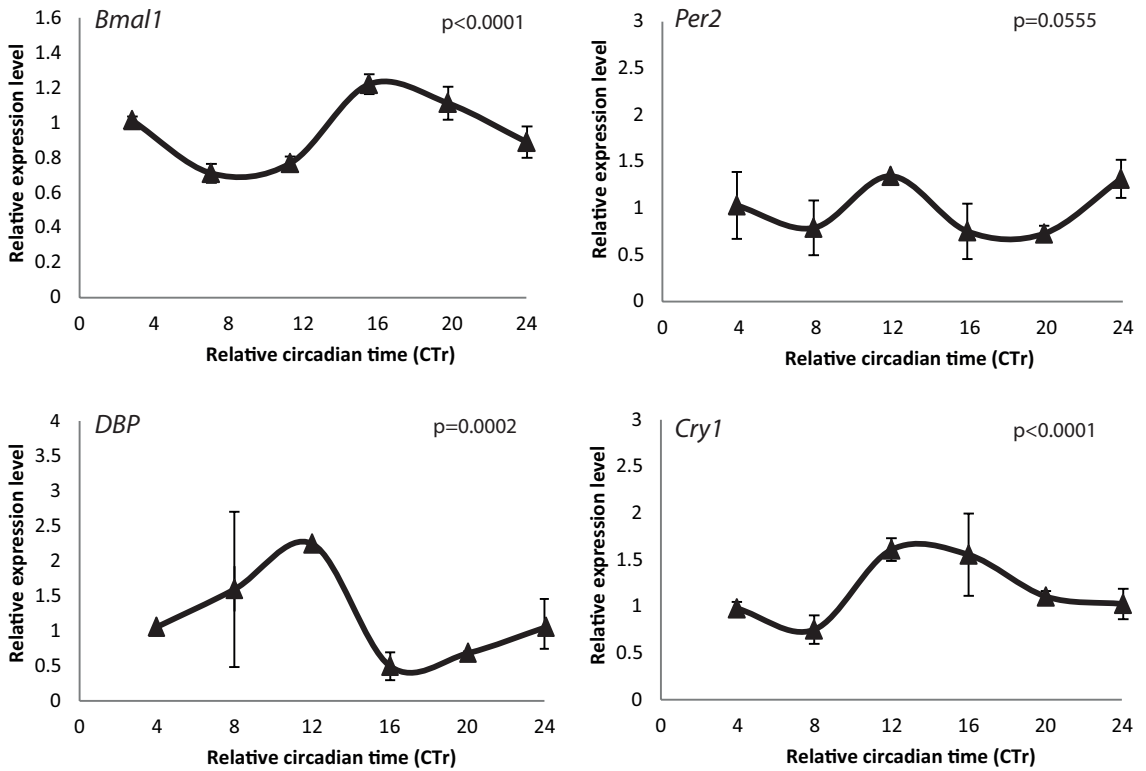
Figure S3. Clock and clock-controlled gene expression in mouse primary hepatocytes (B[a]P mutagenesis experiment). RT-qPCR analysis of clock and clock output genes (*Bmal1, DBP, Per2, Cry1*) in control samples at different phases of the clock. Line represents the average of 3 samples ± SD in one experiment, calculated from the expression values of three housekeeping genes. P-value for significance of rhythmicity was determined using harmonic regression (CircWave) for an oscillation with a period of 24 hours and α=0.05, using the complete dataset.

A
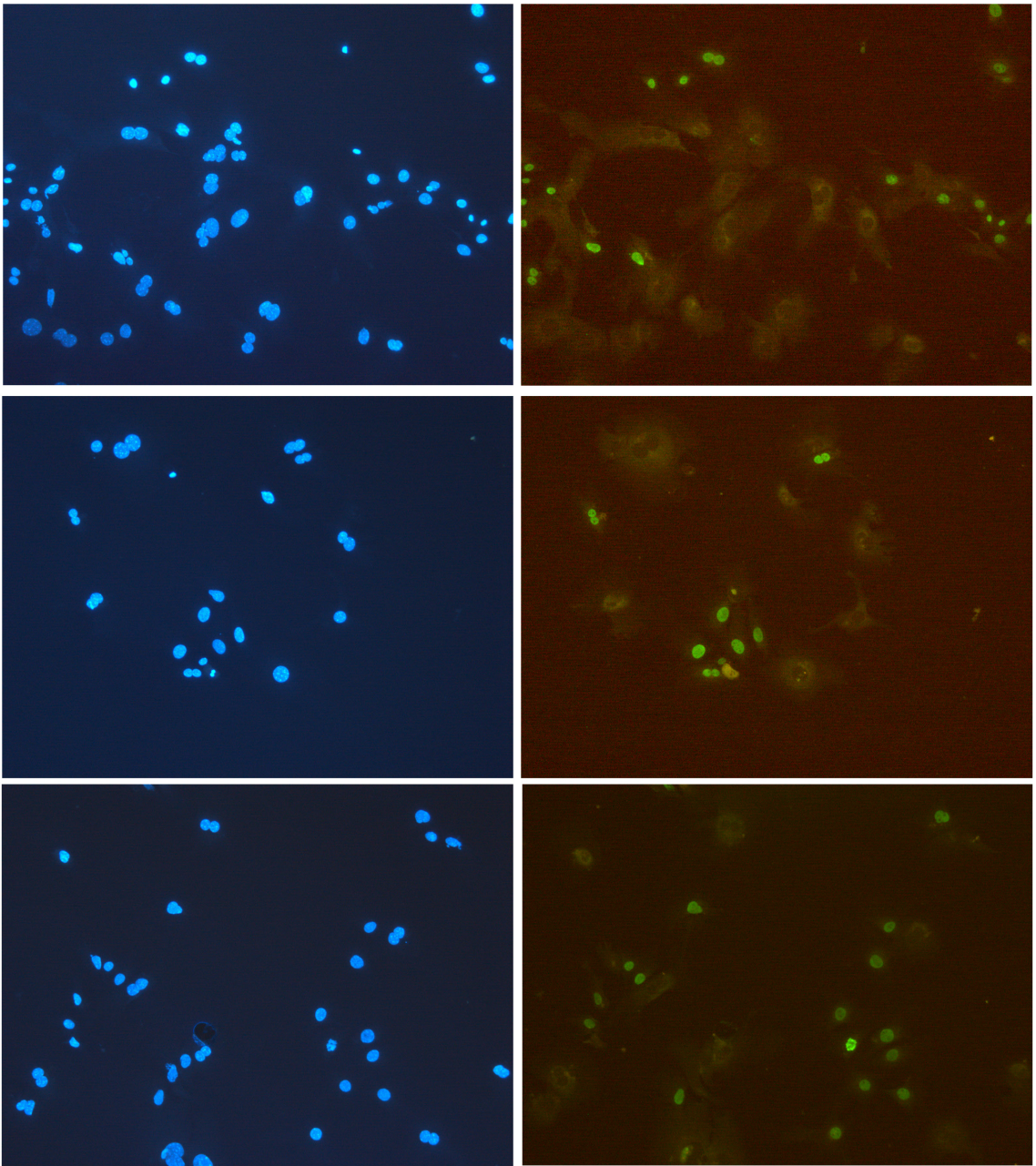
B

3
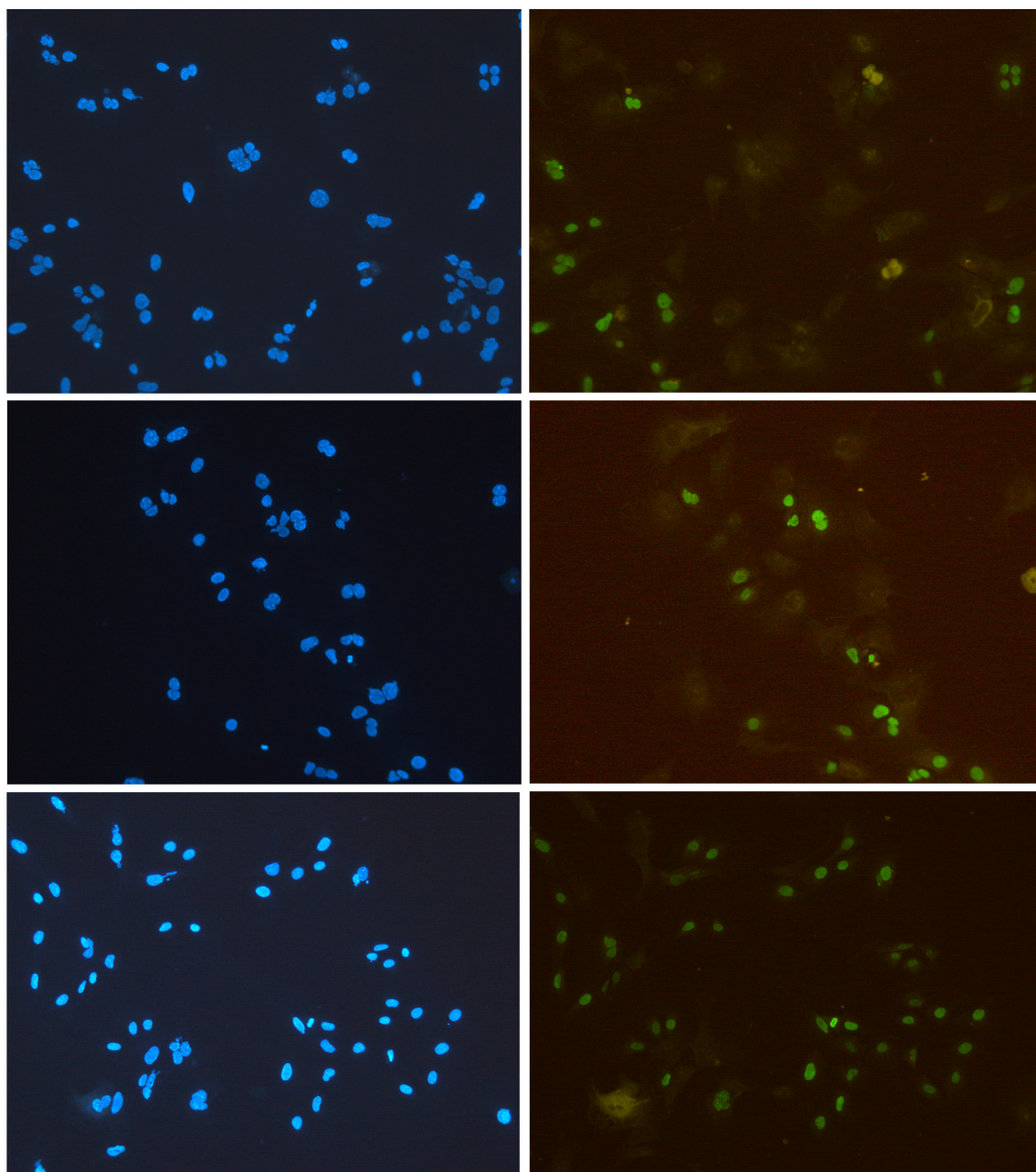
Figure S4. BrdU staining of mouse primary hepatocytes (B[a]P mutagenesis experiment). BrdU staining of primary hepatocytes at day 3-4 (A) and day 4-5 (B). The exposure experiment was performed at day 3 and cell lysis was performed at day 5. Cumulative positive nuclei from day 3-5 represent >50% of total number of nuclei. For each day, photographs of three separate glass coverslips are shown. Blue = DAPI, bright green = BrdU positive nuclei.

3

Chapter 4

SIMH4: a novel Spontaneously Immortalized Mouse Hepatocyte cell line with primary hepatocyte-like characteristics and high metabolic competence

Annelieke S. de Wit, Inês Chaves, Peter de Bruijn, Gijsbertus T.J. van der Horst

Abstract

In genotoxic risk analysis, many studies are focusing on finding *in vitro* alternatives for *in vivo* testing to ultimately replace the use of laboratory animals in drug development and safety investigations. Because of the major role of the liver in xenobiotics metabolism, many studies are focusing on this organ. Current models comprise slices, isolated hepatocytes and immortalized cell lines, but these are hindered either by availability and skill requirements or by reduced metabolic competence. In the present study, we characterized a novel cell line of spontaneously immortalized mouse hepatocytes, SIMH4, derived from a male C57BL/6J-*Period2::luciferase* mouse. SIMH4 cells, other than commercially available cell lines, retain a cuboidal hepatocyte-like appearance and high hepatocyte-specific gene expression and protein production levels under standard culturing conditions. The response to the chemical toxins benzo[a]pyrene and cyclosporine A was more similar to that in mouse primary hepatocytes than to other commonly used established cell lines and we have demonstrated that exposure eventually leads to the induction of apoptosis and cholestasis, two common forms of drug induced liver injury. Additionally, SIMH4 cells were able to metabolize the pharmaceutical drugs sunitinib and tamoxifen at higher rates than other cell lines. Last, we optimized conditions to use SIMH4 cells in the micronucleus test and found significant increases in the formation of micronuclei after exposure to mitomycin C, cyclophosphamide and benzo[a]pyrene. Therefore we suggest that this cell line can be used in genotoxic risk analysis and and in high throughput (toxicity) screens on drug development programs.

Introduction

Given that we are daily exposed to a variety of toxic chemicals, as present in food, cosmetics and pharmaceutical drugs, as well as in our environment, our society demands the testing of new and existing chemicals. On the other hand, as chemical risk assessment still requires the use of many laboratory animals, our society calls for a drastic reduction, and ultimately banning of animal experiments. Therefore, worldwide efforts are being made in setting up and validating *in vitro* alternatives, combined with toxicogenomics-based biomarker assays. With these sensitive mechanism-based assays chemicals can be tested for hazardous health effects, which not only reduces environmental risk but also benefits the pharmaceutical drug development trajectory by limiting late-stage candidate failure.

The liver is the major site of xenobiotic metabolism, involving both activation and detoxification of environmental pollutants and drugs. As such, chemically induced toxicity, notably drug-induced liver injury is still the major cause of hepatic injury (Davila et al., 2008), accounting for 50% of cases of acute liver failure (Lee, 2003). Steatosis, cholestasis, apoptosis/necrosis and carcinogenesis are common forms of liver disease, which often occur in parallel. Steatosis is a condition in which large quantities of fatty acids accumulate in liver vesicles (Janorkar et al., 2009), while cholestasis is characterized by obstruction of bile flow and intracellular accumulation of toxic bile acids (Chiang, 2013). Both conditions can be caused by various processes, amongst which drug induced injury plays a major role (Davila et al., 2008). Cell death can be induced by the triggering of death receptors and changes in glutathione levels, common by-effects of chemotherapy (Thatishetty et al., 2013), or as a secondary effect of other types or damage. Hepatic cell death appeals on the regenerative capacity of the liver, restoring cell mass but increasing the risk of mutagenesis and ultimately cancer (Gupta, 2000). This process is very complex and likely multifactorial (Harris and Sun, 1984; Wogan, 2000) and is therefore difficult to study when focusing on a specific target gene or enzyme. In *in vitro* assays, cholestatic processes can easily be overlooked because of the rapid onset of apoptotic phenotypes (Faubion et al., 1999).

Drug-induced liver injury (DILI), notably unforeseen drug-drug interactions (DDIs), causes research to focus on methods for more accurate predictions of drug toxicity (Rostami-Hodjegan, 2010; Shitara et al., 2005; Yoshida et al., 2012). Therefore it is not only necessary to establish *in vitro* assays that closely mimic the *in vivo* situation, but also to identify early markers of both

preclinical (Dambach et al., 2005; Gomez-Lechon et al., 2010b) and diagnostic (Lemmer et al., 2006) hepatic injury and include these parameters in high throughput *in vitro* screens in order to meet the requirements for testing large numbers of compounds (Bayliss and Cross, 2000; Judson et al., 2011).

An *in vitro* system to screen for hepatocyte injury should at least possess a normal and balanced set of xenobiotic activating and detoxifying enzymes, intact oxidative metabolism, an antioxidant defense system, uptake and efflux transporters, and healthy mitochondria (Godoy et al., 2013). The most important use of *in vitro* systems is to gain knowledge on the metabolism of a given chemical, as well as the molecular mechanisms by which such chemicals induce or inhibit enzymes, in order to use this knowledge for chemical safety assessment or pharmaceutical drug development (Riley, 2001). Because the metabolism of drugs is highly variably amongst humans due to genetic background, age and diet (Lin and Lu, 2001), such mechanisms are difficult to expose. Therefore the use of hepatic systems derived from genetically homogeneous laboratory animals is a necessary step. Moreover, mice are especially eligible because many transgenic models with divergent metabolic deficiencies exist, improving our knowledge on the interplay between metabolic pathways and drug-drug interactions.

An additional requirement for an *in vitro* system is that it allows phenotypic anchoring and repeated exposure. Many *in vitro* studies are focusing solely on differential gene expression after a single exposure to a compound, but because a compound can cause liver injury by more than one mechanism, screens must rely on a biologically relevant phenotype or end point. Ample inconsistencies in gene expression profiles have been observed in response to chemicals when comparing differential gene expression profiles between mice and humans and between *in vivo* and *in vitro* conditions, while the biological endpoint is similar (Kienhuis et al., 2013). Moreover, Zhang and coworkers analyzed gene expression profiles of different species and compounds and found that the initial xenobiotic response is highly conserved, but downstream effectors are often very different (Zhang et al., 2013). Therefore, phenotypic anchoring is more reliable when setting up *in vitro* assays in order to identify the type of injury a specific compound may eventually cause *in vivo*.

At present, human primary hepatocytes are regarded the preferred *in vitro* liver system because this cell type most closely resembles the human *in vivo* situation (Gomez-Lechon et al., 2010a) and express the full spectrum of drug metabolizing enzymes and transporters (Hewitt et al., 2007). However, limited availability, large batch variations (Gomez-Lechon et al., 2003; Kanebratt and Andersson, 2008), demanding isolation procedures and culturing conditions (LeCluyse et al., 2005), and limited survival *in vitro* (Gomez-Lechon et al., 2004) are enormous drawback for routine testing of drugs. Primary hepatocytes and liver slices derived from laboratory animals (van Swelm et al., 2013) reduce the availability and variability limits, but still involve time consuming and skill demanding techniques (Godoy et al., 2013). Accordingly, for high throughput screens, human and non-human hepatocarcinoma-derived, virus-transformed or oncogene expressing transgenic animal-derived cell lines are often the preferred cell type of choice (reviewed by (Castell et al., 2006). These cell lines can be used unlimitedly, but on average have limited expression of important hepatocyte-specific drug-metabolizing enzymes (Donato et al., 2008; Rodrigues-Antona et al., 2002), for which reason they do not represent a true replacement for primary hepatocytes. Xenobiotic metabolism studies in these cells require either transfection or infection of cells with expression vectors for genes encoding metabolizing enzymes (Castell et al., 2006; Godoy et al., 2013; Tolosa et al., 2012) or supplementation of cell cultures with a subcellular fraction containing functional enzymes (S9) (Madle et al., 1986), but both options have their limitations. Transfection often results in uncontrolled expression levels of CYPs (Frederick et al., 2011) and inadequate electron transport (Gonzalez and Korzekwa, 1995) leading to an unbalanced metabolic capacity, while microsomal fractions do not contain the full spectrum of phase I, II and III enzymes (Castell et al., 2006). Intermediate systems such as the highly differentiated HepaRG cells (Guillouzo et al., 2007; Kanebratt and Andersson, 2008), hepatocyte-like cells (HLC) from induced pluripotent stem (iPS) cells (reviewed by (Godoy et al., 2013), proliferating human hepatocytes (Burkard et al., 2012) or 3D-structures such as organoids (Mitaka and Ooe, 2010; Takahashi et al., 2010) and

4

4

cells seeded on or in hydrogels, scaffolds of hepatospheres (reviewed by (Godoy et al., 2013) have greatly ameliorated the predictive value of the spectrum of *in vitro* systems, but are time and cost consuming because they generally take long time to differentiate or grow into the desired structures.

In the present study, we established a Spontaneously Immortalized Mouse Hepatocyte line (SIMH4) that (i) combines primary hepatocyte-like characteristics with high xenobiotic metabolic competence under standard 2D culturing conditions, (ii) is not subject to dedifferentiation, even at high passage number, and (iii) allows phenotypic anchoring of toxicogenomics data. We propose this cell line as the ideal replacement for mouse primary hepatocytes and human and mouse hepatocarcinoma derived cell lines. Establishing SIMH lines from a variety of transgenic and/or reporter mice will further add to our understanding of toxic mechanisms and development of risk assessment assays, while concomitantly reducing the number of laboratory animals in toxicological research.

Materials & methods

Animals
Male C57BL/6J *Per2::Luc* mice (Chaves et al., 2011) were housed at the Animal Resource Center of the Erasmus University Medical Center, which operates in compliance with the European guidelines (European Community 1986) and The Netherlands legislation Dutch legislation for the protection of laboratory animals. Animals were kept in a 12:12 hour light/dark cycle with ad libitum access to water and pelleted food. This animal study was approved by DEC Consult, an independent Animal Ethical Committee (Dutch equivalent of the IACUC) under permit numbers EMC2027 and EMC2382.

Isolation and maintenance of primary hepatocytes
Primary hepatocytes were isolated from 10-16 week old male *Per2::Luc* mice by a two-step collagenase perfusion method (Seglen, 1976), with modifications. In short, animals were anesthetized with an overdose of pentobarbital (300 μg/g body weight; IP injection) and. the liver was perfused in situ via cannulation of the abdominal vena cava using wash buffer, composed of Hank's balanced salt solution (HBSS; Invitrogen) and 10 mM Hepes (Lonza) and 16mM $NaHCO_3$) at a temperature of 37^0C and a flow rate of 7 ml/min. After 10 minutes the was buffer was substituted by perfusion buffer (wash buffer supplemented with 150 U/ml collagenase type IV (Sigma) and 5mM $CaCl_2$) and perfusion was continued for 12 – 16 minutes, depending on the size of the liver. After perfusion, the liver was excised and cells were filtered using a sterile 70 μm filter in primary hepatocyte culture medium (DMEM containing 10% FCS (Gibco), 100 U/ml pen/strep, 0.5 U/ml insulin (Sigma), 20 ng/ml EGF (Sigma), 7 ng/ml glucagon (Sigma) and 7.5 μg/ml hydrocortisone (Sigma)). Cells were centrifuged 3 times (4^0C, 50 g) and during the last centrifugation step Percoll (GE Healthcare) in 1x HBSS was added to separate viable cells from dead cells and debris. Yield and viability (ca. 90% for all mice) were determined using Trypan Blue exclusion.

SIMH generation and cell culture
SIMH cell lines were established from primary hepatocytes seeded at around $6x10^5$ cells in 6-wells plates. Cells were maintained in primary hepatocyte medium without FCS for 1 week with daily medium change before gradually changing to SIMH culturing medium, consisting of William's E (Lonza), containing 10% FCS, 100 U/ml pen/strep, 2 mM Ultraglutamine 1 (Lonza) and 1x ITS-X mix (Gibco)). Medium was changed every 3-4 days until cells started to form colonies, which took between 3 to 12 weeks, depending on the cell line. All the SIMH cell lines were subcultured every 3-4 days after immortalization and maintained in a humidified incubator at 37^0C and 5% CO_2. For SIMH4, cells started to form islands after 4 weeks. Unless stated otherwise, experiments with SIMH4 were performed with passage numbers 15-40.

Hepa1-6 and HepG2 cells were maintained in SIMH medium to eliminate experimental variation due to medium composition. NIH3T3 cells were cultured in DMEM/Ham's F10 (Gibco)

supplemented with 10% FCS and 100 U/ml pen/strep. All cells were subcultured every 3-4 days and maintained in a humidified incubator at 37^0C and 5% CO_2.

For experiments in which hepatocyte-specific characteristics and gene expression of SIMH4 cells, primary hepatocytes (sandwhich cultured), and HepG2 and Hepa1-6 cells were compared, cells were seeded in 6 well-plates in SIMH medium at a density to reach confluency in three days . For experiments testing the cell characteristics in different medium compositions, the medium was changed to SIMH medium with different amounts (10%, 1% or 0%) of FCS at day three and samples were collected daily. Medium samples were collected and centrifuged 1 min at 13.200 g to remove cellular debris and were stored at 4^0C until further use. Cells were lysed according to the specific requirements for each type of test and lysates were stored at -80^0C. All samples were analyzed at once after finishing a set of experiments.

4

Cell proliferation assays
Proliferation rates were determined using the impedance-based xCELLigence RTCA DP system for real time monitoring of cell proliferation and viability and E-plates (ACEA Biosciences) according to the manufacturer's protocol. Population doubling times were calculated using the accessory software. Experiments were performed in triplicate wells.

Protein determination
Unless included in assay kits or stated otherwise, cell cultures were lysed using CelLytic M (Sigma) for 5 min at room temperature. Protein concentration was determined using the Pierce BCA Protein Assay Kit (Thermo Scientific). Absorption at 560 nm was measured in duplicate using a GloMax-96 Microplate Luminometer (Promega).

Secreted albumin and urea assays
Secreted albumin was measured using the Mouse Serum Albumin ELISA Kit (Genway) according to the manufacturer's protocol and measured at 450 nm using a GloMax-96 Microplate Luminometer (Promega). Secreted urea was measured with the Urea Assay Kit (Biochain) according to the manufacturer's protocol and measured at 430 nm using a Varioskan microplate reader (Thermo Scientific). For both assays, values were expressed per mg cellular protein and corrected for albumin or urea levels in the medium.

Cell viability assay
Viability of SIMH cells in confluent cultures or after (geno)toxic exposure was determined by measuring LDH release, using the Cytotoxicity Detection KitPlus (Roche Diagnostics) according to the manufacturer's protocol. Values were background corrected for LDH activity of serum components in the culture medium. Maximum LDH release (indicative for 100% cell death) was determined by lysing parallel cultures containing similar cell numbers with 1% Triton X-100 in medium for 45' at 37^0C. Absorbance at 490 nm was measured using a Varioskan microplate reader (Thermo Scientific).

Reduced glutathione assay
Reduced glutathione in cells was determined using the SensoLyte Glutathione Cellular Assay Kit (Eurogentec) according to the manufacturer's protocol. Fluorescence excitation/emission at 390 nm/480 nm) was measured using a Varioskan microplate reader (Thermo Scientific) at 390/480 nm. Values were expressed per mg cellular protein for each condition separately.

Cell staining
For albumin staining, cells were grown on glass coverslips and fixed with 3.6% paraformaldehyde and 0.15% picric acid for 20 min. Cells were permeabilized and blocked in 0.1% Triton X-100, 1% BSA (Sigma) and 10% horse serum (Sigma) in PBS for 45 min at room temperature. Albumin was visualized by incubating the cells o/n at 4^0C with a primary anti-albumin antibody (ALB(M-140), Santa Cruz) in blocking buffer (1:50). Cells were incubated with a secondary antibody (Alexa Fluor

594 anti-rabbit, Invitrogen) in wash buffer (PBS with 1% BSA) for 45 min at room temperature. Prior to mounting with Vectashield (Vector Laboratories), cell nuclei were stained with DAPI (1 µg/ml in PBS, Sigma) for 5 min. Fluorescence was imaged using a Leica DM4000B microscope.

For the detection of cholestasis, cells were grown on glass coverslips, exposed to cyclosporine A (CsA) or vehicle for 12, 24, 48 or 96 hours and fixed with 4% paraformaldehyde for 20 min. Coverslips were stained for 5 minutes with Fouchet solution (25% trichloroacetic acid (Sigma) and 10% ferric chloride hexahydrate (Sigma)) and counterstained for 2 minutes with Van Gieson solution (0.65% picric acid (Sigma) and 0.08% acid fuchsin (Sigma)) at room temperature. Pictures were taken using a Olympus BX40 microscope.

Total Bile Acid determination

Confluent cultures of SIMH4 cells were exposed to different concentrations of CsA or 0.1% DMSO (vehicle) for 4 hours in conditioned medium (i.e. medium taken from the cell cultures prior to chemical exposure). After exposure cells were washed with pre-warmed PBS and received conditioned medium without CsA or DMSO, in which they were allowed to recover for different amounts of time. Samples were stored at 4^{0}C until analysis. Intracellular bile acids were determined quantitatively with the Total Bile Acid Colorimetric Assay Kit (BQ kits) according to the manufacturer's protocol for microplate use at 560 nm with a Glomax-96 microplate reader (Promega). Values were expressed as µmol/µg protein..

Apoptosis Assay

Confluent cultures of SIMH4 cells were exposed to different concentrations of B[a]P or 0.1% DMSO (vehicle (DMSO) for 4 hours in conditioned medium. After exposure cells were washed with pre-warmed PBS and received conditioned medium without B[a]P or DMSO, in which they were allowed to recover for 20 hours. Samples were stored at -80^{0}C until analysis and intracellular amounts of cleaved caspase-3 were analyzed using the Caspase-3 Fluorescence Assay Kit (Cayman Chemicals)) according to the manufacturer's protocol at 485/535 nm using a Glomax 96-wells microplate reader (Promega). Values were expressed as µmol/µg protein.

7-ethoxyresorufin O-deethylase activity (EROD) assay

SIMH4, HepG2, Hepa1-6 and collagen sandwich cultured mouse primary hepatocytes were cultured in 6-wells plates to reach early confluency and were either left untreated or exposed to different concentrations of B[a]P or 0.1% DMSO (vehicle) for 4 or 24 hours continuously in conditioned medium. After exposure, cells were washed with ice-cold PBS and after aspiration of fluids, plates were quickly frozen on dry ice and stored at -80^{0}C for max. 3 days. The EROD assay was performed as described previously (Donato et al., 1993), with modifications for the use of frozen culture dishes (see Suppl. Figure S1). In short, plates were quickly thawed in a 37^{0}C water bath and kept on ice, after which culturing medium supplemented with 0.5 mM NADPH, 8 µM 7-ER, 10 uM dicumarol (Sigma) and 1.5 mM salicylamide (Sigma) was added. After 1 hour incubation at 37^{0}C, 75 µl assay medium was transferred to black-walled 96-wells plates in duplicate and incubated for another hour at 37^{0}C with 15 Fishman units of β-glucuronidase and 120 Roy units of arylsulfatase (Roche Diagnostics) in 25 µl of enzyme solution to hydrolyze resorufin conjugates. After terminating the reaction with ethanol, P450 activity at 535/590 nm was measured using a Glomax 96-wells microplate reader (Promega). Values were expressed per µg protein and determined using a standard curve prepared with resorufin dye (Sigma).

DCFDA assay

Oxidized DCF disposition in the canalicular domains was performed as described by Zhang et al, with modifications. In short, cells were incubated with 5 µM 5-(and-6)-chloromethyl-2',7'-dichloro-dihydrofluorescein diacetate acetyl ester (DCFDA, Invitrogen) for 20 min at 37^{0}C, washed 3 times with pre-warmed PBS and analyzed using a Leica DFC300-FX microscope.

Quantitative RT-qPCR

Total RNA was isolated using TriPure reagent (Roche Diagnostics) according to the manufacturer's protocol. Following analysis of RNA quality and concentration using the NanoDrop ND1000 (NanoDrop Technologies), 1 µg of RNA was used for cDNA preparation using iScript (Biorad) according to the manufacturer's protocol. RT-qPCR was performed using Platinum Taq DNA polymerase (Invitrogen) according to the manufacturer's protocol on a Biorad C1000 Touch Thermal Cycler using a standard 2-step amplification program with annealing/extension at 60^0C. Reactions for samples with housekeeping transcripts (*B2M, Hprt* and/or *Gapdh*) were always included on the same plate as reactions for transcripts of interest. All samples were analyzed in triplicate and expression levels were normalized separately to 3 housekeeping genes. Afterwards, the average of these 3 analyses was used for calculations. The following primers were used: (mouse) *B2M* Fwd 5'-CCG GCC TGT ATC CAG AAA-3' Rev 5'-ATT TCA ATG TGA GGC GGG TGG AAC-3'; *Hprt* Fwd 5'-CGA AGT GTT GGA TAC AGG CC-3' Rev 5'-GGC AAC ATC AAC AGG ACC TCC-3'; *Gapdh* Fwd 5'-CAG AAC ATC ATC CCT GCA TCC-3' Rev 5'-GTC ATC ATA CTT GGC AGG TTT CTC-3'; *Alb* Fwd 5'-TAA GAA ACA AAC GGC TCT TGC T -3' Rev 5'-GAA GCA GGT GTC CTT GTC AG-3'; *CK18* Fwd 5'-TTG CCG CCG ATG ACT TTA GA -3' Rev 5'GGA TGT CGC TCT CCA CAG AC-3'; *cMet* Fwd 5'-TCT GGG AGC TCA TGA CGA GA-3' Rev 5'-ATC CTG GAG ACC AGT TCG GA-3'; *GluI* Fwd 5'-AAA GTC TTC GCA CAC CCG AT-3' Rev 5'-GGG GAC AAA TGC GGA GGT TA-3'; *Pck1* Fwd 5'-TGC GGA TCA TGA CTC GGA TG-3' Rev 5'-AGG CCC AGT GTT GA CCA AA-3'; *Asl1* Fwd 5'-CTA TGA CCG GCA TCT GTG GAA-3'Rev 5'-AGC AAC CTT GTC CAA CCC TTG-3'; *Gsr* Fwd 5'-GAC ACC TCT TCC TTC GAC TAC C-3' Rev 5'-GAC ATC CAA CAT TCA CGC AAG-3'; *FXR* Fwd 5'-TGG GCT CCG AAT CCT CTT AGA-3' Rev 5'-TGG TCC TCA AAT AAG ATC CTT GG-3'; *Bsep (Abcb11)* Fwd 5'-CAG AAG CAA AGG GTA GCC ATC-3' Rev 5'-GGT AGC CAT GTC CAG AAG CAG-3'; *Mrp2* Fwd 5'-TCA TGG ACA GTG ACA AGA TAA TGG-3' Rev 5'-GGC CAT CAA GTA GAA GGG AC-3'; *Mrp3* Fwd 5'-CTC TCA GCT CAC CAT CAT CC-3' Rev 5'-TGG CCA ACA CTG AGA TTA TCC-3'; *Afp* Fwd 5'-AGT TTC CAG AAC CTG CCG AG-3' Rev 5'-ACC TTG TCG ACT GAG CAG C-3'; *Cyp1a1* Fwd 5'-GCA CTA CAG GAC ATT TGA GAA GG-3' Rev 5'-AAT CAC TGT GTC TAG TTC CTC C-3'; (human): *B2M* Fwd 5'-CTC TTG TAC TAC ACT GAA TTC A-3' Rev 5'-CCT CCA TGA TGC TGC TTA CA-3'; *HPRT* Fwd 5'-TGG AGT CCT ATT GAC ATC GCC AGT-3' Rev 5'-AAC AAC AAT CCG CCC AAA GGG AAC-3'; *GAPDH* Fwd 5'-AAG GTG AAG GTC GGA GTC AA-3' Rev 5'-ACC ATG TAG TTG AGG TCA ATG-3'; *CYP1A1* Fwd 5'-GAC CAA GAG GAG CTA GAC ACA G-3' Rev 5'-CCC ATA GCT TCT GGT CAT GGT-3'. Relative gene expression was calculated using the comparative C(t) method described previously and normalized to relative expression after exposure to the vehicle (relative expression = 1) (Schmittgen and Livak, 2008).

Tamoxifen and sunitinib metabolism

HepG2 and SIMH4 cells were seeded at $4*10^5$ and $2*10^5$ cells/well in 6-wells plates 3 days prior to exposure. Sunitinib (10 µM) and tamoxifen (10 µM) were added to conditioned medium and after incubation for 1, 2, 3 and 5 hours cell lysates and medium were analyzed. Materials from cells exposed to sunitinib were collected in the dark. Cell pellets were homogenized in plasma and sonicated for 30 min at room temperature and homogenates were frozen at -70ºC. After thawing at room temperature, homogenates were sonicated again for 30 min. Tamoxifen and three of its main phase I metabolites were determined using a validated ultraperformance liquid chromatography tandem triple quadruple mass spectrometry (UPLC-MS/MS) assay by dilution of cell lysates in human lithium heparinized plasma (Binkhorst et al., 2011). The lower limit of quantitation was 5 nM for tamoxifen and n-desmethyl-tamoxifen and 0.5 nM for 4-hydroxy-tamoxifen and endoxifen. Sunitinib and its n-desethyl metabolite SU12662 were determined using a validated UPLC-MS/MS assay by dilution of cell lysates in human potassium EDTA plasma (Bruijn et al., 2010). The lower limit of quantitation was 0.2 ng/ml for both sunitinib and the n-desethyl metabolite SU12662.

Micronucleus assay

IC50 values for vinblastine, mitomycine C (MMC), cyclophosphamide (CP) and benzo[a]pyrene

(B[a]P) (all Sigma) were determined in proliferating cultures of SIMH4 cells using the Alamar-Blue Cell Viability assay (Invitrogen) according to the manufacturer's protocol, with an incubation time of 2 hours. Fluorescence was measured using a Glomax-96 Microplate reader (Promega) at 560/590 nm. At least triplicate wells per concentration were analyzed and experiments were performed at least three times. IC_{50} was defined as the average concentration of the chemical at which 50% maximal fluorescence was measured. For micronucleus counting, SIMH4 cells were seeded at $6x10^3$ cells per well on glass coverslips in 24-well plates and allowed to proliferate for 3 days. Cells were exposed for 4 hours to aforementioned chemicals at their IC_{50} concentrations in conditioned medium. After washing with pre-warmed PBS, conditioned medium with 0.15 µg/ml cytochalasin B (Cayman Chemicals) was added and cells were allowed to recover for 20 hours. Next, cells were fixed with 4% paraformaldehyde and stained with 50 µg/ml acridine orange (Sigma) and 1 ug/ml DAPI (Sigma) for 5 min at room temperature. Coverslips were mounted using Vectashield and analyzed using a Leica DM4000B microscope. Per condition 10 fields of cells were analyzed from four coverslips , containing at least 1000 cells and micronucleus counting was performed manually by 2 independent researchers. No statistical significant differences were found between counts from both researchers.

Statistical analysis
Statistical analysis was performed in Microsoft Excel using a Student's paired two-tailed t-test. For gene expression experiments with large interexperimental but similar intraexperimental differences, results were analyzed separately and p-values represent the average of these calculations. P-values >0.05 were considered not significant .
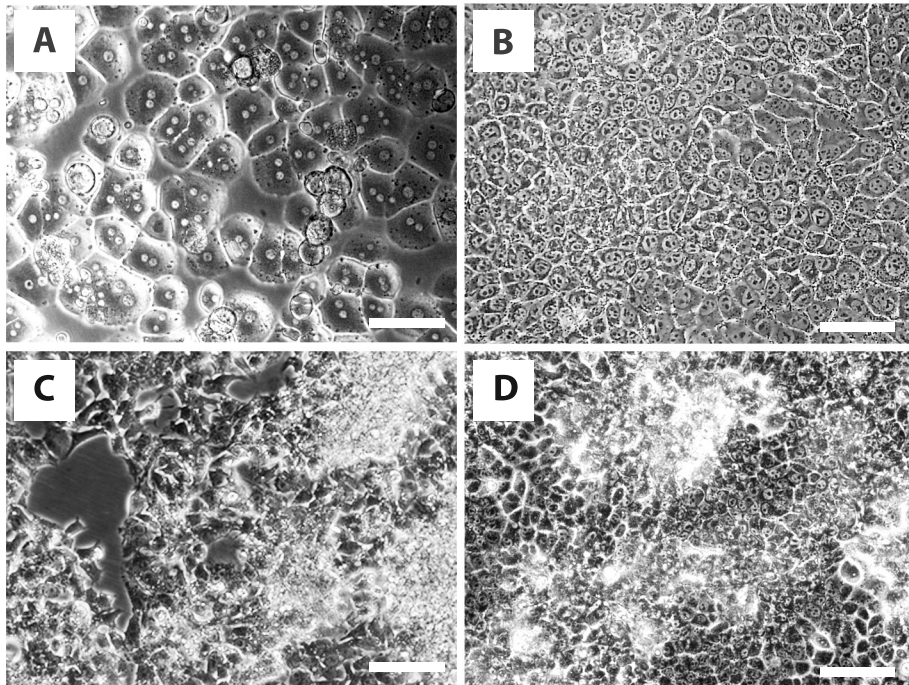
Figure 1. Morphology of SIMH4 cells. Phase contrast micrographs of sandwich cultured mouse primary hepatocytes (A), SIMH4 (B), HepG2 (C) and Hepa1-6 (D) cells under standard culturing conditions. Pictures were taken at 200x magnification. Bars represent 20 µm.
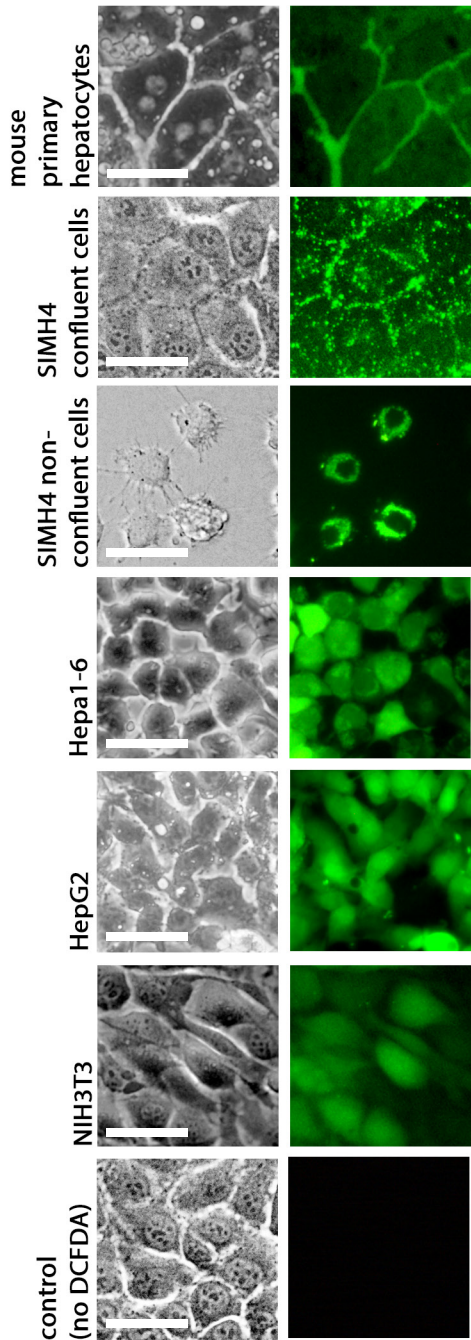
Figure 2. Polarized structure of SIMH4 cells. DCFDA staining of sandwich cultured mouse primary hepatocytes, (confluent and non-confluent) SIMH4 cells, Hepa1-6, HepG2 and NIH3T3 cells. DCFDA (5 μM final concentration) was added to the medium 20 minutes prior to microscopic analysis. Shown are phase contrast micrographs (left panels) and DCF fluorescence (right panels). Note the excretion of DCF in canalicular structures in mouse primary hepatocyte and SIMH4 cell cultures, indicative for the presence of polarized structure. All pictures were taken at 200x magnification. Bars represent 20 μm.

Results

SIMH4 cells retain cell cuboidal morphology and polarized structure

Spontaneously Immortalized Mouse Hepatocyte (SIMH) cell lines were established from primary hepatocytes (C57BL/6J genetic background) by keeping cells in culture for up to 12 weeks under regular medium changes until islands of proliferating cells started to appear (for a detailed description, see Materials & methods section). We have selected the SIMH4 cell line for an in depth characterization, including a comparison with commonly used hepatocarcinoma cell lines such as human HepG2 and mouse Hepa1-6.

Proliferating SIMH4 cells show a population doubling time of ca. 10-12 hours in log phase (Suppl. Figure S2), to ultimately form a uniform monolayer of closely attached cells (Figure 1B). As such, they contrast HepG2 and Hepa1-6 cells which form multilayered colonies and/or often detach from cell clusters (Figure 1C and D). Furthermore, SIMH4 cells retain a distinct cuboidal morphology, resembling that of primary mouse hepatocytes (compare Figure 1A and B, Suppl. Figure S3), while HepG2 and Hepa1-6 cells show a more epithelial-like morphology (Figure 1C and D). Importantly, SIMH4 cells can be kept in culture for over 100 passages.

Primary hepatocytes grown in sandwich configuration have been shown to polarize and form bile canaliculi, which can be visualized by 5-(and 6)-carboxy-2'-7'-dichlorofluorescein diacetate (DCFDA) staining. In the presence of functional drug transporters, DCFDA is internalized by hepatocytes and metabolized into fluorescent 5-(and 6)-carboxy-2'-7'-dichlorofluorescein (CDF), which in turn is excreted into the bile canaliculi via the multi-drug resistance protein 2 (MRP2) (LeCluyse et al., 2005; Turncliff et al., 2006; Zhang et al., 2013) Like primary hepatocytes, DCFDA treated SIMH4 cells in confluency are able to actively export DCF at the apical membrane into the canalicular intercellular space (Figure 2, Suppl. Figure S3). In contrast, at low density SIMH4 cells internalize and metabolize DCFDA but, in the absence of cell-cell contacts, fail to excrete CDF (Figure 2B). Hepatocarcinoma cell lines have been reported to lack expression of many liv-

4
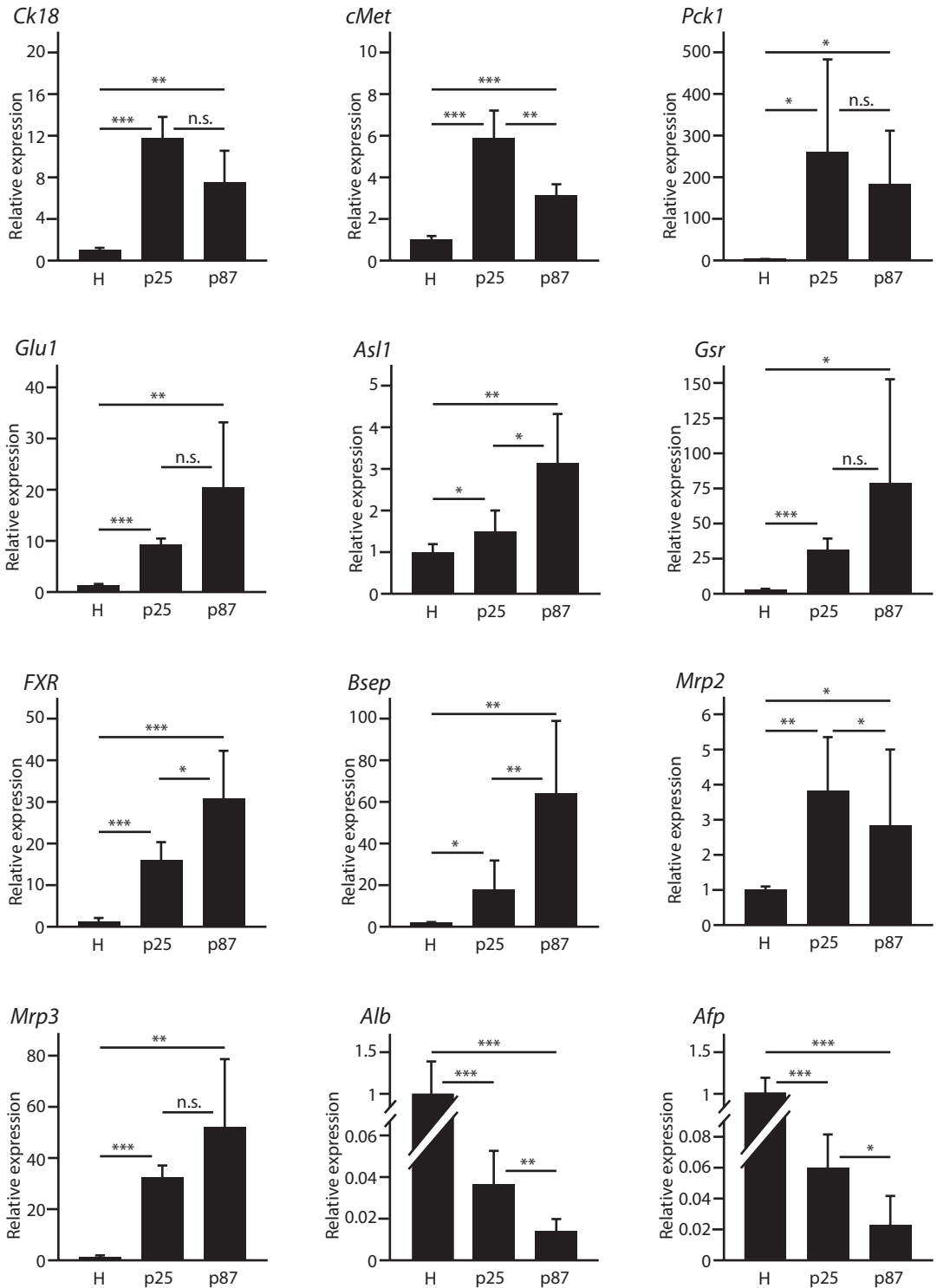
Figure 3. Differentiation status of SIMH4 cells. Comparison of hepatocyte-specific gene expression in Hepa1-6 (H) and SIMH4 cells (passage p25 and p87). Gene expression was determined by RT-qPCR and relative expression level in Hepa1-6 cells is set as 1 (n=2 experiments, triplicate measurements per experiment). Error bars represent SD (*** p<0.001, ** p<0.01, * p<0.05, ns non-significant).

er-specific transporters (Godoy et al., 2013). Indeed, Hepa1-6 and HepG2 cells metabolize DCF-DA, but appear not able to secrete CDF into the extracellular space (Figure 2B). In conclusion, SIMH4 cells retain cell polarization capacity in confluent 2D standard cultures and form canalicular structures.

SIMH4 cells retain expression of hepatocyte specific enzymes and transporters

To validate the differentiated status of SIMH4 cells and compare it with that of a hepato-carcinoma cell line, the expression of hepatocyte specific genes was measured in SIMH4 cells at different passage number and in murine Hepa1-6 cells. Relative expression levels in Hepa1-6 cells were set as 1. As shown in Figure 3, the relative expression levels of Keratin 18 (*CK18)*, Met proto-oncogene (*cMet*), Glutamate-ammonia ligase (*Glul*) and Phosphoenolpyruvate carboxyki-nase 1 (*Pckl*) all highly expressed in the adult liver, as well as genes involved in the urea cycle (Argininosuccinate lyase, *Asll*), glutathione metabolism (Glutathione reductase, *Gsr*), bile acid metabolism (Farnesoid X receptor, *FXR*) or encoding transmembrane transporters (Bile salt export pump, *Bsep*; Multidrug resistance protein 2, *Mrp2*; Multispecific organic anion transporter 3, *Mrp3*) are significantly higher in SIMH4 cells than in Hepa1-6 cells, regardless of the passage number. In marked contrast, the Albumin (*Alb*) mRNA level (the most abundant mRNA species in hepatocytes (Dennis et al., 2002)) appears lower in SIMH4 cells, as compared to Hepa1-6 cells. We also analyzed expression levels of Alpha-fetoprotein (*Afp*), encoding a fetal liver enzyme and silenced in normal adult liver, but upregulated in liver tumors and most hepatocarcinoma cell lines (Abelev and Eraiser, 1999). In line with their neoplastic origin, *Afp* mRNA levels are significantly higher in Hepa1-6 cells, as compared to SIMH4 cells.

As the *Alb* and *Afp* genes are part of the same locus (Kajiyama et al., 2006) and share regulatory elements, it is well possible that the reactivation of *Afp* in neoplastic cells also affects expression of the *Alb* gene and that accordingly, the difference in *Alb* expression between SIMH4 and Hepa1-6 cells reflects high expression of *Alb* in Hepa1-6 cells, rather than low expression in SIMH4 cells. We therefore also analyzed albumin protein expression levels in SIMH4, Hepa1-6 and primary mouse hepatocytes by immunocytochemistry (Figure 4) and observed comparable levels of albumin staining, indicating that albumin expression is normal in SIMH4 cells.

We next examined other hepatocyte specific functions and measured the secretion of albumin and urea in the medium by confluent populations of SIMH4 cells (Figure 5, solid lines). Albumin and urea are both steadily secreted in the medium when in culture for one week. When comparing early and late passage number confluent cultures of SIMH4 cells, we did not observe significant differences in the average levels of albumin and urea secretion and neither in LDH leakage and cellular GSH levels (Figure 6), indicating that hepatocyte specific functions remain constant during prolonged culturing.

Taken together, these results indicate that SIMH4 show highly differentiated, hepatocyte specific (functional) characteristics that are maintained at high passage numbers.

SIMH4 cells retain metabolic competence

To investigate the metabolic competence of SIMH4 cells and compare it to that of primary hepatocytes and hepatocarcinoma derived HepG2 and Hepa1-6 cells, we first performed an exposure study with the model carcinogen benzo[a]pyrene (B[a]P), a common environmental pollut-ant found in exhaust fume and cigarette smoke. B[a]P is a promutagen that requires cytochrome P450-mediated conversion into B[a]P-7,8-diol 9,10-epoxide (BPDE), which causes DNA adducts that can eventually lead to mutagenesis and apoptosis (reviewed by de Wit et al., 2014). B[a]P is known to bind to the aryl hydrocarbon receptor (AHR), resulting in the activation of the *Cyp1a1* gene via a xenobiotic responsive element (XRE) at its promoter.

We exposed SIMH4 cells, as well as primary mouse hepatocytes, HepG2 and Hepa1-6 cells for 4 hours to different concentrations of B[a]P and measured induction of *Cyp1a1* expression. As shown in Figure 7a, the dose-response curve of B[a]P-mediated *Cyp1a1* induction in SIMH4 cells well follows that in primary hepatocytes, although induction levels are on average 20-30% lower. In marked contrast, *Cyp1a1* expression was only minimally induced in HepG2 and
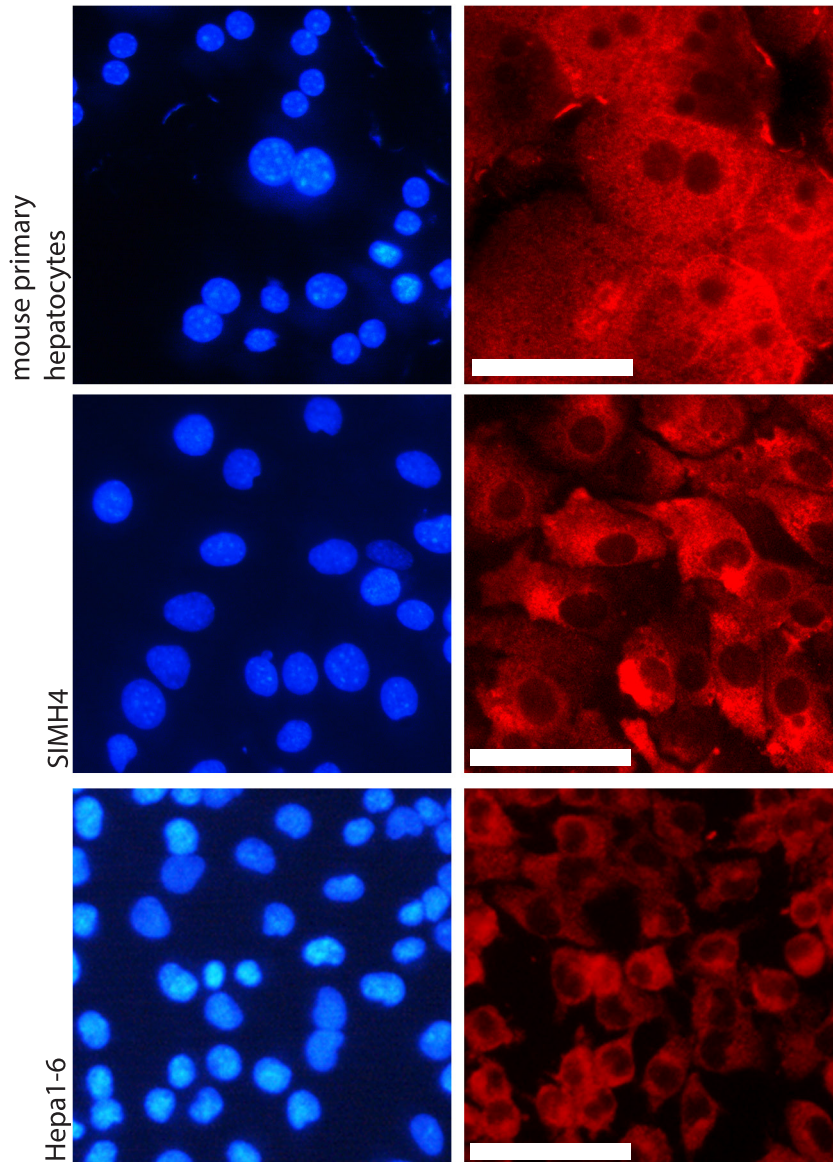
93

4

Figure 4. Albumin synthesis by SIMH4 cells. Albumin synthesis in sandwich cultured mouse primary hepatocytes, SIMH4 and Hepa1-6 cells. Shown are immunocytochemical staining of albumin (red; right panels) and DAPI staining of nuclei (blue; left panels). Pictures were taken at 400x magnification. Bars represent 20 μm
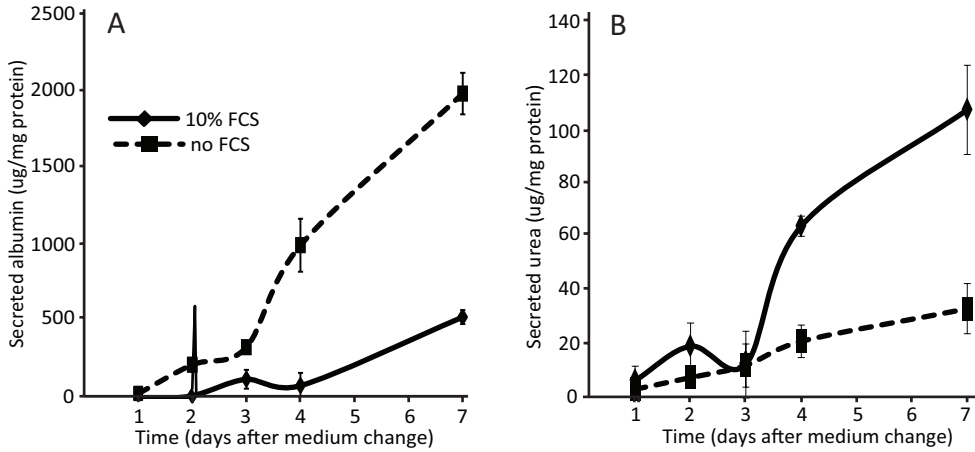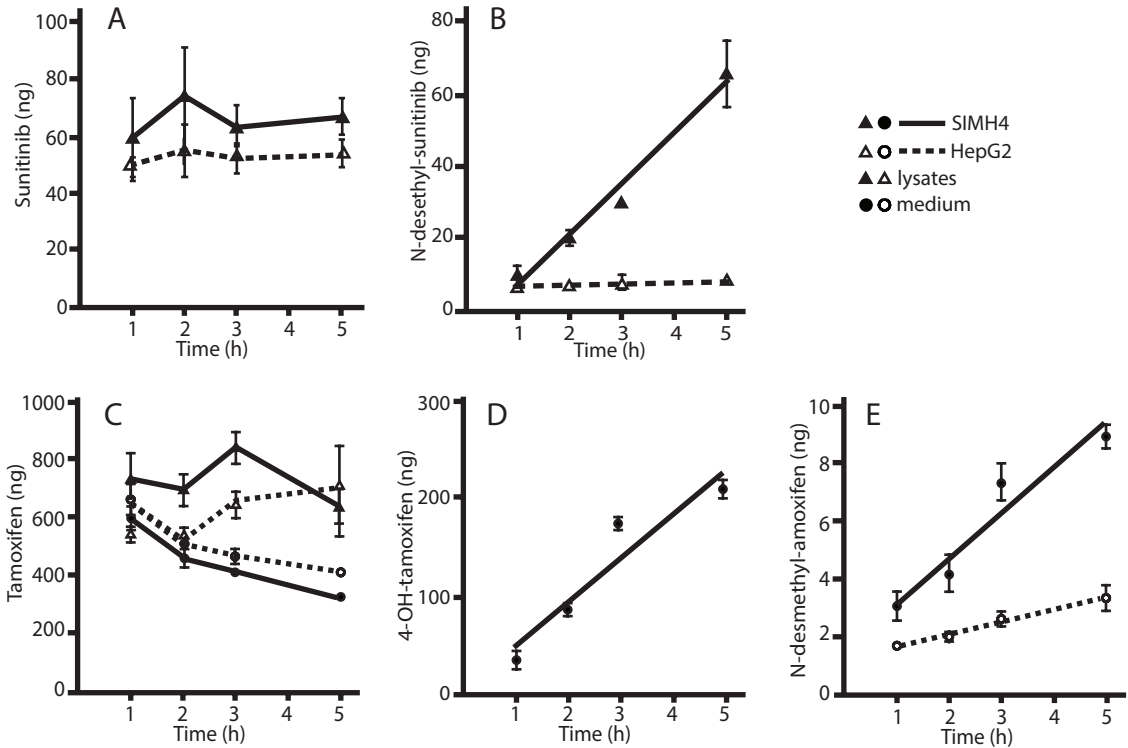
Figure 5. Albumin and urea secretion by SIMH4 cells. Albumin (A) and urea (B) secretion by confluent cultures of SIMH4 cells in the absence (dotted lines) or presence of 10% FCS (solid lines). Values are corrected for background albumin and urea levels originating from the medium (n=2 experiments, triplicate samples per experiment). Error bars represent SD.
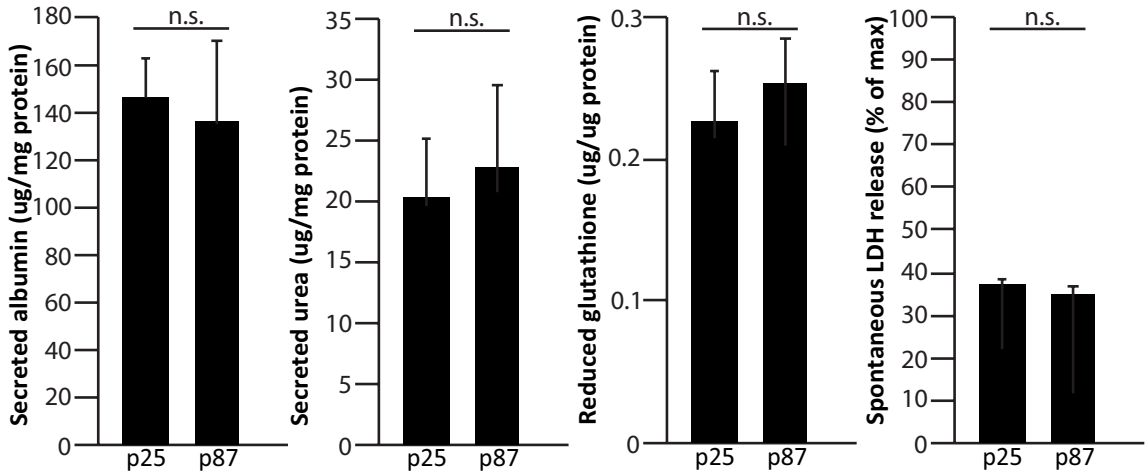
Figure 6. Albumin and urea secretion and intracellular GSH in early and late passage SIMH4 cells. Albumin secretion(A), urea secretion (B), intracellular GSH levels (C), and LDH leakage (D) in SIMH4 cells at passage number 25 and 87 (n=2 independent experiments, triplicate samples per experiment). Error bars represent SD.

4
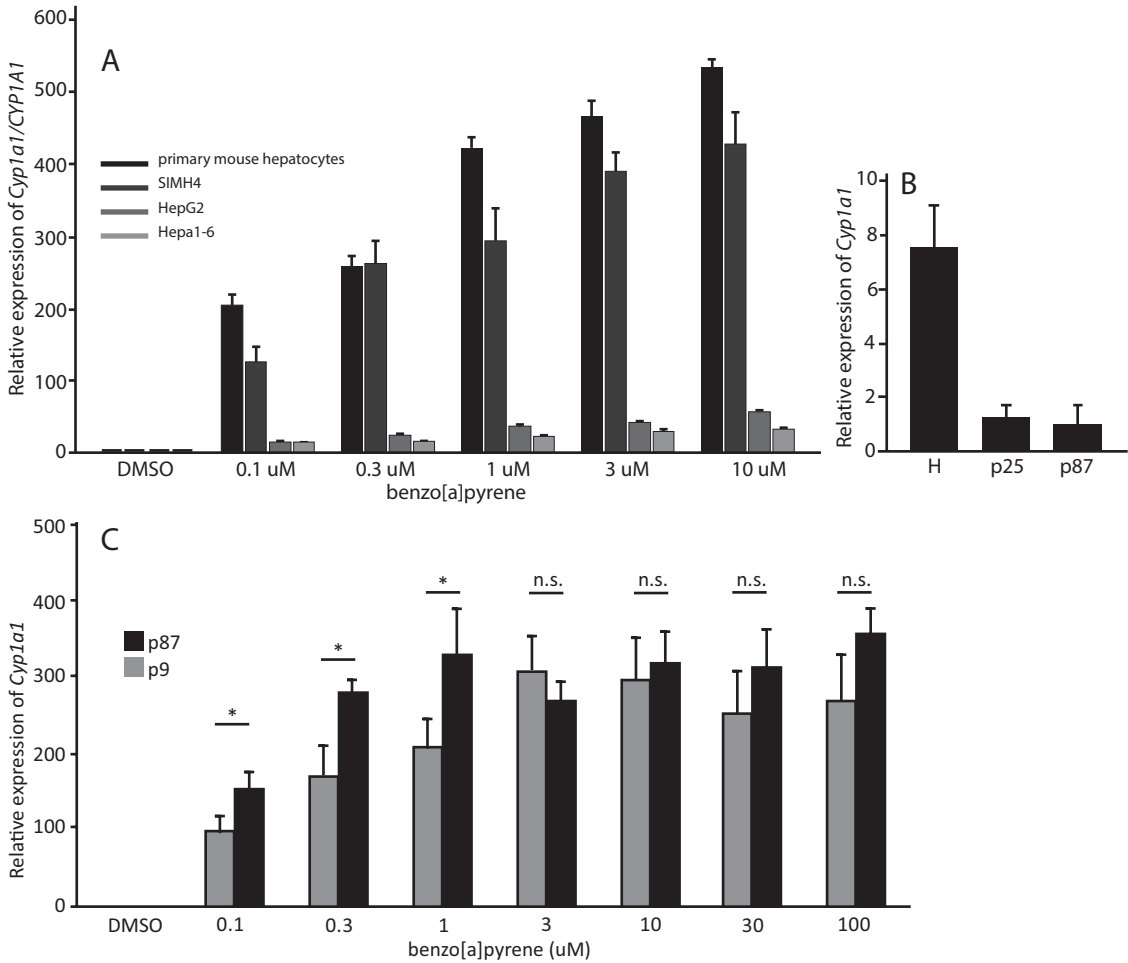
Figure 7. *Cyp1a1* induction in B[a]P exposed SIMH4 cells. Mouse primary hepatocytes, SIMH4, HepG2 and Hepa1-6 cells were either left untreated or exposed to increasing doses of B[a]P or its solvent (0.1% DMSO). (A) Dose response curve for B[a]P-induced *Cyp1a1* expression in the various liver cell lines. (B) Endogenous expression of *Cyp1a1* in Hepa1-6 and SIMH4 cells at passage 25 and 87. (C) Dose response curve for B[a]P-induced *Cyp1a1* induction in SIMH4 cells at passage number 9 and 87. n=2 experiments, triplicate samples per experiment. Error bars represent SD.
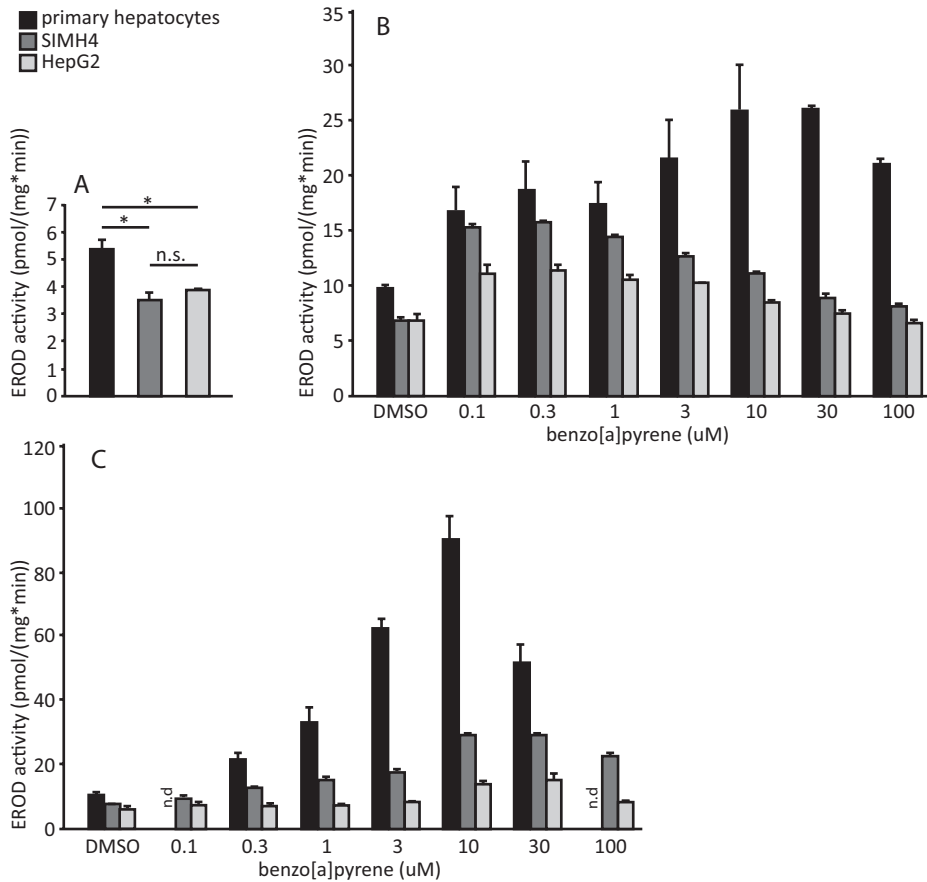
	Endogenous	Fold maximum induction (4h)	Fold maximum induction (24h)
Primary hepatocytes	5.5	~2.5	~9
SIMH4	3.4	~2	~4
HepG2	3.9	~1.5	~2

Figure 8. Endogenous (A) and B[a]P-induced EROD activity in SIMH4 cells. EROD activity was measured in SIMH4 cells, mouse primary hepatocytes and HepG2 cells in the absence of genotoxic treatment (A) or after 4 hour (B) and 24 hour (C) continuous exposure to B[a]P or its solvent 0.1% DMSO. Maximal induction (irrespective of dose) after 4 and 24 hour exposure is calculated by dividing peak of B[a]P-induced EROD activity by the EROD activity in DMSO treated cells (D) n=2-3 independent experiments, measurements in triplicate. Error bars represent SD. N.d. = not determined.

4

Figure 9. Sunitinib and tamoxifen metabolizing capacity of SIMH4 cells. Conversion of sunitinib (A) into n-desethyl-sunitinib (B) and of tamoxifen(C) into 4-OH-tamoxifen (D) and n-desmethyl-tamoxifen (E) by SIMH4 cells (closed symbols, solid lines) and HepG2 cells (open symbols, dotted lines). Note that 4-OH-tamoxifen could not be detected in HepG2 cells. N=1 experiment with triplicate samples. Error bars represent SD.

Figure 10. B[a]P-mediated induction of apoptosis in SIMH4 cells. Cleaved caspase 3 activity (A), total amount of protein (B) and total amount of reduced glutathione (C) in SIMH4 cells after 4 hour exposure to B[a]P and subsequent culturing for 20 hour . N=2 experiments with triplicate samples. Error bars represent SD.

Hepa1-6 cells (Figure 7a). The approximately 10 fold difference in *Cyp1a1* induction in SIMH4 and Hepa1-6 cells is even an underestimation as the latter cells show 7-fold higher basal *Cyp1a1* expression levels (Figure 7b). We also compared B[a]P-induced *Cyp1a1* expression in SIMH4 cells at early (p9) and late (p87) passage. Within the B[a]P dose range tested, p9 and p87 SIMH4 cells reached comparable maximum induction levels, though at lower concentrations (<3 µM) p87 cells appear more sensitive.

To evaluate the CYP1A1 enzyme activity levels, we compared both endogenous and B[a]P-induced CYP1A1 activity in SIMH4, HepG2 and primary mouse hepatocytes with the ethoxy-resorufin-O-deethylase (EROD) assay. As compared to primary hepatocytes, we observed an approximately 30% reduction in the endogenous EROD activity in SIMH4 and HepG2 cells, with no significant difference between the latter two cell lines (Figure 8A). We next exposed cells to different concentrations of B[a]P or its solvent DMSO (0.1%) for 4 and 24 hours (Figure 8B and C). After 4 hour exposure, despite marked changes in *Cyp1a1* mRNA levels (Figure 7), a relatively small (1.5-2.5 fold) dose dependent increase in EROD activity was observed, reaching a maximum at 10-30 µM for primary hepatocytes, and 0.1-1 µM for SIMH4 and HepG2 cells, and decreasing at higher doses, possibly reflecting apoptosis (Figure 8B). After 24h hours, a further dose dependent increase in EROD activity was observed for primary hepatocytes (±9-fold induction) and SIMH4 cells (±4 fold induction), with a maximum around 10 µM B[a]P (Figure 8C). This further elevation in EROD activity likely reflects the *Cyp1a1* induction early after B[a]P exposure (Figure 7). In contrast, and in line with the relative small induction in *CYP1A1* gene expression (Figure 7), the EROD activity in HepG2 cells did not significantly increase upon prolonged exposure to B[a]P (Figure 8C).

In conclusion, SIMH4 cells retain the ability to induce *Cyp1a1* expression and, to a lesser extent CYP1A1 enzymatic activity, upon exposure to B[a]P and as such more closely resemble primary hepatocytes than HepG2 and Hepa1-6 cells.

SIMH4 cells metabolize pharmaceutical drugs

We next explored the metabolic competence of SIMH4 cells towards the anticancer drugs sunitinib and tamoxifen. In mice, CYP3A11 (equivalent of human CYP3A4) is the main enzyme responsible for the metabolic conversion of sunitinib into n-desethyl-sunitinib, while CYP2D10 and CYP2D22 (equivalents of human CYP2D6) are responsible for the conversion of tamoxifen into 4'-OH-tamoxifen and n-desmethyl-tamoxifen (Chow and Eckhardt, 2007; Kiyotani et al., 2012). Uptake of both drugs is largely dependent on transporters, encoded by the *Abcb1a (Abcb1)* and *Abcg2* genes *(Abcg2)* (Bisht et al., 2013; Kiyotani et al., 2012). For the evaluation of the metabolic competence for these drugs in SIMH4 and HepG2 cells, we analyzed cellular uptake and conversion after exposure.

Sunitinib was taken up by both SIMH4 and HepG2 cells during the 5 hour exposure period, as indicated by the constant intracellular concentration of this anticancer drug (Figure 9a). However, while SIMH4 cells metabolized sunitinib into N-desethyl-sunitinib linear with time, HepG2 hardly any conversion was observed in HepG2 cells (Figure 9b). Likewise, tamoxifen was actively transported into SIMH4 and HepG2 cells (Figure 9c). After 3 hours, the intracellular tamoxifen concentration in SIMH4 cells decreased, which can likely be attributed to efficient conversion into the metabolites. The primary metabolite 4-OH-tamoxifen increased linearly in time in SIMH4 cells, while this metabolite was not measurable in HepG2 cells (Figure 9d). The secondary metabolite n-desmethyl-tamoxifen was formed at higher rate in SIMH4 cells than in HepG2 (Figure 9e). These data demonstrate that the metabolic competence of SIMH4 cells exceeds that of HepG2 cells.

SIMH4 cells and in vitro cellular hepatotoxic endpoints

Liver disease is a multifactorial phenotype at the end of a cascade of events. We next investigated whether SIMH cells can be used for *in vitro* analysis of hepatotoxicity related biological endpoints.

We first determined induction of apoptosis by the genotoxic agent B[a]P, which is known
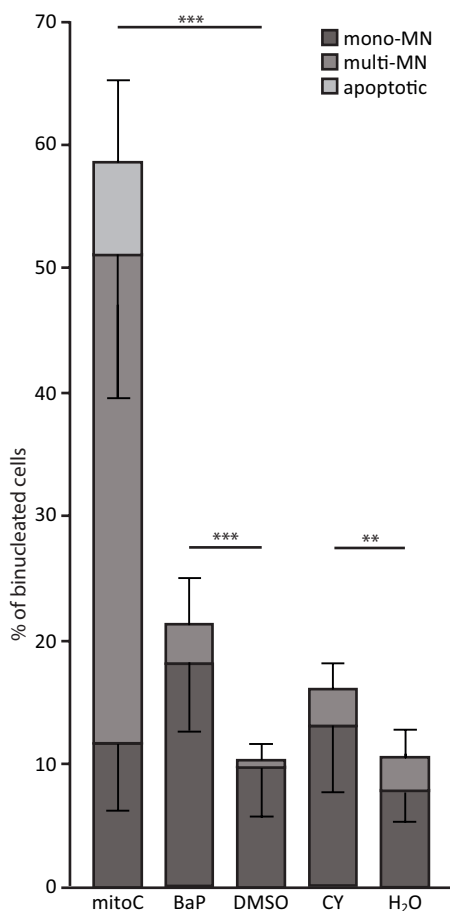
to induce apoptosis *in vivo* and *in vitro* by increasing ROS and activating p53 dependent genes (Yang et al., 2011). SIMH4 cells were exposed to increasing doses of B[a]P for 4 hours, after which culturing was continued for 20 hour. Total protein content and intracellular GSH levels were not significantly altered by the exposure ($p > 0.05$), indicating the cells were not severely affected (Figure 10b and c). However, we observed a dose-dependent increase in cleaved caspase-3 activity in B[a]P exposed SIMH4 cells. As compared to vehicle treated cells, indicative for the induction of apoptosis.

We next applied the micronuclei assay to determine whether SIMH4 cells can be used to measure the clastogenic potential of chemicals that require metabolic activation. After determination of the IC_{50} dose (Suppl. Figure S4), SIMH4 cells were exposed for 4 hours to B[a]P (3.8 μM) and cyclophosphamide (CP; 4.5 μg/ml), at concentrations around their IC_{50} dose. As a positive control, we used the DNA cross-linking agent mitomycin C (MMC; 4 μg/ml), which does not require metabolic activation. Following a recovery period of 20 hours in the presence of 0.15 μg/ml cytochalasin B, cells were scored for the presence of micronuclei (MN). As shown in Figure 11, in comparison to the background levels of mono-MN and multi-MN in water or DMSO treated cells, exposure to the positive control compound MMC resulted in an increase in multi-MN, but not mono-MN, indicating that micronuclei induction can be detected in SIMH4 cells. Exposure of SIMH4 cells to B[a]P and CP caused a significant increase in mono-MN. Only MMC exposure led to apoptotic cells (>5 MN per cell). These data demonstrate that SIMH4 cells can be used to detect micronuclei formation by chemicals that require metabolic activation.

Cholestasis is a hepatic pathological condition characterized by impairment of bile acid export by pumps localized in the cell membrane, and several other clinical parameters such as elevated levels of AST, ALT and bilirubin in the blood. Intracellular accumulation of bile acids is very toxic to the cell and can lead to apoptosis. To investigate whether the SIMH4 line can be used to detect cholestasis, we exposed cells for 4 hour to the cholestatic model compound cyclosporin A (CsA) (Falck et al., 2007) and measured the accumulation of intracellular bile acids (total bile acids, TBA) 48, 72 and 96 hour after the start of the exposure. We observed a dose- and time-dependent increase in total bile acid levels in CsA treated SIMH4 cells (Suppl. Figure S5), reaching significance at a dose of 100 μM CsA (Figure 12). Similarly, medium LDH levels increased with CsA concentration and ex-

Figure 11. Micronuclei formation in SIMH4 cells. SIMH4 cells were exposed for 4 hours to the clastogens mitomycine C (MMC, in 0.1% DMSO), B[a]P (in 0.1% DMSO) or cyclophosphamide (CP in water), as well as the corresponding solvent, and allowed to grow for another 20 hour in the presence of cytochalasin B (for a detailed description, see Materials & Methods section). For each condition, comparable numbers of binucleated cells were observed and at least 1000 cells were analyzed for the presence of one (mono-MN) or more (multi-MN) micronuclei. N=1 experiment with 2 coverslips per condition. 5 pictures per coverslip were taken for counting. Error bars represent SD (*** $p < 0.001$, ** $p < 0.01$).

posure time, indicating that the toxic accumulation of bile acids is also causing cell death in this setup. In an attempt to visualize intracellular bile acid accumulation, we performed a Fouchet-Von Gieson staining on SIMH4 cells, exposed to 10 µM CsA. As shown in Figure 13, we could not detect bile acids in CsA exposed SIMH4 cells. Interestingly however, and in line with previous findings in CsA treated liver slices (Szalowska et al., 2013), we observed an accumulation of vacuoles in time after CsA, but not after DMSO (vehicle) exposure. These vesicles were not observed in CsA-treated non-liver cells (i.e. U2OS cells).The question to which extent these vesicles represent a cholestatic phenotype remains to be answered.

Discussion

Because the liver is the major organ involved in xenobiotics metabolism, large research efforts have been made in establishing *in vitro* systems as reliable alternatives for animal based studies on compound-induced toxicity in the liver. Here, we present a novel established liver cell line of Spontaneously Immortalized Mouse Hepatocytes (SIMH4) that combines ease of use in standard culturing conditions with high metabolic competence that is stable over time.

Although human primary hepatocytes are generally recognized as the system that predicts human toxicity the most reliable, inter-donor variability is unacceptably high to draw mechanistic conclusions and limited availability poses a large drawback (Gomez-Lechon et al., 2003; Kanebratt and Andersson, 2008; Lin and Lu, 2001). It is unlikely that an *in vitro* system will ever completely replace rodent *in vivo* experiments. A trade off must be made in order to find an optimal balance between predictive value, reproducibility, ease of handling and testing large numbers and combinations of compounds. Freshly isolated human and rodent primary hepatocytes are very similar to the *in vivo* situation but are subject to extensive temporal changes in gene expression and enzyme activity when placed in culture (Boess et al., 2003; Harris et al., 2004). Therefore this system is not suited for repeated or chronic exposure studies, especially for drugs obstructing bile export *in vivo* and causing intracellular bile accumulation, requiring cells with a stable polarized architecture.

HepaRG, a fairly new cell line studied by an increasing number of researchers has been proven to show high resemblance to human primary hepatocytes regarding expression of genes involved in drug metabolism (activation as well as detoxification) and transport, but is derived from a single human donor and requires extended periods in culture before reaching the maximal hepatocyte-like potential (Kanebratt and Andersson, 2008; Klein et al., 2013; Mueller et al., 2014). Moreover, results are subject to high variability due to batch differences, percentage of hepatocyte-like cells within the differentiated population and culturing conditions (Jetten et al., 2013; Schulze et al., 2012). HepG2, an extensively studied human hepatocarcinoma cell line, shows lower variability when kept at similar culturing conditions, but lacks expression of most endogenous drug-metabolizing genes (Castell et al., 2006), thus impeding its predictive value. Nonetheless, both HepaRG and HepG2 cells have successfully been used in 3D-type of structures, augmenting their hepatocyte-like function. For HepaRG cells, Mueller et al. have demonstrated that the EC_{50} value for compounds studied in 3D spheroids was significantly lower than in 2D cultures, increasing the predictive value, but lowering the possibilities for use in high throuput screens (Mueller et al., 2014).

In vivo toxicity studies still comprise a major part of the field, not in the last place to validate the *in vitro* models. Hepa1-6 cells, a murine equivalent of HepG2 that is often used when comparing mouse *in vivo* and *in vitro* data, have been shown to be more sensitive than HepG2 cells (Weiller et al., 2004). For a more direct comparison of gene expression, we compared the gene expression levels of SIMH4 cells to those in Hepa1-6 rather than those in HepG2 cells in order not to include technical inconsistencies in our RT-qPCR analysis. We found that, with the exception of *Alb* and *Afp*, all tested genes expressed at high levels in adult hepatic tissues (*CK18, cMet, GluI, Pckl*), involved in the urea cycle (*AslI*), glutathione metabolism (*Gsr*), bile acid metabolism (*FXR*) or coding for transporters (*Bsep, Mrp2, Mrp3*) are expressed at levels higher than in the Hepa1-6 cell line and at different passages of SIMH4 cells. We observed differences
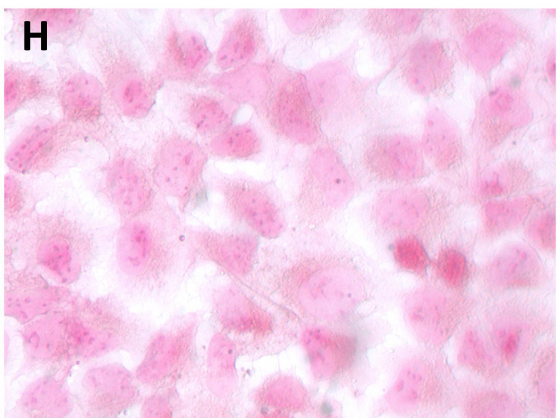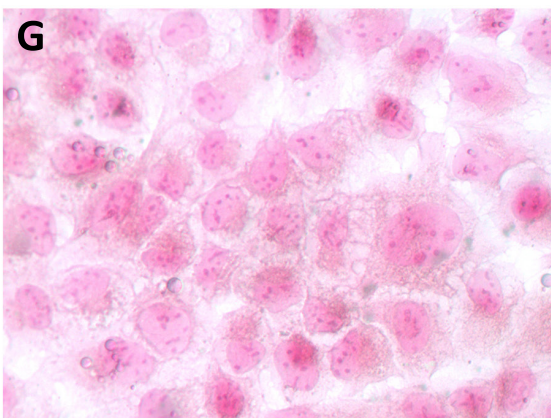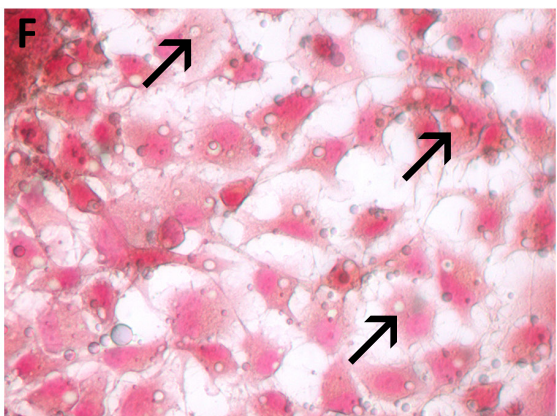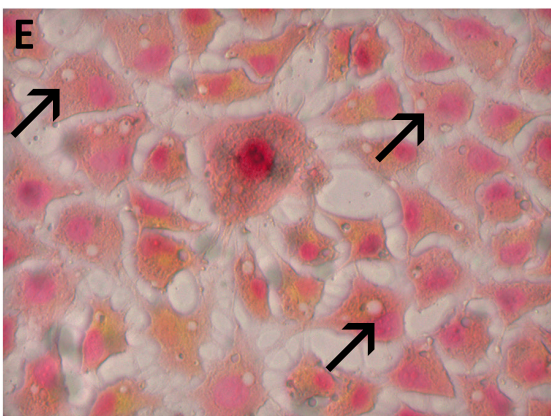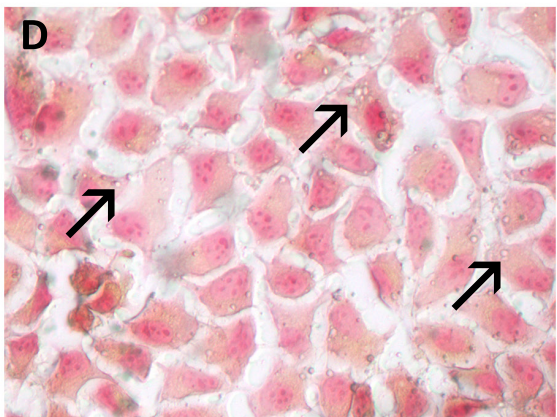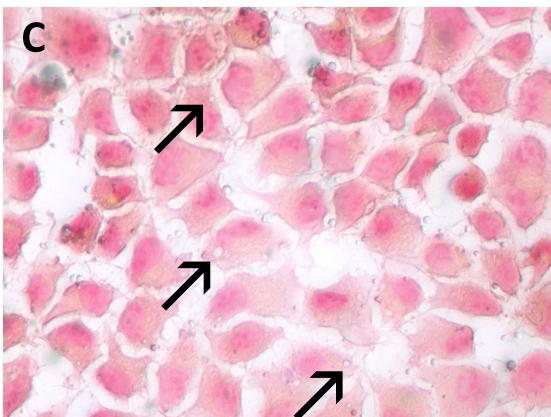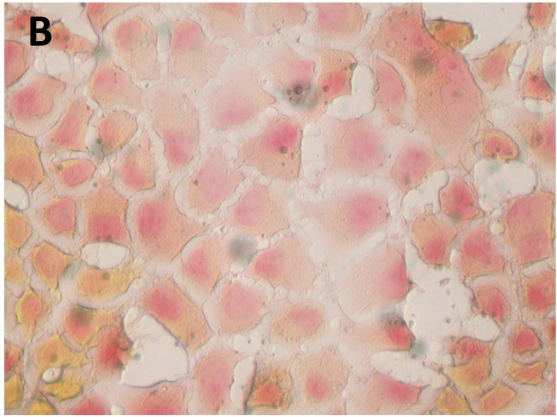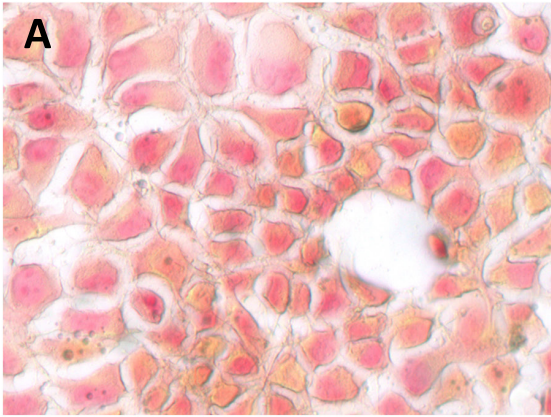
4

Figure 12: Accumulation of bile acids in CsA exposed SIMH4 cells. SIMH4 cells were exposed to the cholestatic compound CsA (100 µM) or its solvent DMSO (0.1%) for 4 hours. Intracellular accumulation of total bile acids was measured 48, 72 and 9h hours after the start of exposure. N= 2 experiments with triplicate samples. Error bars represent SD (** p<0.01).
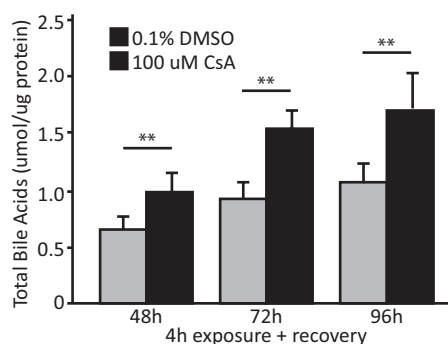

Figure 13: Induction of cholestasis in CsA exposed SIMH4 cells. DMSO exposed SIMH4 cells, 12h (A) and 96 h (B). 10 µM CsA exposed SIMH4 cells, 12h (C), 24h (D), 48h (E) and 96h (F). DMSO exposed U2OS cells, 96h (G). 10 µM CsA exposed U2OS cells, 96h (G). Arrows indicate accumulation of vesicles in CsA-treated SIMH4 cells. All pictures were taken using 400-fold magnification.

in expression levels between the passage numbers, both up and down, but when compared at the functional level no differences were measured. Both *Afp* and *Alb* were higher expressed in Hepa1-6 cells than SIMH4 cells. Because albumin is an important hepatocyte-specific product, we analyzed the production by immunofluorescence and secretion by ELISA and found that SIMH4 cells have high protein levels of albumin. *Afp* is associated with neoplasm and shares its locus with *Alb* (Kajiyama et al., 2006). We suggest that both genes amplify each other at the gene expression level while this is not necessarily mirrored at the protein level. The low expression of *Afp* in SIMH4 cells is therefore an important feature to show that although SIMH4 are immortalized, they were not derived from tumorigenic tissue.

An important feature of hepatocytes *in vivo* is their distinct cuboidal shape with polarized expression of transporters at either the sinusoidal or the canalicular membrane. Immortalized cell lines that retain polarized cell architecture are better able to demonstrate the phenotypic anchoring of chemicals inducing liver injury, especially cholestasis. Similar to the findings of Zhang et al. in primary mouse hepatocytes we observed activity of MRP2 at the canalicular membranes of SIMH4 cells, indicating that these cells retain their polarity in standard 2D culturing conditions when they are able to form cell-cell contact, where both Hepa1-6 and HepG2 cells were unable to do so in similar conditions (Zhang et al., 2005).

In order to analyze the xenobiotic metabolism activity of SIMH4 cells in these conditions, we compared gene expression between SIMH4, HepG2 and Hepa1-6 cells to primary mouse hepatocytes by exposing the cells to different concentrations of benzo[a]pyrene, a known inducer of *CYP1a1/Cyp1a1,* and found that induced gene expression of SIMH4 was around 70-80% of levels observed in primary hepatocytes, while levels in HepG2 and Hepa1-6 only reached 10 and 5%, respectively. SIMH4 cells were slightly more sensitive to benzo[a]pyrene at higher passage numbers. Because the vehicle of benzo[a]pyrene, DMSO, induces *Cyp1a1* expression, we compared basal expression levels between Hepa1-6 and different passages of SIMH4 cells in a separate assay. Basal expression levels were Hepa1-6 >> SIMH4 (low PN) > SIMH4 (high PN), indicating that this is of influence to the inducibility of *Cyp1a1*. Because the range for inducibility in HepG2 and Hepa1-6 is very small, drawing proper conclusions from *CYP1A1/Cyp1a1* induction is difficult. In order to draw conclusions from basal expression levels in SIMH4 cells, these should be compared to basal expression levels in mouse primary hepatocytes. Additionally, differences between high and low passage numbers of SIMH4 cells should be addressed more thoroughly, for example in terms of karyotyping and assessing genetic variation between subcultured populations.

Most studies concerning xenobiotic exposure involve exposure times of 24 hour or longer. Indeed, Mathijs et al. concluded that discrimination between different types of toxic compounds increased with exposure time (Mathijs et al., 2009). This is mainly because of the lower number of genes

4

induced directly after exposure compared to the number of genes differentially regulated later on. On the other hand, Zhang et al. concluded that most of these differentially expressed genes were species and compound specific, impinging on very specific metabolic pathways. The early response to toxic exposure is often more similar, dependent on the class of chemicals but independent of species (Zhang et al., 2013). While gaining knowledge on the specific effects of any compound, these findings are often difficult to extrapolate to other systems or species.

To investigate xenobiotic metabolism protein expression and activation we also compared CYP1A1/Cyp1a1 enzyme activity between primary hepatocytes, HepG2 and SIMH4 cells. There was no difference in endogenous activity of CYP1A1/Cyp1a1 between HepG2 and SIMH4 cells, while the activity in primary mouse hepatocytes was higher. After 4 hours of exposure to benzo[a] pyrene, slight increase in enzyme activity was observed in HepG2 and SIMH4 levels, while significant activation was observed in the primary hepatocytes. Interestingly, activation in the cell lines mainly occurred at low concentrations, while the increase in activity in primary hepatocytes was dose dependent up to 10 uM. After 24 hours of continuous exposure, a dose dependent increase in activity was observed for all cell types in the order primary hepatocytes > SIMH4 > HepG2. These data show that SIMH4 cells are more sensitive to toxic exposure involving the CYP1A1/ Cyp1a1 signaling pathway than HepG2 and Hepa1-6 cells and more resembles that of cultured primary mouse hepatocytes.

We exposed SIMH4 cells for a short period of 4 hours to compounds inducing apoptosis (benzo[a]pyrene), mutagenesis (benzo[a]pyrene, cyclophosphamide, vinblastine and mitomycine C) or accumulation of bile acids (cyclosporine A), after which they were allowed to recover in medium without these chemicals for at least 20 hours and measured early markers of cell death, carcinogenesis or cholestasis. We found that apoptosis and cholestasis could be induced in a dose dependent manner, and mutagenesis could be induced with all compounds including the promutagens cyclophosphamide and benzo[a]pyrene, requiring activation by phase I enzymes before becoming mutagenic. We also exposed SIMH4 cells to the chemotheurapeutic drugs sunitinib and tamoxifen and compared rates of uptake and conversion into metabolites with those observed in HepG2 cells and found that SIMH4 cells were faster in both uptake and metabolism for both drugs. Taken together, these exposure studies underline the intact xenobiotic metabolic competence of SIMH4 cells and its usefulness for the development of *in vitro* alternatives for rodent studies.

In conclusion, SIMH4 cells are a valuable novel tool for toxicogenomics assays, combining ease of use with high hepatocyte specific behavior and xenobiotic metabolism, which makes this cell line extremely useful for use in high throughput studies.

An obvious improvement of these short exposure studies would be to optimize the SIMH4 cells for long term maintenance and chronic low-dose, or repeated dose exposure to better mimic real life situations. Therefore we analyzed a set of parameters to study the hepatocyte like behavior of SIMH4 cells in serum free culturing conditions, inhibiting cell proliferation and thereby improving the formation of cell-cell interactions (appendix to this chapter). We found that cell polarization was enhanced in serum free conditions and that gene expression levels were either unchanged or higher compared to cells cultured in medium containing 10% serum after three days. Klein et al. published a similar analysis of HepaRG and found that the medium was nutrient depleted after two or three days for cells cultured without or with serum, respectively (Klein et al., 2013). Similar to our study, serum free conditions favored the secretion of albumin but inhibited that of urea. The latter supports our hypothesis that for a proper functioning of the urea cycle and secretion of urea, medium precursors are necessary as input. We suggest that a higher frequency of medium change combined with the addition of specifically optimized growth factors is likely to improve long term culturing of SIMH4 The drawback of HepaRG cells is that they take weeks to differentiate and form. We want to emphasize that SIMH4 cells are maintained and grown in standard culturing conditions and have high proliferative capacity while retaining high hepatocyte specific behavior and xenobiotic metabolism, making them very valuable in setting up high throughput assays. Reversing between proliferative and non-proliferative states will make the cells useful in chronic and repeated dose exposure studies, further adding to their use in testing large numbers

of and interactions between chemicals. Because of the murine background of these cells, similar cell lines from mutant mice with various metabolic deficiencies can be obtained. Moreover, *in vitro* data can directly be compared to similar *in vivo* studies in rodents if necessary, thereby gaining knowledge on the extrapolation from *in vitro* to *in vivo*.

Acknowledgements

References

Abelev, G.I., Eraiser, T.L., 1999. Cellular aspects of alpha-fetoprotein reexpression in tumors. Semin. Cancer Biol. 9, 95–107.

Bayliss, M.K., Cross, D.M., 2000. The importance of hepatocytes in drug metabolism studies: an industrial perspective, The Hepatocyte Review.

Binkhorst, L., Mathijssen, R.H.J., Moghaddam-Helmantel, I.M.G., Bruijn, P. de, Gelder, T. van, Wiemer, E.A.C., Loos, W.J., 2011. Quantification of tamoxifen and three of its phase-I Metabolites in human plasma by liquid chromatography/triple quadrupole mass spectrometry. J. Pharm. Biomed. Anal. 56, 1016–1023.

Bisht, S., Feldmann, G., Brossart, P., 2013. Pharmacokinetics and pharmacodynamics of sunitinib for the treatment of advanced pancreatic neuroendocrine tumors. Expert Opin. Drug Metab. Toxicol. 9, 777–788.

Boess, F., Kamber, M., Romer, S., Gasser, R., Muller, D., Albertini, S., Suter, L., 2003. Gene expression in two hepatic cell lines, cultured primary hepatocytes, and liver slices compared to the in vivo liver gene expression in rats: possible implications for toxicogenomics use of in vitro systems. Toxicol. Sci. 73, 386–402.

Bruijn, P. de, Sleijfer, S., Lam, M.-H., Mathijssen, R.H.J., Wiemer, E.A.C., Loos, W.J., 2010. Bioanalytical method for the quantification of sunitinib and its n-desethyl metabolite SU12662 in human plasma by ultra performance liquid chromatography/tandem triple-quadrupole mass spectrometry. J. Pharm. Biomed. Anal. 51.

Burkard, A., Dähn, C., Heinz, S., Zutavern, A., Sonntag-Buck, V., Maltman, D., Przyborski, S., Hewitt, N.J., Braspenning, J., 2012. Generation of proliferating human hepatocytes using Upcyte® technology: characterisation and applications in induction and cytotoxicity assays. Xenobiotica. 42, 939–56.

Castell, J., Jover, R., Martinez-Jimenez, C., Gomez-Lechon, M., 2006. Hepatocyte cell lines : their use, scope and limitations in drug metabolism studies. Expert Opin. Drug Metab. Toxicol. 2, 183–212.

Chaves, I., Nijman, R., Biernat, M., Bajek, M., Brand, K., Carvalho da Silva, A., Saito, S., Yagita, K., Eker, A., van der Horst, G., 2011. The Potorous CPD photolyase rescues a cryptochrome-deficient mammalian circadian clock. PLoS One 6, e23447.

Chiang, J.Y.L., 2013. Bile Acid Metabolism and Signaling. Compr. Physiol. 3, 1191–1212.

Chow, L.Q.M., Eckhardt, S.G., 2007. Sunitinib: From Rational Design to Clinical Efficacy. J. Clin. Oncol. 25, 884–896.

Dambach, D.M., Andrews, B.A., Moulin, F., 2005. New Technologies and Screening Strategies for Hepatotoxicity: Use of In Vitro Models. Toxicol Pathol 33, 17–26.

Davila, J.C., Xu, J.J., Hoffmaster, K.A., P.J., O., Storm, S.C., 2008. Current in vitro models to study drug-induced liver injury, in: Hepatotoxicity (ed S. C. Sahu), John Wiley & Sons, Ltd, Chichester, UK.

De Wit, A.S., Nijman, R., Destici, E., Chaves, I., van der Horst, G.T.J., 2014. Hepatotoxicity and the circadian clock, a timely matter, in: Toxicogenomics-Based Cellular Models: Alternatives to Animal Testing for Safety Assessment. Academic Press, pp. 251–270.

Dennis, M.S., Zhang, M., Meng, Y.G., Kadkhodayan, M., Kirchhofer, D., Combs, D., Damico, L. a, 2002. Albumin binding as a general strategy for improving the pharmacokinetics of proteins. J. Biol. Chem. 277, 35035–35043.

Donato, M., Gomez-Lechon, M., Castell, J., 1993. A microassay for measuring cytochrome P450IA1 and P450IIB1 activities in intact human and rat hepatocytes cultured on 96-well plates. Anal Biochem 213, 29–33.

Donato, M., Lahoz, A., Castell, J., Gomez-Lechon, M., 2008. Cell lines: a tool for in vitro drug metabolism studies. Curr Drug Metab 9, 1–11.

Falck, P., Guldseth, H., Asberg, A., Midtvedt, K., Reubsaet, J., 2007. Determination of ciclosporin A and its six main metabolites in isolated T-lymphocytes and whole blood using liquid chromatography-tandem mass spectrometry. J Chromatogr B Anal. Technol Biomed Life Sci. 852, 345–352.

Faubion, W.A., Guicciardi, M.E., Miyoshi, H., Bronk, S.F., Roberts, P.J., Svingen, P.A., Kaufmann, S.H., Gores, G.J., 1999. Toxic bile salts induce rodent hepatocyte apoptosis via direct activation of Fas. J Clin Invest 103, 137–145.

Frederick, D., Jacinto, E., Patel, N., Rushmore, T., Tchao, R., Harvison, P., 2011. Cytotoxicity of 3-(3,5-dichlorophenyl)-2,4- thiazolidinedione (DCPT) and analogues in wild type and CYP3A4 stably transfected HepG2 cells. Toxicol Vitr. 25, 2113–2119.

Godoy, P., Hewitt, N.J., Albrecht, U., Andersen, M.E., Ansari, N., et al., 2013. Recent advances in 2D and 3D in vitro systems using primary hepatocytes, alternative hepatocyte sources and non-parenchymal liver cells and their use in investigating mechanisms of hepatotoxicity, cell signaling and ADME, Archives of toxicology.

Gomez-Lechon, M., Castell, J., Donato, M., 2010a. The use of hepatocytes to investigate drug toxicity. Methods Mol Biol 640, 389–415.

Gomez-Lechon, M., Donato, M., Castell, J., Jover, R., 2003. Human hepatocytes as a tool for studying toxicity and drug metabolism. Curr Drug Metab 4, 292–312.

Gomez-Lechon, M., Donato, M., Castell, J., Jover, R., 2004. Human hepatocytes in primary culture: the choice to investigate drug metabolism in man. Curr Drug Metab 5, 443–462.

Gomez-Lechon, M., Lahoz, A., Gombau, L., Castell, J., Donato, M., 2010b. In Vitro Evaluation of Potential Hepatotoxicity Induced by Drugs. Curr. Pharm. Des. 16, 1963–1977.

Gonzalez, F., Korzekwa, K., 1995. Cytochromes P450 expression systems. Annu Rev Pharmacol Toxicol 35, 369–390.

Guillouzo, A., Corlu, A., Aninat, C., Glaise, D., Morel, F., Guguen-Guillouzo, C., 2007. The human hepatoma HepaRG cells: a highly differentiated model for studies of liver metabolism and toxicity of xenobiotics. Chem. Biol. Interact. 168, 66–73.

Gupta, S., 2000. Hepatic polyploidy and liver growth control. Semin. Cancer Biol. 10, 161–171.

Harris, A.J., Dial, S.L., Casciano, D. a, 2004. Comparison of basal gene expression profiles and effects of hepatocarcinogens on gene expression in cultured primary human hepatocytes and HepG2 cells. Mutat. Res. 549, 79–99.

Harris, C.C., Sun, T., 1984. Multifactoral etiology of human liver cancer. Carcinogenesis 5, 697–701.

Hewitt, N.J., Lechón, M.J.G., Houston, J.B., Hallifax, D., Brown, H.S., Maurel, P., Kenna, J.G., Gustavsson, L., Lohmann, C., Skonberg, C., Guillouzo, A., Tuschl, G., Li, A.P., LeCluyse, E., Groothuis, G.M.M., Hengstler, J.G., 2007. Primary hepatocytes: current understanding of the regulation of metabolic enzymes and transporter proteins, and pharmaceutical practice for the use of hepatocytes in metabolism, enzyme induction, transporter, clearance, and hepatotoxicity studies. Drug Metab. Rev. 39, 159–234.

Janorkar, A., King, K., Megeed, Z., Yarmush, M., 2009. Development of an in vitro cell culture model of hepatic steatosis using hepatocyte-derived reporter cells. Biotechnol Bioeng 102, 1466–1474.

Jetten, M.J. a, Kleinjans, J.C.S., Claessen, S.M., Chesné, C., van Delft, J.H.M., 2013. Baseline and genotoxic compound induced gene expression profiles in HepG2 and HepaRG compared to primary human hepatocytes. Toxicol. Vitr. 27, 2031–40.

Judson, R., Kavlock, R., Setzer, R., Hubal, E., Martin, M., Knudsen, T., Houck, K., Thomas, R., Wetmore, B., Dix, D., 2011. Estimating toxicity-related biological pathway altering doses for high-throughput chemical risk assessment. Chem Res Toxicol 24, 451–462.

Kajiyama, Y., Tian, J., Locker, J., 2006. Characterization of distant enhancers and promoters in the albumin-alpha-fetoprotein locus during active and silenced expression. J. Biol. Chem. 281, 30122–31.

Kanebratt, K.P., Andersson, T.B., 2008. Evaluation of HepaRG Cells as an in Vitro Model for Human Drug Metabolism Studies □ ABSTRACT : Drug Metab Dispos 36, 1444–1452.

Kienhuis, A., Vitins, A., Pennings, J., Pronk, T., Speksnijder, E., Roodbergen, M., Van Delft, J., Luijten, M., Van der Ven, L., 2013. Cyclosporine A treated in vitro models induce cholestasis response through comparison of phenotype-directed gene expression analysis of in vivo Cyclosporine A-induced cholestasis. Toxicol Lett 221, 225–236.

Kiyotani, K., Mushiroda, T., Nakamura, Y., Zembutsu, H., 2012. Pharmacogenomics of tamoxifen: roles of drug metabolizing enzymes and transporters. Drug Metab Pharmacokinet 27, 122–131.

Klein, S., Mueller, D., Schevchenko, V., Noor, F., 2013. Long-term maintenance of HepaRG cells in serum-free conditions and application in a repeated dose study. J. Appl. Toxicol.

LeCluyse, E.L., Alexandre, E., Hamilton, G.A., Viollon-Abadie, C., Coon, D.J., Jolley, S., Richert, L., 2005. Isolation and Culture of Primary Human Hepatocytes. Methods Mol. Biol. 290, 207–229.

Lee, W., 2003. Drug-induced hepatotoxicity. N Engl J Med 349, 474–485.

Lemmer, E.R., Friedman, S.L., Llovet, J.M., 2006. Molecular Diagnosis of Chronic Liver Disease and Hepatocellular Carcinoma: The Potential of Gene Expression Profiling. Semin Liver Dis 26, 373–384.

Lin, J.H., Lu, A.Y., 2001. Interindividual variability in inhibition and induction of cytochrome P450 enzymes. Ann Rev Pharmacol Toxicol 41, 535–567.

Lushchak, V., 2012. Glutathione Homeostasis and Functions: Potential Targets for Medical Interventions. J. Amino Acids 2012.

Madle, E., Tiedemann, G., Madle, S., Ott, A., Kaufmann, G., 1986. Comparison of S9 mix and hepatocytes as external metabolizing systems in Mammalian cell cultures: Cytogenetic effects of 7,12-dimethylbenzanthracene and aflatoxin B1. Environ. Mutagen. 8, 423–437.

Mathijs, K., Brauers, K.J.J., Jennen, D.G.J., Boorsma, A., Herwijnen, M.H.M. van, Gottschalk, R.W.H., Kleinjans, J.C.S., Delft, J.H.M. van, 2009. Discrimination for Genotoxic and Nongenotoxic Carcinogens by Gene Expression Profiling in Primary Mouse Hepatocytes Improves with Exposure Time. Toxicol. Sci. 112, 374–384.

Mitaka, T., Ooe, H., 2010. Characterization of hepatic-organoid cultures. Drug Metab Rev 42, 472–481.

Mueller, D., Krämer, L., Hoffmann, E., Klein, S., Noor, F., 2014. 3D organotypic HepaRG cultures as in vitro model for acute and repeated dose toxicity studies. Toxicol. In Vitro 28, 104–12.

Riley, R., 2001. The potential pharmacological and toxicological impact of P450 screening. Curr Opin Drug Discov Devel 4, 45–54.

Rodrigues-Antona, C., Donato, M., Boobis, A., Edwards, R., Watts, P., Vicente Castell, J., Gomez-Lechon, M., 2002. Cytochrome P450 expression in human hepatocytes and hepatoma cell lines: molecular mechanisms that determine lower expression in cultured cells. Xenobiotica 32, 505–520.

Rostami-Hodjegan, A., 2010. Translation of in vitro metabolic data to predict in vivo drug-drug interactions: IVIVE and modeling and simulations, Springer, New York. Springer, New York.

Schmittgen, T.D., Livak, K.J., 2008. Analyzing real-time PCR data by the comparative CT method. Nat. Protoc. 3, 1101 – 1108.

Schulze, A., Mills, K., Weiss, T.., Urban, S., 2012. Hepatocyte polarization is essential for the productive entry of the hepatitis B virus. Hepatology 55, 373–383.

Seglen, P., 1976. Preparation of isolated rat liver cells. Methods Cell Biol 13, 29–83.

Shitara, Y., Sato, H., Sugiyama, Y., 2005. Evaluation of drug-drug interaction in the hepatobiliary and renal transport of drugs. Annu. Rev. Pharmacol. Toxicol. 45, 689–723.

Szalowska, E., Stoopen, G., Groot, M.J., Hendriksen, P.J., Peijnenburg, A.A., 2013. Treatment of mouse liver slices with cholestatic hepatotoxicants results in down-regulation of Fxr and its target genes. BMC Med. Genomics 6, 39.

Takahashi, R., Sonoda, H., Tabata, Y., Hisada, A., 2010. Formation of hepatocyte spheroids with structural polarity and functional bile canaliculi using nanopillar sheets. Tissue Eng Part A 16, 1983–1995.

Thatishetty, A. V., Agresti, N., O'Brien, C.B., 2013. Chemotherapy-Induced Hepatotoxicity. Clin. Liver Dis. 17, 671–686.

Tolosa, L., Donato, M., Perez-Cataldo, G., Castell, J., Gomez-Lechon, M., 2012. Upgrading cytochrome P450 activity in HepG2 cells co-transfected with adenoviral vectors for drug hepatotoxicity assessment. Toxicol Vitr. 26, 1272–1277.

Turncliff, R., Tian, X., Brouwer, K., 2006. Effect of culture conditions on the expression and function of Bsep, Mrp2, and Mdrla/b in sandwich cultured rat hepatocytes. Biochem Pharmacol 71, 1520–1529.

Van Swelm, R.P.L., Hadi, M., Laarakkers, C.M.M., Masereeuw, R., Groothuis, G.M.M., Russel, F.G.M., 2013. Proteomic profiling in incubation medium of mouse, rat and human precision-cut liver slices for biomarker detection regarding acute drug-induced liver injury. J. Appl. Toxicol.

Weiller, M., Latta, M., Kresse, M., Lucas, R., Wendel, A., 2004. Toxicity of nutritionally available selenium compounds in

primary and transformed hepatocytes. Toxicology 201, 21–30.

Wogan, G.N., 2000. Impacts of chemicals on liver cancer risk. Semin. Cancer Biol. 10, 201–210.

Yang, G., Jiang, Y., Rao, K., Chen, X., Wang, Q., Liu, A., Xiong, W., Yuan, J., 2011. Mitochondrial dysfunction and trans-activation of p53-dependent apoptotic genes in BaP-treated human fetal lung fibroblasts. Hum. Exp. Toxicol. 30, 1904.

Yoshida, K., Maeda, K., Sugiyama, Y., 2012. Prediction of the degree of transporter-mediated drug-drug interactions involving OATP substrates based on in vitro inhibition studies. Clin. Pharmacol. Ther. 91, 1053–1064.

Zhang, J., Berntenis, N., Roth, A., Ebeling, M., 2013. Data mining reveals a network of early-response genes as a consensus signature of drug-induced in vitro and in vivo toxicity. Pharmacogenomics J. 1–9.

Zhang, P., Tian, X., Chandra, P., Brouwer, K.L.R., 2005. Role of Glycosylation in Trafficking of Mrp2 in Sandwich-Cultured Rat Hepatocytes. Mol. Pharmacol. 67, 1334–1341.

4

Supplementary figures
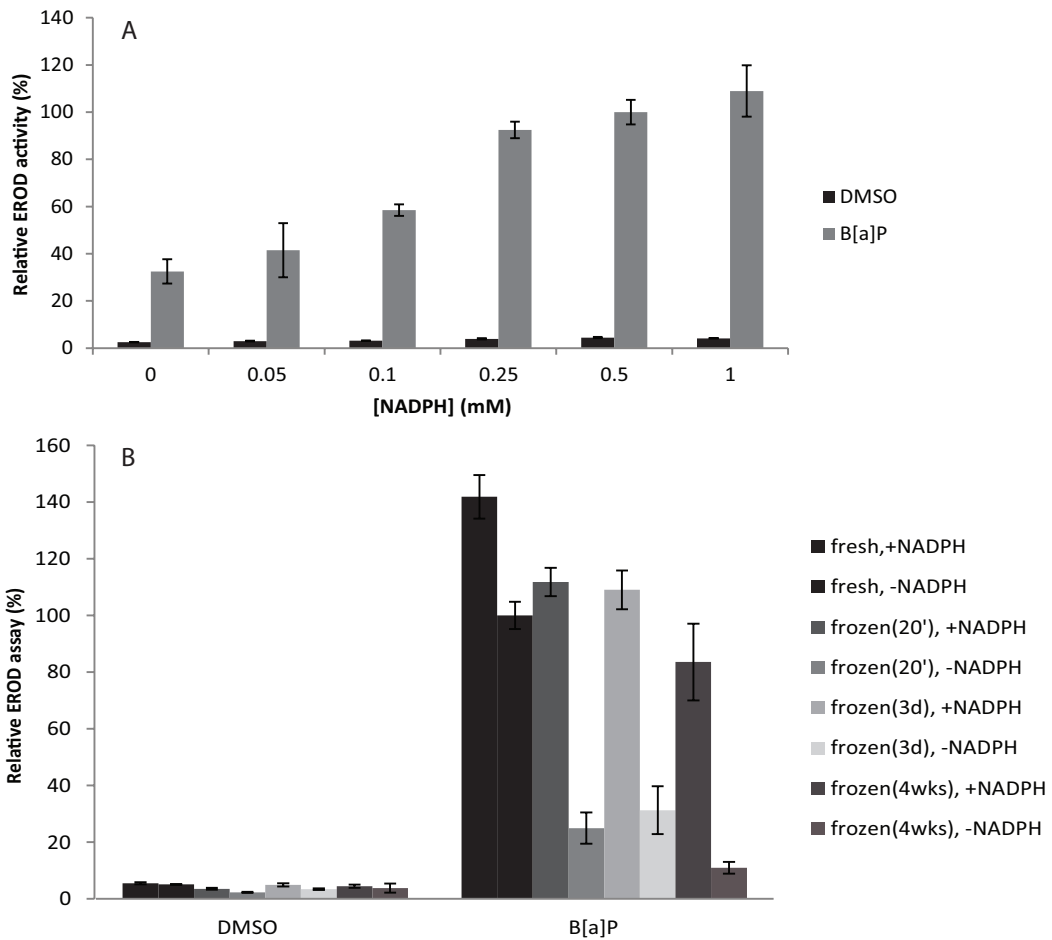
Figure S1. Optimization of the EROD assay for snap frozen samples. Titration of NADPH to reactions in snap frozen samples of B[a]P or DMSO treated SIMH4 cells (A) and performance of snap frozen samples thawed after different periods at -800C (B). Note that in the presence of 0.5 mM NADPH, EROD activity in frozen samples is comparable to that in fresh samples without NADPH when measured within 3 days.. n=2 experiments with triplicate samples. Error bars represent SD.
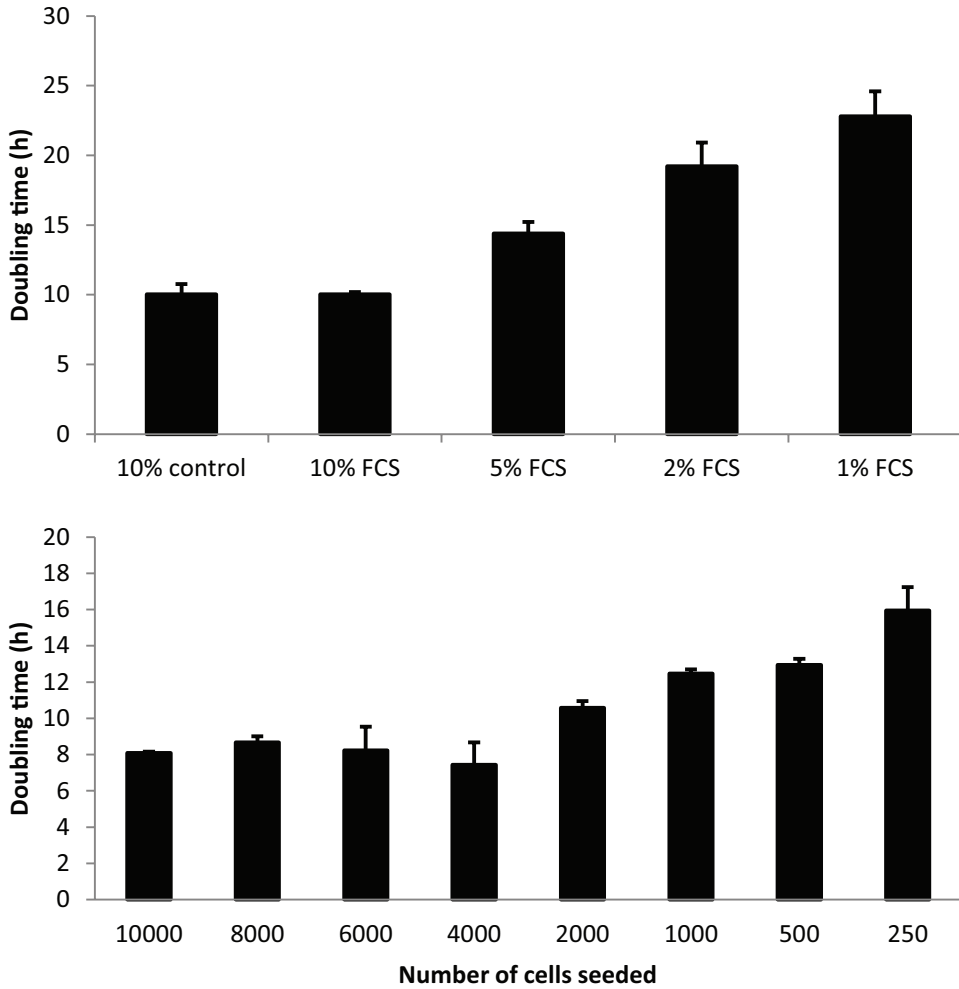
Figure S2. Proliferation rate of SIMH4 cells. Population doubling time of SIMH4 cells in log phase, as determined in 96-well plates using the xCELLigence system for real time monitoring of proliferation (A) in the presence of 10% FCS after seeding of cells at different densities and (B) in the presence of varying concentrations of FCS (2000 cells/well). In the later experiment, medium containing different concentrations of FCS was applied 24 hour after seeding, while for the '10% control' sample, medium was not replaced (n=2 experiments, measurements in triplicate). Doubling times were determined from the slopes of the curves in the log phase from xCELLigence data and plotted as mean ± SD.

4

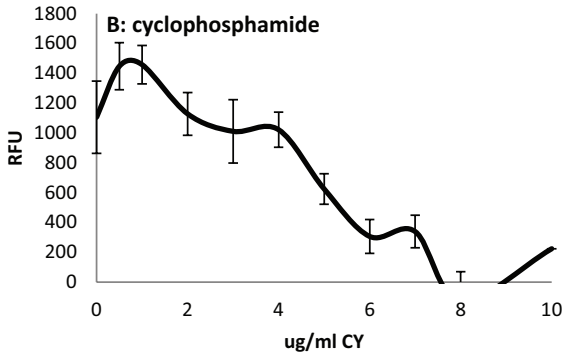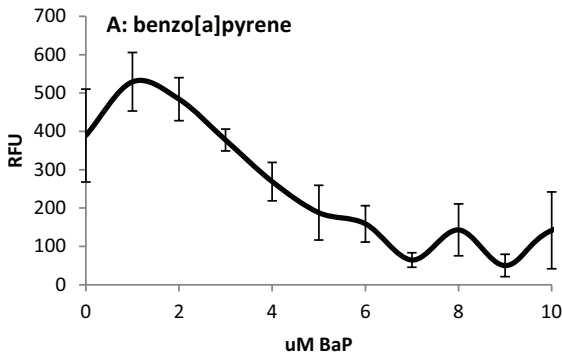**mouse primary hepatocytes**
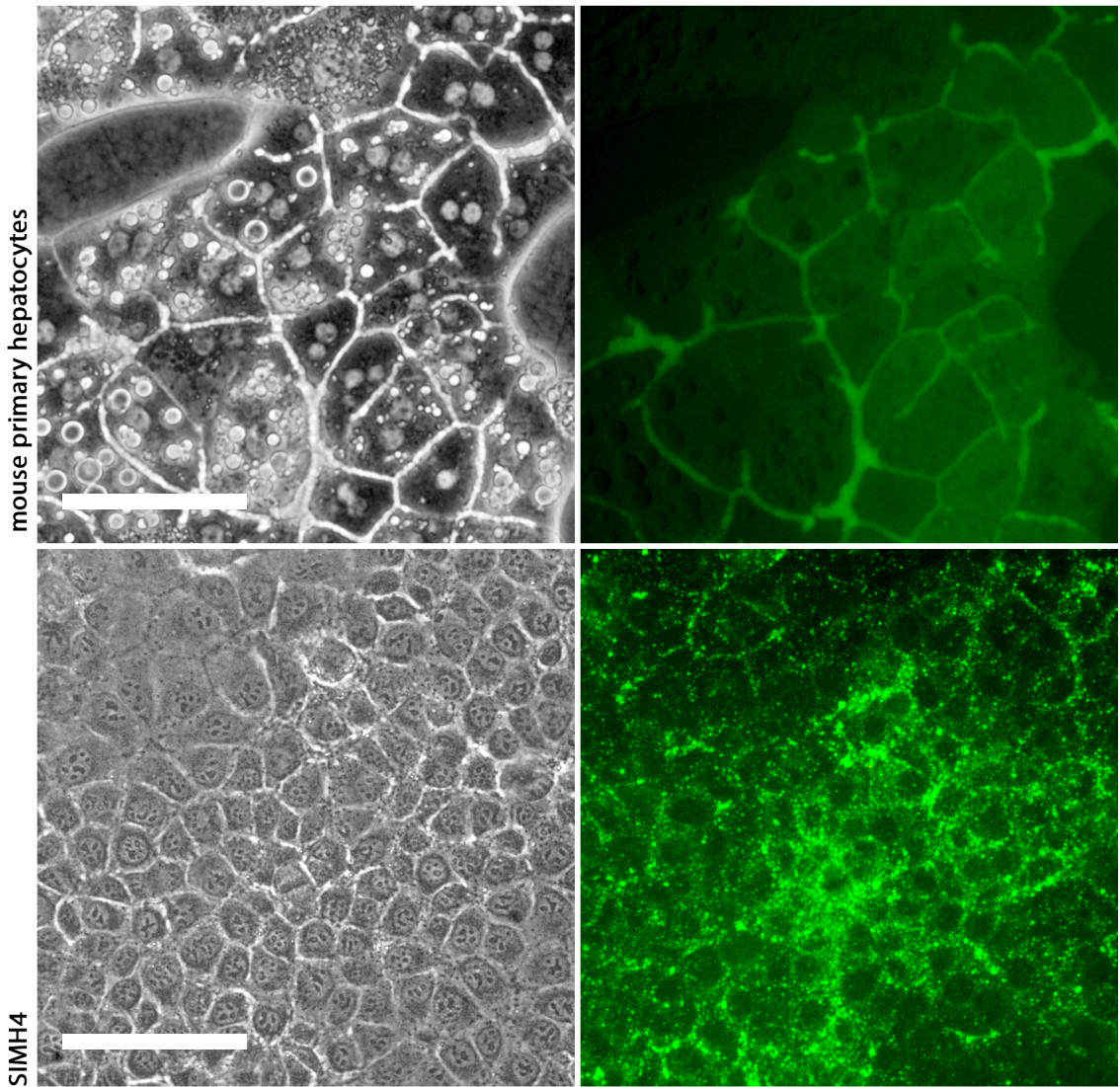
SIMH4

Figure S3. Morphology and polzarized structure of SIMH4 cells, overview pictures. Phase contrast micrographs (left panels) and DCFDA staining (right panels) of sandwich cultured mouse primary hepatocytes and HepG2 cells. Pictures were taken at 400x magnification. Bars represent 20 µm.

SIMH4: a novel Spontaneously Immortalized Mouse Hepatocyte cell line with primary hepatocyte-like characteristics and high metabolic competence
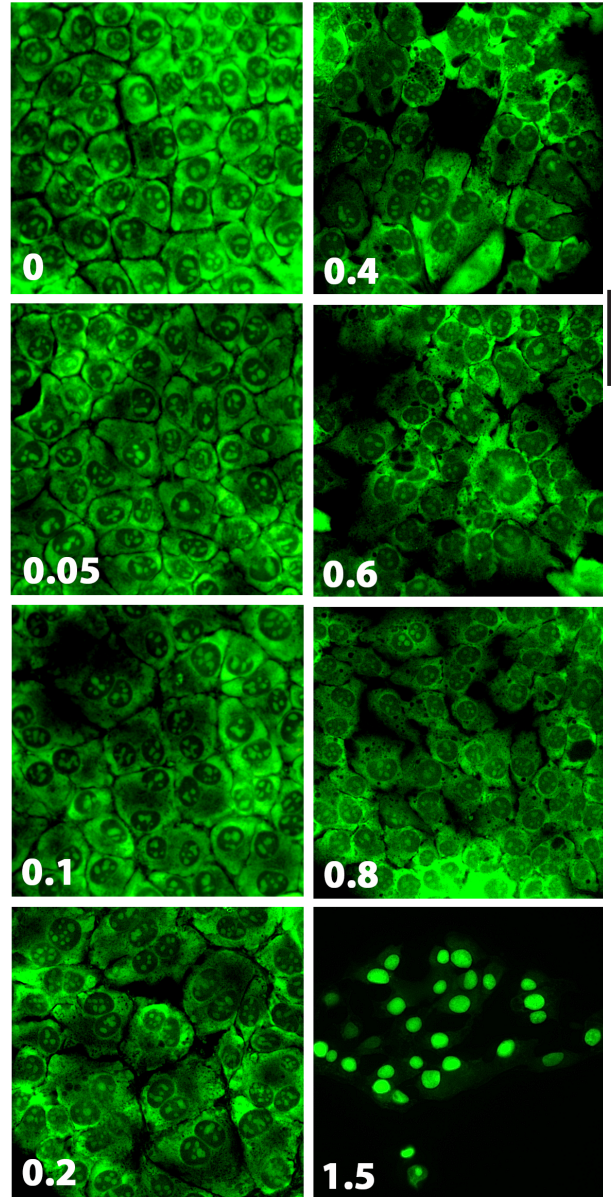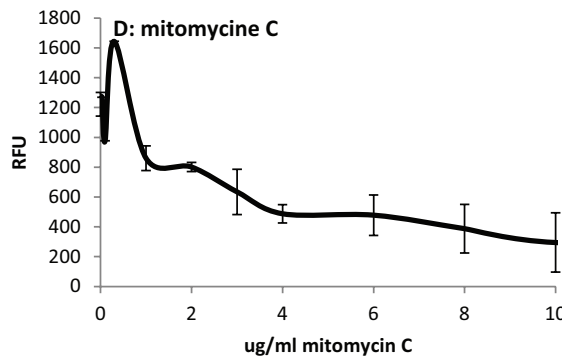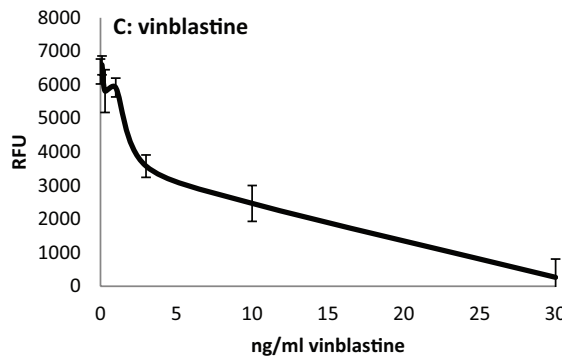
Figure S4. IC$_{50}$ dose determination. SIMH4 cells were exposed to clastogens for 4 hours and allowed to recover for 20 hours. Cytotoxicity was determined using alamar blue and 2 hours of incubation. Estimated IC$_{50}$ doses: (A) B[a]P: 3.8 μM, (B) CP: 4.5 μg/ml), (C) vinblastine 3 ng/μl, and (D) MMC 4 μg/ml (n=3 experiments, triplicate measurements per experiment). Error bars represent SD. (E) SIMH4 cells were exposed to different doses of cytochalasin B for 20 hours and stained with acridine orange.

113

4
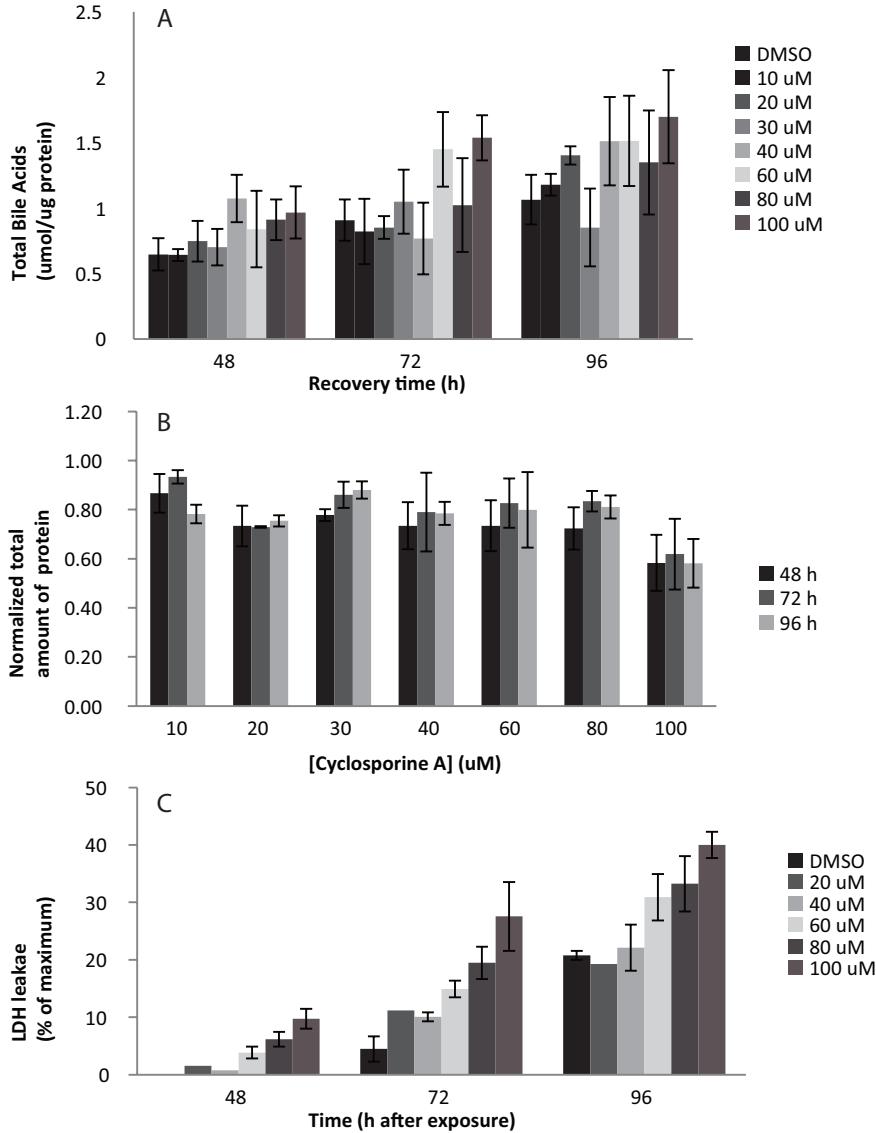
two-tailed paired t-test	48h	72h	96h
DMSO vs 10 uM	0.459	0.278	0.352
DMSO vs 20 uM	0.197	0.386	0.219
DMSO vs 30 uM	0.294	0.104	0.196
DMSO vs 40 uM	0.030	0.285	0.108
DMSO vs 60 uM	0.194	0.022	0.158
DMSO vs 80 uM	0.038	0.379	0.269
DMSO vs 100 uM	0.001	0.002	0.014

Figure S5. (A) Total bile acids in SIMH4 cells after 4 hour exposure to different concentrations of cyclosporine A and 44, 68 or 92 hour recovery. N=3 ± SD (n=6 for DMSO and 100 μM). (B) Ratio between protein content in vehicle (DMSO) treated samples vs cyclosporine A treated samples, normalized for each time point separately. At each time point (48, 72, 96 h), "1" represents the amount of protein in the vehicle treated samples. N=3 ± SD (n=6 for 100 μM). (C) LDH leakage of CsA treated cells, corrected for values prior to exposure. N=3 ±SD.

Appendix to chapter4

Hepatocyte specific behavior in SIMH4 cells is retained for several days in confluent cultures and can be enhanced by inhibition of proliferation by serum depletion

In order to measure biological endpoint for which the phenotype takes several days to emerge such as cholestasis and/or to be able to perform semi-chronic exposure studies, it is important that the cells can be maintained in culture undisturbed after reaching a confluent status, to best mimic the non- or slow-proliferating status of most hepatocytes in vivo.

While SIMH cells were never observed to form colonies and only grow in a monolayer, they proliferate at a lower rate with spatially restricted cytokinesis, leading to populations with a high density of cells with only a minimum amount of cytoplasm. We observed that hepatocyte specific behavior is increased in confluent populations (figure 2) and therefore we investigated whether we could maintain confluent cultures of SIMH cells for an increased period by manipulating the culturing conditions, without impinging on normal metabolic behavior to a large extent. In figure S2 we show that de doubling time of SIMH4 cells rapidly increases when the serum concentrations in the medium are lowered. When the cells were maintained in medium without serum, we measured a population doubling time of ca. 60 ± 15 hours, due to residual intracellular serum in the cells and/or cells already past S-phase. In order to test the influence of maintaining SIMH4 cells in medium depleted of serum or with low starting levels of serum (1%), we allowed the cells to grow into confluent populations for three days, after which the medium of the dishes was replaced with fresh medium containing either 10% (standard condition), 1% or no serum. We measured total protein content, LDH and GSH levels (figure 10a,b and c) from the day of medium change (day 0) until day 7 and found that there were no significant changes between low serum or serum depleted levels compared to standard culturing conditions until day 2. We did also not observe major changes in cell morphology (figure S4). Between 2 and 4 days after medium change, serum depleted cells started to suffer from starvation and showed increased levels of LDH and decreased levels of total protein and GSH. 7 days after the medium change, LDH and protein levels were comparable to those at day 4, indicating that after this period, most cells had started apoptotic trajectories. This was also observed in the overall morphology of the cells. After 7 days, groups of cells in all conditions still survived with normal morphology, indicating that a subpopulation of cells can survive for a prolonged period without any serum. Further optimization will allow for the whole population to survive and for chronic exposure studies in the future.

Albumin secretion was 4-fold higher in conditions without serum, while urea secretion was a 3-fold lower (figure 5). Cell culturing serum contains a high concentration of albumin, as this is a very abundant component of the blood, possibly inhibiting albumin secretion by cells in standard culturing conditions. Activity and output of the urea cycle are dependent on the amount of substrates for all enzymes. The main substrates for enzymes involved in the urea cycle, L-aspartate and L-glutamate, will quickly be depleted after removing the serum or only adding a low percentage. Although the urea cycle is most likely fully functional in serum depleted cultures, the net output is very low.

Hepatocyte specific gene expression was calculated for cells cultured for three days in different culturing conditions and normalized to expression levels at day 0 (before medium change) (figure 10b). Because the cells were allowed to grow into confluency in this condition, it is likely that serum was depleted or at very low levels. In concordance with the results from secreted albumin and urea, *Alb* gene expression was suppressed in the presence of serum, while in the absence of serum, expression levels were comparable to those at day 0. Expression levels of *Asl1* were unchanged, supporting our notion on the functionality of the urea cycle in these cells.

Compared to day 0, *Gsr* levels were reduced in all conditions but mostly in standard medium. Reduced glutathione, the product of GSR activity, was increased in all conditions (figure 10c), protecting the cells from oxidative stress. Because GSH synthesis is regulated via a negative feedback loop (Lushchak, 2012), it is very likely that the increased levels of GSH suppress the expression of *Gsr*.

Hepatocyte specific gene expression was either unchanged (*FXR, Mrp3*), lower than at day 0 but without differences between culturing conditions (*CK-18, cMet*), lower than at day 0 for cell cultured with serum but comparable in conditions inhibiting proliferation (*GluI, Bsep*) or unchanged in medium with serum but upregulated in conditions without serum. *Afp* is the only gene that was upregulated in conditions with and without serum compared to day 0, but downregulated in conditions with low serum levels.

The upregulation of the canalicular transporters *Bsep* en *Mrp2* are good indicators that conditions inhibiting proliferation promote hepatocyte specific behavior. To test whether MRP2 was also functional, we performed the DCF assay as described before for cells maintained in the different culturing conditions and found that, indeed, DCF export into the canalicular space was increased in medium with low concentrations of or without serum (figure S4). Taken together, we conclude that it is possible to maintain confluent cultures of SIMH4 in order to test liver specific biological endpoints, that proliferation can successfully be inhibited by depriving the cells from serum in the medium and that hepatocyte specific behavior is enhanced in populations of non-proliferating cells without any effect for at least 2 days. Further optimization of culturing conditions is likely to enable SIMH4 cells to be cultured for a prolonged period without proliferation and without losing hepatocyte-specific functions, in order to perform chronic, repeated dose or complex exposure studies, and/or further studying cell-cell interactions.
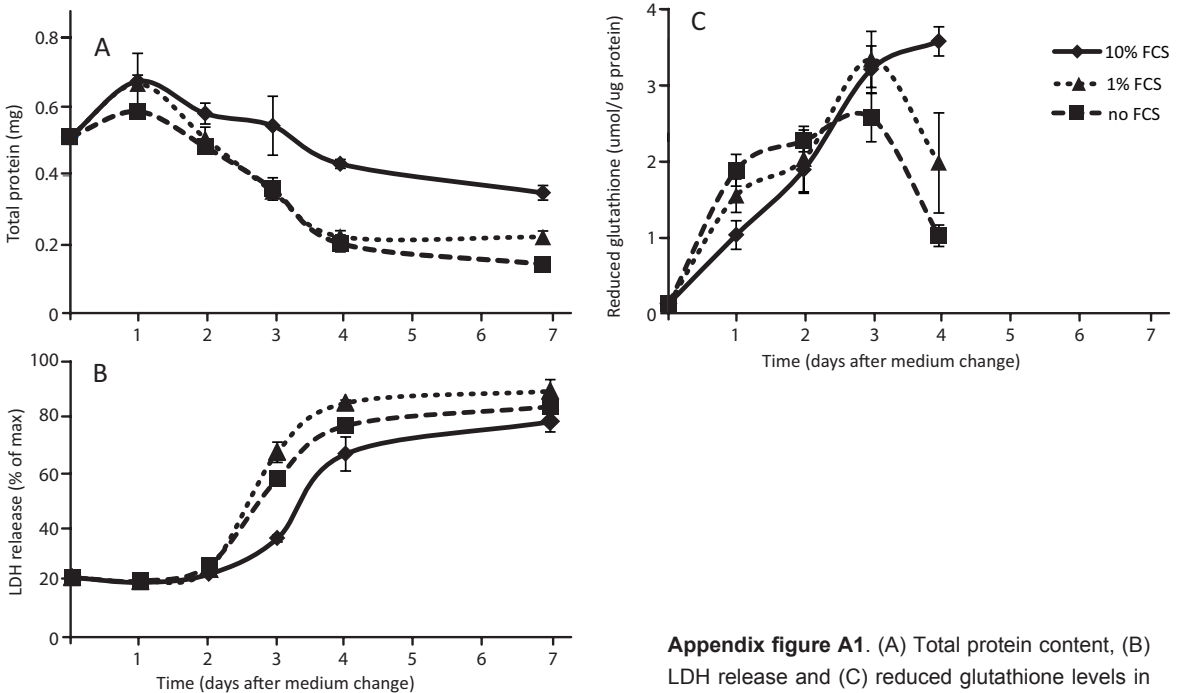
Appendix figure A1. (A) Total protein content, (B) LDH release and (C) reduced glutathione levels in SIMH4 cells when cultured in confluence in different types of medium (10%, 1% or no FCS). 100% LDH is determined by exposing the cells to 1% Triton X-100 in medium, 45'@ 37^0. Total GSH is corrected for protein content. n=3 ± SD. (D) Hepatocyte specific gene expression in confluent SIMH4 cells in the presence of 10%, 1% or no FCS. N= 6± SD.
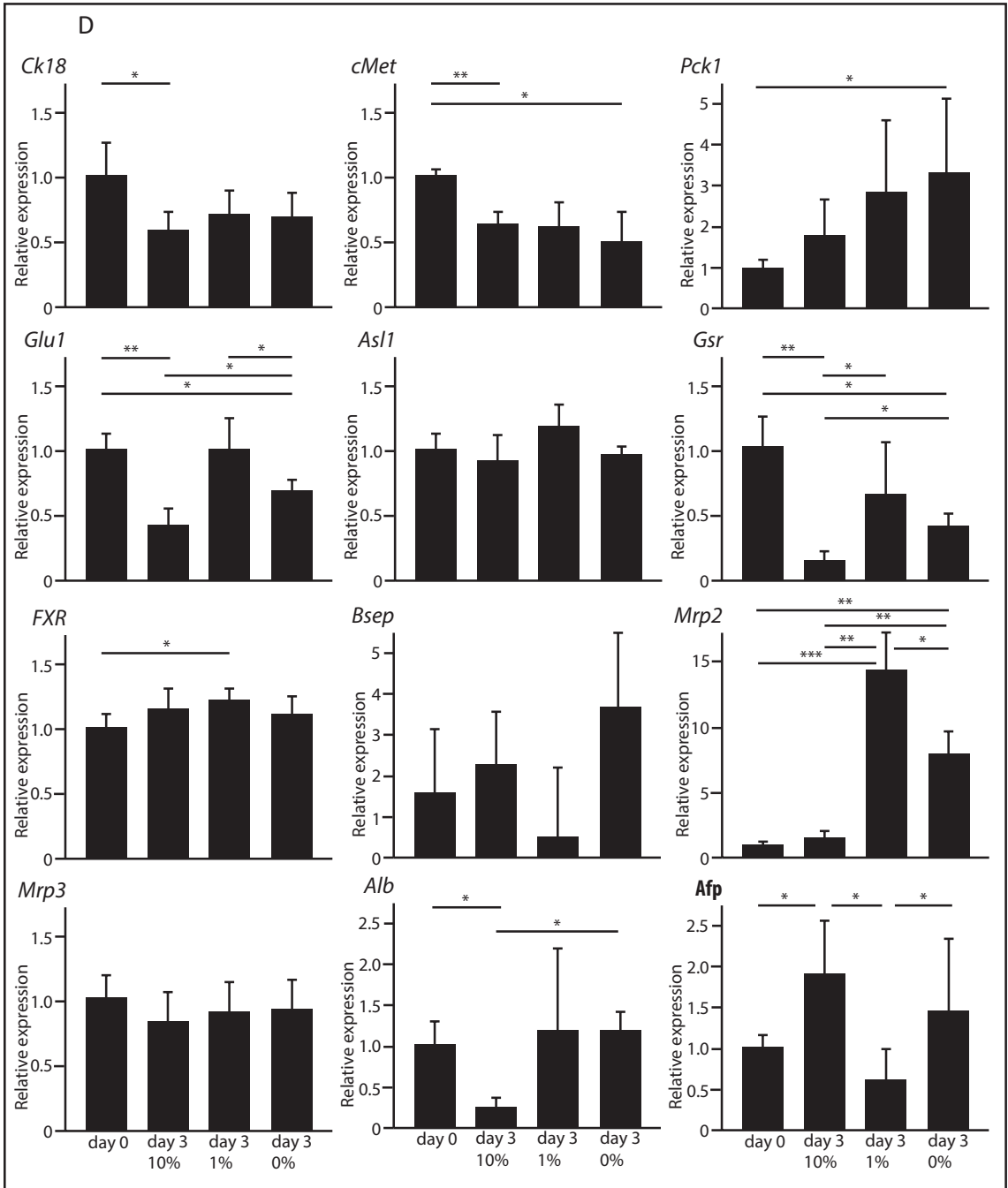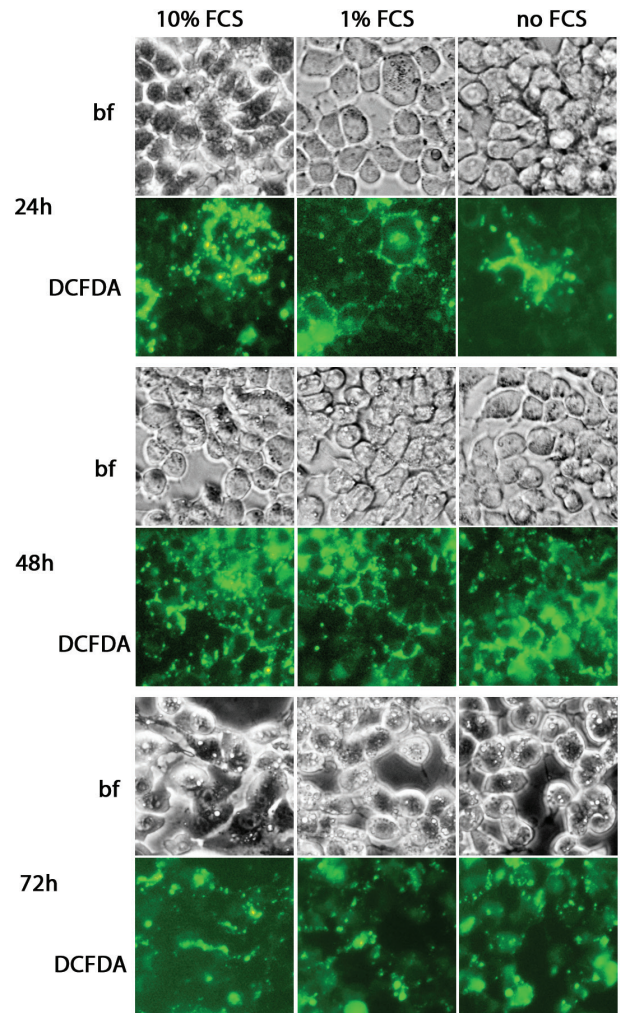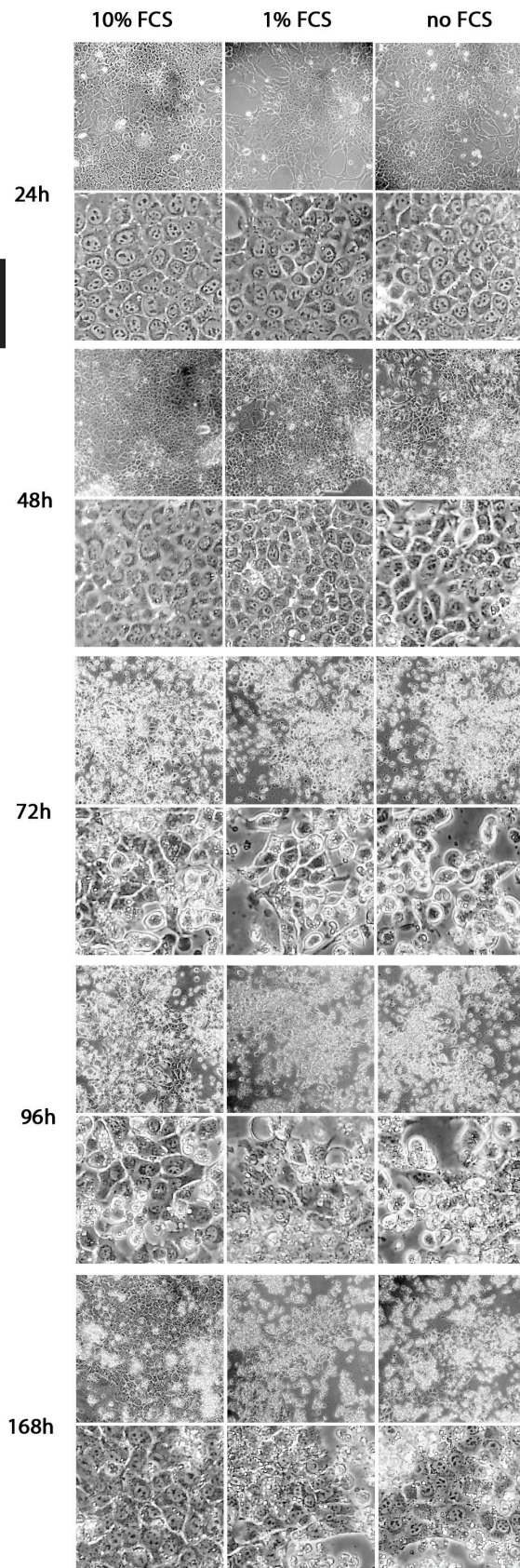
Appendix supplementary figure AS1. Cell morphology and DCF export in confluent SIMH4 cells in the presence of 10%, 1% or no FCS.

4

Chapter 5

SIMH^{CLOCK}, a Spontaneously Immortalized Mouse Hepatocyte cell line for identification of chronotoxic properties of chemicals

Annelieke S. de Wit, Inês Chaves, Gijsbertus T.J. van der Horst

5

Abstract

In the course of finding alternatives for animal testing, we developed a spontaneously immortalized mouse hepatocyte line, SIMH[CLOCK]. This novel, non-cancer derived liver cell line demonstrates a robust, synchronizable circadian clock with a period of 24.7 ± 0.6 hours under normal culturing conditions, as judged by real time bioluminescence recording of *Per2::Luc* clock reporter gene expression, RT-qPCR and transcriptome (RNA seq) analysis. Core clock, as well as major clock controlled genes involved in (xenobiotic) metabolism, are rhythymically expressed with a phase distribution similar to that observed *in vivo* in the mouse liver. RNA sequencing analysis revealed that 11.8% of the annotated transcripts display significant oscillations (p<0.05). Exposure of SIMH[CLOCK] cells at defined phases of the circadian clock to 0.5 µM benzo[a]pyrene (B[a]P) resulted in highly significant (p<0.0001) circadian pattern of *Cyp1a1* induction with peak values at relative circadian time CTr4-8 (in which CTr0 refers to the trough of *Per2* expression), indicative for the chronotoxic properties of this pro-carcinogen. Likewise, induction of *DnaJb9* gene expression by exposure to 5 µM cyclosporine A (CsA) appears time of day dependent with a significant (p=0.0016) peak around CTr16-20 on top of an endogenous 12 hour rhythm in vehicle exposed cells (p<0.0001). Analysis of levels of cleaved caspase 3 revealed time of day dependent variations in background levels of apoptosis in unexposed (p=0.0001) and vehicle exposed (p=0.0031) cells. Exposure to 30 or 100 µM B[a]P for 4 hour induced apoptosis at all time points (p<0.0001), with highest induction of caspase 3 measured at CTr12, indicating that chronotoxic exposure leads to time of day dependent differences in gene expression and ultimately biologic end points.

Introduction

In order to comply with European legislations, stating that the experiments with laboratory animals should be reduced and ultimately replaced, various efforts are undertaken to create *in vitro* alternatives for chemical testing and genotoxic risk analysis. Because the liver is the major organ involved in xenobiotics metabolism, most *in vitro* systems have focused on this organ. Alternatives include liver slices, isolated primary hepatocytes and immortal (often cancer derived) cell lines, which all have their own applications and limits (reviewed by De Wit et al., 2014). An important drawback of most *in vitro* systems is that they do not take into account day-night variation in biological processes.

The circadian clock is an internal timing mechanism, which is present in every cell of our body (Reppert and Weaver, 2002) and orchestrates diurnal variations in behavior, physiology and metabolism in order to adapt to environmental changes. At the cellular level, rhythms are generated by a molecular oscillator, composed of a set of clock genes and proteins that rhythmically turn each other on and off with a near (circa) 24 hour (dies) periodicity (reviewed by Dibner et al., 2010). In turn, this molecular clock drives rhythmic expression of approximately 10% of a tissues transcriptome (Akhtar et al., 2002; Hughes et al., 2009; Panda et al., 2002). Increasing evidence is emerging that this internal timekeeper plays an important role in key metabolic processes (Mazzoccoli et al., 2012). Chronic disruption of the circadian system, for instance by jet lag or shift work, has been associated with the development of various metabolism related pathogenic conditions such as diabetes and obesitas (Hotamisligil, 2008) and has also been linked to cardiovascular problems, mutagenesis and cancer (Innominato et al., 2010; Savvidis and Koutsilieris, 2012; Smith and Eastman, 2012). Moreover, metabolism of many xenobiotics present in food, drugs and the environment, for instance, is dependent on the phase of the clock at some point along the route. Because of the pivotal role of circadian rhythms in xenobiotic metabolism, diurnal variations in metabolic competence can be imperative in defining optimal moments for pharmacological drug administration (Innominato et al., 2010) or determining the least hazardous moment for the occupational handling of toxic compounds.

In order to implement time of day dependent genotoxic risk assessment, extensive knowledge of the basal clock machinery is essential. Moreover, it requires the development of new

methods for reproducible and easy screening. The liver is the major organ involved in xenobiotic metabolism and therefore much research has focused on this organ. However, despite multiple studies showing that many central genes involved in metabolism are oscillating (Zhang et al., 2009), few genotoxic risk assessment studies have taken the phase of the clock into account. Using mouse liver slices and primary hepatocytes, we have shown that toxic responses (e.g. gene induction, mutagenesis) display time of day dependency (known as chronotoxicity) (chapter 2). We have previously established, and extensively characterized, a Spontaneously Immortalized Mouse Hepatocyte line, SIMH4, which combines high metabolic competence with the potency for use in high throughput screening programs (chapter 4). Interestingly, this hepatocyte line was isolated from a *Per2::Luc* circadian clock reporter mouse, thus allowing real time monitoring of circadian clock phase. In the present paper, we have investigated the potential use of this SIMH4 line (hereafter referred to as SIMH^{CLOCK}) for chronotoxic risk identification. We have focused on the two most common types of xenobiotics induced liver injury, apoptosis and cholestasis by benzo[a] pyrene (B[a]P) and cyclosporine A (CsA), respectively. B[a]P, a polycyclic aromatic hydrocarbon present in e.g. cigarette exhaust fumes is a promutagen and its binding affinity is dependent on the phase of the clock (Anderson et al., 2013). Upon entering the cell via the aryl hydrocarbon receptor, cytochrome P450 1a1 (CYP1A1) metabolizes B[a]P into its mutagenic form benzo[a] pyrene diolepoxide (BPDE). The antisuppressant drug CsA is often used after renal transplantation and can lead to cholestasis by inhibiting canalicular transport of intracellular toxic bile acids (Trauner et al., 1999). We demonstrate that upon synchronization, the circadian clock can be followed for several days in SIMH^{CLOCK} cells and that, similar to primary hepatocytes, time of day dependent effects in the toxic response to CsA and B[a]P exposure can be detected. Moreover, we validated the significance of these findings by demonstrating that time of day dependent exposure leads to diurnal variation in the level of B[a]P-induced apoptosis (Riedl and Shi, 2004).

Materials & methods

Cell culture
SIMH^{CLOCK} cells, originating from male *Per2::Luc* mice in a C57BL/6J genetic background (Chaves et al., 2011) and originally referred to as SIMH4 cells, have been described previously (de Wit et al., 2014). Cells were maintained in SIMH culturing medium, consisting of William's E (Lonza), containing 10% FCS, 100 U/ml pen/strep, 2 mM UltraGlutamine 1 (Lonza) and 1x ITS-X mix (Gibco)). Medium was changed every 3-4 days and cells were kept in a humidified incubator at 37^{0}C and 5% CO$_2$. All experiments were performed with cells at passage numbers 20-40.

Real time recording of circadian performance
To monitor circadian clock phase, SIMH^{CLOCK} cells were cultured in 35 mm dishes. Real time bioluminescence recording of luciferase activity (60 sec measurements at 10 min intervals) were performed using a LumiCycle 32-channel automated luminometer (Actimetrics), placed in a dry incubator at 37^{0}C. Prior to placing dishes in the LumiCycle, the lid was replaced by a glass coverslip and sealed with parafilm. Data were analyzed using Actimetrics software.

In vitro exposure
Confluent cultures of SIMH^{CLOCK} cells, maintained in SIMH culturing medium were treated with 100 nM dexamethasone to synchronize the circadian clocks of the individual cells. Starting 24 hours after synchronization, cells were exposed to benzo[a]pyrene (B[a]P; Sigma) (0.5 µM for RT-qPCR or 30 and 100 µM for apoptosis), cyclosporine A (CsA; Sigma) (5 µM) or the solvent DMSO (0.1%) at 4 hour intervals for 4 hours in conditioned medium, pooled per time point to prevent unexpected synchronization by medium composition. At the end of the exposure, cells were either harvested for RNA isolation or cultured for another 20 hours in conditioned medium to determine other biological endpoints (i.e. apoptosis).

5

Quantitative real time PCR

Total RNA was isolated using TriPure reagent (Roche Diagnostics) according to the manufacturer's protocol. RNA quality and concentrations were analyzed using the Nanodrop ND1000 (NanoDrop Technologies) and 1 µg of RNA was used for cDNA preparation using iScript (Biorad) according to the manufacturer's protocol. RT-qPCR was performed using Platinum Taq DNA polymerase (Invitrogen) according to the manufacturer's protocol on a Biorad C1000 Touch Thermal Cycler, using a standard 2-step amplification program with annealing/extension at 60^{0}C and SYBR Green. Expression levels were normalized using beta-2-microglobulin (*B2M*) (clock genes), or *B2M, Hprt* and *Gapdh* mRNA levels and plotted relative to the first time point. The generation of specific PCR products was confirmed by melting curve analysis and each primer pair was tested with a serial dilution of a cDNA mix that was used to calculate the primer pair efficiency. The following primers were used: *B2M* Fwd 5'-CCG GCC TGT ATC CAG AAA-3' Rev 5'-ATT TCA ATG TGA GGC GGG TGG AAC-3'; *Hprt* Fwd 5'-CGA AGT GTT GGA TAC AGG CC-3' Rev 5'-GGC AAC ATC AAC AGG ACC TCC-3'; *Gapdh* Fwd 5'-CAG AAC ATC ATC CCT GCA TCC-3' Rev 5'-GTC ATC ATA CTT GGC AGG TTT CTC-3'; *Cyp1a1* Fwd 5'-GCA CTA CAG GAC ATT TGA GAA GG-3' Rev 5'-AAT CAC TGT GTC TAG TTC CTC C-3'; *Bmal1* Fwd 5'-GCA CTG CCA CTG ACT ACC AAG A-3' Rev 5'- TCC TGG ACA TTG CAT TGC AT-3'; *DBP* Fwd 5'-ACC GTG GAG GTG CTA ATG AC-3' Rev 5'-CCT CTT GGC TGC TTC ATT GTT-3'; *Per2* Fwd 5'-GGC TTC ACC ATG CCT GTT GT-3' Rev 5'-GGA GTT ATT TCG GAG GCA AGT GT-3'; *Cry1* Fwd 5'-CAG ACT CTC GTC AGC AAG ATG-3' Rev 5'-CAA ACG TGT AAG TGC CTC AGT-3'; *DnaJb9* Fwd 5'-TCA GAG CGA CAA ATC AAA AAG GC-3' Rev 5'-CTA TTG GCA TCC GAG AGT GTT T-3'. Relative gene expression was calculated using the comparative C(t) method described by Schmittgen et al and normalized to relative expression after exposure to the vehicle (relative expression = 1) (Schmittgen and Livak, 2008).

RNA Seq analysis

To analyse circadian gene expression in the SIMH^CLOCK line, cells were seeded in 35 mm dishes at a density of 2 x 10^5 cells and allowed to grow to confluency. Subsequently, cells were synchronized with 100 nM dexamethasone and lysed at 1.5 hour intervals, starting 24 hours after synchronization until 67.5 hours after synchronization. RNA was isolated and purified with the NucleoSpin kit (Machery-Nagel) according to the manufacturer's protocol. Prior to processing samples for RNA Seq analysis, the quality of the experiment (i.e. synchronization) was confirmed by qPCR analysis of clock and clock-controlled gene expression as described above. For RNA sequencing, quality control and sequencing was performed at ServiceXS (Leiden, The Netherlands).

Apoptosis assay

SIMH^CLOCK cells were exposed to B[a]P as described above. At the end of the experiment, cells were lysed in 500 µl of buffer provided in the Caspase-3 Fluorescence Assay Kit (Cayman Chemicals) and cell lysates were stored at -80^{0}C until further analysis. Caspase 3 activity, a marker for apoptosis, was analyzed according to the manufacturer's protocol. Fluorescence was determined at 485/535 nm using a Glomax 96-wells microplate reader (Promega). Total protein was determined using the BiCinchoninic Acid (BCA) assay (Thermo Scientific) and read in duplicate at 560 nm. Values were expressed as relative fluorescence units (RFU) per µg protein.

Cell viability assay

Viability of SIMH cells in confluent cultures or after (geno)toxic exposure was determined by measuring LDH release, using the Cytotoxicity Detection KitPlus (Roche Diagnostics) according to the manufacturer's protocol. Values were background corrected for LDH activity of serum components in the culture medium. Maximum LDH release (indicative for 100% cell death) was determined by lysing parallel cultures containing similar cell numbers with 1% Triton X-100 in medium for 45' at 37^{0}C. Absorbance at 490 nm was measured using a Varioskan microplate reader (Thermo Scientific).

Statistical analysis

To identify genes with circadian expression, RT-qPCR results or the FPKM expression values (RNA Seq data) were analyzed using CircWave Batch for cosinor analysis with a 24 hour wave, with forward linear harmonic regression using an F-test. User defined alpha was 0.05 (courtesy of Dr. R.A. Hut). For RNA Seq data, a p value cut-off of 0.001 was used to eliminate false positives (Oster et al., 2006). The group of genes displaying circadian oscillation was further analyzed with the DAVID gene ontology tool (Huang et al., 2009a, 2009b).

Results

SIMH[CLOCK] cells demonstrate robust 24 hour rhythms in core clock and clock output genes

For the real time observation of circadian clock cycling we monitored expression of *Period2::luciferase* in a Lumicycle device in SIMH[CLOCK] cells after synchronization with dexamethasone. *Per2::Luc* bioluminescence followed a sinusoidal expression pattern with a period of 24.7 ± 0.6 hours (Figure 1a). The phase of the clock could be followed for at least 7 days, but similar to results obtained in other cell lines (Oklejewicz et al., 2008), the amplitude of the oscillation was reduced after several days due to desynchronization. Next, we isolated RNA from SIMH[CLOCK] cells every 1.5 hours starting 24 hours after synchronization and analyzed expression of several clock genes (Figure 1b). Analysis of clock gene expression (*Bmal1, Per2, Cry1, DBP*) shows that RNA levels in these cells underwent 1 complete cycle and kept oscillating afterwards, indicating that core clock components were expressed in a circadian manner throughout the whole experiment.

Characterization of the transcriptome of SIMH[CLOCK]

As described above, RNA was collected from SIMH[CLOCK] cells at 1.5 hour intervals during almost two complete circadian cycles (43.5 hours). The expression levels were analyzed by RNA sequencing, as described in methods. In order to identify transcripts with circadian expression, the FPKM expression values obtained were analyzed using harmonic regression (Circwave Batch, courtesy of R.A. Hut). Only transcripts detected in more than 5 of the 30 time points were analyzed. Table 1 shows the number of identified transcripts with circadian expression, using different p-value cut-offs, and comparing the whole data set with the annotated transcripts. For gene ontology analysis, we focused on the annotated genes with a $p<0.001$ (Figure 2). A similar approach was used by Oster and coworkers in an expression array analysis, where a p-value cut-off of 0.001 was selected for Circwave analysis in order to eliminate false positives (Oster et al., 2006). Table 2 shows the list of genes, ordered by F value (largest to smallest) and P value (smallest to largest). The F value indicates to what extent the curve fit deviates from a linear fit, and is a read out for robustness of oscillation. As shown in Figure 2, gene ontology analysis revealed that more than 50% of the genes with circadian expression is related to metabolic processes, indicating that, similar to *in vivo*, many metabolic processes oscillate in a circadian manner.

Gene induction after cyclosporine A and benzo[a]pyrene exposure is time of day dependent

Table 1. Transcript analysis of RNA sequencing. Analysis of annotated and non-annotated oscillating transcripts with cutoff values of 0.05 or less.

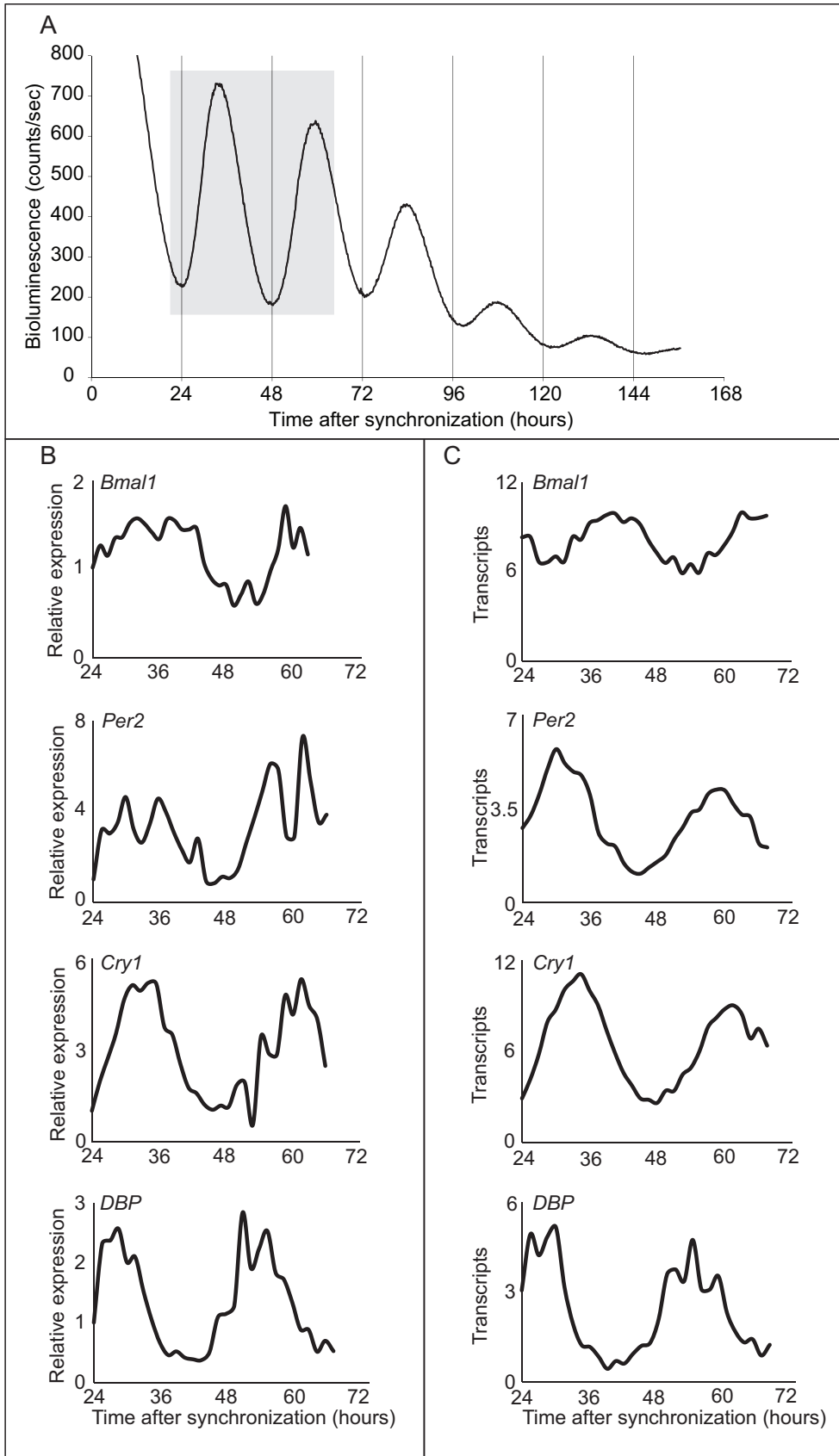|	Transcripts: total (n=22515)		annotated (n=14765)	
	n	%	n	%
p<0.05	2324	10.3	1742	11.8
p<0.01	656	2.9	519	3.5
p<0.005	403	1.8	331	2.2
p<0.001	147	0.6	124	0.8

5

Figure 1. Circadian performance of SIMH^CLOCK cells. (A) Representative example of real time bioluminescence recordings in confluent SIMH^CLOCK cells after dexamethasone-mediated synchronization of the circadian clock. (B) Core clock gene expression profiles in confluent SIMH^CLOCK cells, starting 24 hours after dexamethasone synchronization. mRNA levels are expressed relative to *B2M* mRNA levels. (C) As panel B, except that number of transcripts were determined by RNA Seq.
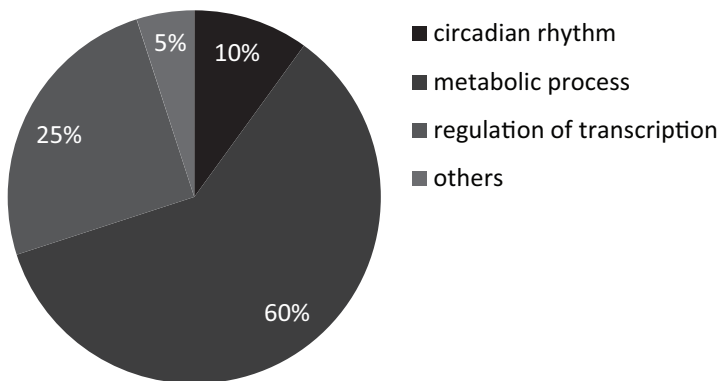

5

Figure 2. Pathway analysis of oscillating genes with p<0.001. GO-term analysis (DAVID) of significantly oscillating genes (p<0.001, as determined by CircWave analysis), described in Table 2. Pathways are classified as circadian rhythm, metabolic processes, regulation of transcription or other.
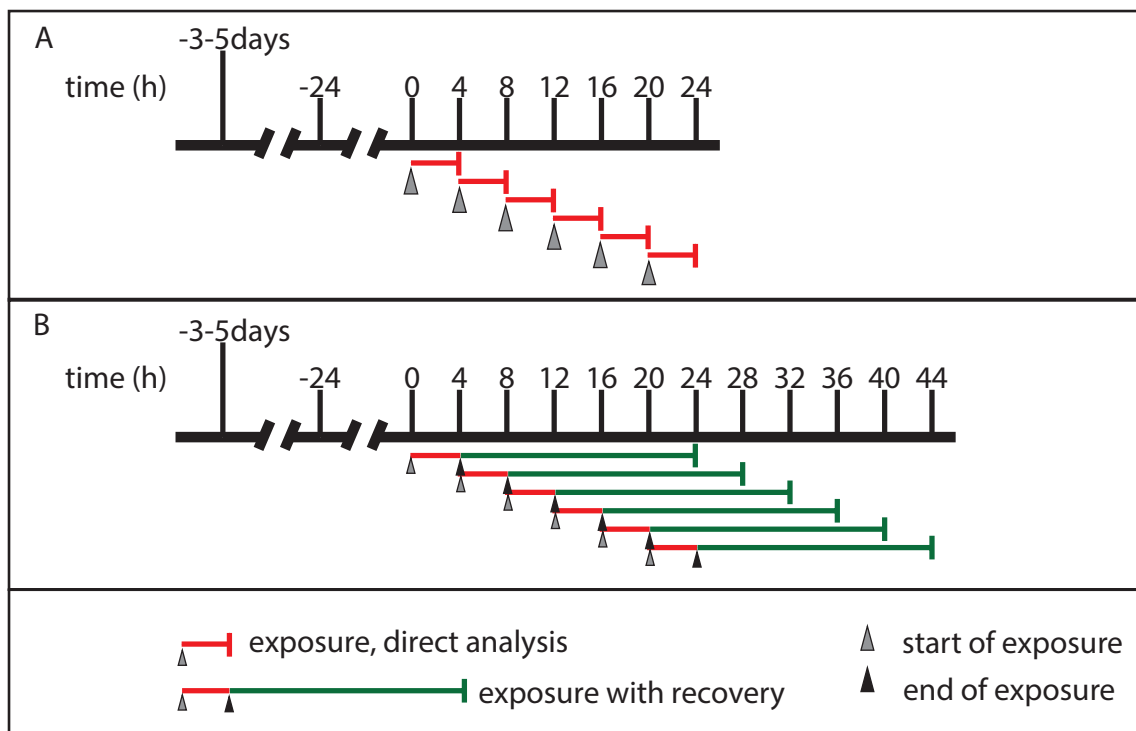

Figure 3. Experimental set up of chronotoxicity assays. SIMH^CLOCK cells were synchronized 24 hours prior to starting the experiment and exposed for 4 hours to a toxic compound, starting at defined phases of the circadian clock. 0/24 refers to the trough, and 12 refers to the peak of *Per2::Luc* expression, as determined by real time bioluminescence recording. (A) Cells were harvested directly after exposure. (B) cells were washed and allowed to recover for 20 hours after exposure before harvesting.

Table 2. Oscillating genes with p<0.001. List of annotated genes with significantly oscillating transcripts (p<0.001, as determined by CircWave analysis). Genes are sorted based on p-value and core clock genes are indicated in bold text.

Gene	Ftest	P value	Gene	Ftest	P value	Gene	Ftest	P value	Gene	Ftest	P value
Arntl	78.2	0.0000	Zfand5	14.5	0.0001	*Per1*	11.7	0.0002	Nadk	10.0	0.0006
Eif5a2	60.7	0.0000	Hmgn5	14.4	0.0001	Siae	11.5	0.0002	Dag1	10.0	0.0006
Nr1d1	52.9	0.0000	Wwc2	14.1	0.0001	Scel	11.4	0.0003	Acot10	10.0	0.0006
Dbp	48.7	0.0000	Fus	14.1	0.0001	Klf3	11.4	0.0003	*Cry2*	10.0	0.0006
Tef	48.5	0.0000	Il33	13.9	0.0001	Lmo7	11.3	0.0003	Plk3	9.9	0.0006
Rorc	48.0	0.0000	Tnfrsf21	13.8	0.0001	Cenpf	11.2	0.0003	Ahr	9.9	0.0006
Cry1	44.1	0.0000	Pdha1	13.8	0.0001	Ephx1	11.1	0.0003	Upf3b	9.8	0.0006
Nr1d2	34.0	0.0000	Chac1	13.6	0.0001	Ppil2	11.0	0.0003	n-R5s15	9.8	0.0006
Per2	33.5	0.0000	Ryk	13.5	0.0001	Rnf130	11.0	0.0003	Rplp1-ps1	9.7	0.0007
Coq10b	26.8	0.0000	Pam16	13.2	0.0001	Isoc2a	10.9	0.0003	Mex3a	9.6	0.0007
Tenc1	25.9	0.0000	Stx3	13.1	0.0001	Nup210l	10.9	0.0003	Rnf126	9.5	0.0008
Ypel2	19.8	0.0000	Foxq1	13.1	0.0001	Dlc1	10.8	0.0004	Arhgef26	9.4	0.0008
Ccna2	19.7	0.0000	Adora1	13.1	0.0001	Pawr	10.7	0.0004	Dusp5	9.3	0.0008
Clec2d	18.4	0.0000	Pxdc1	13.1	0.0001	Akap8	10.6	0.0004	Itga6	9.3	0.0008
Cebpb	18.4	0.0000	Myo1c	13.0	0.0001	Ptrf	10.6	0.0004	Wbscr27	9.3	0.0008
Ppp1r14b	17.8	0.0000	Agfg1	12.9	0.0001	Aldh6a1	10.5	0.0004	Fam83h	9.3	0.0008
Veph1	17.2	0.0000	Magi3	12.9	0.0001	Sdha	10.5	0.0004	Gprc5a	9.3	0.0009
Blcap	17.1	0.0000	Cbx1	12.7	0.0001	Tmem171	10.5	0.0004	Mcm7	9.2	0.0009
Sorbs2	16.5	0.0000	Hist3h2a	12.7	0.0001	Arfip1	10.4	0.0004	Arrdc4	9.2	0.0009
Spg11	16.5	0.0000	Leo1	12.6	0.0001	Cab39	10.4	0.0004	Afg3l2	9.2	0.0009
Ubl3	16.4	0.0000	Rps6ka4	12.5	0.0001	Pdzk1ip1	10.4	0.0005	Lfng	9.2	0.0009
Soat1	15.6	0.0000	Atp1a2	12.4	0.0002	*Per3*	10.3	0.0005	Mterfd3	9.2	0.0009
Nrn1	15.5	0.0000	Hes1	12.3	0.0002	Plin2	10.3	0.0005	Snora43	9.1	0.0009
Pard6b	15.0	0.0000	Atp1a1	12.3	0.0002	Fech	10.3	0.0005	Atp5a1	9.1	0.0009
Lingo4	14.9	0.0000	Igf2bp2	12.3	0.0002	Eif2d	10.3	0.0005	Ubl5	9.1	0.0010
Eepd1	14.9	0.0000	Osgep	11.9	0.0002	Impa2	10.2	0.0005	Sgk3	9.1	0.0010
Kpna2	14.8	0.0000	Wdr36	11.8	0.0002	Nol9	10.2	0.0005	Ier5	9.0	0.0010
Por	14.8	0.0000	Oip5	11.8	0.0002	Lamp3	10.1	0.0005	Chst1	9.0	0.0010
Mical2	14.7	0.0000	Cenpb	11.8	0.0002	Fosl1	10.0	0.0005	Sfxn1	9.0	0.0010
Mcm5	14.6	0.0000	Hibadh	11.8	0.0002	Tmem71	10.0	0.0006	Aplp2	9.0	0.0010
Gcnt2	14.6	0.0001	Scamp1	11.7	0.0002	Eif2a	10.0	0.0006	Acat1	9.0	0.0010

In order to test the time of day dependent toxicity and determine a suitable concentration of the antisuppressant cyclosporine A (CsA), we tested several responsive genes for 24 hour exposure published earlier (Van den Hof et al., 2014) for responsiveness after 4 hours in SIMH^CLOCK cells (Figure S1a). We decided to further test *DnaJb9*, coding for a protein involved in endoplasmatic reticulum stress and prevention from apoptosis, because of the dose responsiveness at fairly low doses (Figure S1b). From this data, we determined the optimal concentration of CsA for 4 hour exposure for gene expression analysis to be 5 µM, which is lower than the concentrations necessary to induce intracellular accumulation of toxic bile acids (chapter 4).

Similar to experiments described before in mouse primary hepatocytes (chapter 3) we exposed synchronized populations of SIMH^CLOCK cells to CsA at different phases of the clock, starting 24 hours after dexamethasone synchronization (Figure 3a) and analyzed induction of *DnaJb9* in each of these phases compared to background expression in vehicle exposed cells (figure 4a). We observed a 12 hour rhythm in expression of *DnaJb9* in vehicle exposed samples (p<0.0001) in accordance with rhythms observed in wild type mouse livers (Hughes et al., 2009). After exposure to CsA, gene expression of *DnaJb9* was upregulated 4-6 fold at all time points (p=0.0004 for 12h rhythm). When gene expression of CsA exposed cells was divided by gene expression of DMSO exposed cells for each time point separately, *DnaJb9* was upregulated 3-5 fold (Figure 4b). P-values for 12 and 24 hour rhythm were 0.0114 and 0.0016, respectively, indicating that it is likely that there is a 24 hour rhythm in *DnaJb9* inducibility on top of the endogenous 12 hour rhythm. The
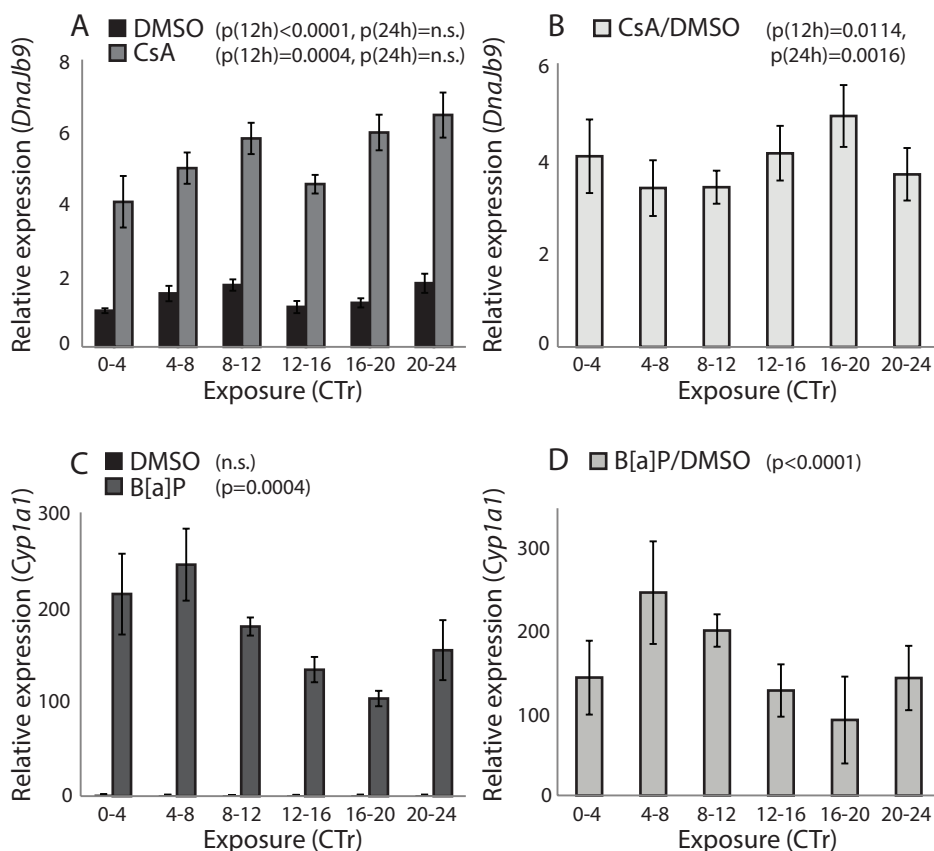
5

Figure 4. Time of day of exposure dependent gene induction by CsA and B[a]P. Induction of *DnaJb9* and *Cyp1a1* gene expression after exposure of SIMH^CLOCK cells to CsA and B[a]P, respectively. Values are relative to expression values of housekeeping genes and normalized to expression after exposure to 0.1 % DMSO at CTr0-4 (panels A and C), or as the average of CsA or B[a]P exposed samples divided by the average of DMSO exposed samples per time point (panels B and D). n=2 experiments (measurements in triplicate) for CsA and n=3 experiments (measurements in triplicate) for B[a]P. Error bars represent SD.

largest peak of this inducibility was observed around CTr16-20, where CTr0/24 and 12 refer to the trough and peak of *Per2* expression, respectively.

Next we exposed synchronized SIMH[CLOCK] cells to B[a]P, a polycyclic aromatic hydrocarbon (PAH) commonly found in exhaust fumes, with highly mutagenic metabolites after activation by CYP1a1. The optimal concentration of B[a]P in SIMH[CLOCK] cells was previously determined to be around 0.5 µM (chapter 4). *Cyp1a1* was induced at all time points compared to the vehicle exposed samples, with values between 100 and 250 fold, with the larges induction around CTr4-8 (figure 4c and d). There was no circadian oscillation in induction by DMSO, whereas p-values for B[a]P exposed samples were very small (p=0.004). Dividing induction levels of B[a]P exposed samples by those in DMSO exposed samples for each time point further increased significance (p<0.0001).

B[a]P induced apoptosis is dependent on the moment of exposure

The formation of the primary mutagenic metabolite of B[a]P, benzo[a]pyrene diolepoxide (BPDE), is dependent on the activity of the aryl hydrocarbon receptor (AhR) and therefore on the inducibility of *Cyp1a1*, both of which are under circadian control (Anderson et al., 2013). The mutagenic potential of B[a]P, eventually leading to apoptosis, may consequently be dependent
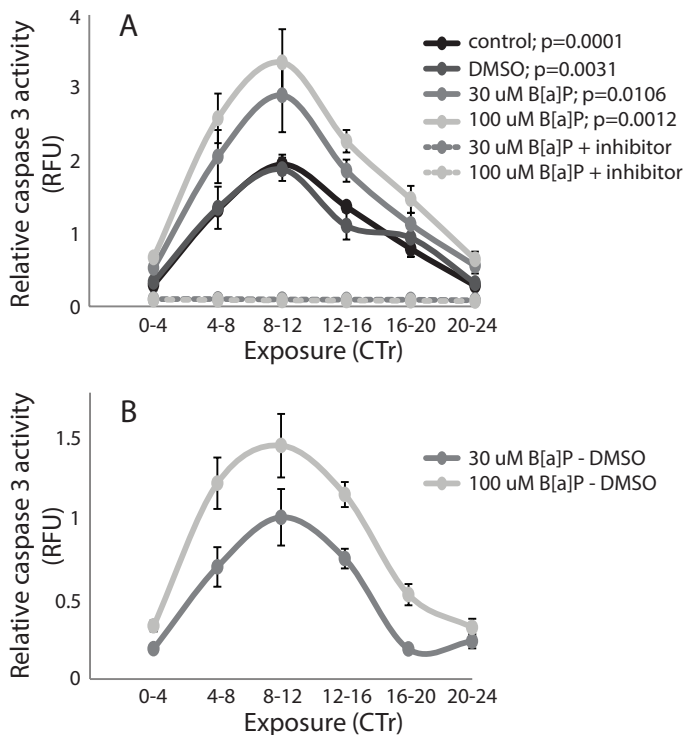

Figure 5. Time of day dependent induction of apoptosis. Induction of apoptosis after exposure of SIMH[CLOCK] cells for 4 hours to B[a]P at defined circadian phase and a 20 hour recovery period. (A) Relative amount of caspase-3 activity; a relative activity of 1 is defined as the average value measured in DMSO exposed samples for all time points; n=2 experiments with 3 or 4 samples per experiment. Error bars represent SD. The control samples were not exposed to DMSO or B[a]P. In the presence of caspase-3 inhibitors, no fluorescence could be detected in B[a]P exposed samples. (B) Relative amount of cleaved caspase-3 in B[a]P exposed minus DMSO exposed samples for each time point separately. (C) Relative amount of LDH leakage after exposure and recovery. No differences could be detected between B[a]P and DMSO exposed samples versus unexposed (control) samples.

on the phase of the clock at the moment of exposure. To investigate this hypothesis, we exposed synchronized SIMH^CLOCK cells to B[a]P or DMSO at different phases of the clock and measured the caspase-3 activity after 24 hours (figure 3b). In Figure 5, we show that there are significant diurnal variations in background levels of apoptosis (Figure 5a) in vehicle (DMSO) or unexposed (control) cells (p=0.0031 and 0.0001, respectively). In samples exposed to B[a]P, the amount of active caspase-3 was higher at all time points (p=0.0094 for 30 μM and p=0.0012 for 100 μM B[a]P), and when the background caspase-3 activity was subtracted from the induction levels in exposed samples, the results show a highly significant (p<0.0001) circadian oscillation in the inducibility of apoptosis on top of the background variation with the highest induction levels around CTr12 (figure 5b). Microscopic evaluation and measurement of LDH levels showed no difference in cell morphology or cell death, indicating that these cells are in an early stage of apoptosis only.

Discussion

Using both real time bioluminescence and qPCR analysis, we have demonstrated that SIMH^CLOCK cells line show robust synchronizable circadian rhythmicity with an average period of 24.7 ± 0.6 hours, which is similar to that observed in mouse primary hepatocytes (chapter 3) and *in vivo* data based on liver transcriptome analysis (Hughes et al., 2009; Panda et al., 2002; Storch et al., 2002; Ueda et al., 2002). After several cycles, the amplitude decreases, indicating that cells become asynchronous in the absence of synchronizing stimuli (Reppert and Weaver, 2002), which has been observed in multiple other cell lines previously e.g. (Oklejewicz et al., 2008). The average signal of bioluminescence also decreases in time, indicating decreased viability most likely due to depletion of nutrients in the medium (Klein et al., 2013). We were able to follow the phase of the clock using real time *Per2::Luc* based bioluminescence measurements for at least 7 days. These results are similar to rhythmicity observed in mouse primary hepatocytes (chapter 3) and in contrast to those observed in human hepatocarcinoma cells (HepG2). In HepG2 cells, we were unable to follow the phase of the clock for more than 48 hours in any condition tested (data not shown), which is similar to the period in which genes have been reported to oscillate in this cell line (Takiguchi et al., 2007).

RNA sequencing analysis demonstrated that 11.8% of the annotated transcripts are oscillating with p<0.05 and oscillation of clock genes was confirmed by RT-qPCR. Gene ontology analysis of transcripts oscillating with p<0.001 indicated that the top oscillating genes, apart from genes involved in the core clock machinery and in regulation of transcription, consists of genes involved in metabolic processes. The RNA sequencing experiment thus confirms robust oscillation and knowledge on the oscillating or non-oscillating character of genes and pathways are imperative to understanding (and predicting) chronotoxic properties of chemicals. Combined with our previous demonstration of the high metabolic competence of SIMH^CLOCK cells (chapter 4), we conclude that these cells are highly suitable for chronotoxic exposure studies.

The endogenous expression of *DnaJb9* in the chronotoxicity study with CsA showed a distinct 12 hour rhythm, which is in accordance with results obtained by Hughes et al. (Hughes et al., 2009). After exposure to CsA at CTr0-4, 4-8, 8-12, 12-16 and 16-20, another rhythm on top of the 12 hour basal rhythm was uncovered with a significant 24 hour oscillation, showing chronotoxicity at the gene expression level for CsA. The peak value of exposed vs unexposed levels of *DnaJb9* was observed at CTr16-20, which is in concordance with the previously reported peak in *Cyp3a11*, the primary gene involved in the metabolism of CsA (Zhang et al., 2009). In mouse primary hepatocytes, we were unable to uncover a circadian oscillation for *DnaJb9* induction, but values at CTr8-12, 12-16 and 16-20 were significantly higher than those at CTr20-24, 0-4 and 4-8 (chapter 3). Average expression levels of *DnaJb9* were comparable between primary and immortalized hepatocytes, indicating that the SIMH^CLOCK cell line may yield more reproducible results in chronotoxicity studies.

Time of day dependent exposure to B[a]P in SIMH^CLOCK cells presented similar results as those observed in mouse primary hepatocytes (chapter 3), with average values comparable to those observed in unsychronized SIMH^CLOCK cells (chapter 4). Background levels of *Cyp1a1* were

similar at all time points, but induction after B[a]P exposure was highly clock phase dependent. The highest induction for gene expression was observed at CTr4-8, whereas in mouse primary hepatocytes this maximum induction was reached at CTr8-12. This difference could be due to the sampling period of 4 hours, with true maximum values reached between CTr4-8 and 8-12. On the other hand, we can not exclude that the proliferating status of SIMH[CLOCK] cells versus the mostly non-proliferating status of primary hepatocytes may influence the rates of metabolism. It has been demonstrated *in vivo* that there are large differences in lag time between gene expression and protein cycles over the day (Robles et al., 2014). If the metabolism in SIMH[CLOCK] cells is significantly faster than in primary hepatocytes, this may be causal for a faster path from attachment to the aryl hydrocarbon receptor, formation of the AHR-ARNT complex, translocation to the nucleus and activation of the dioxin response element, eventually leading to transcription of *Cyp1a1* (Mimura and Fuji-Kuriyama, 2003).

Because B[a]P is a promutagen that becomes toxic after conversion into BPDE by CYP1a1, the mutagenic potential of B[a]P is likely to be dependent on the rate at which this metabolite is produced. To our knowledge, no studies have been presented showing that there is a link between xenobiotic induced apoptosis and the circadian clock. We hypothesized that the main difference would be observed in the onset of apoptosis and therefore we studied caspase 3 activity, which is increased in early stages of apoptosis and in multiple apoptotic pathways (Riedl and Shi, 2004; Salvesen, 2002). Here, we demonstrated that there is an endogenous oscillation caspase 3 activity, with peak values observed around CTr12. Next to these background values, induction of apoptosis after B[a]P exposure was significantly higher in samples exposed at CTr8-12 than 20-24, leading to 3-4 fold differences in induction of apoptosis between these time points.

In conclusion, we observed differential gene expression after exposure to CsA and B[a]P at different phases of the clock, in accordance with our previous results in mouse primary hepatocytes. Moreover, we have linked these differences to variations in the occurrence of apoptosis, thereby connecting time-of-day dependent induction of gene expression to time-of-day dependent cell death.

Acknowledgements

References

Akhtar, R.A., Reddy, A.B., Maywood, E.S., Clayton, J.D., King, V.M., Smith, A.G., Gant, T.W., Hastings, M.H., Kyriacou, C.P., 2002. Circadian cycling of the mouse liver transcriptome, as revealed by cDNA microarray, is driven by the suprachiasmatic nucleus. Curr. Biol. 12, 540–50.

Anderson, G., Beischlag, T. V, Vinciguerra, M., Mazzoccoli, G., 2013. The circadian clock circuitry and the AHR signaling pathway in physiology and pathology. Biochem. Pharmacol.

Chaves, I., Nijman, R., Biernat, M., Bajek, M., Brand, K., Carvalho da Silva, A., Saito, S., Yagita, K., Eker, A., van der Horst, G., 2011. The Potorous CPD photolyase rescues a cryptochrome-deficient mammalian circadian clock. PLoS One 6, e23447.

De Wit, A.S., Nijman, R., Destici, E., Chaves, I., van der Horst, G.T.J., 2014. Hepatotoxicity and the circadian clock, a timely matter, in: Toxicogenomics-Based Cellular Models: Alternatives to Animal Testing for Safety Assessment. Academic Press, pp. 251–270.

Dibner, C., Schibler, U., Albrecht, U., 2010. The mammalian circadian timing system: organization and coordination of central and peripheral clocks., Annual review of physiology.

Hotamisligil, G., 2008. Inflammation and endoplasmic reticulum stress in obesity and diabetes. Int J Obes 2, S52–54.

Huang, D., Sherman, B., Lempicki, R., 2009a. Systematic and integrative analysis of large gene lists using DAVID Bioinformatics Resources. Nat. Protoc 4, 44–57.

Huang, D., Sherman, B., Lempicki, R., 2009b. Bioinformatics enrichment tools: paths toward the comprehensive functional analysis of large gene lists. Nucleic Acids Res. 37, 1–13.

Hughes, M.E., DiTacchio, L., Hayes, K.R., Vollmers, C., Pulivarthy, S., Baggs, J.E., Panda, S., Hogenesch, J.B., 2009. Harmonics of circadian gene transcription in mammals. PLoS Genet. 5, e1000442.

Innominato, P.F., Lévi, F. a, Bjarnason, G. a, 2010. Chronotherapy and the molecular clock: Clinical implications in oncology. Adv. Drug Deliv. Rev. 62, 979–1001.

Klein, S., Mueller, D., Schevchenko, V., Noor, F., 2013. Long-term maintenance of HepaRG cells in serum-free conditions and application in a repeated dose study. J. Appl. Toxicol.

Mazzoccoli, G., Pazienza, V., Vinciguerra, M., 2012. Clock genes and clock-controlled genes in the regulation of metabolic rhythms. Chronobiol. Int. 29, 227–51.

Mimura, J., Fuji-Kuriyama, Y., 2003. Functional role of AhR in the expression of toxic effects by TCDD. Biochim Biophys Acta 1619, 263–268.

Oklejewicz, M., Destici, E., Tamanini, F., Hut, R. a, Janssens, R., van der Horst, G.T.J., 2008. Phase resetting of the mammalian circadian clock by DNA damage. Curr. Biol. 18, 286–91.

Oster, H., Damerow, S., Hut, R., Eichele, G., 2006. Transcriptional profiling in the adrenal gland reveals circadian regulation of hormone biosynthesis genes and nucleosome assembly genes. J Biol Rhythm. 21, 350–361.

Panda, S., Antoch, M.P., Miller, B.H., Su, A.I., Schook, A.B., Straume, M., Schultz, P.G., Kay, S.A., Takahashi, J.S., Hogenesch, J.B., 2002. Coordinated transcription of key pathways in the mouse by the circadian clock. Cell 109, 307–20.

Reppert, S.M., Weaver, D.R., 2002. Coordination of circadian timing in mammals. Nature 418, 935–41.

Riedl, S.J., Shi, Y., 2004. Molecular mechanisms of caspase regulation during apoptosis. Nat. Rev. Mol. Cell Biol. 5, 897–907.

Robles, M.S., Cox, J., Mann, M., 2014. In-vivo quantitative proteomics reveals a key contribution of post-transcriptional mechanisms to the circadian regulation of liver metabolism. PLoS Genet. 10, e1004047.

Salvesen, G., 2002. Caspases: opening the boxes and interpreting the arrows. Cell Death Differ 9, 3–5.

Savvidis, C., Koutsilieris, M., 2012. Circadian rhythm disruption in cancer biology. Mol Med 18, 1249–1260.

Schmittgen, T.D., Livak, K.J., 2008. Analyzing real-time PCR data by the comparative CT method. Nat. Protoc. 3, 1101 – 1108.

Smith, M.R., Eastman, C.I., 2012. Shift work: health, performance and safety problems, traditional countermeasures, and innovative management strategies to reduce circadian misalignment. Nat. Sci. Sleep 4, 111–132.

Storch, K.-F., Lipan, O., Leykin, I., Viswanathan, N., Davis, F.C., Wong, W.H., Weitz, C.J., 2002. Extensive and divergent

5

circadian gene expression in liver and heart. Nature 417, 78–83.

Takiguchi, T., Tomita, M., Matsunaga, N., Nakagawa, H., Koyanagi, S., Ohdo, S., 2007. Molecular basis for rhythmic expression of CYP3A4 in serum-shocked HepG2 cells. Pharmacogenet. Genomics 17, 1047–1056.

Trauner, M., Meier, P.J., Boyer, J.L., 1999. Molecular regulation of hepatocellular transport systems in cholestasis. J. Hepatol. 31, 165–78.

Ueda, H.R., Chen, W., Adachi, A., Wakamatsu, H., Hayashi, S., Takasugi, T., Nagano, M., Nakahama, K., Suzuki, Y., Sugano, S., Iino, M., Shigeyoshi, Y., Hashimoto, S., 2002. A transcription factor response element for gene expression during circadian night. Lett. to Nat. 418, 534–539.

Van den Hof, W.F.P.M., Ruiz-Aracama, A., Van Summeren, A., Jennen, D.G., Gaj, S., Coonen, M.L., Brauers, K., Wodzig, W.K., Kleinjans, J.C., Van Delft, J.., 2014. Integrating multiple omics to unravel mechanisms of Cyclosporin A induced hepatotoxicity in vitro. BMC Syst. Biol. Submitted.

Zhang, Y.J., Yeager, R.L., Klaassen, C.D., 2009. Circadian Expression Profiles of Drug-Processing Genes and Transcription Factors in Mouse Liver. Drug Metab. Dispos. 37, 106–115.

5
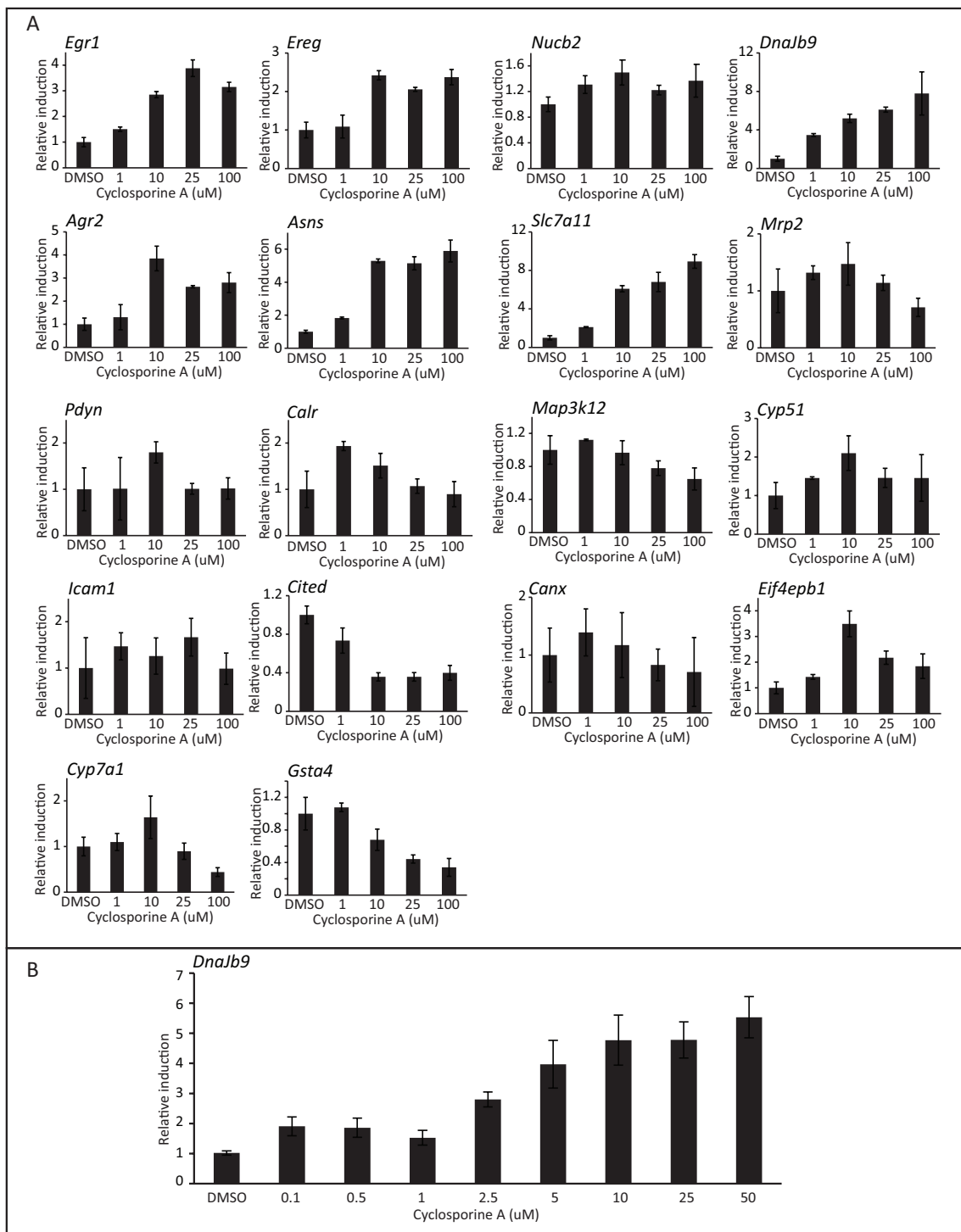
Supplementary figures

Supplementary Figure 1. (A) RT-qPCR data for dose range experiment for CsA responsive genes in SIMH^CLOCK cells after 4 hours of exposure; (B) more detailed dose range for DnaJb9. N=3, error bars represent SD.

Chapter 6

Time of day dependent toxic exposure increases specificity and sensitivity in chemical risk analysis

Annelieke S. de Wit, Gijsbertus T.J. van der Horst, Inês Chaves

Abstract

The circadian clock plays a major role in (xenobiotic) metabolism *in vivo* and therefore should be acknowledged in setting up *in vitro* alternatives for animal testing. Here, we use populations of synchronous and non-synchronous SIMH[CLOCK] cells (spontaneously immortalized mouse hepatocytes). Lumicycle and RT-qPCR analysis showed a clear difference between these populations, in which core clock genes were either oscillating with a period of ca. 24 hours or completely flat, whereas analysis of random populations of non-synchronized cells often demonstrated (partial) clock synchrony, explaining inter-experimental variations in many studies. Exposure to 0.5 µM benzo[a]pyrene (B[a]P) starting 24, 28, 32, 36, 40 and 44 hours after (mock) synchronization demonstrated clear time of day dependent induction of *Cyp1a1* in synchronous populations ($p < 0.0001$) but not in non-synchronous populations ($p > 0.05$), in which there was a 3-fold difference between the moment of highest and lowest induction in synchronous populations and a 2-fold difference between the highest induction in synchronous populations compared to non-synchronous populations. We therefore conclude that chronotoxic exposure leads to higher sensitivity and specificity than standard toxic exposure regimens.

Introduction

The circadian clock is an internal timing mechanism, orchestrating diurnal variations in behavior, physiology and metabolism, aimed to best prepare us for daily recurring changes in our environment such as temperature and light/dark cycles. At the cellular level, circadian rhythms are generated by a molecular oscillator that consists of two main transcription translation feedback loops (TTFLs) in which expression of the heterodimeric CLOCK/BMAL1 complex induces transcription of *Cry* and *Per* genes via E-box elements in their promoter regions, and expression of CRY/PER complexes dislocate the CLOCK/BMAL1 complex, thereby inhibiting their own transcription. This molecular clock work is coupled to rhythmic output processes via a set of clock controlled genes, many of which also contain E-box elements in their promoter regions (Lowrey and Takahashi, 2011). Following this mechanism, over 10% of our genes is under circadian control (Akhtar et al., 2002; Hughes et al., 2009; Panda et al., 2002).

Every cell has its own clock, which is kept in phase by a central clock residing in the suprachiasmatic nucleus (SCN) in our brain. When cells or tissues are taken from the body and cultured *in vitro*, they retain their endogenous clocks (Lowrey and Takahashi, 2004), but in the absence of synchronizing stimuli from the SCN, they eventually run out of phase. Although cell cultures initially have been considered clock-asynchronous, it has become known that *in vitro*, cellular clocks can be resynchronized by a number of events such as, but not limited to, medium refreshment (through components present in serum), changes in temperature, induction of DNA damage (i.e. toxic exposure) or treatment with a variety of other compouns (e.g. endothelin, forskolin, dexamethasone) (Balsalobre et al., 2000; Buhr et al., 2010; Oklejewicz et al., 2008; Schibler et al., 2003). Because of the vast number of synchronizing events and in case of non-standardized culturing and experimental conditions, cells *in vitro* are often (partially) synchronized, unknowingly or unintentionally, which as a consequence can give rise to large inter-experimental, as well as intra- and inter-laboratory variation.

Worldwide, many efforts are undertaken to find alternative methods for animal testing in order to reduce, refine and replace such experiments, many of which are focusing on genotoxic risk analysis. However, most of those studies are not considering the influence of the circadian clock. We have recently shown that the phase of the circadian clock can have a dramatic effect on the response of the liver transcriptome in *in vivo* and *in vitro* toxic exposure studies, as evident from the large time-of-day of exposure dependent differences in the number and kind of differentially expressed genes and pathways (Van Dycke et al., 2014; chapter 2). This phenomenon is referred to as chronotoxicity and is well exemplified by the time-of-day dependent effects of the carcinogen benzo[a]pyrene (B[a]P). We have previously demonstrated that mouse liver slices, as well as primary and established mouse hepatocytes, exposed to B[a]P at different phases of their

clock, show a clear circadian variation in *Cyp1a1* gene induction (chapters 2, 3 and 5). Eventually this leads to time of day dependent differences in induction of apoptosis (chapter 5).

Previously, we have hypothesized that, apart from providing information on chronotoxic properties of chemicals, the sensitivity of toxic exposure studies may benefit from an approach in which the circadian clocks of cells in culture are synchronized prior to treatment and exposure is performed at the circadian phase at which the magnitude of the response (i.e. gene induction) is maximal (Destici et al., 2009). In the present study, we have investigated this concept by comparing the B[a]P sensitivity of asynchronous and clock-synchronized populations of cells. Apart from demonstrating that unsynchronized populations are not necessarily nonsynchronous, we show that a the use of synchronized cells increases the sensitivity of genotoxic risk analysis studies.

Materials & methods

Cell culture
SIMH[CLOCK] cells, originating from a male *Per2::Luc* mouse in a C57BL/6J genetic background (Chaves et al., 2011), were maintained as described before (chapter 4). In short, cells were maintained in SIMH culturing medium, consisting of William's E (Lonza), containing 10% FCS, 100 U/ml pen/strep, 2 mM UltraGlutamine 1 (Lonza) and 1x ITS-X mix (Gibco)). Medium was changed every 3-4 days and cells were kept in a humidified incubator at 37^0C and 5% CO_2. All experiments were performed with cells at passage numbers 20-40. For experiments involving real time recording of circadian clock phase, cells were cultured in SIMH medium, supplemented with 0.1 mM luciferin (Sigma) and 10 mM Hepes buffer (Lonza).

Real time recording of circadian performance
Real time bioluminescence recording of luciferase activity (60 sec. measurements at 10 min. intervals) were performed using a LumiCycle 32-channel automated luminometer (Actimetrics) in a dry incubator at 37^0C. Prior to placing the dishes in the LumiCycle, the lid was replaced by a glass coverslip and sealed with parafilm. Data were analyzed using Actimetrics software. For synchronization, the coverslip was removed and dexamethasone (final concentration 100 nM) or it's solvent (0.1% ethanol) was added to the cell cultures,.

In vitro exposure
Confluent cultures of SIMH[CLOCK] cells were exposed to 0.5 µM B[a]P (Sigma) or its solvent DMSO (0.1%) for 4 hours, and at 4 hour intervals, starting at least 24 hours after dexamethasone-mediated clock synchronization or mock treatment. B[a]P and DMSO were added to conditioned medium, pooled per condition in triplicate. At the end of the exposure, cells were harvested for RNA isolation.

Semi-quantitative real time PCR
Total RNA was isolated using TriPure reagent (Roche Diagnostics) according to the manufacturer's protocol. Following RNA quality analysis and concentration determination using the Nanodrop ND1000 (NanoDrop Technologies), 1 ug of RNA was used for cDNA preparation using iScript (Biorad) according to the manufacturer's protocol. Semi-quantitative RT-qPCR was performed using Platinum Taq DNA polymerase (Invitrogen) according to the manufacturer's protocol on a Biorad C1000 Touch Thermal Cycler using a standard 2-step amplification program with annealing/extension at 60^0C. Reactions for samples with housekeeping genes (*B2M, Hprt* and/or *Gapdh*) were always performed within the same plate as reactions for genes of interest. qPCR data represents the average of 2 housekeeping genes. The following primers were used: *B2M* Fwd 5'-CCG GCC TGT ATC CAG AAA-3' Rev 5'-ATT TCA ATG TGA GGC GGG TGG AAC-3'; *Hprt* Fwd 5'-CGA AGT GTT GGA TAC AGG CC-3' Rev 5'-GGC AAC ATC AAC AGG ACC TCC-3'; *Gapdh* Fwd 5'-CAG AAC ATC ATC CCT GCA TCC-3' Rev 5'-GTC ATC ATA CTT GGC AGG TTT CTC-3'; *Cyp1a1* Fwd 5'-GCA CTA CAG GAC ATT TGA GAA GG-3' Rev 5'-AAT CAC TGT GTC TAG TTC CTC C-3'; *Bmal1* Fwd 5'-GCA CTG CCA CTG ACT ACC AAG A-3' Rev 5'- TCC

TGG ACA TTG CAT TGC AT-3'; *Per2* Fwd 5'-GGC TTC ACC ATG CCT GTT GT-3' Rev 5'-GGA GTT ATT TCG GAG GCA AGT GT-3'; *Cry1* Fwd 5'-CAG ACT CTC GTC AGC AAG ATG-3' Rev 5'-CAA ACG TGT AAG TGC CTC AGT-3. Relative gene expression was calculated using the comparative C(t) method described by Schmittgen et al. and normalized to relative expression after exposure to the vehicle (relative expression = 1) (Schmittgen and Livak, 2008).

Statistical analysis
Harmonic regression analysis of circadian oscillation was performed using CircWave Batch v5.0 for cosinor analysis with a 24 hour wave, with forward linear harmonic regression using an F-test. User defined alpha was 0.05.

Results

In our experience, most populations of cells are not asynchronous, but rather demonstrate full or partial clock synchrony. These observations were made with cell types of different origin and species (data not shown). In order to perform exposure studies in synchronized versus non-synchronized populations of cells, we optimized culturing conditions for SIMH[CLOCK] cells to obtain fully asynchronous populations, i.e. in which *Per2::Luc* bioluminescence rhythms are flat and the expression level of clock genes is constant, independent of the time of analysis. To get true asynchronous populations, it proved necessary to seed SIMH[CLOCK] cells at medium to low density and allow them to proliferate for at least 2 days to reach confluency without medium changes or additions, and transport cells with prewarmed heat blocks (data not shown).

Commonly used clock synchronizing protocols involve a serum shock or treatment of cell cultures with forskolin or dexamethasone. For standardization of toxic exposure studies, we prefer not so use a serum shock as the composition of serum varies between batches. We have chosen to use dexamethasone (see also chapter 5). When SIMH[CLOCK] cells are cultured under the conditions described above, dexamethasone treatment provokes a clear high amplitude oscillation of *Per2::Luc* bioluminescence (Figure 1). In marked contrast, after mock treatment with DMSO, cells remain largely unsynchronized.

In vivo exposure studies in mice have revealed that dexamethasone activates PXR, CAR and CYP3A11 (Gentile et al., 1996; Scheer et al., 2010), which though activation of the P450 system, is considered to have a protective effect against the toxicity of some drugs, In literature, there is no clear convergence on the rate of metabolism or decay of dexamethasone. In dexamethasone treated mice, this compound could no longer be detected from 4 hours after administration (Scheer et al., 2010), while *in vitro* dexamethasone no longer influence membrane permeability 6 hours after addition (Fischer et al., 2001). Although there are considerable differences in metabolic rates between species (Tomlinson et al., 1997), experiments with human microsomes showing a half-life of dexamethasone of 42 minutes at 37[0]C (Obach, 1999) indicate that dexamethasone in the presence of an intact P450 system is removed from the medium quickly. In order to allow the P450 activity in the cells return to normal values and to be able compare between dexamethasone and mock treated cells, we started experiments 24 hours after synchronization.

Routine exposure experiments with SIMH[CLOCK] cells are preferably performed under standard culturing conditions in humidified incubators, rather than in dry incubators, as used for real time clock recording. We therefore first compared circadian clock performance (i.e. amplitude and phase) in synchronized and non-synchronized SIMH[CLOCK] cells grown under standard conditions (clock gene expression) or under "LumiCycle" conditions. Starting 24 hours after dexamethasone or vehicle addition, RNA was collected and relative levels of clock genes *Per2, Bmal1, Rev-erbα* and *Cry1* were measured. As expected, expression levels of *Cry1* and *Bmal1* are clearly oscillating in dexamethasone treated cells, indicating that the cellular clocks are synchronized, while flat expression levels are observed in mock treated cells, demonstrating asynchrony (Figure 2a and b). Because the ratio between clock genes oscillating in different phases is a robust way of demonstrating either synchrony or asynchrony, we analyzed the ratio of *Cry1/Bmal1* for both populations. As shown in Figure 2c, we found clear time of day dependent differences in dexa-

methasone treated (pink lines) but not in ethanol treated cells (blue lines). For each time point, we also plotted the expression levels of *Cry1* and *Bmal1* relative to the expression levels at time point 24, where we defined both expression levels as 1 (point 1,1). Because the expression levels of both genes are time of day dependent in synchronous cells, depicting the relation between them this way leads to the formation of a circle-like figure, whereas all data points for asynchronous populations are similar and thus centered around a single point.

  Cyp1a1 is the primary responsive gene after *in vivo* or *in vitro* exposure to the environmental pollutant (B[a]P). Accordingly, induction of *Cyp1a1* expression serves as a reliable readout for the cellular response to B[a]P exposure. SIMH^CLOCK cells were exposed to B[a]P for 4 hours, starting 24, 28, 32, 36, 40 and 44 hours after dexamethasone or mock treatment. In order to exclude possible influence of dexamethasone in the medium, cells were synchronized at least 24 hours prior to exposure to B[a]P or DMSO. Variations in medium composition and cell passage number were excluded by performing the experiment in triplicate for each condition and repeating the complete procedure with different batches of cells. Absence of the influence of environmental changes (e.g. temperature) on the sensitivity of the cells was verified by exposing a parallel set of cells to DMSO in each experiment. In clock-synchronized cultures, B[a]P addition resulted in highly significant time of day dependent induction of *Cyp1a1* ($p<0.0001$, as revealed by CircWave analysis), peaking and troughing 28 and 40 hours after the synchronization step, while in mock treated cells no significant rhythm in *Cyp1a1* induction was observed (Figure 3). As expected, DMSO did not induce *Cyp1a1* significantly in either condition. Moreover, the induction of *Cyp1a1* in mock treated cells was similar to the average of *Cyp1a1* induction of all time points in dexa-
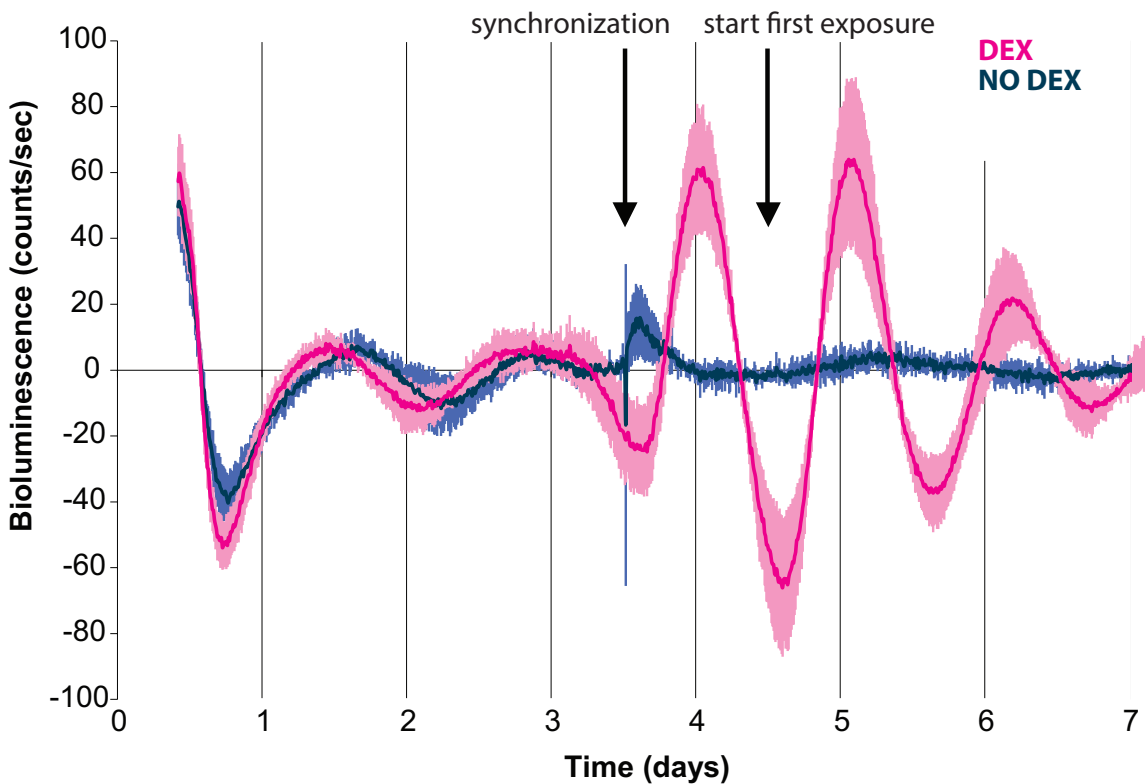
6

Figure 1. Circadian performance of dexamethasone-synchronized and non-synchronized SIMH^CLOCK cell populations. *Per2::Luc* mediated bioluminescence rhythms in SIMH^CLOCK cells, before and after clock synchronization with dexamethasone (pink) or mock treatment with its solvent ethanol (blue). Average bioluminescence signals (triplicate samples in one experiment) are indicated by solid lines and colored background represents standard deviation. Exposure to B[a]P was performed starting 24 hours after dexamethasone/EtOH treatment.
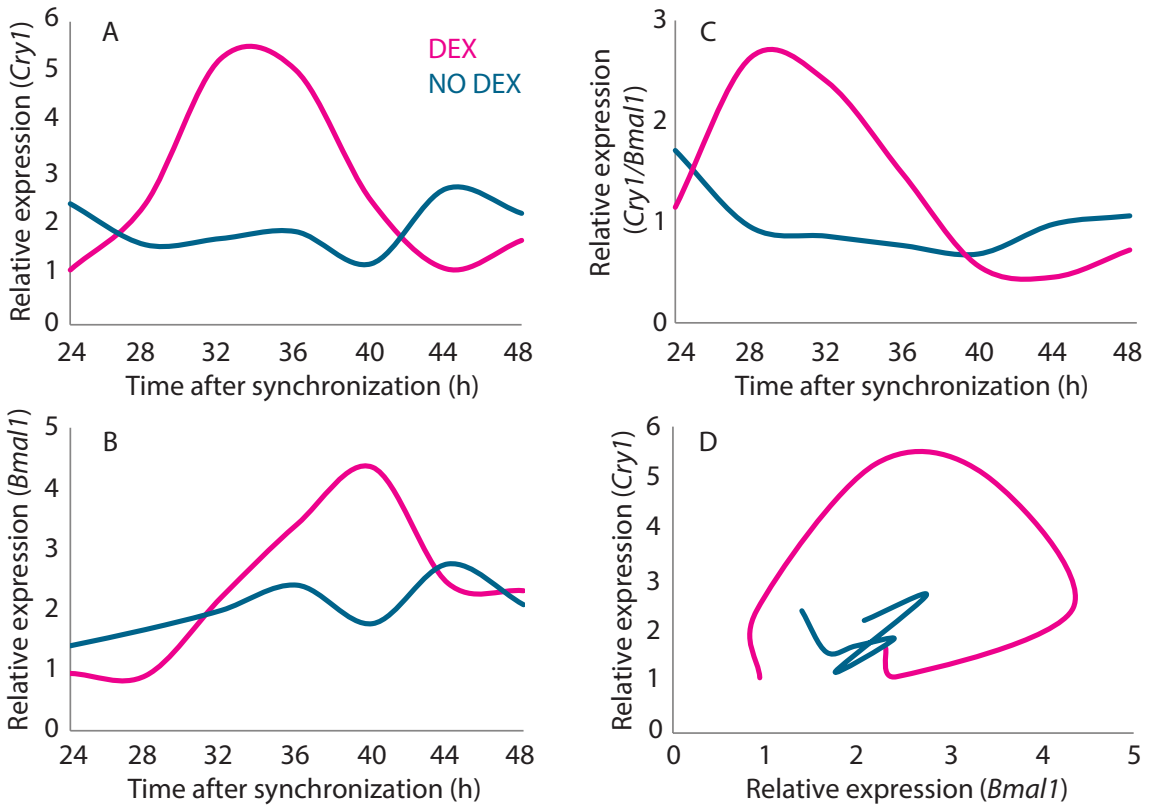
Figure 2. *Cry1* and *Bmal1* expression in synchronized and nonsynchronous SIMH^CLOCK cells. Graphical representation of *Cry1* and *Bmal1* clock gene expression in synchronized versus nonsynchronous populations of SIMH^CLOCK cells. RNA was isolated starting 24 hours after dexamethasone synchronization (pink) or ethanol treatment (blue) treatment. Shown are relative expression levels of *Cry1* (A), and *Bmal1* (B), as well as the ratio between relative *Cry1* and *Bmal1* expression levels (C) and a double plot of *Cry1* and *Bmal1* relative expression levels in which the values on the axes represent expression values relative to time point 24 (expression in synchronized cells at time point 24 is set as 1,1). Significant changes in both expression levels and ratios between *Cry1* and *Bmal1* for synchronized, but not for nonsychronous cell populations are observed.
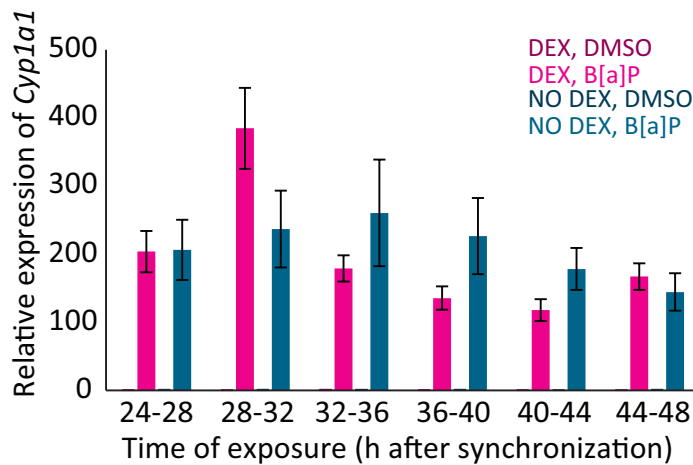
Figure 3. Time of day dependent induction of Cyp1a1 by B[a]P in synchronized and nonsynchronous SIMH^CLOCK cells. Starting 24 hour after dexamethasone clock synchronization or mock treatment, SIMH4CLOCK cells were exposed to 0.5 µM B[a]P or its solvent, 0.1% DMSO for 4 hours. At the end of the exposure period, Cyp1a1 gene expression was measured by RT-qPCR (n=2 experiments, measurements in triplicate). Error bars represent SD.

methasone treated cells (ca. 200x relative induction compared to DMSO exposed cells). These results therefore provide experimental proof for the suggestion that performing toxicological or toxicogenomics experiments with clock synchronized cells increases the sensitivity of the assay (Destici et al., 2009).

Discussion

In the course of these experiments, we observed that most cell populations of which the individual clocks were not intentionally synchronized demonstrated at least partial synchrony. We observed this in multiple experiments with various cell types of different origin and species. It is likely that in classical *in vitro* assays that do not acknowledge the influence of the circadian clock, this is causal for both intra- and inter-experimental variations as experiments may be performed at different (and unknown) phases of the clock. Moreover, it has been demonstrated that DNA damage is often able to reset the phase of the clock (Oklejewicz et al., 2008), at best leading to possible false positive results by classifying differentially expressed genes as genotoxic respon-sive genes while in fact these are clock controlled genes as a result of unrecognized clock syn-chronization (Destici et al., 2009), and at worst missing important toxic responses because there is no consensus between experimental setups. Both of these add to the difficulties in extrapolating *in vitro* data to *in vivo* systems. Therefore, it is important to know both the phase of the clock prior to toxic exposure, as well as the possible phase resetting abilities of the compounds investigated.

Here, we demonstrate a proof of principle experiment in which we compare the genotoxic reponse to the dioxin benzo[a]pyrene (B[a]P) between synchronized and nonsynchronous popu-lations of cells. It was suggested that chronotoxic exposure compared to standard toxic exposure would increase the sensitivity of the assay for compounds whose metabolism is dependent on clock controlled genes (Destici et al., 2009). We demonstrated earlier that there is a time of day dependent response to B[a]P (chapters 2, 3 and 5) and in the current study, we prove chrono-toxic exposure studies more sensitive than standard exposure studies by showing that the toxic response in true nonsynchronous populations is independent on the time of the day, and that this response is the average of the induction in synchronized populations. The induction of *Cyp1a1* at the most sensitive moment in synchronized populations is a 2 fold increase of the response on nonsynchronous populations of SIMH[CLOCK] cells. These insights have major implications for opti-mizing and standardizing risk identification and assessment regimens. Next to the higher level of detail in toxicogenomics studies that follows from decreasing false positives and interexperimental variability, studies can address issues regarding chronotoxicity of hazardous materials or phar-maceutical drugs, leading to chronomodulated protocols for labor hygiene and clinical treatment, respectively.

In conclusion, to our best knowledge, this is the first study demonstrating that acknowl-edging the influence of the clock increases the sensitivity of genotoxic exposure assays. This further emphasizes the influence of the circadian clock on *in vitro* studies.

Acknowledgements

References

Akhtar, R.A., Reddy, A.B., Maywood, E.S., Clayton, J.D., King, V.M., Smith, A.G., Gant, T.W., Hastings, M.H., Kyriacou, C.P., 2002. Circadian cycling of the mouse liver transcriptome, as revealed by cDNA microarray, is driven by the supra-chiasmatic nucleus. Curr. Biol. 12, 540–50.

6

Balsalobre, A., Marcacci, L., Schibler, U., 2000. Multiple signaling pathways elicit circadian gene expression in cultured Rat-1 fibroblasts. Curr. Biol. 10, 1291–4.

Buhr, E.D., Yoo, S.-H., Takahashi, J.S., 2010. Temperature as a Universal Resetting Cue for Mammalian Circadian Oscillators. Science (80-.). 330, 379–385.

Chaves, I., Nijman, R., Biernat, M., Bajek, M., Brand, K., Carvalho da Silva, A., Saito, S., Yagita, K., Eker, A., van der Horst, G., 2011. The Potorous CPD photolyase rescues a cryptochrome-deficient mammalian circadian clock. PLoS One 6, e23447.

Destici, E., Oklejewicz, M., Nijman, R., Tamanini, F., van der Horst, G.T.J., 2009. Impact of the circadian clock on in vitro genotoxic risk assessment assays. Mutat. Res. 680, 87–94.

Fischer, S., Renz, D., Schaper, W., Karliczek, G.F., 2001. In vitro effects of dexamethasone on hypoxia-induced hyperpermeability and expression of vascular endothelial growth factor. Eur. J. Pharmacol. 411, 231–43.

Gentile, D., Tomlinson, E., Maggs, J., Park, B., Back, D., 1996. Dexamethasone metabolism by human liver in vitro. Metabolite identification and inhibition of 6-hydroxylation. J Pharmacol Exp Ther 277, 105–112.

Hughes, M.E., DiTacchio, L., Hayes, K.R., Vollmers, C., Pulivarthy, S., Baggs, J.E., Panda, S., Hogenesch, J.B., 2009. Harmonics of circadian gene transcription in mammals. PLoS Genet. 5, e1000442.

Lowrey, P., Takahashi, J., 2011. Genetics of circadian rhythms in Mammalian model organisms, in: Adv Genet. pp. 74:175–230.

Lowrey, P.L., Takahashi, J.S., 2004. Mammalian circadian biology: elucidating genome-wide levels of temporal organization. Annu. Rev. Genomics Hum. Genet. 5, 407–41.

Obach, R.S., 1999. Prediction of human clearance of twenty-nine drugs from hepatic microsomal intrinsic clearance data: An examination of in vitro half-life approach and nonspecific binding to microsomes. Drug Metab. Dispos. 27, 1350–9.

Oklejewicz, M., Destici, E., Tamanini, F., Hut, R. a, Janssens, R., van der Horst, G.T.J., 2008. Phase resetting of the mammalian circadian clock by DNA damage. Curr. Biol. 18, 286–91.

Panda, S., Antoch, M.P., Miller, B.H., Su, A.I., Schook, A.B., Straume, M., Schultz, P.G., Kay, S.A., Takahashi, J.S., Hogenesch, J.B., 2002. Coordinated transcription of key pathways in the mouse by the circadian clock. Cell 109, 307–20.

Scheer, N., Ross, J., Kapelyukh, Y., Rode, A., Wolf, C.R., 2010. In Vivo Responses of the Human and Murine Pregnane X Receptor to Dexamethasone in Mice. Drug Metab. Dispos. 38, 1046–1053.

Schibler, U., Ripperger, J., Brown, S., 2003. Peripheral circadian oscillators in mammals: time and food. J Biol Rhythm. 18, 250–260.

Schmittgen, T.D., Livak, K.J., 2008. Analyzing real-time PCR data by the comparative CT method. Nat. Protoc. 3, 1101 – 1108.

Tomlinson, E.S., Maggs, J.L., Park, B.K., Back, D.J., 1997. Dexamethasone metabolism in vitro: Species differences. J. Steroid Biochem. Mol. Biol. 62, 345–352.

Van Dycke, K.C.G., Nijman, R.M., Wackers, P.F., Jonker, M.J., Rodenburg, W., van Oostrom, C.T.M., Salvatori, D.C.F., Breit, T.M., van Steeg, H., Luijten, M., van der Horst, G.T.J. (2014), 2014. A day and night difference in the response of the hepatic transcriptome to cyclophosphamide treatment. Arch. Toxicol. In press.

6

Chapter 7

General discussion
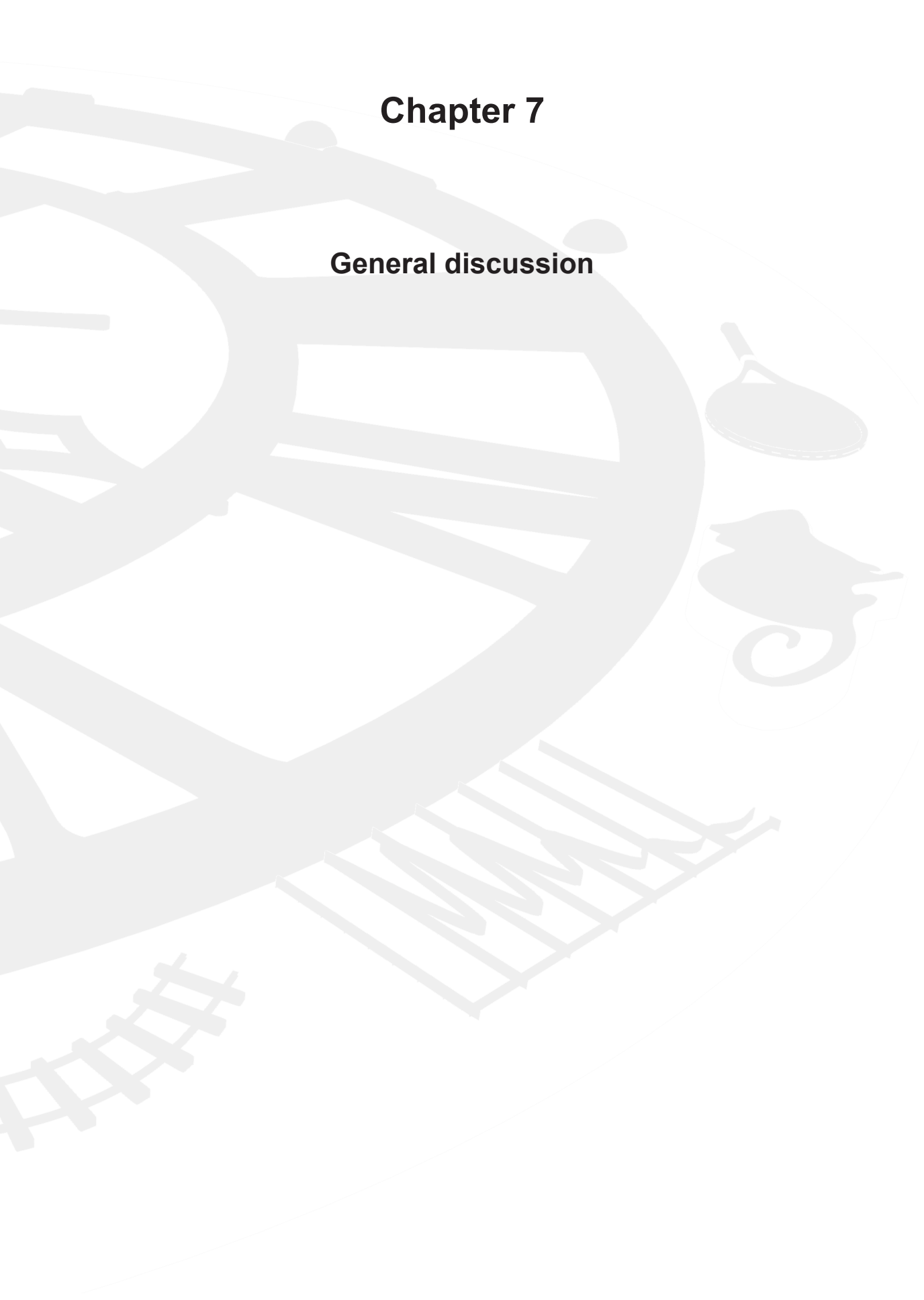
In vitro alternatives for genotoxic risk analysis studies & the influence of the circadian clock

In the past decades various methods have been set up and described for chemical risk analysis assays for new and existing compounds in our environment. Most often, these assays are being carried out with the aid of laboratory animals, of which rodents represent the largest group. European legislations demand that animal studies are reduced, refined and replaced (3R's), leading to the development of numerous *in vitro* alternatives, using no or a reduced number of animals.

Most of these newly developed *in vitro* systems have focused solely on altered gene expression after exposure to one or more compounds and the results of these genotoxic risk analysis studies are mostly obtained using microarray and RT-qPCR systems. In addition, genetic pathways are found for genes involved in altered processes. These pathways are often similar between (i) classes of compounds, (ii) different studies, (iii) different laboratories and (iv) different species, but specific genes involved are frequently not. This phenomenon can be explained by various reasons, mainly being a) differences in the free drug concentration (apart from different starting concentrations, variations in culturing media have ample influence on the intracellular concentrations) (Kramer et al., 2012; Mueller et al., 2014), b) differences in cell type or subtype, even within the same cell line (for instance, the HepaRG cell line consist of different cell types and exact composition is variable) (Cerec et al., 2007; Schulze et al., 2012), c) variations in medium composition (Klein et al., 2013, chapter 4) and d) the age of the cells in culture (cells undergo major temporal changes causing differences in the cell's behavior and xenobiotic metabolism) (Baker et al., 2001; Harris et al., 2004; Luttringer et al., 2002, chapter 3, chapter 4).

Another major, yet poorly recognized, reason for inconsistencies between studies or even within studies is the influence of the circadian clock. This internal timing mechanism, present in all cells (Reppert and Weaver, 2002), affects many cellular processes causing extensive interplay between circadian rhythmicity and metabolic pathways. Even though a substantial percentage of genes oscillates during the day (e.g. around 10% in the liver transcriptome (Akhtar et al., 2002; Hughes et al., 2009; Panda et al., 2002)) and thus affect essentially all processes, most alternative assays for animal studies do not acknowledge the influence of the circadian clock, whilst the time of day plays a large role in animal exposure studies. This can lead to false positives when genes with altered expression after exposure are considered genotoxic responsive genes instead of genes with endogenously different expression levels depending on the time of day (Destici et al., 2009). This might explain many inconsistencies between studies and projects. The liver is the major organ involved in (xenobiotic) metabolism and therefore the majority of genotoxicity studies are being performed in systems derived from the liver. Additionally, acute liver failure is still a major reason for drug withdrawal after entering the market (Davila et al., 2008). In this thesis, we have therefore focused on the liver.

Various liver derived systems have been described previously, such as immortal cells derived from hepatocarcinomas, primary cells infected with oncogenes and induced pluripotent stem cells (iPSC) from different species, cultured in 2D systems or in different types of 3D structures (Godoy et al., 2013), as well as primary hepatocytes and precision cut liver slices (Szalowska et al., 2013), but none of those acknowledge the influence of the circadian clock. It is our belief that when the phase of the clock is taken into account when performing chemical exposure studies, the results of these experiments will better resemble *in vivo* toxicity and therefore increase the predictive value for toxic exposure. Moreover, present studies in which false positives or false negatives are found after genotoxic exposure because the response is the average of the responses in individual cells could be ameliorated by exposing synchronized cells at their most or least sensitive clock phase.

The extrapolation from results obtained with *in vitro* research to effects observed *in vivo* is subject to many pitfalls. Apart from the reasons mentioned above, the more different a system is from the *in vivo* situation, e.g. considering the structural environment of cells, the more differences can be expected when looking at gene expression one to one. For instance, organ slices retain the cellular architecture observed *in vivo* with different cell types and cell-cell interactions, where cultures of an isolated type of cells often do not. On the other hand, studying processes in

7

a specified cell type is nearly impossible in slices because of the presence of multiple cell types. Immortalized cell types no longer require the use of animals and can be used unlimitedly, but may demonstrate altered behavior compared to primary material. Therefore, looking at gene expression patterns solely, few consistencies might be found even while the ultimate biological end point of a process is equal. For this reason the inclusion of biologic (pathogenic) end points should be considered when studying xenobiotic metabolism *in vitro*. When this is similar between different systems, gene expression can be used to find early responsive genes so as to detect early stages of pathogenic processes, which may be dissimilar dependent on the system used. Within the Netherlands Toxicogenomics Centre, we have conducted experiments with slices, primary cells and immortalized cells of mouse liver to find (dis)similarities between all systems, in order to find a systematic response to toxic exposure, in which the liver plays a major role. The projects in our laboratory have focused on these responses with regard to the circadian clock, i.e. in what way the xenobiotic metabolism is dependent on the phase of the clock. With knowledge thus obtained, *in vitro* results in general can represent better the results observed *in vivo*, leading to more accurate predictions about genotoxic risk analysis and ultimately a significant reduction in the number of laboratory animals needed.

Mouse liver slices and mouse primary hepatocytes

Our first efforts in setting up and validating *in vitro* assays comprised *ex vivo* slices and *in vitro* primary hepatocytes derived from mice. In this thesis, we optimized culturing conditions for long-term culturing, allowing monitoring clock phase prior to toxic exposure. Historically, experiments using liver slices and primary hepatocytes of any species tend to be performed as soon as possible after isolation, because cells quickly lose their metabolic competence. In order to prevent these cells from running low on any nutrients, a highly nutrient rich medium is used, which is usually replaced daily. In our opinion, this method has two pitfalls. First, multiple studies have demonstrated that major temporal changes take place in the first (approximately 48) hours after cell collection, leading to large inter- and possibly intra-experimental variations. Second, a nutrient rich medium is very likely to contain clock synchronizing compounds, but time of medium refreshment and exposure are generally not standardized. Within one experiment this may lower variability because all cells are in a similar (yet unknown) clock phase, but when a second experiment is conducted under slightly different working schedules or lab routines, this rapidly leads to variation that can be the result of the circadian clock instead of other parameters. For our experimental setup, it was necessary to control both problems in order to find what effects were the result of exposure at different phases of the clock. We optimized culturing conditions and found that mouse primary hepatocytes settled in their new environment after ca. 4 days, also leading to a re-established network of bile canaliculi that was disrupted by collecting the cells. Medium replacement indeed resynchronized the individual cellular clocks, most likely due to the presence of glucagon.

Spontaneously Immortalized Mouse Hepatocytes (SIMH4/SIMH^CLOCK^)

The ultimate goal in genotoxic risk analysis is an immortal cell line, needing no further animals, which is able to grow fast and in standardized 2D, high throughput conditions while retaining all metabolic features of *in vivo* cells, including a functional clock. Preferably this cell line would be of human origin, but major drawbacks here are that it is impossible to standardize the human response upon toxic exposure because of differences in genetic makeup and life style, next to obvious difficulties of directly comparing *in vitro* responses to those obtained *in vivo*. In order to unravel molecular mechanisms involved in xenobiotic metabolism, a murine cell line is more convenient because the mice within a mouse line are genetically identical, many mouse lines harboring specific genetic improvements or defects exist so these can be studied in detail and results can be compared to extensive *in vivo* data if necessary. We have developed a murine hepatic cell line from a male C57Bl6/J mouse with a *Period2::luciferase* reporter to follow the phase of the clock in real time using bioluminescence: Spontaneously Immortalized Mouse Hepatocytes (SIMH4 or SIMH^CLOCK^). These cells were derived from primary hepatocytes by refreshing the medium until

some cells started to proliferate spontaneously, so no oncogenes were introduced. Additionally, we established other SIMH cell lines from male and female mice with different defects (e.g. *Ercc1*, *Xpc* and clock mutations) and/or reporters (e.g. fluorescent XPB-GFP or XPC-GFP).

For the experiments described in this thesis, we focused solely on SIMH4/SIMH[CLOCK] cells. SIMH4/SIMH[CLOCK] cells have been characterized extensively, and have demonstrated to express various genes specific for adult liver as well as genes involved in the urea cycle, glutathione and bile acid metabolism and transmembrane transporters (chapter 4) in standard culturing conditions. A comparison between different passages has shown that these features are not altered when cells are kept in culture for long time. On the other hand, culturing conditions (e.g. the presence of different concentrations of serum) do have a major influence on many parameters. In short, serum deprivation leads to higher liver specific function, as was shown earlier for HepaRG cells (Klein et al., 2013), but after a period of 4 days cells starve because of a lack of nutrients. Ideally, more research should be conducted for optimizing these culturing conditions, enabling long-term cell culture, which in turn paves the way for complex genotoxic risk analyses, repeated dose or chronic exposure regimens. The perspective is that optimizing medium composition and refreshment regime will further improve the hepatocyte specific behavior of SIMH4 cells.

In SIMH4/SIMH[CLOCK] cells, endogenous P450 activity is retained at both gene expression and protein levels and show a more similar response after exposure to benzo[a]pyrene (B[a]P) to mouse primary hepatocytes than to commercially available cell lines (HepG2 and Hepa1-6), indicating a larger metabolic competence as compared to other cell lines, as also shown for the the pharmaceutical drugs tamoxifen and sunitinib. Concerning the biological significance of altered gene expression, we demonstrated time and dose dependent increases for both apoptosis and the accumulation of intracellular bile acids, which eventually leads to cholestasis. These findings are highly important for future research, because it enables the optimization of exposure assays for high throughput assays based on liver pathology-related endpoints. Biological end point parameters are likely more predictive for the type of risk associated with a compound, or a combination of compounds, than differential gene analysis alone. Moreover, this type of analysis is cheaper, faster and more suitable for future high content screens in drug development programs ,and likely also in risk assessment assays, the latter being more and more subject to stringent governmental regulations. Because many chemical compounds are known to induce mutagenesis that can ultimately lead to cancer, the mutagenic potential of a compound is an important factor. To our knowledge no immortal hepatic cell line has been developed previously that was able to metabolize promutagens such as B[a]P in the absence of extracellular P450 enzyme activity (e.g. by adding a S9 mix) at high rates, so that the mutagenic potential of a compound is often difficult to determine. We have demonstrated that different compounds including B[a]P were able to induce mutagenesis in SIMH4/SIMH[CLOCK] cells in normal culturing medium without the addition of external enzymes, leading to the induction of micronuclei. This is an important parameter in toxicology, and therefore this feature further adds to the high throughput potential of SIMH4/SIMH[CLOCK] cells.

Because SIMH4/SIMH[CLOCK] cells were derived from a male mouse, results will better resemble *in vivo* and other *in vitro* data available at this moment, since most studies have been performed with male animals and there is increasing evidence that the P450 system behaves differently between males and females (Lu et al., 2013; Penaloza et al., 2013). It is unlikely that any one *in vitro* alternative derived from any species will ever completely predict genotoxic risk assessment correctly for all types of compounds and damage but the SIMH4/SIMH[CLOCK] cell line has demonstrated to retain high levels of hepatocyte specific behavior and P450 activity, as well as the possibility to measure various biologic end points. Therefore, the SIMH4/SIMH[CLOCK] cell line is a highly valuable addition with the potential to become the new 'golden standard' to the array of *in vitro* systems already available and our efforts in establishing multiple cell lines similar to SIMH4/SIMH[CLOCK] cells with different genetic makeup (sex, mutations, background) further add to this. Additional perspectives are the establishment of SIMH lines with bioluminescent or fluorescent reporters for marker genes or biological endpoints (e.g. apoptosis), allowing assessment of (toxic) responses after addition of (a) chemical compound(s) in real time. This can be achieved in cell populations (using similar techniques as described in this thesis), but also allows for single cell

analysis. The most important attribute of SIMH cells over other established cell lines is that they can be used to assess biological responses in standard culturing conditions, leading to high(er) throughput testing. In some cases, however, the goal is to create a system with the highest possible predictive value, so SIMH cells can be used to form organoids, similar to those created with other liver cell lines. In this case, the high proliferative capacity is likely to result in faster creation of these structures, compared to HepaRG cells, for instance. Subsequently, these organoids can be used in complex serial structures combining cell types derived from multiple organs, thus creating a miniscule gastro-intestinal tract using microfluidics, or to study the interaction between healthy and cancer cells ('cancer on a slide').

Time of day dependent toxicity (chronotoxicity)

The circadian clock plays an important role in many if not all cellular processes. We have focused on the interplay between the circadian clock and chemical-induced toxicity. Destici and coworkers have suggested earlier that in various studies regarding chemical risk assessment *in vitro*, many false positives can be found for genotoxic responsive genes (Destici et al., 2009). In short, all cells retain their endogenous clock (Reppert and Weaver, 2002) but in the absence of humoral stimuli from the central clock, cells *in vitro* tend to desynchronize. When the clock phase of a cell culture is followed in time, e.g. with the use of bioluminescent clock reporter, the average bioluminescent signal at the population level is constant, even though individual cells retain a circadian rhythm. Many chemicals possess the ability to resynchronize the clocks in such a non-synchronous population, e.g. by introducing DNA damage (Oklejewicz et al., 2008). After chemical exposure, the average output of the population is a circadian rhythm, so a gene with altered expression on the population level can be the result of the chemical exposure, but could also be the effect of the clock synchronization (see figure 2 in chapter 1). In order to circumvent this, it is suggested to synchronize the cells in the population prior to chemical exposure, and preferably perform the chemical exposure experiment at different phases of the clock in order to find true genotoxic responsive genes and in many cases, differential response depending on the phase of the clock at the moment of exposure.

Using mouse liver slices, we have shown large differences in the toxic response to B[a]P when slices are exposed at CTr12 compared to CTr0 or 24 (CTr0 refers to the through of *Per2::luciferase* expression, as measured by bioluminescence recording in a LumiCycle device (chapter 2). *Cyp1a1*, the primary gene involved in the metabolism of B[a]P, is induced most prominent after exposure from CTr8-12. In order to find out whether this chronotoxic response can also be visualized in mouse primary hepatocytes and SIMH cultures, we first optimized culturing conditions for both cell types for semi long term culturing with robust and synchronizable clock gene expression (chapters 2, 3 and 4). We exposed both primary hepatocytes and SIMH4/SIMH[CLOCK] cells, to B[a]P and cyclosporine A (CsA) for 4 hours, starting at CTr 4, 8, 12, 16, 20 and 24, and analyzed RNA expression levels directly after exposure (chapters 3 and 5). For B[a]P, similar to liver slices, the highest induction of *Cyp1a1* was observed for exposure from CTr8-12 in primary hepatocytes, with 3-fold difference between the highest and lowest induction. A similar fold change (2.5 x) was observed in SIMH4/SIMH[CLOCK] cells, but in this system the peak of induction was observed for exposure from CTr4-8. We hypothesize that the reason for this shift in peak inducibility is caused by the faster metabolism and proliferation of SIMH4/SIMH[CLOCK] cells. Hepatocytes *in vivo* retain their capability for proliferation but healthy cells rarely divide. Liver slices as well as primary hepatocytes hence contain only few proliferating cells while the immortalized SIMH4/SIMH[CLOCK] cells have a population doubling time of around 10-14 hours when in non-confluence. In confluence this doubling time is obviously lower but it is likely that the rate of metabolism in such cells is higher than in primary cells or slices.

In order to determine whether differential gene expression at different phases of the clock leads to differential induction of apoptosis, we exposed SIMH4/SIMH[CLOCK] cells to B[a]P and allowed them to recover for 24 hours. Analysis of cell lysates showed that indeed, amounts of cleaved caspase 3 were present in highly significant differential numbers, ranging from 5-7 fold changes between peak and through, depending on the concentration of B[a]P used. Interestingly,

7

peak values for cleaved caspase 3 were found for exposure from CTr8-12, possibly due to lag times between gene expression and protein formation (Robles et al., 2014). Another interesting finding is that background values for cleaved caspase 3, in unexposed or DMSO exposed cells, also showed significant circadian variations with peak values around CTr12. Exposed minus unexposed values were always positive, ranging from around 0.4 to 1.5 fold more cleaved caspase 3 depending on the time point and concentration.

DnaJb9, an early responsive gene used in this thesis for determining the response to cyclosporine A exposure, has an endogenous rhythm of 12 hours *in vivo* (Hughes et al., 2009), which is in concordance with our results in both primary hepatocytes and SIMH4/SIMH[CLOCK] cells (chapters 2 and 4). After exposure to CsA, *DnaJb9* was upregulated at all time points. CYP3A11 is the primary member of the P450 family involved in metabolism of CsA and is expressed in a circadian manner with peak expression around our CTr20 (Takiguchi et al., 2007; Zhang et al., 2009). When we divided induced values of *DnaJb9* after CsA exposure by background values in DMSO exposed samples, we found a 24 hour circadian rhythm with high significance in SIMH4/SIMH[CLOCK] cells, with highest induction indeed found for exposure from CTr16-20. In primary hepatocytes, we observed higher expression for exposure from CTr8-12, 12-16 and 16-20 and lower for exposure from CTr20-24, 0-4 and 4-8, but we were not able to derive a significant circadian oscillation. These results suggest that the cholestatic phenotype observed *in vivo* after CsA exposure is highly likely to show circadian oscillation in these *in vitro* setups.

A second suggestion made by Destici and coworkers was that, when cell populations are synchronized prior to toxic exposure, results of gene expression would not only by more specific by lowering false positives but also more sensitive because in this setup, the true maximum value of gene induction and biologic end point can be assessed by exposing the cells at their most sensitive moment of the clock. When nonsynchronous populations are exposed to a toxicant, the result of the exposure represents the average of the whole population, where in synchronous populations values are dependent on the moment of exposure. In chapter 6, we prove this hypothesis true by showing an average response to B[a]P exposure in nonsynchronous SIMH4/SIMH[CLOCK] cells compared to synchronized populations, in which induction of *Cyp1a1* is higher or lower than the average depending on the phase of the clock. In our opinion, using synchronized cell populations in chronotoxic exposure studies not only enhances specificity and sensitivity, but also the speed and therefore high throughput potential of chemical risk assessment; for many compounds the primary enzyme involved in metabolism is known, so therefore cells can be exposed around the phase of the clock at which this enzyme is expressed highest or lowest depending on the question. This ensures maximum output of the exposure experiment and faster data collection. Another important issue uncovered during these comparisons is that for most cell types it is very difficult to obtain true nonsynchronous populations of cells. Due to many experimental (e.g. DNA damage induction) and external (e.g. medium change, temperature differences) influences, populations become at least partly synchronized. Therefore, when conducting experiments in unsynchronized populations, cells are not necessarily and most likely not nonsynchronous. Again, this lead to inexplicable interexperimental variations and should therefore be avoided when performing any *in vitro* experiment.

Perspectives

In the field of toxicology, a lot of resources are invested in finding the best *in vitro* alternative for *in vivo* testing. As stated previously, it is unlikely that any one cell line or system will completely replace animal testing in short time, because all findings have to be evaluated against data obtained *in vivo*. We believe one of the most important neglected differences between *in vivo* and *in vitro* testing is the disregarding of the circadian clock. Therefore, performing toxic exposure studies in a chronotoxic risk analysis setup will likely lead to more representative and more reproducible results with *in vitro* systems by standardizing exposure regimens.

First, our novel cell line SIMH4/SIMH[CLOCK] combines easy handling and perspective for use in a high throughput setup with high endogenous metabolic competence, polarized cell archi-

tecture and fast proliferation. The high throughput setup requires further development because safety assessment programs for drug discovery, facilitating early go/no go decisions, will be a major asset in cost savings. Additionally, the possibility of assessing possible chronotoxicity of chemicals further refines these programs, thereby adding to safety in labor hygiene and personalized medicine.

Second, in order to use this cell line to its full potential, future research efforts should also focus on the optimization of long term culturing, for instance by determining optimal concentrations of serum, DMSO and growth factors without disturbing the circadian clock. This way, the SIMH4/SIMH[CLOCK] cells can be used for chronic (4D) exposure in nonsynchronous populations, or in chronotoxic repeated dose exposure studies, in which the same cells are exposed to a certain toxicant for a short period in a specific phase of the clock at subsequent days. The latter represents better exposure to, for instance, pharmacological drug use for patients and exposes molecular mechanisms that are only activated after a longer period of exposure to lower concentrations. Unexpected interplay between multiple drugs, as can be a side effect when combining drug in the clinic, will also be discovered sooner, adding to safer drug administration. Better knowledge about the interactions between the circadian clock and the effects of time-of-day dependent drug administration will eventually lead to increased used of chronotherapy, in which patients can be treated more efficiently with fewer adverse effects.

Third, since molecular mechanisms and pathways may differ between specific compounds and species but biologic end points are often more similar, we propose that more resources should be invested in optimizing assays for other types or liver damage such as steatosis and necrosis. These assays, as well as exposure to a cholestasis-inducing compound such as CsA should be performed at different time points around the day in synchronized populations of SIMH4/SIMH[CLOCK] cells in order to determine if these end points follow a circadian pattern similar to that observed for apoptosis after exposure to B[a]P.

Last, SIMH4/SIMH[CLOCK] cells, as well as other SIMH lines, create ample possibilities for introducing additional (fluorescent) markers for identifying single cell behavior (generally and after toxic exposure), optimizing culturing conditions for growing cells in organoids to further increase predictive capacity, or to be used in simulations of the gastro-intestinal tract or to study the interactions between healthy and cancer cells, eventually leading to finding novel methods to treat liver cancer.

References

Akhtar, R.A., Reddy, A.B., Maywood, E.S., Clayton, J.D., King, V.M., Smith, A.G., Gant, T.W., Hastings, M.H., Kyriacou, C.P., 2002. Circadian cycling of the mouse liver transcriptome, as revealed by cDNA microarray, is driven by the suprachiasmatic nucleus. Curr. Biol. 12, 540–50.

Baker, T.K., Carfagna, M.A., Gao, H., Dow, E.R., Li, Q., Searfoss, G.H., Ryan, T.P., 2001. Temporal gene expression analysis of monolayer cultured rat hepatocytes. Chem. Res. Toxicol. 14, 1218–1231.

Cerec, V., Glaise, D., Garnier, D., Morosan, S., Turlin, B., Drenou, B., Gripon, P., Kremsdorf, D., Guguen-Guillouzo C, and C.A., 2007. Transdifferentiation of hepatocyte-like cells from the human hepatoma HepaRG cell line through bipotent progenitor. Hepatology 45, 957–967.

Davila, J.C., Xu, J.J., Hoffmaster, K.A., P.J., O., Storm, S.C., 2008. Current in vitro models to study drug-induced liver injury, in: Hepatotoxicity (ed S. C. Sahu), John Wiley & Sons, Ltd, Chichester, UK.

Destici, E., Oklejewicz, M., Nijman, R., Tamanini, F., van der Horst, G.T.J., 2009. Impact of the circadian clock on in vitro genotoxic risk assessment assays. Mutat. Res. 680, 87–94.

Godoy, P., Hewitt, N.J., Albrecht, U., Andersen, M.E., Ansari, N., et al., 2013. Recent advances in 2D and 3D in vitro systems using primary hepatocytes, alternative hepatocyte sources and non-parenchymal liver cells and their use in in-

vestigating mechanisms of hepatotoxicity, cell signaling and ADME, Archives of toxicology.

Harris, A.J., Dial, S.L., Casciano, D. a, 2004. Comparison of basal gene expression profiles and effects of hepatocarcino-gens on gene expression in cultured primary human hepatocytes and HepG2 cells. Mutat. Res. 549, 79–99.

Hughes, M.E., DiTacchio, L., Hayes, K.R., Vollmers, C., Pulivarthy, S., Baggs, J.E., Panda, S., Hogenesch, J.B., 2009. Harmonics of circadian gene transcription in mammals. PLoS Genet. 5, e1000442.

Klein, S., Mueller, D., Schevchenko, V., Noor, F., 2013. Long-term maintenance of HepaRG cells in serum-free conditions and application in a repeated dose study. J. Appl. Toxicol.

Kramer, N.I., Krismartina, M., Rico-Rico, A., Blaauboer, B.J., Hermens, J.L., 2012. Quantifying processes determining the free concentration of phenanthrene in Basal cytotoxicity assays. Chem. Res. Toxicol. 25, 436–445.

Lu, Y.-F., Jin, T., Xu, Y., Zhang, D., Wu, Q., Zhang, Y.-K.J., Liu, J., 2013. Sex Differences in the Circadian Variation of Cytochrome P450 Genes and Corresponding Nuclear Receptors in Mouse Liver. Chronobiol. Int. 30, 1135–1143.

Luttringer, O., Theil, F.P., Lavé, T., Wernli-Kuratli, K., Guentert, T.W., de Saizieu, A., 2002. Influence of isolation proce-dure, extracellular matrix and dexamethasone on the regulation of membrane transporters gene expression in rat hepato-cytes. Biochem. Pharmacol. 64, 1637–50.

Mueller, D., Krämer, L., Hoffmann, E., Klein, S., Noor, F., 2014. 3D organotypic HepaRG cultures as in vitro model for acute and repeated dose toxicity studies. Toxicol. In Vitro 28, 104–12.

Oklejewicz, M., Destici, E., Tamanini, F., Hut, R. a, Janssens, R., van der Horst, G.T.J., 2008. Phase resetting of the mammalian circadian clock by DNA damage. Curr. Biol. 18, 286–91.

Panda, S., Antoch, M.P., Miller, B.H., Su, A.I., Schook, A.B., Straume, M., Schultz, P.G., Kay, S.A., Takahashi, J.S., Ho-genesch, J.B., 2002. Coordinated transcription of key pathways in the mouse by the circadian clock. Cell 109, 307–20.

Penaloza, C., Estevez, B., Han, D., Norouzi, M., Lockshin, R., Zakeri, Z., 2013. Sex-dependent regulation of cytochrome P450 family members Cyp1a1, Cyp2e1, and Cyp7b1 by methylation of DNA. FASEB J published , fj.13–233320.

Reppert, S.M., Weaver, D.R., 2002. Coordination of circadian timing in mammals. Nature 418, 935–41.

Robles, M.S., Cox, J., Mann, M., 2014. In-vivo quantitative proteomics reveals a key contribution of post-transcriptional mechanisms to the circadian regulation of liver metabolism. PLoS Genet. 10, e1004047.

Schulze, A., Mills, K., Weiss, T.., Urban, S., 2012. Hepatocyte polarization is essential for the productive entry of the hep-atitis B virus. Hepatology 55, 373–383.

Szalowska, E., Stoopen, G., Groot, M.J., Hendriksen, P.J., Peijnenburg, A.A., 2013. Treatment of mouse liver slices with cholestatic hepatotoxicants results in down-regulation of Fxr and its target genes. BMC Med. Genomics 6, 39.

Takiguchi, T., Tomita, M., Matsunaga, N., Nakagawa, H., Koyanagi, S., Ohdo, S., 2007. Molecular basis for rhythmic ex-pression of CYP3A4 in serum-shocked HepG2 cells. Pharmacogenet. Genomics 17, 1047–1056.

Zhang, Y.J., Yeager, R.L., Klaassen, C.D., 2009. Circadian Expression Profiles of Drug-Processing Genes and Transcrip-tion Factors in Mouse Liver. Drug Metab. Dispos. 37, 106–115.
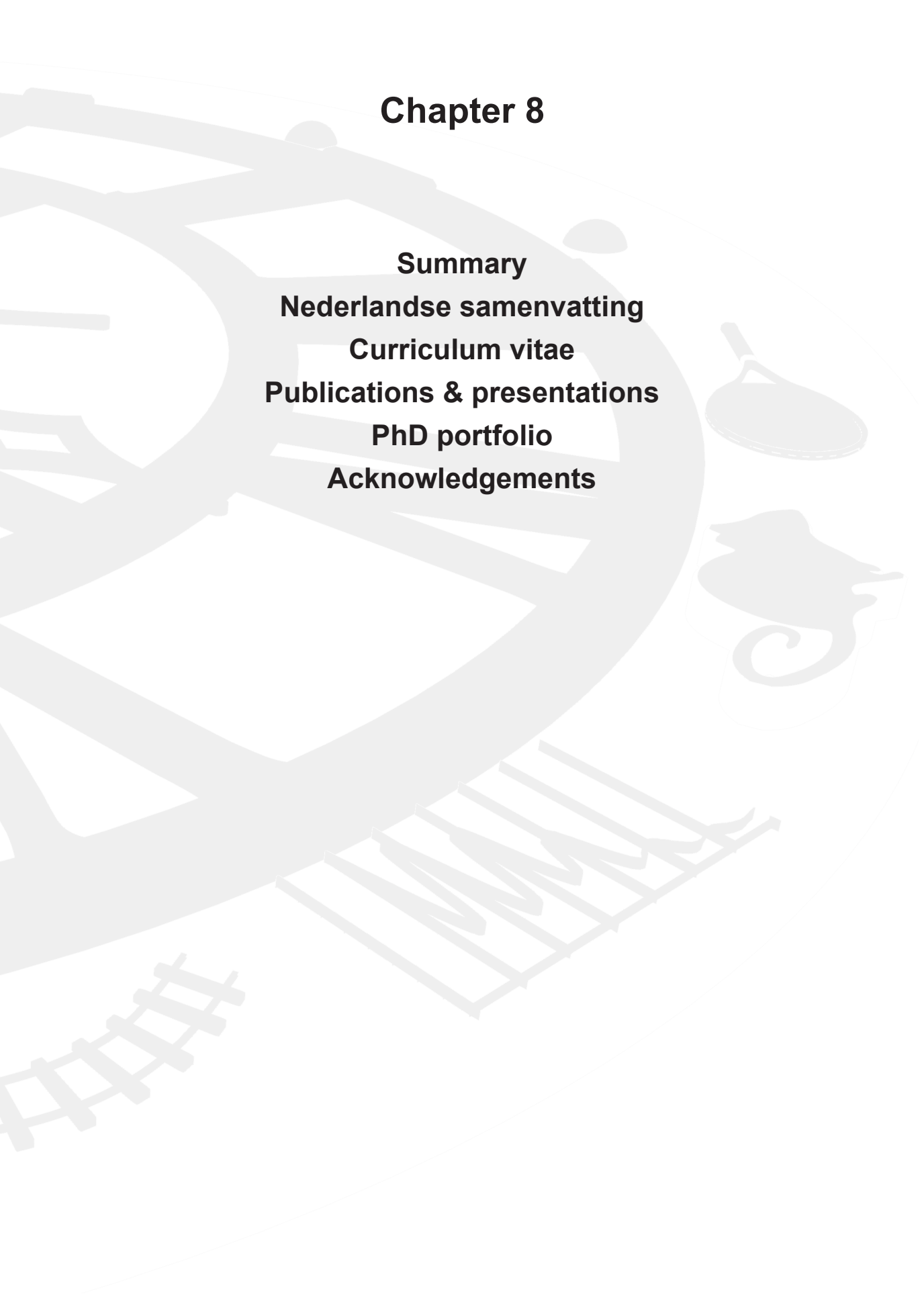
7

Chapter 8

Summary
Nederlandse samenvatting
Curriculum vitae
Publications & presentations
PhD portfolio
Acknowledgements

Summary

In order to adapt to environmental changes, life has acquired an internal timing mechanism that plays a role in circadian (Lat. circa = around, dies = day) oscillations in physiology, metabolism and our sleep/wake cycle, for instance. In mammals, the central clock resides in the suprachiasmatic nucleus in the brain, and is reset daily by light via the retinohypothalamic tract. Peripheral clocks in all other organs and cells are synchronized by hormonal stimuli originating from the brain. When organs or cells are explanted from the body, they retain their endogenous clocks but in the absence of synchronizing events, individual clocks desynchronize *ex vivo*. At the cellular level, the mammalian circadian clock is composed of a series of transcription translation feedback loops (TTFLs). The TTFLs drive the transcription and translation of core clock genes, which in turn are able to rhythmically repress their own expression with a periodicity of approximately 24 hours. The main loop consists of heterodimeric complexes of BMAL1/CLOCK containing a basic-helix-loop-helix/PER-ARNT-Sim (BHLH/PAS) domain, which induces transcription of *Cry1/Cry2* and *Per1/Per2* through E-box elements in their promoter regions. PER/CRY complexes in turn dislocate BMAL1/CLOCK complexes from these regions, thus inhibiting their own transcription. Similarly, other genes containing E-box elements in their promoter regions are rhythmically expressed. We refer to these genes as clock controlled genes (CCGs). In the liver, approximately 10% of genes is under circadian control. In **chapter 1** we first review the crosstalk between the core clock machinery and the pathogenesis of chronic metabolic diseases relying on disruption of fatty acid and cholesterol or bile acid metabolism. Second, we evaluate how circadian oscillations impinge on xenobiotic metabolism and the diurnal variations in the cell's efficiency in chemical detoxification and DNA damage pathways. Consequently, the toxic properties of many chemical compounds are dependent on the time of day of exposure; we refer to this as chronotoxicity. The chronotoxic properties of compounds can be used in therapeutical drug administration to maximize efficacy or in determining the least harmful time of exposure in occupational toxic exposure. Conversely, when the influence of the clock is not recognized in animal exposure studies or in drug administration, this can cause large variations in outcome.

Next to more information on chemical safety, our society also demands a large reduction in the use of laboratory animals. Therefore, many studies in toxicology are setting up *in vitro* alternatives for animal testing. Because the liver is the major organ involved in xenobiotic metabolism, the focus is often on the liver. However, despite increasing evidence on the influence of the clock, few studies acknowledge the impact of circadian rhythmicity on *in vitro* experiments. **Chapter 2** describes the differences in biological response to genotoxic exposure to the environmental pollutant benzo[a]pyrene (B[a]P) in mouse liver slices when they are exposed at opposite phases of the clock. In **chapter 3** we also optimized mouse primary hepatocytes, for chronotoxic exposure studies. We investigated the temporal changes the hepatocytes undergo in culture and concluded that profound changes in gene expression are observed during the first 48 hours in culture and that gene expression and hepatocyte specific product secretion (albumin, urea) are stable for at least 12 days after this period. Cellular clocks were synchronized by replacing the medium and clock dependent bioluminescence by *Period2::luciferase* was followed in real time prior to exposure. Chronotoxic exposure to B[a]P and the immunosuppressant drug cyclosporine A (CsA) were performed during 6 periods of 4 hours in different populations, in which the relative time point 0 or 24 refers to the trough, and relative time point 12 to the peak of *Per2::luc* expression. We found significant circadian rhythmicity in activation of the primary gene involved in B[a]P detoxification, *Cyp1a1*, with the highest induction found for exposure between relative time point 8 and 12 which is in accordance with results in mouse liver slices. For CsA, we used *DnaJb9* to measure the influence of chronotoxic exposure and found higher induction for exposure ending at relative time points 12, 16 and 20 than at 0, 4 and 8. No circadian oscillation could be found for in this data.

In order to further improve the reduction in numbers of laboratory animals, we investigated the characteristics of an in house developed immortalized hepatocyte cell line, which we refer to as Spontaneously Immortalized Mouse Hepatocytes, or SIMH4/SIMH[CLOCK]. In **chapter 4** we demonstrate that SIMH4/SIMH[CLOCK] cells retain a cuboidal morphology typical for primary

hepatocytes, high hepatocyte specific gene expression and functional polarized cell architecture in confluent populations. The latter two are further improved when cells are cultured in serum free conditions. The perspective is that optimizing medium composition and medium refreshment regimes will promote cell survival, enhancing the cell line's ability to be used in chronic or repeated dose exposure studies. Upon exposure to B[a]P, SIMH4/SIMH^{CLOCK} cells demonstrate higher gene induction and protein expression than commonly used immortalized hepatocyte cell lines such as HepG2 and Hepa1-6, and more resemble the response in mouse primary hepatocytes, signifying an intact P450 system. Only slight differences were found in basal gene expression and xenobiotic gene inducibility between passages of SIMH4/SIMH^{CLOCK} cells, indicating that hepatocyte specific functions are not lost in higher passage numbers but the sensitivity to a chemical compound should be tested prior to any experiment, similar to other cell lines.

Gene expression analysis is a powerful tool in genotoxic exposure studies, but for chemical risk analysis it is important to know what is the ultimate biologic significance of altered gene expression, especially to better predict *in vivo* toxicity. B[a]P is a known inducer of apoptosis and mutagenesis *in vivo* and here, we show that SIMH4/SIMH^{CLOCK} cells can indeed be used to induce apoptosis, assessed by increased levels of cleaved caspase 3, and mutagenesis, assessed by optimizing SIMH4/SIMH^{CLOCK} cells for the micronucleus assay. Cholestasis is a common side effect of CsA and we have demonstrated that the intracellular accumulation of toxic bile acids can correspondingly be measured in SIMH4 cells.

In **chapter 5** we tested expression of genes involved in general and xenobiotic metabolism in SIMH4 cells depending on the time of day. Overall these results resembled gene expression observed *in vivo*. We then exposed SIMH4/SIMH^{CLOCK} cells to B[a]P and CsA similar to experiments performed in mouse primary hepatocytes. *Cyp1a1* again showed a distinct circadian induction pattern, but the peak of induction was now observed around relative time point 8. Chronotoxic exposure to B[a]P, followed by a recovery period of 20 hours demonstrated clear circadian variation in induced levels of cleaved caspase 3 on top of endogenous circadian oscillations in levels of caspase 3; both oscillations have their peak around relative time point 12. The earlier peak in gene expression compared to primary hepatocytes and liver slices is likely due to higher rates of metabolism needed to sustain high proliferative capacity, and the relative delay in the peak of apoptosis to the time needed between gene expression and protein assembly. This data shows, for the first time, that both endogenous levels of apoptosis as well as inducibility of apoptosis are dependent on the phase of the clock. *DnaJb9* demonstrated an endogenous 12 hour ultradian expression with peaks around relative time points 12 and 24. After exposure to CsA, a 24 hour circadian expression pattern emerged compared to vehicle exposed cells, with the peak around relative time point 20, which coincides with peak expression of the primary gene involved in CsA metabolism *in vivo*, *Cyp3a11*.

It has been suggested earlier that time of day dependent toxic exposure not only increases specificity of chemical risk analysis by eliminating false positive genotoxic responsive genes that are in fact clock controlled genes, but also the sensitivity of the assay. We therefore performed proof of principle experiments in **chapter 6** with populations of synchronized versus nonsynchronous SIMH4/SIMH^{CLOCK} cells and indeed demonstrated that *Cyp1a1* induction in nonsynchronous populations were similar for all time points and around the average value observed for synchronized populations. Additionally, we found that nonsynchronized populations are not necessarily, and in fact most often, not fully nonsynchronous, which likely contributes to intra- and interexperimental variation in genotoxic exposure studies.

Nederlandse samenvatting

Om zich aan te kunnen passen aan veranderingen in de omgeving heeft het leven een intern klokmechanisme ontwikkeld dat een rol speelt in dagelijkse oscillaties in onder andere onze fysiologie, metabolisme en slaap/waak cycli: de circadiane klok (Lat. circa = rondom, dies = dag). In zoogdieren bevindt de centrale klok zich in de suprachiasmatische kern in de hersenen, en wordt dagelijks gesynchroniseerd door licht via de retinohypothalamische route. Perifere klokken in alle andere organen en cellen worden gesynchroniseerd door hormonen die vanuit de hersenen worden aangestuurd. Wanneer organen of cellen uit het lichaam worden getransplanteerd behouden zij hun endogene klokken maar in de afwezigheid van synchroniserende signalen lopen de individuele klokken *ex vivo* snel uit de pas. Op celniveau bestaat de klok van zoogdieren uit een serie van transcriptie translatie feedback loops (TTFL's). Deze TTFL's regelen de transcriptie en translatie van kernklokgenen, die op hun beurt hun eigen expressie ritmisch onderdrukken met een periode van ongeveer 24 uur. De belangrijkste serie bestaat uit heterodimerische complexen van BMAL1/CLOCK, die een basic-helix-loop-helix/PER-ARNT-Sim (BHLH/PAS) domein hebben waarmee ze transcriptie van *Cry1/Cry2* en *Per1/Per2* induceren door middel van E-box elementen in hun promotergebieden. Complexen van PER/CRY verwijderen de BMAL1/CLOCK complexen op hun beurt weer van deze gebieden, waarmee ze hun eigen transcriptie tegengaan. Op dezelfde manier worden anderen genen die E-box elementen in hun promotergebieden bezitten ritmisch tot expressie gebracht. Deze genen noemen we klokgereguleerde genen (CCG's). In de lever wordt ongeveer 10% van alle genen circadiaan gereguleerd. In **hoofdstuk 1** hebben we eerst een overzicht gemaakt van de invloed van de klokgenen op de pathogenese van chronische ziektes die veroorzaakt worden door de verstoring van vetzuur- en galzoutmetabolisme, en vice versa. Daarna hebben we geëvalueerd hoe de circadiane klok inwerkt op het metabolisme van xenobiotische stoffen en op de dagelijkse variaties in de efficiëntie waarmee een cel chemische stoffen kan opruimen en DNA-schade kan herstellen. Daardoor is de hoeveelheid schade die een toxische stof kan aanrichten afhankelijk van het moment van blootstelling, een verschijnsel dat we chronotoxiciteit noemen. De chronotoxische eigenschappen van een stof kunnen in ons voordeel werken wanneer men denkt aan het toedienen van medicijnen om de werkzaamheid te maximaliseren, of aan het bepalen wat het minst schadelijke moment is om beroepshalve met een bepaalde stof te werken. Wanneer de invloed van de klok daarentegen niet wordt erkend in dierproeven of bij medicijngebruik kan dit leiden tot grote variaties in de uitkomsten.

Naast het vergaren van meer informatie over de veiligheid van chemische stoffen verlangt onze maatschappij ook een grote vermindering in het gebruik van proefdieren. Daarom worden binnen de toxicologie vele *in vitro* studies opgezet als alternatief voor het gebruik van deze proefdieren. Omdat de lever het belangrijkste orgaan is in het onschadelijk maken van xenobiotische stoffen focussen de meeste studies op dit orgaan, maar ondanks toenemend bewijs voor de invloed van de klok houden slechts weinig van deze *in vitro* studies rekening met circadiane ritmen. **Hoofdstuk 2** beschrijft de verschillen in biologische respons na genotoxische blootstelling aan de milieuverontreinigende stof benzo[a]pyreen (B[a]P) in muizenleverplakjes wanneer deze worden blootgesteld op tegengestelde fasen van de klok. In **hoofdstuk 3** hebben we ook primaire muizenhepatocyten geoptimaliseerd voor chronotoxische blootstellingsstudies. We hebben onderzocht welke veranderingen plaatsvinden in hepatocyten wanneer deze in kweek worden gebracht, en vonden grote veranderingen in genexpressie in de eerste 48 uur na uitzaaien. Genexpressie en de uitscheiding van hepatocytspecifieke producten zoals albumine en ureum waren stabiel in de 12 dagen daarna. De individuele klokken werden gesynchroniseerd door het medium te verversen en real-time bioluminescentie afkomstig van *Period2::luciferase* kon worden gevolgd voordat cellen werden blootgesteld aan chemische stoffen. Chronotoxische blootstelling aan B[a]P en het immuunsysteemonderdrukkende medicijn cyclosporine A (CsA) werd uitgevoerd gedurende 6 perioden van 4 uur in afzonderlijke celpopulaties, waarin relatief tijdspunt 0 refereert aan het dal, en 12 aan de piek van *Per2:luciferase* expressie. Dit leidde tot significante circadiane ritmen in de activatie van *Cyp1a1*, het primaire gen dat betrokken is bij de afbraak van B[a]P, met de hoogste inductie wanneer cellen werden blootgesteld vanaf relatief tijdspunt 8 tot 12. Dit is in

overeenstemming met eerdere resultaten die werden gevonden in experimenten met leverplakjes van de muis. Voor CsA werd *DnaJb9* gebruikt om de invloed van chronotoxische blootstellingen te meten en hierbij vonden we een hogere inductie wanneer cellen werden blootgesteld met eindtijden op relatieve tijdspunten 12, 16 en 20 dan op 0, 4 en 8. In deze data konden we geen significante circadiane oscillaties vinden.

Om het gebruik van proefdieren verder te verminderen hebben we de kenmerken van een huisgemaakte cellijn van hepatocyten onderzocht, die we Spontaan Geïmmortaliseerde Muis Hepatocyten (SIMH4/SIMH^{CLOCK}) noemden. In **hoofdstuk 4** laten we zien dat SIMH4/SIMH^{CLOCK} cellen een kubusachtige morfologie behouden die typerend is voor primaire hepatocyten, alsmede hoge leverspecifieke genexpressie en functionele gepolariseerde celstructuren in confluente populaties. Deze laatste twee kenmerken werden bovendien verbeterd wanneer cellen werden gekweekt in serumvrij kweekmedium. Het vooruitzicht is dan ook dat het optimaliseren van de mediumsamenstelling en het verversingsregime het overleven van deze cellen zal verbeteren, waardoor de mogelijkheid om deze cellen te gebruiken in chronische or herhaaldelijke- dosisstudies zal toenemen. Wanneer SIMH4/SIMH^{CLOCK} cellen worden blootgesteld aan B[a]P vertonen zij een hogere geninductie en eiwitexpressie dan algemeen gebruikte geïmmortaliseerde hepatocytencellijnen zoals HepG2 en Hepa1-6, en lijkt de respons meer op die van primaire muis- hepatocyten, wat duidt op een intact systeem van P450-genen. We vonden slechts kleine verschillen in basale genexpressie en induceerbaarheid van genen die zijn betrokken bij het onschadelijk maken van toxische stoffen tussen verschillende passages van SIMH4/SIMH^{CLOCK} cellen, wat erop wijst dat hepatocytspecifieke functies niet verloren gaan wanneer de cellen vaak worden doorgezet. De gevoeligheid van SIMH4/SIMH^{CLOCK} cellen voor een chemische stof moet wel telkens worden bepaald voorafgaand aan een blootstellingsexperiment, net als bij andere cellijnen.

Analyse van genexpressie is een goede methode voor gebruik in genotoxische bloot- stellingsstudies, maar voor de risicoanalyse van chemische stoffen is het belangrijk om te weten wat de uiteindelijk biologische betekenis is van veranderingen in genexpressie, om zo betere voorspellingen te doen voor *in vivo* toxiciteit. Het is bekend dat B[a]P apoptose en mutagenese induceert *in vivo* en hier laten we zien dat SIMH4/SIMH^{CLOCK} cellen gebruikt kunnen worden om beide gevolgen aan te tonen door middel van toegenomen hoeveelheden actief caspase 3 voor apoptose, en door SIMH4/SIMH^{CLOCK} cellen te optimaliseren voor micronucleusexperimenten voor mutagenese. Cholestase is een veelvoorkomend neveneffect van CsA en we hebben aangetoond dat de intracellulaire ophoping van toxische galzouten inderdaad kan worden gemeten in SIMH4/ SIMH^{CLOCK} cellen.

In **hoofdstuk 5** hebben we gekeken naar de expressie van genen die betrokken zijn bij algemeen metabolisme en bij het omzetten van xenobiotische stoffen. Tezamen kwamen deze resultaten overeen met de resultaten *in vivo*. Daarna hebben we SIMH4/SIMH^{CLOCK} cellen blootgesteld aan B[a]P en CsA op verschillende momenten van de dag en gevonden dat *Cyp1a1* ook hier een significante circadiane oscillatie geeft, in dit geval met de maximale inductie wanneer cellen werden blootgesteld van relatief tijdspunt 4 tot 8. Chronotoxische blootstelling aan B[a]P gevolgd door een rustperiode van 20 uur liet zien dat er ook significante verschillen zijn in de hoeveelheid actief caspase 3 bovenop een endogene circadiane oscillatie. Beide patronen lieten een piek zien voor behandelingen van relatief tijdspunt 8 tot 12. De vroegere piek in genexpressie vergeleken met primaire hepatocyten en leverplakjes kan waarschijnlijk worden toegeschreven aan een sneller metabolisme als gevolg van een hoge groeisnelheid, en de vertraging in de piek van apoptose aan de tijd die nodig is voor de productie van eiwitten als gevolg van genexpressie. Het is niet eerder aangetoond dat zowel endogene als induceerbare hoeveelheden apoptose afhankelijk zijn van de fase van de klok. *DnaJb9* liet een endogeen expressiepatroon zien van 12 uur, met pieken rondom relatief tijdspunt 12 en 24. Na behandeling met CsA verscheen er een 24- uurs patroon ten opzichte van onbehandelde cellen, met een piek voor behandeling eindigend op relatief tijdspunt 20. Dit valt samen met de piek in genexpressie van *Cyp3a11*, het voornaamste gen dat betrokken is bij het metabolisme van CsA.

Eerder werd geopperd dat chronotoxische blootstellingen niet alleen de specificiteit van chemische risicoanalyse zou vergroten door vals-positieven te elimineren van genen die niet be-

trokken zijn bij genotoxische responsen maar eigenlijk klokgereguleerde genen zijn, en ook de gevoeligheid van deze experimenten. Daarom hebben we een proof of principle experiment uitgevoerd in **hoofdstuk 6** met populaties gesynchroniseerde versus ongesynchroniseerde SIMH4/SIMH^{CLOCK} cellen. De inductie van *Cyp1a1* in asynchrone cellen was inderdaad vergelijkbaar tussen alle tijdspunten en slechts gelijk aan de gemiddelde inductie in gesynchroniseerde cellen. Daarbovenop hebben we aangetood dat niet-gesynchroniseerde celpopulaties niet per se hetzelfde zijn als asynchrone celpopulaties. In de praktijk zijn niet-gesynchroniseerde celpopulaties niet of niet volledig asynchroon, wat waarschijnlijk bijdraagt aan intra- en interexperimentele variaties in genotoxische blootstellingsstudies.

8

Curriculum vitae

Personal information

Name	Annelieke Suzanne de Wit
Born	April 22nd, 1985 in Amsterdam

Education

2007-2009	MSc Life Science & Technology, Leiden University & Delft University of Technology
2003-2008	BSc Life Science & Technology, Leiden University & Delft University of Technology
1997-2003	Gymnasium, Spinozalyceum Amsterdam

Research experience

2009-2014	PhD project (Genetics, Erasmus MC, prof. G.T.J. van der Horst) Cellular models for liver toxicity: keeping track of time
2009	Master thesis (Enzymology, TU Delft, prof. S. de Vries) Characterization of bacterial terminal oxidases: inhibition of *Paracoccus denitrificans* aa3 and cbb3 oxidase by nitric oxide and identification of *Escherichia coli* bd-I and bd-II oxidase
2008	iGEM project: international Genetically Engineered Machine (Synthetic biology, Groningen University, prof. O. Kuipers & MIT) Conway's Game of Life
2007	Master design project (TU Delft, Wageningen University & Organon) Enzymatic production of nucleotide sugars for the synthesis of glycosaminoglycans
2006	Bachelor thesis (Solid State NMR, Leiden University, prof. F. Buda) Vibrational properties of methyl substituted retinylidene chromophores

8

Teaching / mentoring experience

2013	Supervisor for 3rd year student from Avans University of Applied Science, Breda
2003-2009	Student assistant practicals for first year LST students (Leiden University) Teacher practical courses for high school students (Reizende DNA Labs, TU Delft & Leiden University) Teacher high school exam training (SSL Leiden, statistics) Supervisor in homework classes for high school students (Descartes, Leiden) Mentor for first year LST students (Leiden University)

Publications

De Wit, A. S., Nijman, R., Destici, E., Chaves, I., & van der Horst, G. T. J. (2014). Hepatotoxicity and the circadian clock, a timely matter. In Toxicogenomics-Based Cellular Models: Alternatives to Animal Testing for Safety Assessment (pp. 251–270). Academic Press.

Bombardieri, C. R., Sepe, S., Payan Gomez, C., Wamelink, M. M., De Wit, A. S., Leen, R., Hamilton, B., Van Kuilenburg, A. B. P., Hoeijmakers, J. H. J. & Mastroberardino, P.G. (2014). DNA damage-induced transcription arrest elicits allosteric redesign of metabolism and activation of longevity pathways (in preparation).

Presentations

2013   NTC Annual meeting, Amsterdam: Chronotoxicity in primary and immortalized mouse hepatocytes: an *in vitro* model to determine time-of-day dependent differences in compound toxicity (oral)

2013   MGC Symposium, Düsseldorf: Liver chronotoxicity *in vitro* using primary and immortalized mouse hepatocytes (oral)

2012   MGC Symposium, Maastricht: Primary and immortalized mouse hepatocytes in chronotoxicicity assays (poster)

2012   NTC Annual meeting, Amsterdam: Primary and immortalized mouse hepatocytes in chronotoxicicity assays (poster)

2011   NTC Annual meeting, Amterdam: The circadian clock in cultured hepatocytes and liver slices: Towards an *in vitro* hepatochronotoxicity assay (poster)

8

PhD portfolio

2010
Epigenetic Regulation
Animal Imaging
Technology Facilities
Genome Maintenance & Cancer
Cell and Developmental Biology
Basic Data Analysis on Gene Expression Arrays
Genetics
Microarray Analysis
Biophysics
Basic & Translational Oncology
Veilig Werken in Laboratoria

2011
Project Management
Get Out Of Your Lab Days
Signal Transduction Pathways and Disease
MGC Literature Discussions

2012
SRBR Meeting Florida
Loopbaanoriëntatie voor Wetenschappers

2013
Postdoc Retreat (PCDI)

8

Acknowledgements

Eindelijk!! De experimenten, het schrijven, de figuren en de lay-out: het is klaar! Net zoals velen vóór mij schrijf ik deze laatste bladzijden als allerlaatste, terwijl ik weet dat het door de meesten van jullie als eerste gelezen wordt... Tenslotte vraag je je nu vooral af of ik je niet heb overgeslagen!

Lieve familie, vrienden, collega's en –genoten: ik wil jullie graag allemaal bedanken. Niet alleen voor de afgelopen 4 (vooruit 4,5) jaar, maar uiteraard ook voor de tijd ervoor. Sommigen van jullie ken ik nog niet erg lang, anderen houden het al langere tijd met mij vol. Hoe dan ook had ik het zonder jullie steun, hulp en feedback niet gekund.

Bert, via een omweg langs Roland Kanaar en Jan Hoeijmakers belandde ik bij de klokgroep. Ondanks mijn minder toepasselijke achtergrond stelde je het vertrouwen in mij om dit project op te zetten en tot een goed einde te brengen. Bedankt voor je ideeën, hulp, kritiek maar vooral ook voor je geduld met mijn soms iets te directe benadering. Ik heb veel van je mogen leren! Filippo, thank you for your help to get started with a lot of little things in the lab. Inês, na 2,5 jaar experimenteren werd jij mijn nieuwe begeleider/copromotor; we hebben dag en nacht samen staan pipetteren, soms met wel 6 tijdpunts-experimenten tegelijk, waardoor dit een stuk gezelliger en efficiënter werd! 1+1 was zeker meer dan 2 bij het honderden epjes schrijven en uitgebreide planningen maken, maar ook bij onze pizza-en-film-op-het-lab-avonden, koffiemomentjes en shop-activiteiten. Bedankt voor je hulp met de kleine en grote dingen, maar vooral voor je vriendschap: ik hoop deze zeker voort te zetten!

In en rond het lab heb ik het genoegen gehad om samen te werken met veel gedreven, goede, grappige, serieuze, leuke en intelligente collega's en studenten. Aida, Andre, Anke, António, Arjan, César, Chiara, Cíntia, Ed, Eugin, Franzi, Giulia, Gosia, Hannes, Henk, Hervé, Humaira, Inês, Jacqueline, Joris, Jurgen, Kira, Kyra, Karen, Kasper, Karl, Lieneke, Loes, Magda, Maikel, Marco, Maria, Marjolein, Marshall, Monique, Özge, Peter, Petra, Pier, grote Pim, kleine Pim, Renata, Roel, Romana, Sander Ba, Sander Bo, Sara, Shoko, Stefanie, Sylvia, Wilbert, Wim, Yanto, Yvette, Yvonne; farmacokinetiek-buddies Jacqueline, Lisette en Peter; dames van de keuken; Jan de Wit; dames van het secretariaat; Jan Hoeijmakers; heren van de IT; Enno, Koos, Leo, Melle; NTC-genoten Anke, Ewa, Wim en andere WP4-members; RIVM'ers Edwin, Harry, Kirsten, Mirjam, Petra en Wendy; Geert en Freddy bij Janssen; Mary Harrington & coworkers; mijn commissiegenootjes bij de party committee en MGC-commissie en andere collega's van het Erasmus: zonder jullie was het nooit gelukt!

Natuurlijk moet ik ook mijn leescommissie niet vergeten: Harry, Leon en Ron, bedankt voor jullie tijd en bij het verbeteren van de tekst en verwijzingen!

Mama, papa en Marilene: ik was niet altijd de gemakkelijkste dochter/ zus, maar jullie hebben altijd achter mij gestaan in alle keuzes die ik maakte. Bedankt dat jullie er altijd voor mij waren! Dit geldt natuurlijk ook voor alle andere familieleden, "schoonfamilie" en "zwagers" (;)). Jullie aanhoudende interesse in de onbegrijpelijke dingen die ik probeerde uit te leggen betekende voor mij dat jullie graag wilden weten wat mij bezig hield, zelfs op de momenten dat ik dat zelf even niet zo interessant vond: bedankt!

Ook mijn cordialgenootjes Anjo, Annelies, Ilse, Jeanile, Laura, Maaike, Michelle, Pauline, Puck, Risha en Tessa; LST-vriendinnetjes Bo, Claire, Fenna, Hilde, Stephanie en natuurlijk jullie mannen; tennisvriendjes- en vriendinnetjes van At Risk en Obvius met de Utrecht-gang Sanne en Melchior in het bijzonder en Octo'ers met poezen wil ik graag bedanken voor jullie vriendschap, gezelligheid, discussies, etentjes, feestjes en verdere activiteiten. Jullie maakten mij mee op mijn beste en slechtste momenten, en juist doordat jullie mij af en toe ook op mijn plaats zetten

waardeer ik jullie allemaal enorm!

Mijn paranimfen Marilene en Yvonne, eerder al genoemd, wil ik ook graag nog speciaal bedanken hiervoor. Jullie enorme inzet maakt deze promotie voor mij nog feestelijker! Yvonne, op jouw vrije dagen was het in ons lab nooit zo gezellig als met jouw aanwezigheid. Ik heb gezien hoe hard je werkt en hoop dat je ook in de toekomst wordt beloond hiervoor. Marilene, jouw creativiteit is ongeëvenaard, kijk maar naar de omslag; ik hoop dat je deze creativiteit ook in je zzp-projecten kwijt kunt. Ik ben ontzettend blij dat ik zo'n bijzonder zusje heb!

Last but not least: Lars. Ik vind het heerlijk dat we zo veel interesses delen en fantastisch om nieuwe dingen te ontdekken, variërend van duiken en golfen tot een wijncursus en 1,5 meter kookboek. Jij bent er altijd voor mij, ook op de mindere momenten, en kan mij altijd weer opvrolijken. Jouw relativeringsvermogen houdt mij met beide benen op de grond. Ik ben ontzettend blij met al onze avonturen en hoop dat we er nog veel meer zullen beleven!

Liefs, Annelieke

8